2014

Extreme Value Analysis of Rainfall Events Over the Kennedy Space Center Complex

Adam David Schnapp
Embry-Riddle Aeronautical University - Daytona Beach

EXTREME VALUE ANALYSIS OF RAINFALL EVENTS OVER THE KENNEDY SPACE CENTER COMPLEX

Adam David Schnapp

A Thesis Submitted to the College of Aviation, Department of Graduate Studies,
in Partial Fulfillment of the Requirements for the Degree of
Master of Science in Aeronautics

Embry-Riddle Aeronautical University
Daytona Beach, Florida
July 2014

EXTREME VALUE ANALYSIS OF RAINFALL EVENTS OVER THE KENNEDY SPACE CENTER COMPLEX

by

Adam David Schnapp

This Thesis was prepared under the direction of the candidate's Thesis Committee Chair, Dr. John M. Lanicci, Professor, Daytona Beach Campus, and Thesis Committee Members Dr. Christopher G. Herbster, Associate Professor, Daytona Beach Campus, and Dr. Jennifer E. Thropp, Assistant Professor, Daytona Beach Campus, and has been approved by the Thesis Committee. It was submitted to the Department of Graduate Studies in partial fulfillment of the requirements for the degree of Master of Science in Aeronautics

Thesis Committee:

John M. Lanicci, Ph.D.
Committee Chair

Christopher G. Herbster, Ph.D.
Committee Member

Jennifer E. Thropp, Ph.D.
Committee Member

John M. Lanicci, Ph.D.
Graduate Program Chair
Graduate Studies

Alan Stolzer, Ph.D.
Associate Dean
Research and Graduate Studies

Tim Brady, Ph.D.
Dean, College of Aviation

Robert Oxley, Ph.D.
Associate Vice President of Academics

12-9-14
Date

Acknowledgements

I would like to thank my advisor, Dr. John Lanicci, who guided me through a challenging and rewarding research experience. He always provided positive and insightful feedback that facilitated my efforts. He read and revised numerous drafts that have assisted me with writing a thesis that I am proud to submit.

I would also like to thank committee members, Dr. Jennifer Thropp and Dr. Christopher Herbster, who contributed their knowledge toward my research efforts. I am appreciative of my friends and family for their continuous support of my studies. Finally, I would like to acknowledge the aid I have received from NASA Award #NNX12AF58G that has supported this research.

Abstract

Researcher: Adam David Schnapp

Title: Extreme Value Analysis of Rainfall Events Over the Kennedy Space Center Complex

Institution: Embry-Riddle Aeronautical University

Degree: Master of Science in Aeronautics

Year: 2014

The use of observational datasets to determine the occurrence frequencies of extreme weather events has gained a lot of recent interest due to concerns about the potential regional impacts from global climate change. Extreme-value theory can quantify the return frequency of the most extreme events, using climatologically short data sets and the assumption that such short climatological periods are stationary. However, the resulting analyses must be used with caution since they may not accurately reflect the potential of extreme events in the future due to climate change and variability. Accurately predicting extreme-event likelihood is important for building realistic long-range planning scenarios for a number of weather- and climate-sensitive interests.

This study used extreme-value theory to analyze a short period (15-year), high-density rainfall dataset from NASA Kennedy Space Center's observational network. This data was acquired through the Tropical Rainfall Measurement Mission archive website. The researcher employed the National Center for Atmospheric Research's Extremes statistical software package for the analysis of 24-hour rainfall at the locations of the 32 tipping-bucket gauges in the network. This type of analysis is highly sensitive to data that may have been misreported, invalid, or missing, therefore, additional quality

control was required. The quality-controlled rainfall gauge data was subsequently gridded using a Barnes-style objective analysis with minimal smoothing, in order to estimate missing values while preserving maxima in the initial data. The high-resolution gridded rainfall data was used by the Extremes program to estimate a series of event return levels over the studied region.

Analyses of the gridded data show that that the 100-year events are around 315 mm and 433 mm for 24-hour and 72-hour durations, respectively. The wet-season analysis 100-year event estimation was around 426 mm and is similar to the yearly analysis, indicating that the majority of the annual extremes are from wet-season events. The yearly and wet-season 100-year return levels appear to be realistic and consistent with previous literature and estimates from the longer period of record at Titusville; however, some results from the dry-season analysis do not appear to be realistic, as they indicate the rainfall frequency distribution has an abnormally bounded tail shape. The dry-season 100-year return-levels are likely greater than the 170 mm model consensus produced from the analysis of the gridded data. The better-behaved Titusville analysis suggests the dry-season 100-year return level is around 250 mm. Findings indicate large uncertainty associated with long-period estimates and high spatial variations in rainfall extremes across the Kennedy Space Center region.

Table of Contents

List of Tables

List of Figures

Chapter I

Introduction

Kennedy Space Center (KSC) plays a significant role in the National Aeronautics and Space Administration's (NASA) operations. The center is responsible for NASA space shuttle and rocket launches, and research and development. KSC is on a barrier island (Merritt Island) in east-central Florida surrounded by several bodies of water, including the Atlantic Ocean (east), Banana River (south), Indian River (west), and Mosquito Lagoon (north). The complex sits very close to sea level and is exposed to a variety of weather hazards, from tropical systems, to wildfires, and thunderstorms.

The Intergovernmental Panel on Climate Change (IPCC) Fifth Assessment Report (AR5) on climate change summarizes the state of the global climate (IPCC, 2013). The report covers the major climate forcings and produces multiple climate-change projections based on greenhouse gas emission scenarios. AR5 estimates with 95% certainty that human activity is the dominant cause of observed warming since the mid-20th century. The effects of global climate change will differ by geographic region, and there is still little certainty as to how the frequency distributions of some weather variables may change with the climate (IPCC, 2013).

Significance of the Study

This study is part of a NASA-funded Research Opportunities in Space and Earth Sciences (ROSES) group within the Climate Adaptation Science Investigator (CASI) working group. The groups consist of NASA researchers and NASA-funded university and private-sector researchers (Rosenzweig et al., 2014). CASI's mission statement is "to advance and apply NASA's scientific expertise and products to develop climate adaptation strategies that support NASA's overall mission by minimizing risks to each center's operations, physical and biological assets, and personnel" (Rosenzweig & Horton, 2011). Minimizing risk at NASA centers requires an understanding of the hazards that affect them. This study focused specifically on advancing local climatological knowledge of the KSC region through analysis of extreme rainfall-event occurrence frequencies. The research group conducting the vulnerability analysis of KSC is collecting archived meteorological and geological data sets in order to build the current "climate picture". The group proposes that observed weather and climate anomalies can be used with downscaled global climate model output to project extreme-event trends over the next 20-40 years at NASA facilities across the U.S. (Rosenzweig et al., 2014).

Statement of the Problem

NASA centers, including KSC, have historically been impacted by numerous anomalous events associated with normal climate variability and change. According to AR5 (2013), extreme weather and climate events are increasing in frequency and/or magnitude in many locations around the world. These events include, but are not limited to, drought, wildfires, and flooding (IPCC, 2013). Extreme events put personnel, infrastructure, and the environment at risk. Extreme events at critical locations can have cascading impacts across the country. For example, in 2005, Hurricane Katrina's strike on the Gulf Coast destabilized the Gulf Coast states and the entire country. The storm devastated life and property along the Gulf Coast states. The Federal Response to Hurricane Katrina Lessons Learned report compares the loss of life and devastation to the terrorist attacks on 9/11 (DOHS, 2006). Katrina shut down 33% of U.S. oil and natural gas refining capabilities and caused shortages across the country. Gas prices increased around the world as supplies were diverted away from Europe and Asia to ease pressure in the U.S. Gas prices increased by 33% in Europe and 13% in Asia after Katrina (Cheatle, 2006). Appropriate planning and risk-management strategies can reduce loss of life and local and regional impacts of environmental hazards on the nation's valuable assets and critical infrastructure.

The use of observational datasets to determine the occurrence frequencies of extreme weather events has gained a lot of recent interest due to concerns about the potential regional impacts from global climate change. Extreme-value theory can quantify the probabilities of extreme events using climatologically short data sets and the assumption that such short climatological periods are stationary (i.e., no trends exist). However, the resulting analyses should be used with caution since they may not accurately reflect the potential for extreme events to occur in the future due to climate change and variability. Gilleland (2005) developed the Extremes Toolkit to promote the use of extreme-value theory in the atmospheric sciences over the use of traditional statistical distributions where applicable.

Estimating risk requires anticipating the loss from potential hazards and predicting the likelihood of hazards. Although there is often large uncertainty associated with estimating the probabilities of weather hazards, it is ethical to act on best estimates when hazards can have severe consequences. The potential outcomes from operational decisions should be carefully considered during the decision-making process (Tannert, Elvers, & Burkhard, 2007).

Purpose Statement

The goals of this study were to describe the extreme rainfall climatology of the

KSC region and estimate the likelihood of extreme rainfall events. An extreme-value analysis (EVA) was used to describe the extremes (right tail) of the rainfall-amount frequency distribution, and as a tool for predicting the likelihood of extreme rainfall events. A 15-year period of record (POR) from the KSC region was analyzed in this study.

Research Questions

This study addressed the following research questions:

Question 1: How does the right tail of the rainfall-amount frequency distribution at KSC behave over the 15-year POR?

Question 2: What can the right tail of the rainfall-amount frequency distribution tell us about the return level of extreme rainfall events at KSC?

Question 3: Does a seasonal spatial signal show up in the KSC rainfall data?

Delimitations

This study analyzed a 15-year POR between 1998 and 2012 from the KSC region. This period was chosen because fewer observations from the network were missing during this time and it was more reliable than measurements before 1998. Quality control was performed on the data, however, radar-derived precipitation was not used due to availability and time constraints. Quality control is addressed in the Methodology chapter.

Limitations and Assumptions

For this study, the researcher assumed all rain gauges were in appropriate locations for representative rainfall “catch”, and environmental obstructions did not influence gauge catch. Multiple assumptions were made regarding the rainfall data.

First, all gauge data was assumed to be ground truth, meaning the observation is as close to the "true occurrence" as could be determined. However, further assumptions were made during the data quality-control process, based on the natural ability for tipping-bucket rain gauges to catch and record rainfall. For instance, the researcher assumed that gauges are much more likely to underreport than overreport (Nystuen, 1999). This assumption is important for the quality control process; these assumptions are outlined and justified in the Methodology chapter.

Definitions of Terms

Return level	A value of some variable with "return period" *T*, and has a *1*/*T* exceedance probability (Katz, n.d.).
Return period	Sometimes referred to as waiting time, where on average *T* years must pass until the next occurrence of the "return level" (Katz, n.d.).
Scale parameter	Specifies the "spread" of the Generalized Extreme Value (GEV) and Generalized Pareto Distributions (GPD) (Katz, Brush, & Parlange, 2005).
Shape parameter	Specifies the tail behavior of the GEV and GPD ($\xi = 0$, light-tailed; $\xi > 0$, heavy-tailed; $\xi < 0$, bounded) (Katz et al., 2005).
Tipping bucket rain gauge	A rain gauge which measures rain by counting the tips that occur when a predetermined amount of water falls into the gauge (AMS Glossary, n.d.).

List of Acronyms

AR5	IPCC Fifth Assessment Report
ASOS	Automated Surface Observing System
CASI	Climate Adaptation Science Investigator Work Group
CLT	Central Limit Theorem
DOT	Department of Transportation

EVA	Extreme Value Analysis
FAWN	Florida Automated Weather Network
GEV	Generalized Extreme Value
GPD	Generalized Pareto Distribution
IDF	Intensity-Duration-Frequency
IID	Independently Identically Distributed
IPCC	Intergovernmental Panel on Climate Change
KSC	Kennedy Space Center
MRL	Mean Residual Life
NASA	National Aeronautics and Space Administration
NCAR	National Center for Atmospheric Research
NOAA	National Oceanic and Atmospheric Administration
PDF	Probability Distribution (Density) Function
POI	Point of Interest
POR	Period of Record
POT	Peaks Over Threshold
ROSES	Research Opportunities in Space and Earth Sciences
SFL	South Florida Water Management
STJ	St. Johns River Water Management
TC	Tropical Cyclone
TRMM	Tropical Rainfall Measuring Mission

Chapter II

Review of the Relevant Literature

Extreme Events at KSC

During the 2004 tropical season, four hurricanes (Charlie, Frances, Ivan, and Jeanne) struck the Florida Peninsula. KSC was closed twice for extended periods of time because of these storms and their threat to the center and those living in the adjacent coastal region. The storms resulted in significant damage, which was documented in the 2004 Hurricane Recovery Report (KSC, 2004). The center did not experience sustained hurricane force winds during these events, but the damage done opened eyes to how vulnerable the nation's space centers are to natural hazards. Damage from Hurricane Frances can be seen in Figure 1.

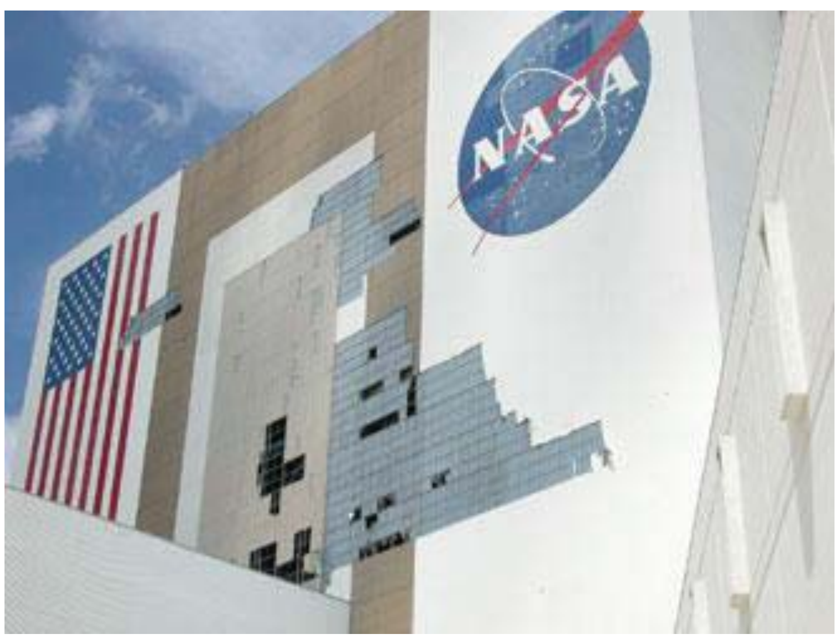

Figure 1. KSC's Vehicle Assembly Building had about 820 panels torn off its south side by Hurricane Frances. *Note.* Reprinted from NASA's 2004 Hurricane Report.

The storms had great impacts on KSC's operational space-launch missions, occupational health, finances, public affairs, and wildlife services. Indoor air quality became a problem following the storms because of water damage to more than 30 major facilities. KSC made a request for $126 million in emergency supplemental funding, which was not approved until October 13, 2004 (KSC, 2004). Delays in the receipt of emergency supplemental funding made for a complicated financial situation, where unobligated operational funds had to be distributed and reimbursed. KSC contractors also had to be reimbursed after the supplemental funding was approved. An estimated $1.4 million in additional revenue was lost from the KSC Visitor Complex because of nine days closure to the public after the storms. The natural environment also suffered significant damage. Many dunes were eroded by waves and animal habitats destroyed (KSC, 2004).

The 2004 hurricane season at KSC was studied and lessons learned were documented in the recovery report. These lessons aim to "improve KSC's emergency response capability to reduce risks and better protect the safety of the center's workforce and other valuable assets" (KSC, 2004, p. vii). Lessons learned focused on leadership and communications, improving safety, preparations, protection of facilities, and logistics, including traffic and power (KSC, 2004).

Climate Statistics

Statistical analyses are often used for describing climate and weather data. Climatological research involves using robust statistical measures of location, spread, and shape for describing how data is distributed. These statistical measures utilize the entire data set and therefore describe the union of the most frequently occurring and the unusual events, which occur less frequently. The body of a probability distribution function (PDF) represents the usual data, while the tails of the distribution represent the unusual data. This type of distribution is shown in Figure 2.

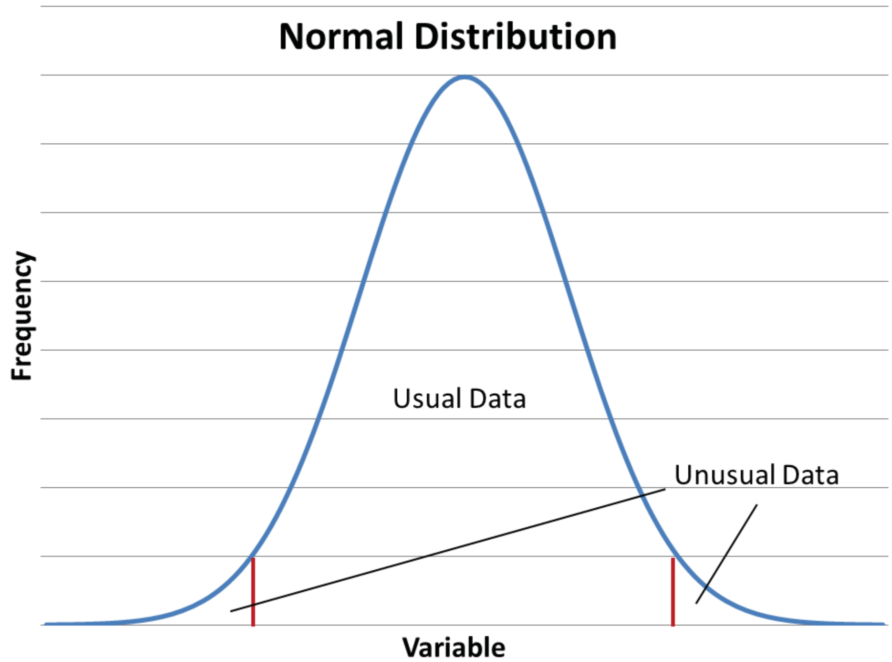

Figure 2. Normal occurrences exist in the body of the normal PDF while the unusual occurrences exist in the tails.

Traditional descriptive statistical measures describe the location, spread, and the shape of the overall frequency distribution of a variable. These statistics can lead to inference of tail shape and location, but can be misleading for modeling the likelihood of rare (unusual) occurrences, which occur in the tails. Statistics based on the normal distribution do not provide a theoretical basis for extrapolation of the tails and predicting the probability of rare events, which may not occur during the sampled period (R.W. Katz, personal communication, February 2, 2014).

Extreme-Value Theory

Weather and climate extremes have been studied more often recently, due to interest in potential regional impacts of global climate change (Katz et al., 2005; Dilumie, Gilleland, Bronaugh, & Wong, 2009; Bodini & Antonio, 2008). Weather extremes are rare; therefore, estimates must be made to quantify the likelihood of events that may have not been actually observed. This is especially needed when the observed POR is not long enough to infer the probability of an event easily, based on the event history. Extreme-value theory and its class of models enable extrapolation of frequency distribution models to values that have not been actually observed. Engineering applications often require estimates based on these extrapolated models. Even with underlying rationale for the models, extrapolation can be dangerous. Coles (2001) acknowledges, "It is easy to be cynical about this strategy", and that "extrapolation of models to unseen levels requires a leap of faith" (p. vii). He also argues that applications *demand* extrapolation, and that it is better to use justifiable techniques that have rationale.

Theoretical background. The Central Limit Theorem (CLT) shows how the means of a sufficiently large number of independently identically distributed (IID) samples approach a Gaussian distribution with a mean equivalent to the population mean. The CLT demonstrates that sample means are asymptotically normally distributed, and normality is often an appropriate assumption when using statistical modeling techniques (Gilleland, 2006).

The Extremal Types Theorem is similar to the CLT and provides asymptotic justification for modeling the tails of a distribution. The Extremal Types Theorem states that infinite sampling of maxima values will approach a Generalized Extreme Value

(GEV) distribution with cumulative distribution function as shown in Equation 1 below:

$$\boldsymbol{F}(\boldsymbol{x};\mu,\boldsymbol{\sigma},\boldsymbol{\xi}) = \begin{cases} \mathbf{exp}\{-\left[\mathbf{1}+\frac{\xi(x-\mu)}{\sigma}\right]^{-\frac{1}{\xi}}\}, \\ \mathbf{1}+\frac{\xi(x-\mu)}{\sigma} > \mathbf{0} \quad \boldsymbol{\xi} \neq \mathbf{0} \\ \\ \mathbf{exp}\left\{-\,\mathbf{exp}\left[-\frac{x-\mu}{\sigma}\right]\right\} \quad \boldsymbol{\xi} = \mathbf{0} \end{cases} \tag{1}$$

The parameters $\mu, \boldsymbol{\sigma}, \textbf{and } \boldsymbol{\xi}$ are termed the location, scale, and shape parameters, respectively. If a random variable *X* has a GEV distribution, then the standardized variable $(\boldsymbol{X}-\mu)/\boldsymbol{\sigma}$ has a distribution that is only dependent on $\boldsymbol{\xi}$. The location parameter specifies where the distribution is “centered”, and the scale parameter specifies the distribution’s “spread” (Katz et al., 2005).

The GEV consists of a family of distributions known as the Fréchet, Gumbel, and Weibull distributions (Coles, 2001; Gilleland, 2006). They are characterized by their various tail behaviors. The Shape Parameter $\boldsymbol{\xi}$ (Shape) of the GEV specifies the tail behavior of the GEV distribution. When $\boldsymbol{\xi} = \mathbf{0}$, the GEV takes on a lightly tailed Gumbel distribution. For $\boldsymbol{\xi} > \mathbf{0}$, the GEV takes on a heavy-tailed Fréchet distribution. If $\boldsymbol{\xi} < \mathbf{0}$, the GEV takes on a bounded Weibull distribution (Katz et al., 2005). Figure 3 shows the three GEV distributions. The tail shapes are described later in this chapter.

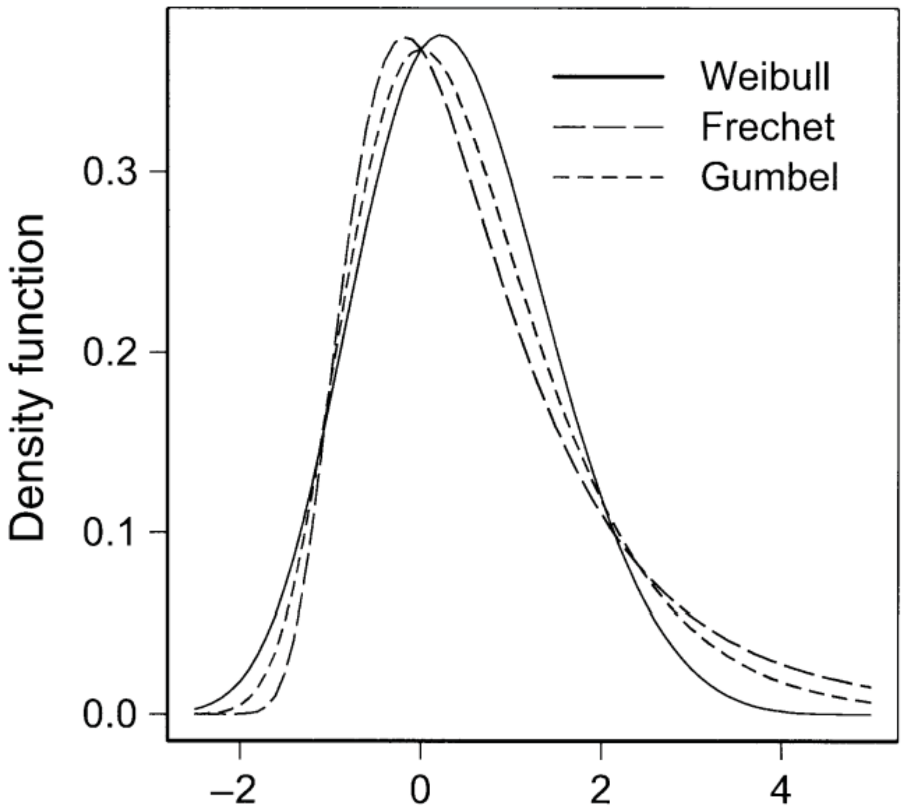

Figure 3. GEV plots with location parameter $\boldsymbol{\mu = 0}$, scale parameter $\boldsymbol{\sigma = 1}$, and shape parameter $\boldsymbol{\xi = -0.2}$ (Weibull type), $\boldsymbol{\xi = 0}$ (Gumbel), and $\boldsymbol{\xi = 0.2}$ (Fréchet). *Note.* Reprinted from Katz, Brush, and Parlange (2005).

Classical extreme-value modeling. Classical extreme-value modeling involves fitting "block maxima" with a GEV distribution through maximum likelihood estimation. This "block maxima" approach involves dividing the sampled period into equal length (time) blocks and fitting the GEV distribution to the maxima from each block. Figure 4 shows a sample data set from Titusville, Florida containing the precipitation maxima from blocks spanning one year.

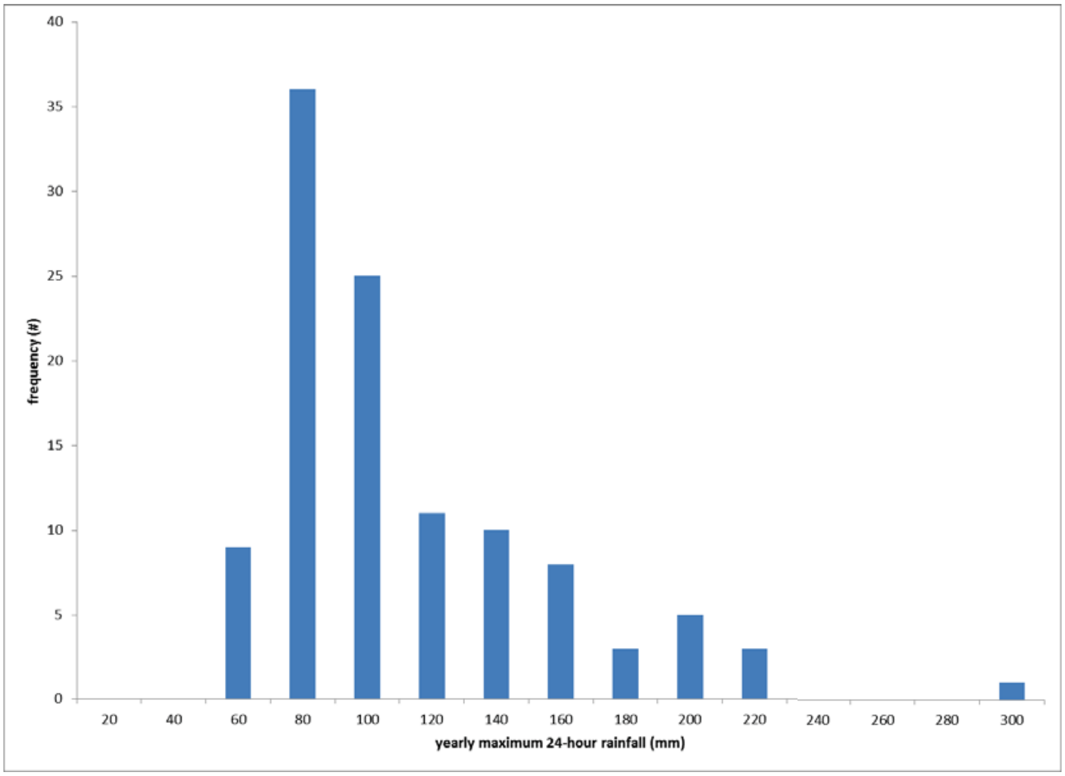

Figure 4. Frequency histogram of annual maximum 24-hour accumulated rainfall at Titusville between 1901 and 2011.

The choice of block size is very important for this analysis. If the block size is too small, the underlying theory behind the approach can be violated and lead to bias in the maximum likelihood estimation and extrapolation of the statistical model. If the block size selected is too large, few maxima will be considered when fitting the model, and lead to high variance of the model estimation. Block sizes of one year are frequently used. Yearly block sizes tend to be more robust, as smaller block sizes are likely to reveal annual variability or data dependencies, which violate the underlying theory that the sample is independent and identically distributed. If smaller blocks are used, it is likely that the greatest precipitation event would be much smaller during blocks which span the dry season than blocks which span the wet season. Failing to account for this effect could lead to inaccurate results (Coles, 2001).

The classical “block maxima” approach can be advantageous when a complete data set is not available, for example, when only the extreme values are known. However, this approach does not maximize the use of information available (in comparison to threshold models) and can be disadvantageous if a long POR is not available (Katz et al., 2005).

Threshold models. The classical GEV model and “block maxima” approach have been adapted to utilize the information available better. Another commonly used approach is the Peaks-Over-Threshold (POT) technique and Generalized Pareto Distribution (GPD). Pickands (1975) justifies the modeling of exceedances above an appropriate threshold with a GPD with cumulative distribution function as shown in Equation 2:

$$\boldsymbol{F(y;\sigma^*,\xi)} = \begin{cases} \boldsymbol{1-\left[1+\xi\left(\frac{y}{\sigma^*}\right)\right]^{-\frac{1}{\xi}}}, \\ \boldsymbol{1+\xi\left(\frac{y}{\sigma^*}\right)>0 \quad \xi \neq 0} \\ \\ \boldsymbol{1-exp\left[-\frac{y}{\sigma^*}\right] \quad \xi = 0} \end{cases} \tag{2}$$

In Equation 2, $\boldsymbol{\sigma^*}$ is the scale parameter and $\boldsymbol{\xi}$ is the shape parameter (Katz et al., 2005). This justification is also summarized by Coles (2001). The shape parameter of the GPD can be interpreted exactly as the shape parameter from the GEV distribution is interpreted, where the sign reveals the tail behavior. If $\boldsymbol{\xi > 0}$, the GPD takes on a heavy tailed Pareto (power law) distribution. If $\boldsymbol{\xi = 0}$, the GPD takes on a lightly tailed exponential distribution. If $\boldsymbol{\xi < 0}$, the GPD takes on a bounded-tail beta distribution.

These distributions are shown in Figure 5. A thick tail means that expected return levels continue to increase for longer return periods, and the cumulative distribution function slowly decreases in the tail. It is typical for rainfall frequency distributions to have thick tails. A thin or bounded tail means that return levels increase very slowly or not at all for longer return periods, and the cumulative distribution function rapidly approaches 0 in the tail. It is typical for a temperature frequency distribution to have a thin or bounded tail. Return levels and return periods are explained later in this chapter.

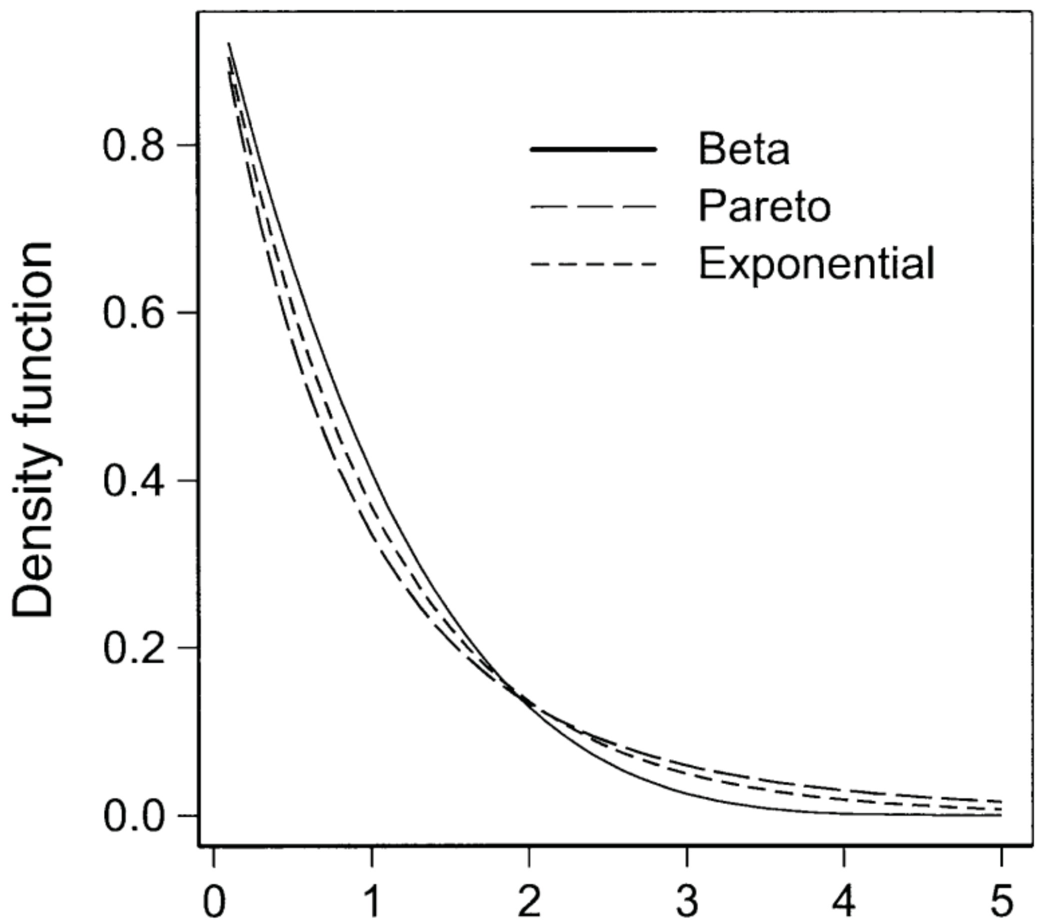

Figure 5. GPD plots with scale parameter $\boldsymbol{\sigma}^* = \mathbf{1}$, and shape parameter $\boldsymbol{\xi} = -\mathbf{0.2}$ (Beta) $\boldsymbol{\xi} = \mathbf{0}$, (exponential), and $\boldsymbol{\xi} = \mathbf{0.2}$ (Pareto). *Note*. Reprinted from Katz et al. (2005).

Threshold models optimize the use of available data but require selection of an appropriate threshold, which is analogous to selection of block size in the block-maxima approach. Selection of too small a threshold will violate the asymptotic basis of the model and lead to bias, while selection of too high a threshold will result in too few threshold exceedances for the model to be estimated, and result in high variance of the model (Coles, 2001).

Threshold selection. There are multiple techniques for threshold estimation. Scarrott and MacDonald (2012) provide a summary and review of threshold-estimation techniques. Generally, the goal of threshold estimation is to balance the bias and variance tradeoffs mentioned above (Scarrott & MacDonald, 2012). Coles (2001) highlights the most common graphical techniques used for threshold estimation. These techniques include the use of a mean residual life (MRL) plot, where mean excess of values exceeding a threshold u is plotted for a range of thresholds. An appropriate threshold can be chosen to be the lowest threshold where mean excess is approximately linear above that threshold. This technique can be very challenging to interpret and is also very subjective. Figure 6 shows how subjective this decision is, and that a *range* of thresholds may be appropriate.

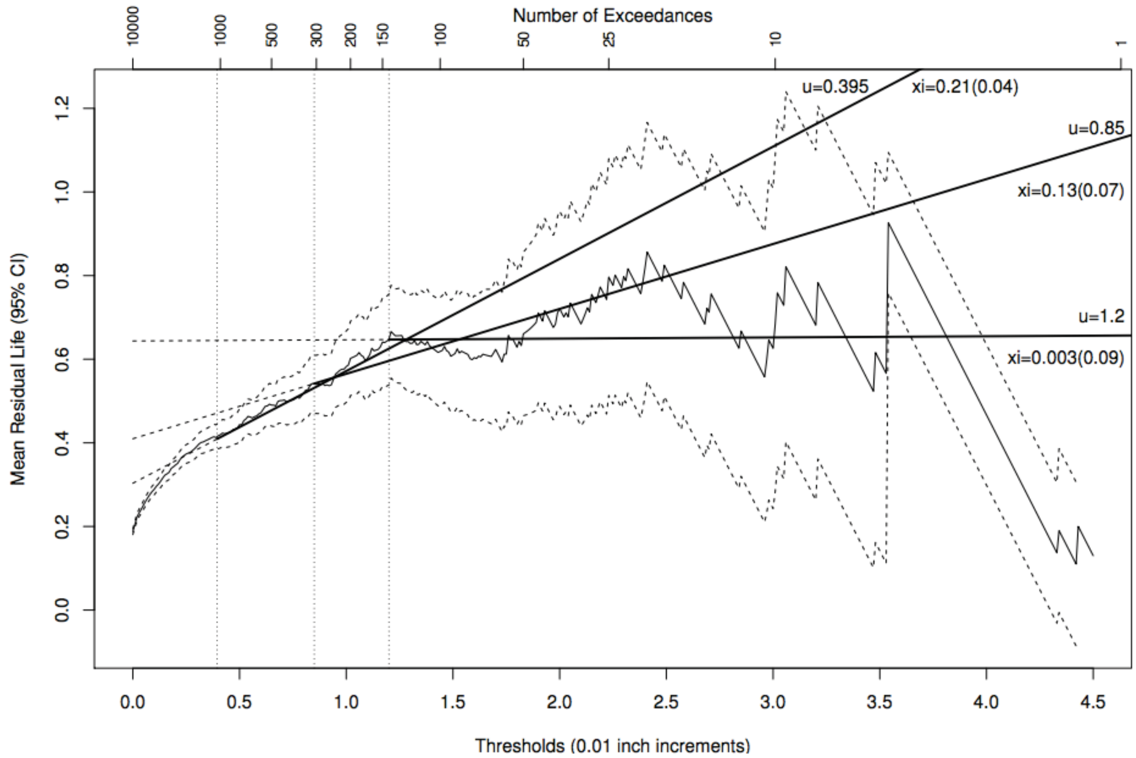

Figure 6. Mean residual life plot of Fort Collins precipitation data. *Note.* The MRL appears to be approximately linear over thresholds of u = 0.395, 0.85, and 1.2. *Note.* Reprinted from Scarrott and MacDonald (2012).

Coles (2001) shows that for a sufficiently high threshold of a distribution where the GPD is a reasonable statistical model of excess, then the GPD of excess of a higher threshold is identical. This suggests that plotting the scale and shape parameters against threshold with confidence intervals, and using the lowest threshold for which the shape parameter remains nearly constant is an appropriate method for threshold selection (Coles, 2001). This method is also very subjective. Figure 7 shows scale and shape parameter estimates of Titusville 24-hour rainfall data for a range of thresholds.

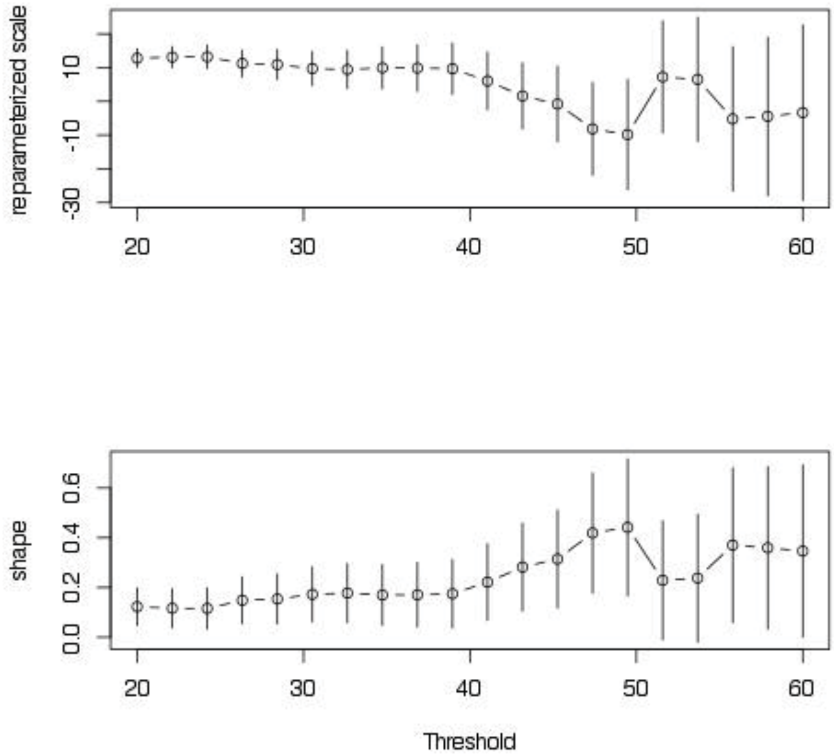

Figure 7. Scale and shape parameters plotted for thresholds of 1980 - 2011 daily precipitation data (mm) at Titusville. *Note.* The shape parameter (lower panel) remains relatively stable for thresholds less than 40 mm, suggesting 40 mm is an appropriate threshold.

Dumouchel (1983) proposes the use of the 90th percentile value of the frequency distribution as a threshold selection that is less subjective. Dumouchel uses the 90th percentile because the upper 10% is often a balance between being sufficiently low enough that an adequate number of observations exceed the threshold for reliable estimation of model parameters, and sufficiently high enough that the asymptotic rationale for the model is valid. Scarrott and MacDonald (2012) noted that this rule of thumb is “inappropriate from a theoretical viewpoint, [but is] frequently used in practice” (p. 41), because it is not subjective.

Dependencies and non-stationarity in EVA. The GEV and GPD extreme-value models are derived under the assumption that the data consists of a sequence of IID values. Often, observational data sets have temporal dependencies and may not be stationary, thus, the assumption that observational data is IID is often a poor one. For example, temperature data may not be stationary due to seasonality and trends over time (i.e., global warming). It is also typical for temperature extremes to be temporally dependent on one another, where extreme days are often followed by more extreme days. A data series may be independent, but not stationary; stationary, but not independent; or neither (Coles, 2001).

These problems can be accounted for by adapting the extreme-value model so that parameter estimates can change with time, and by declustering the series to remove dependencies of extremes. Extreme values can be assumed to be independent if they are far enough apart in time. Runs-declustering removes extreme dependencies that are within a time of length r, where r is the run length. This is done by keeping the most extreme value within the cluster and reducing the other values so they will not impact the EVA. Coles (2001) shows how the extremal index θ is the reciprocal of the average exceedances per cluster, and a series for which $\theta = 1$ means dependence is negligible. Declustering becomes another tradeoff between bias and variance as too small a run length will allow dependencies through while too high a run length will prevent values from getting through that could have been reasonably considered independent (Coles, 2001). Coles (2001) recommends relying on common sense judgment and checking the sensitivity of results to the run length.

Extremes Toolkit. The Extremes Toolkit is a software package used for analyzing extreme-value data. The package was written by National Center for Atmospheric Research (NCAR) scientists Eric Gilleland and Richard Katz to spread the use of extreme-value statistics within the atmospheric sciences. The package uses the R statistical programming language; however, knowledge of R is not necessary to use the package (Gilleland & Katz, 2006). The package provides support for using both the block-maxima and peaks-over-threshold approaches.

Return levels and return periods. The results of an EVA are usually quantified using a return level and return period. These values convey the rarity of events. A return level is a value of some variable with return period *T*, and has a *1*/*T* exceedance probability. The return period is sometimes referred to as waiting time, where on average *T* years must pass until the next occurrence of the event (Katz, n.d.). For example, if the 100-year return level is 300 mm, the expected waiting time to see a 300-mm event is 100 years, and the 300-mm event has 1/100 exceedance probability in any particular year.

Operational Applications of Return Levels

Return periods and return levels are operationally useful for engineers. They use rainfall return levels from Intensity-Duration-Frequency (IDF) plots for operational water management planning. IDF plots present return levels in a compact form for a continuous range of return periods and time durations. Technical Paper 40 (Hershfield, 1961) established initial estimates of rainfall return estimates for time durations ranging from 30 minutes to 24 hours and return periods from 1 to 100 years across the U.S. The National Oceanic and Atmospheric Administration (NOAA) Atlas 14 re-estimated return levels from Technical Paper 40 using updated, longer time series observational data. Both studies used a regional frequency analysis approach, where yearly maxima precipitation amounts were used to estimate return levels (Hershfield, 1961; NOAA Atlas 14, 2013).

Florida Rainfall Climatology

Florida receives its rainfall from four major rainfall-producing phenomena. These phenomena include local deep moist convection, extra-tropical cyclonic storms, tropical disturbances, and tropical cyclones. Local convection contributes to 33% of the yearly precipitation on average (Richards, 1927). Later researchers, including Horace (1948), Gentry (1954), and Frank (1966) found that summer air-mass showers and storms on the Florida Peninsula are caused by low-level convergence forced by sea-breeze interactions. They found the central Florida Peninsula has the highest frequency of summer storms due to the almost daily convergence of sea-breeze fronts from opposite coasts. Frank (1966) used radar data and synoptic-flow regimes to characterize shower distributions for different synoptic-flow regimes across the peninsula. Multiple automatic rainfall observing networks such as the Florida Automated Weather Network (FAWN) have been established more recently, which provide additional observational data for studying rainfall over the peninsula (Florida, n.d.).

Tropical Rainfall Measuring Mission

The Tropical Rainfall Measuring Mission (TRMM) was a joint U.S.-Japan initiative to estimate tropical rainfall amounts from space (Simpson, 1996). The TRMM ground validation program used a network of rainfall gauges and radar-derived precipitation to validate estimates made from the TRMM satellite. Rainfall from the gauge network and radar must be quality controlled before it can be used to validate satellite-based rain estimates (Wang, 2010). TRMM has a high-density rainfall observing network in the KSC coastal region. The network in the KSC region consists of 33 tipping-bucket rain gauges, which are maintained by KSC. A map of rain-gauge networks in central Florida and map of the KSC TRMM network are presented in Figures 8 and 9, respectively.

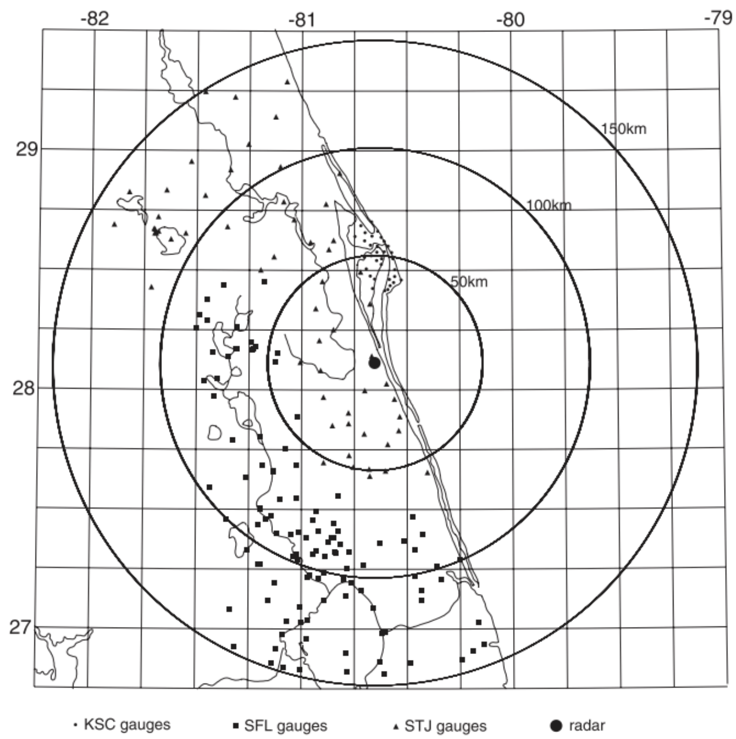

Figure 8. Central Florida map with Melbourne radar, South Florida Water Management (SFL) gauges, St. Johns River Water Management (STJ) gauges, and TRMM KSC gauges. *Note.* Reprinted from Wang (2011).

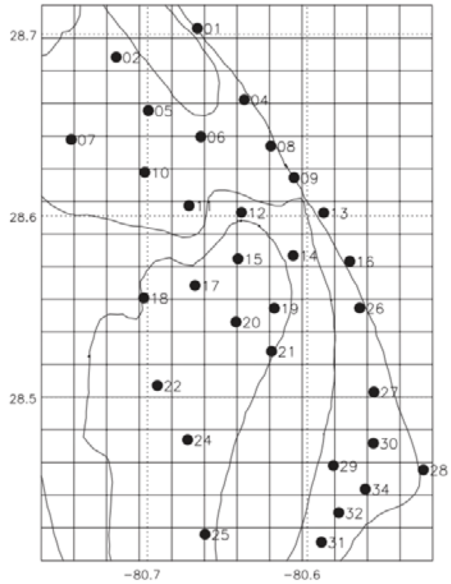

Figure 9. KSC rain gauges with gauge identification numbers. *Note.* The grid shown in this figure is not the same as the objective analysis grid used later in this paper. Reprinted from Wang (2009).

Tipping-Bucket Rainfall Gauges

Tipping-bucket rain gauges are frequently used for automatic rainfall measurements and are used by NOAA at its automated surface observing stations (ASOS). The gauges work by allowing rainfall to flow into them; once a predetermined amount of water (usually 0.254 mm, 0.01 inches) flows into them, the bucket tips and empties the water. The tipping bucket triggers a magnetic switch and records the tip. These rainfall gauges perform best when rainfall rates are light to moderate (< 5 mm/hour) and winds are calm. The gauge's accuracy falls off with a negative bias as rain rate increases (especially above 50 mm/hour) and wind speeds increase. During heavy rainfall, water can be lost between tips, and high winds can reduce the volume of rain that makes its way into the gauge. Generally, tipping-bucket rain gauges perform well at lower rainfall rates and underestimate rainfall at higher rainfall rates (Nystuen, 1999).

One could also assume that gauges may occasionally malfunction or get clogged. A clogged or malfunctioning gauge will most likely report null precipitation values or values significantly lower than the actual rainfall occurrence. In cases where a gauge malfunctions and over-reports, it will usually be obvious.

Summary

Extreme-value statistics and the Extremes Toolkit can be used to model tail behavior of the rainfall frequency distribution at locations such as KSC. Threshold-exceedance models such as the GPD maximize the use of available data and are more viable than the "block-maxima" approach when long periods of data are not available. However, threshold-exceedance models are sensitive to threshold selection. Too large a threshold will result in high variance within the model, and too low a threshold will result in model bias. Therefore, threshold choice should be carefully considered. Graphical tools such as the MRL plot can help with threshold selection, however, there is subjectivity involved in making a threshold selection. A sensitivity analysis can be used to exclude thresholds that would not produce relatively stable results.

An EVA assumes the data is independent and stationary. In cases where data is not stationary due to the nature of the variable, the non-stationarity can be accounted for by adapting the model so that parameter estimates can change in time. In cases where temporal dependencies exist (e.g., extreme temperatures), declustering can remove the dependencies of the extreme values.

The resulting probabilities of occurrence from EVA are expressed as return levels for given return periods. Rainfall return levels are used by engineers and planners for operational decision making. This is especially important for low-lying areas that are prone to flooding during extreme rainfall events.

The resulting shape parameter estimate from an EVA is a best estimate of how thick the extreme tail of the distribution is. Shape-parameter estimates greater than 0 ($\boldsymbol{\xi > 0}$) indicate the frequency distribution has a thick tail and that return levels will continue to increase at high return periods. A shape parameter around or less than zero ($\boldsymbol{\xi = 0}$, $\boldsymbol{\xi < 0}$) indicates the tail is thin or bounded, respectively. This means that the return level will approach a maximum and will no longer increase at very high return periods. A thick tail is often a characteristic of rainfall frequency distributions, while temperature frequency distributions typically have bounded or very light tails.

A large amount of Florida's precipitation comes from local deep moist convection. Convection over the peninsula is caused by low-level convergence, often forced by sea-breeze interactions. Local convection often results in significant geographic variations in rainfall accumulations. The state has multiple rainfall-observing networks, including TRMM and FAWN, which can be used to study precipitation-frequency intensity and duration. The TRMM KSC network consists of 33 tipping-bucket rain gauges that are maintained by KSC. Gauges occasionally malfunction or may get jammed or clogged, which most often results in null precipitation value or values significantly lower than the actual rainfall. Failures over longer periods (i.e., > 2 weeks) are easy to identify and remove, however, failures over short time periods are not. Additionally, it is common for tipping-bucket rain gauges to underreport rainfall amounts during heavy rainfall, especially at rates greater than 50 mm/hour.

Chapter III

Methodology

Daily rainfall totals from the KSC TRMM network were quantitatively analyzed using statistical methods. Extreme-value statistics and descriptive statistics were used to estimate return periods and describe the data.

Research Approach

This descriptive study utilized extreme-value statistics to characterize the likelihood of rare rainfall events in the KSC coastal region. A 15-year POR of daily rainfall totals from 33 tipping-bucket rain gauges was quantitatively analyzed using statistical methods. The Extremes Toolkit from NCAR was used to perform extreme-value analyses of the data.

Apparatus and Materials

This study utilized multiple software tools. The Extremes Toolkit facilitates modeling extreme values using the GEV and GPD extreme-value models (Gilleland & Katz, 2011). The General Meteorology Package (GEMPAK) was used for data visualization and gridding (Unidata, n.d.). GEMPAK is often used for displaying weather-model data and for gridding non-uniform observations. Microsoft Excel® was also used as a multipurpose statistical and visualization tool.

Population/Sample

The data sample consisted of daily rainfall amounts recorded between 1998 and 2012 from 33 rain gauges in the KSC region. The sample represents the daily rainfall that fell in the region. Due to rain gauge under-capture from winds and heavy precipitation, a slight negative bias is expected. The researcher assumed gauge data were ground-truth measurements since the bias is not easy to estimate.

Sources of the Data

Rainfall data was acquired through the data-access section of the TRMM website. Daily rainfall totals from the KSC network were loaded into Microsoft Excel for data visualization. The URL location where data was acquired is available at TRMM GV Gauge Quick Look Products (n.d.). The TRMM website notes that null precipitation events are not differentiated from missing data, and that gaps in the POR can be assumed to usually be periods of non-precipitation. They also note that long periods of missing data should be questioned. It was observed that in many cases, individual gauges reported long periods of null precipitation values while nearby gauges reported multiple days with precipitation. These periods are also in question. Periods from some gauges were removed due to unreliability as noted by the TRMM website, however, many gauges reported multiple shorter periods which also appeared to be unreliable.

Data Collection Device

Tipping-bucket rain gauges from the TRMM network measured rainfall over the POR. Information on tipping-bucket rain gauges was provided in Chapter II.

Instrument reliability. It was assumed that all rainfall gauges were properly calibrated and reliable. If gauges were not reliable, they were most likely removed from the data set during quality control. Quality control is addressed later in this chapter.

Instrument validity. It was assumed that instrument validity is strong and that gauges measured rainfall accurately. This validity assumption is based on the fact that gauges are located in appropriate locations and are not near trees or structures that interfere with rainfall collection.

Treatment of the Data

Long periods of unreliability. An objective quality control method was needed to remove gauge observation data that was unlikely to represent the true occurrence on that day. Some longer periods of unreliability were noted by the TRMM website. These periods of unreliability were also observed by the researcher and removed from the data record. Gauge observation data from gauge 2 was removed from January 1998 through September 1999. Gauge 26 was completely removed. Gauge 9 observations were removed for the whole 1999 calendar year. The locations of these gauges were shown in Figure 9. Although these long periods of unreliable data were removed, the researcher observed many shorter periods of suspicious data.

Quality control. Each gauge within the 33-gauge network is on average 3 km from its nearest neighboring gauge. There are on average 11.7 neighboring gauges within 10 km of any single gauge. Based on the close proximity of gauges, an internal-quality control method was used. This was done by comparing nearby gauges within the network and removing gauge observations that were unlikely to represent the true occurrence.

One of the main problems with the data was the presence of a 0 for null or missing precipitation event where multiple nearby gauges reported precipitation. This meant the researcher could not use all surrounding gauges to check if the value at a gauge location is valid. Due to this problem, the researcher made the assumption that at least half of the observations within 10 km of any gauge location were operating properly, and were representative of the true rainfall occurrence at the gauge location. The researcher also assumed that in most cases, if the gauge observation was misrepresentative of the true occurrence, the gauge observation was lower than the true occurrence, and therefore lower than the majority of surrounding gauge observations. This does not mean that observed values lower than the surrounding gauges are misrepresentative, however, it allowed the researcher to identify a set of neighboring gauge observations which could be compared with the gauge observation of interest.

Based on these assumptions, the median value of gauges within a 10-km radius of any gauge could be a reasonable estimate of the true rainfall occurrence at the gauge location. The median value is a reasonable estimate because it will nearly always be a good representation of the true occurrence near the gauge location on that day. The researcher removed the gauge observation if it was less than 80% of the median value of the neighboring gauges, because it was considerably lower than the reasonable estimate for the true occurrence. The statements below describe the logic of this process:

Let $\mathrm{GOV_i}$ = the gauge observation value at the location, i
Let S_i = the set of gauge observation values within 10 km of i
Let $\mathrm{Mdn_i}$ = the median of S_i

$$\text{Remove } \mathrm{GOV_i} \text{ if } \mathrm{GOV_i} < 0.8\mathrm{Mdn_i}, \text{ for all } i \tag{3}$$

Statement (3) removes $\mathrm{GOV_i}$ when it is less than 80% of the median of surrounding gauge observations.

Due to the chance of high spatial variability in precipitation, an additional check was performed to determine if $\mathrm{GOV_i}$ may have been unusually lower than the median of surrounding gauges *because of high spatial variability on that day*. If $\mathrm{GOV_i}$ was within one standard deviation of the set of values greater than 80% of the median, then it was assumed there was sufficiently high variance in the values to justify re-introduction of GOV_i to the data set. The statements below describe this process.

Let N_i = the new set of observed values within 10 km of the location, *i*.
Let M_i = the mean of N_i
Let SD_i = the standard deviation of N_i

Re-introduce GOV_i if $GOV_i \geq M_i - SD_i$, for all *i* (4)

Statement (4) re-introduces GOV_i when it is within one standard deviation of surrounding gauge observations. The new set of observed values (N_i) does not change as data is re-introduced.

EVA sensitivities. EVA is highly sensitive to the largest values within the POR. Analyzing a time series with large numbers of missing values could result in bias due to missing values on days when it is probable that the location received heavy rainfall. Due to this potential bias, the rainfall gauge data was analyzed onto an evenly spaced grid in order to produce a continuous time series without missing values. This process is known as an objective analysis and involves interpolating irregularly spaced data to fixed grid locations (Koch, desJardin, & Kocin, 1983).

Data gridding. The Barnes objective analysis scheme used for the objective analysis applies Gaussian weighting of observations to grid points. Observations closer to the grid point have more weight, and therefore greater influence on the grid value. Observations that are far from the grid point carry significantly less weight and have less influence on the grid value (Koch et al., 1983). Missing data does not pose a problem to the gridded analysis, because valid data from nearby gauges is used to compute the rainfall values at the grid-point locations.

While gridding the data produces a continuous data series by using surrounding gauge observations to interpolate observational values to grid locations, gridding results in data smoothing, where the maximum-value observations are reduced and minima are increased. These effects can introduce bias into analyses performed, and are of particular concern due to the objective of the study. These biasing effects were minimized by using minimal smoothing while performing the gridded objective analysis. This means the observations closer to any grid point will have a stronger influence at the grid point than if greater smoothing was used. Minimal smoothing preserves the maxima and minima within the observational data. This is very important due to the sensitivity of an EVA to small changes in the extreme values themselves.

For this gridded analysis, the researcher let GEMPAK select an appropriate grid spacing based on the number of observations and their distance spread. GEMPAK recommended using a grid spacing of 0.03 degrees (approximately 3.3 km). The analysis grid covers a 35 by 35 km area and can be seen in Figure 10.

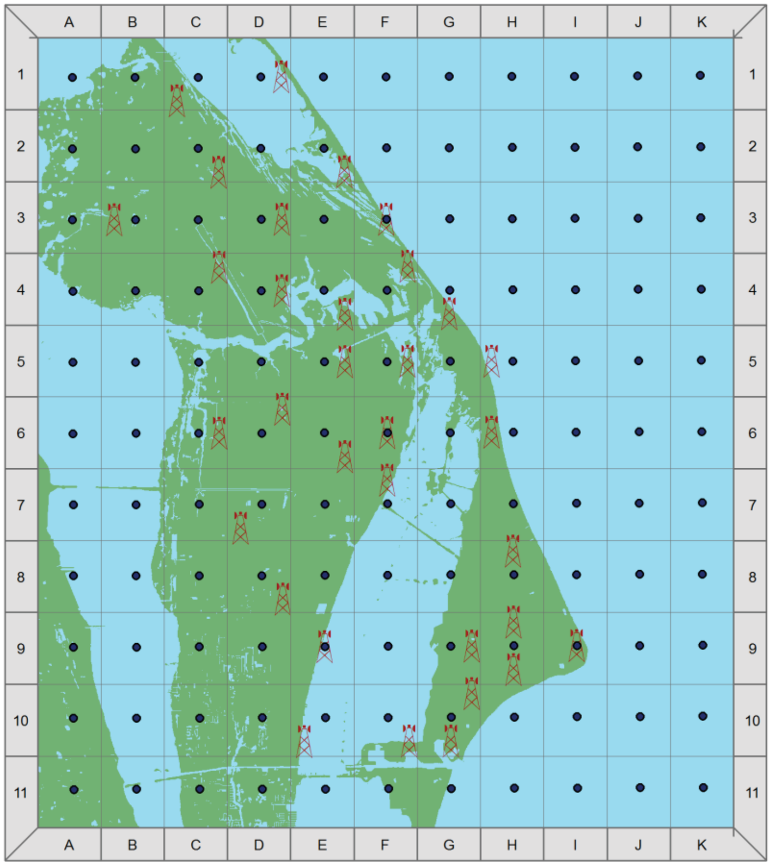

Figure 10. Rainfall objective analysis domain *Note.* Blue dots represent the grid locations and are indexed by horizontal and vertical axis coordinates. The centers of the red towers represent observation sites with tipping-bucket rain gauges.

Grid point population. As a further means of quality control, grid points were populated only if three or more gauge observations were available within the search radius. In the Barnes objective analysis, minimizing smoothing (i.e., the convergence parameter, gamma) consequentially reduces the search radius. Therefore, in some cases where an insufficient number of observations (< 3) lay within the search radius, smoothing (gamma) was increased for the purpose of populating those grid points. The first objective analysis (gamma = .03) populated every grid point using observations within 10 km, and the second objective analysis (gamma = .05) populated grid points using observations within 17 km. Grid points from the second analysis were only used if they were not populated by the first analysis. It should be noted that the resulting gridded data set is a transformation and should be considered “once removed” from the original observational gauge data. As a final quality control measure, the researcher decided to use grid points in the EVA calculations only if gauge observations lie within the grid box or on opposite sides of the grid box. Figure 11 shows the grid points whose values were utilized in this study.

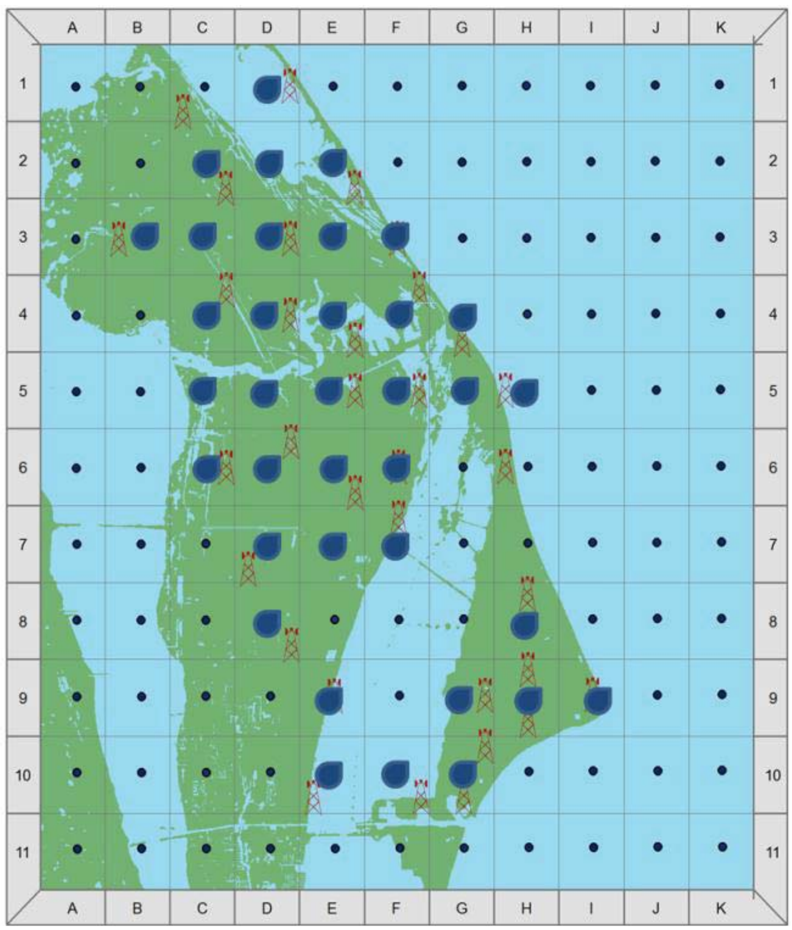

Figure 11. Rainfall analysis domain, with blue dots representing grid locations indexed by horizontal and vertical axis coordinates. *Note.* Blue teardrops are grid locations used in the actual EVA. Red towers represent observation sites with tipping-bucket rain gauges.

Note from Figure 11 that grid cell 6H was not included because rain gauge 26 was removed. Grid cell 1C was not included because the point was not fully populated by the gridded analyses.

Comparing gridded data with the longer POR from Titusville ASOS. The upper tail (72-hour rainfall values above 50 mm) of the gridded data distribution was declustered (threshold = 50, $r = 3$), standardized, plotted, and compared to the standardized upper-tail data from the Titusville ASOS between 1980 and 2011. The 72-hour duration events were used to capture shorter- and longer-period extreme events. The daily measuring times for the two sets of data are different, and examining longer-duration extremes will minimize effects from the different daily measuring times. A tail histogram was produced for each data set to compare the tail shape and occurrence frequency of the extreme events visually. Table 1 contains the standardized data used to plot the standardized rainfall frequency histograms in Figure 12.

Table 1

Tail Histogram Data

Top of Bin (mm)	Standardized Gridded Freq. (year^{-1})	Standardized Titusville Freq. (year^{-1})
100	4.778	4.875
150	0.887	0.969
200	0.169	0.188
250	0.093	0.094
300	0.065	0.000
350	0.026	0.031
400	0.014	0.000
450	0.008	0.000
500	0.008	0.000
550	0.006	0.000
600	0.004	0.000

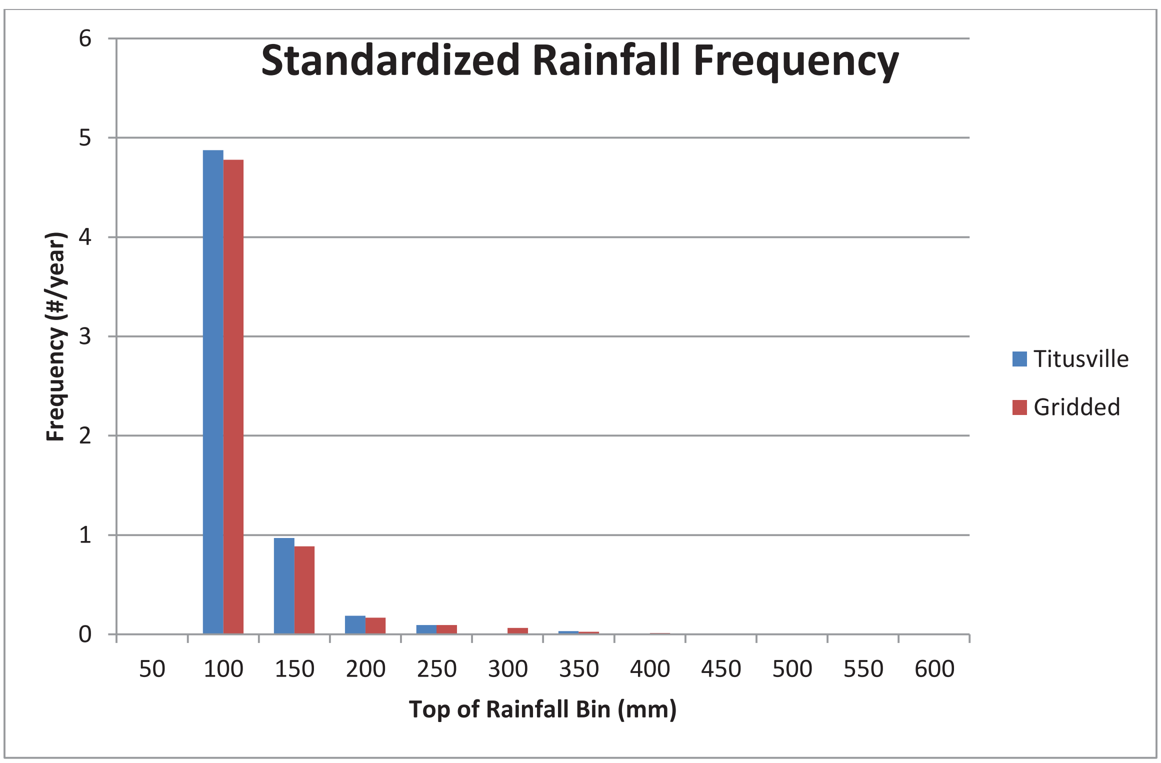

Figure 12. Standardized rainfall frequency histogram of tail data at Titusville ASOS and grid locations.

The gridded data distribution's tail was found to be very similar to that from the 32-year POR from the Titusville ASOS. This gives the researcher confidence that gridding the observed values did not considerably change the tail shape, and that the 15-year POR is not very different from the longer 32-year POR.

EVA of Titusville ASOS and Gridded Domain Data

An EVA was performed on the 24-hour data and 72-hour data for all months, and 72-hour data during the wet (May – October) and dry (November – April) seasons by fitting exceedances above a sufficiently high threshold with a GPD. This approach required that an appropriate threshold be selected. The months of May through October were chosen to define the wet season in order to ensure that extreme rainfall events near the beginning and end of the "official" wet season (May 28 – October 17) were not included in the dry season (Lascody, 2002).

Threshold selection. An EVA is sensitive to threshold selection. If the threshold is too small, a bias will be introduced. If the threshold is too large, too few exceedances will exist for the model parameter estimation, and high variance is introduced into the model. For the purpose of this study, where a separate EVA was performed for each grid location, an objective method for threshold selection was sought.

24-hour threshold selection. As stated in Chapter II, DuMouchel (1983) proposed that the 90th percentile is often an acceptable threshold. In this case, rainfall greater than 0.01 inches occurred on 30% of the days and the 90th percentile of all days was 13 mm. This value was not a sufficiently high threshold according to the subjective graphical tools that Coles (2001) proposes for threshold selection. Figure 13 shows that the shape parameter remains relatively stable at thresholds greater than 13 mm, therefore, the 13-mm threshold is too small. Figure 14 also shows that mean excess does not appear to be approximately linear above 13 mm.

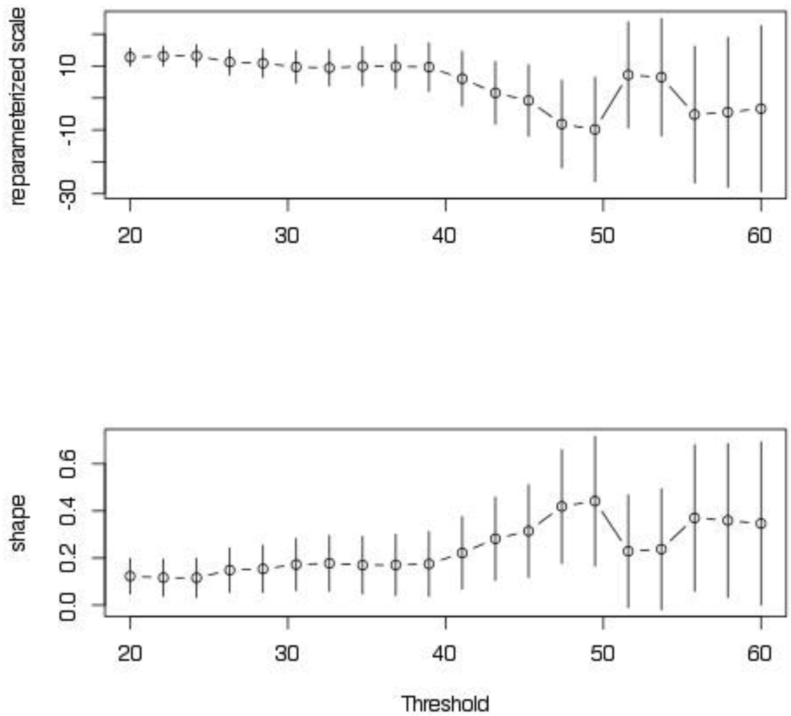

Figure 13. Scale and shape parameters plotted for thresholds of daily precipitation at grid point 7E (mm). *Note.* The shape parameter remains relatively stable for thresholds less than 35 mm, suggesting 35 mm is an appropriate threshold.

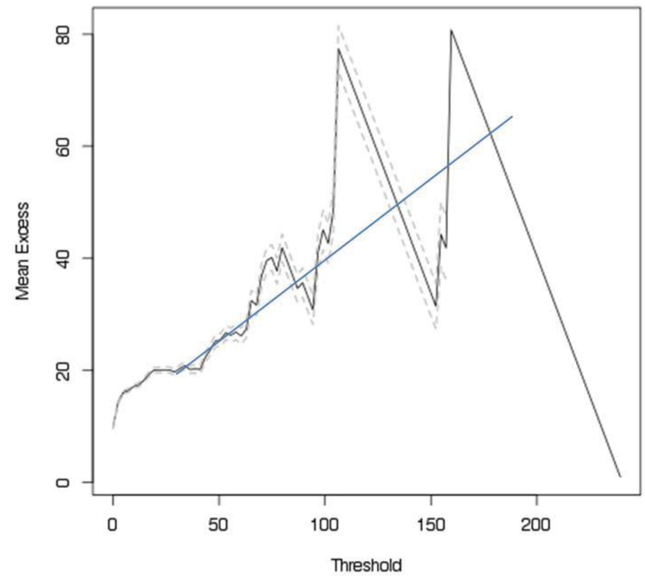

Figure 14. Mean residual life plot of daily precipitation data (mm) from grid point 7E. *Note.* Solid black line is mean excess. Dashed lines are 95% confidence bounds. It appears as if mean excess is approximately linear above a threshold of 35 mm. The blue line is drawn by the researcher to show how the mean excess is approximately linear above 35 mm (compare with Fort Collins example shown in Figure 6).

The 98th percentile amount of 35 mm was found to be appropriate after fitting the data to a GPD over a range of thresholds and plotting a mean residual life plot. This threshold was used for all grid locations and was found to be reasonably appropriate for the gridded locations according to these subjective graphical tools. Since threshold selection is subjective, 25-mm and 30-mm thresholds were also tested.

72-hour threshold selection. The 72-hour rainfall data values are highly dependent on values from previous days, and data declustering was necessary in order to remove the temporal dependencies. The extremal index suggested declustering the data using a run length of $r = 3$, therefore the data was declustered using a threshold of 45 mm and run length of 3. The threshold of 45 mm was found to be appropriate for the EVA.

Additionally, 40-mm and 50-mm thresholds were also tested.

72-hour threshold selection for dry and wet seasons. Declustering was performed using runs declustering and a run length of $r = 3$ for the dry and wet seasons. The same 45-mm threshold was found to be appropriate for the wet season; however, the smaller 25-mm threshold was more appropriate for the dry season. Additionally, 20-mm and 30-mm thresholds were tested for the dry season, and 40-mm and 50-mm thresholds were tested for the wet season.

EVA Performed

Numerous extreme-value analyses were performed on the gridded and longer period observational data from Titusville. See Table 2 for a summary of the analyses performed. Each analysis was done using multiple thresholds to check for stability about that threshold. Recall that lower thresholds are more likely to result in model bias while higher thresholds may have high model variance.

Table 2

EVA Performed Using a GPD to Model Threshold Excess

Data	Season	Duration (hours)	Threshold (mm)	Declustering Run (days)
Titusville	Dry	72	25	3
		72	30	3
		72	35	3
	Wet	72	70	3
		72	80	3
		72	90	3
		72	100	3
	Year	72	70	3
		72	80	3
		72	90	3
		72	100	3
		24	35	0
		24	40	0
		24	45	0
Gridded	Dry	72	20	3
		72	25	3
		72	30	3
	Wet	72	40	3
		72	45	3
		72	50	3
	Year	72	40	3
		72	45	3
		72	50	3
		24	25	0
		24	30	0
		24	35	0

The thresholds for the Titusville analyses were picked independently from the gridded analysis thresholds. Larger thresholds were more appropriate for the Titusville time series because sufficient data existed above the higher thresholds, and they appear to balance the bias and variance tradeoffs mentioned in Chapter 2. Again, multiple analyses were performed across multiple thresholds because threshold selection is subjective.

Descriptive Statistics. Descriptive statistics were computed on the observational (Titusville) and gridded rainfall data. Descriptive statistics were also computed on results from the EVA. These statistics describe the location (mean) and spread (standard deviation) of the return-level estimates.

Chapter IV

Results and Discussion

The results from extreme-value analyses of the 32-year Titusville ASOS data record and 15-year gridded data record are described in this section.

Titusville 24-hour Duration Rainfall

Figure 15 shows the resulting return levels from the analysis of the 24-hour data at Titusville for thresholds of u = 35, 40, and 45 mm. The 100-year return level estimates were 240, 243, and 294 mm, respectively. Figure 16 displays the uncertainty around the 100-year return-level estimates, and shows that for the 45-mm threshold, the 95% confidence interval of the 100-year return-level ranges from 133 mm to 456 mm. Figure 17 shows quality-of-fit diagnostic plots, which describe how well the estimated models fit the empirical data.

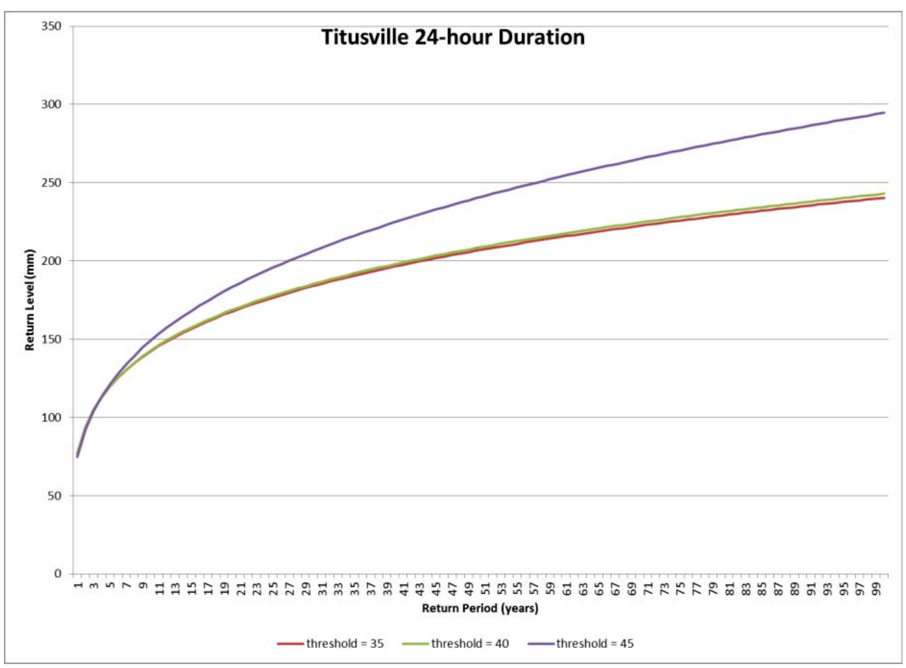

Figure 15. Titusville 24-hour duration return-level estimates plotted for thresholds of 35 mm, 40 mm, and 45 mm.

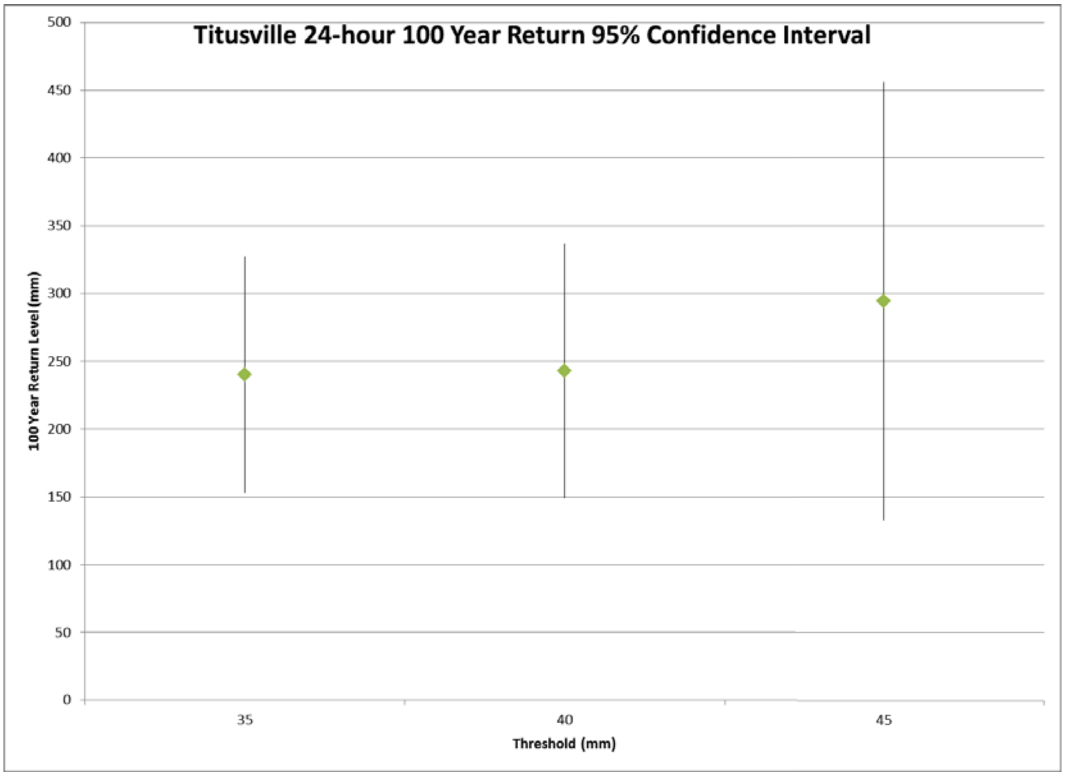

Figure 16. Titusville 24-hour 100-year return level estimates and 95% confidence intervals plotted for thresholds of 35 mm, 40 mm, and 45 mm.

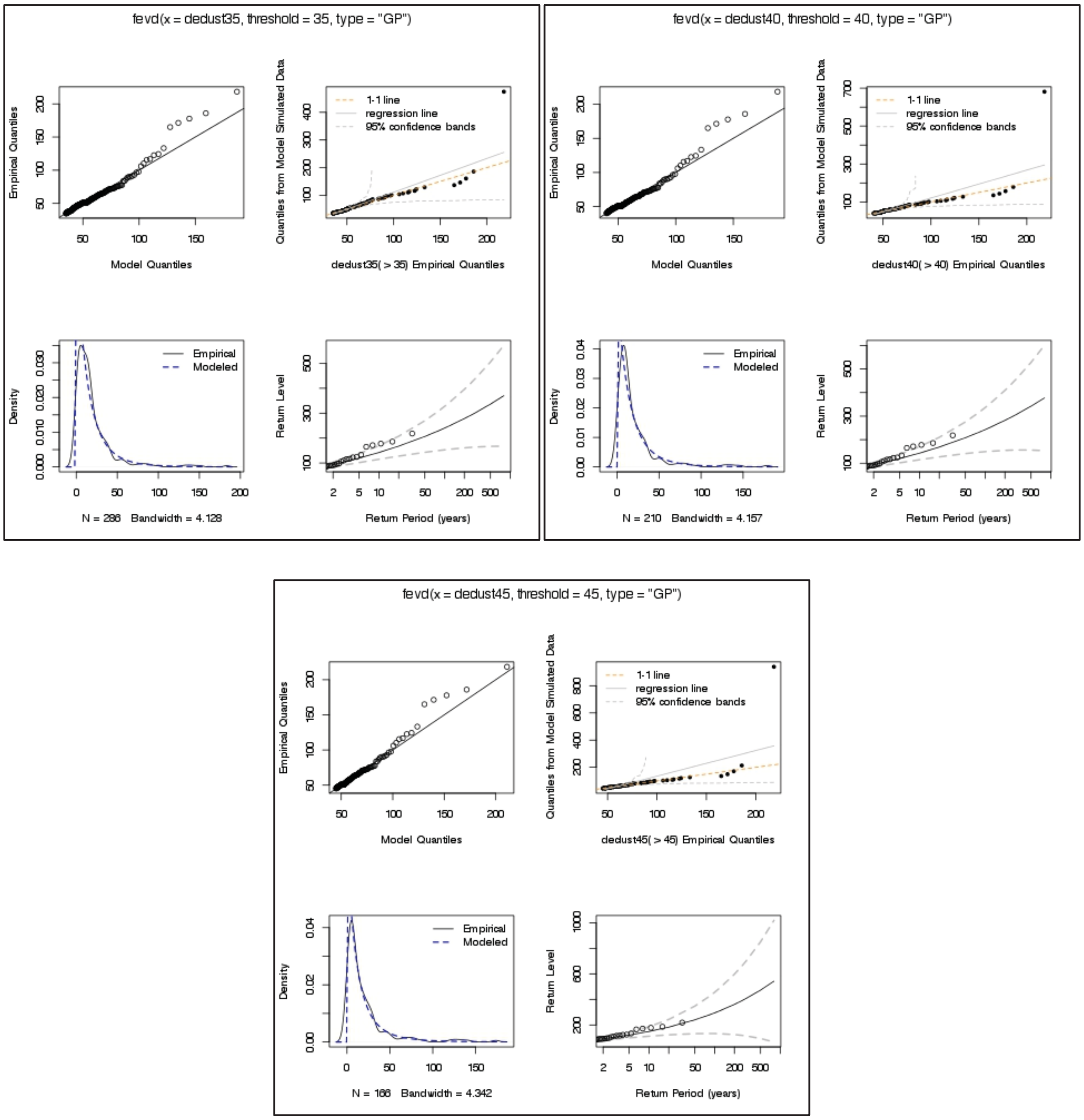

Figure 17. Diagnostic plots of GPD fit of Titusville 24-hour precipitation data for thresholds of 35 mm (top left panel), 40 mm (top right panel), and 45 mm (bottom panel). *Note.* Each diagnostic plot panel contains a quantile plot (top left), probability plot (top right), density plot (bottom left), and return-level plot (bottom right).

According to the diagnostic plots, it appears that the model may be underestimating the longer-period return levels for thresholds of 35 and 40 mm (compare return-level plots in Figure 17). Note that the model estimate performs best for longer return periods in the return-level plots in the 45-mm threshold analysis. This suggests that the 45-mm threshold analysis may be most realistic; however, the entire 95% confidence interval does not appear to be realistic. The low-end estimate of 133 mm is not a realistic 100-year return level, however, the upper-end estimate of 456 mm may be reasonable. The researcher believes that the models with lower thresholds may have a slight negative bias, and that the 45-mm threshold may be more accurate at longer return periods.

Figure 18 displays the shape parameter estimates and their 95% confidence intervals. The shape estimates and confidence intervals from all three threshold-value models suggest that the most probable shape parameter is around 0.2. This means the frequency distribution has a thick tail (Fréchet type; recall Figure 3). Note that by observing the modeled return-level estimates in Figure 15, the return level continues to increase at a considerable rate for longer return periods (50 – 100 years) for all thresholds. This also indicates that the statistical models suggest the frequency distribution has a thick tail ($\xi > 0$). If the statistical models had shown return levels increasing at very slow rates or not at all for longer return periods (50 – 100 years), then the models would suggest that the frequency distribution has a very light or bounded tail ($\xi \leq 0$).

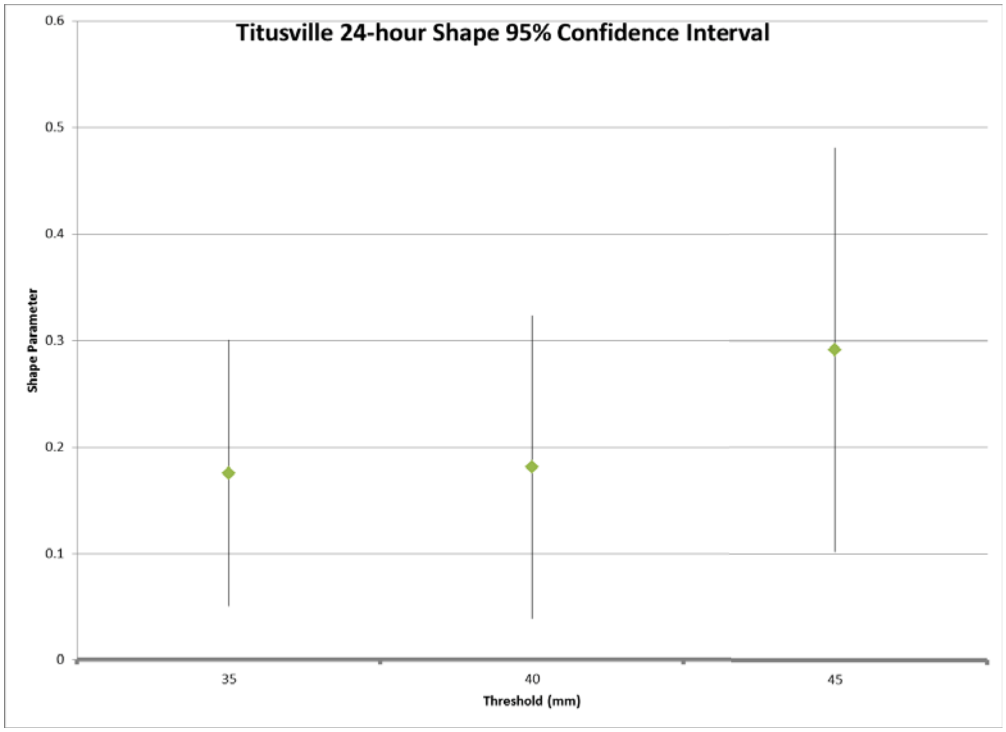

Figure 18. Titusville 24-hour shape estimates and 95% confidence intervals plotted for thresholds of 35 mm, 40 mm, and 45 mm.

Gridded 24-hour Duration Rainfall

Figure 19 shows the resulting return levels from the analysis of the 24-hour data at each of 36 grid locations for thresholds of u = 25, 30, 35 mm, respectively.

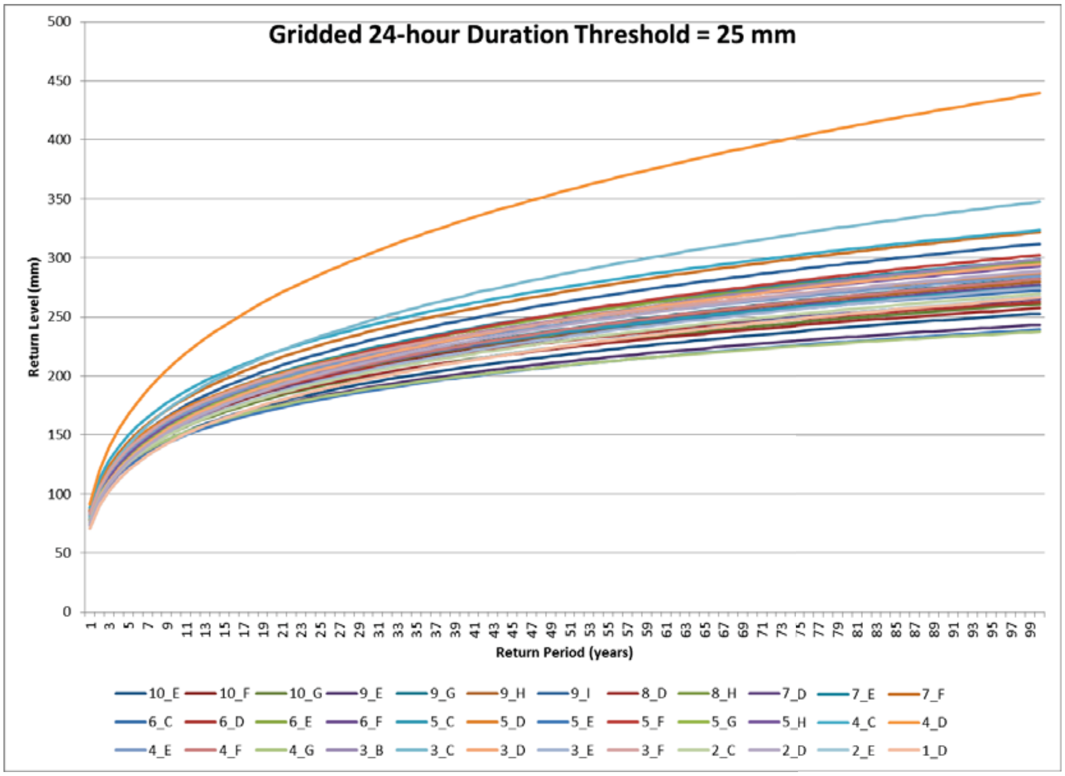
Gridded 24-hour Duration Threshold = 25 mm
Return Level (mm)
Return Period (years)
10_E 10_F 10_G 9_E 9_G 9_H 9_I 8_D 8_H 7_D 7_E 7_F
6_C 6_D 6_E 6_F 5_C 5_D 5_E 5_F 5_G 5_H 4_C 4_D
4_E 4_F 4_G 3_B 3_C 3_D 3_E 3_F 2_C 2_D 2_E 1_D

a

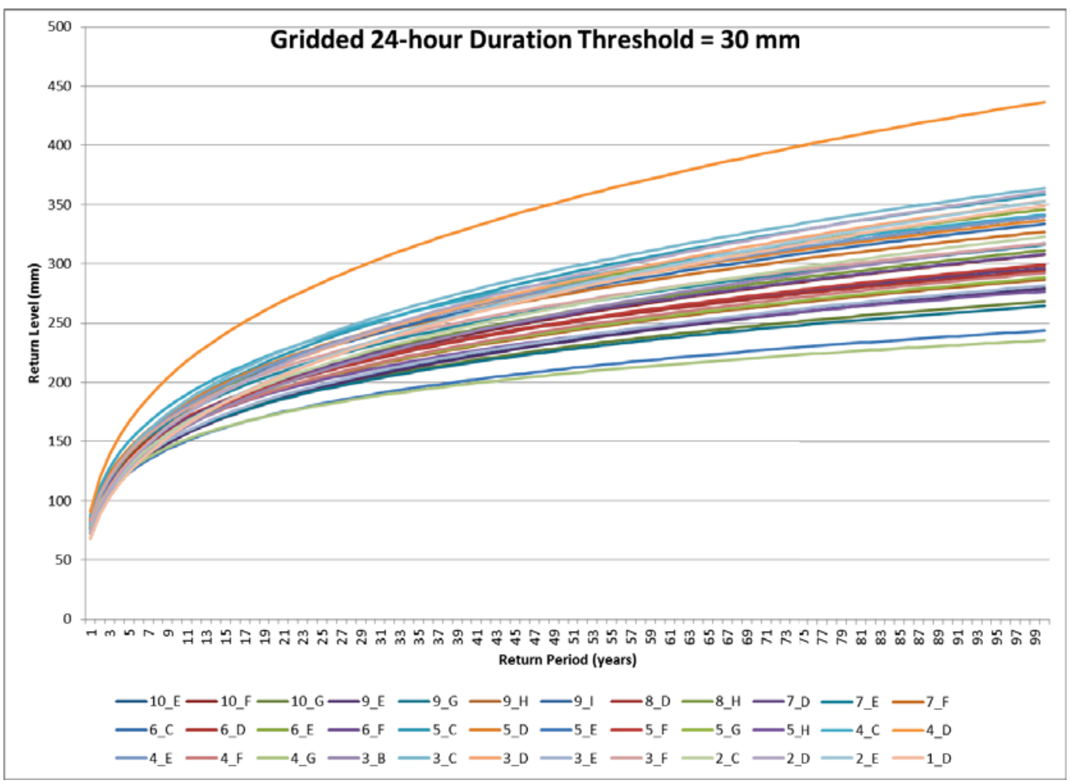
Gridded 24-hour Duration Threshold = 30 mm
Return Level (mm)
Return Period (years)
10_E 10_F 10_G 9_E 9_G 9_H 9_I 8_D 8_H 7_D 7_E 7_F
6_C 6_D 6_E 6_F 5_C 5_D 5_E 5_F 5_G 5_H 4_C 4_D
4_E 4_F 4_G 3_B 3_C 3_D 3_E 3_F 2_C 2_D 2_E 1_D

b

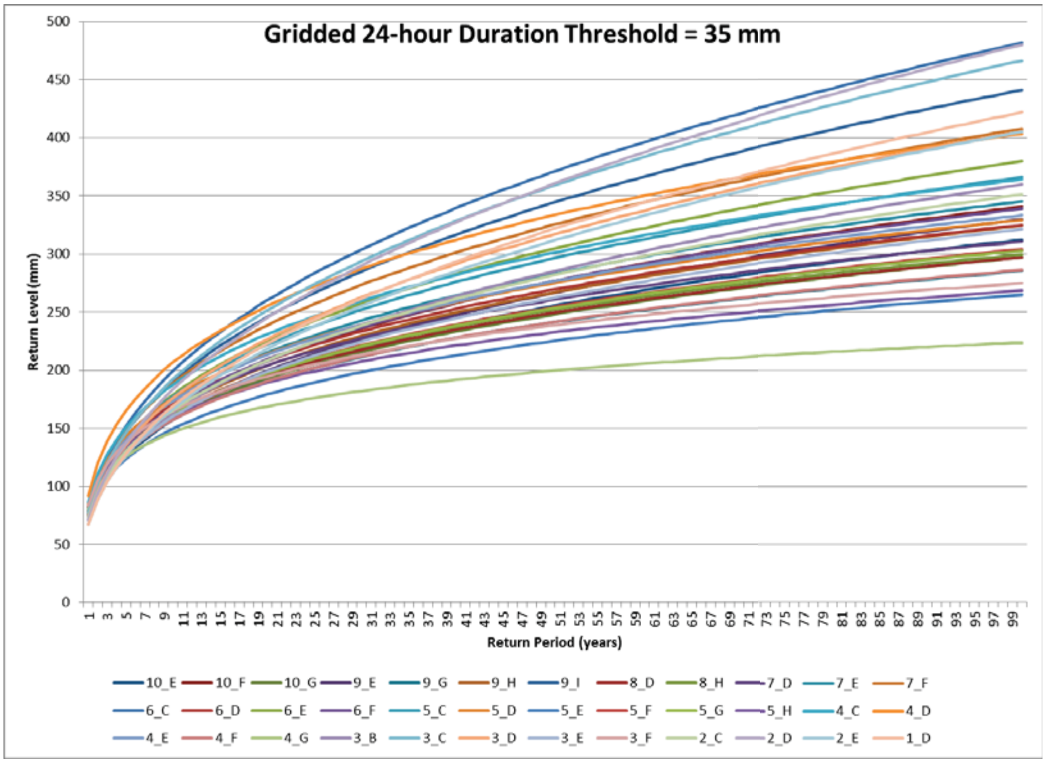

c

Figure 19. Gridded 24-hour duration return-level estimates plotted for thresholds of 25 mm (a), 30 mm (b), and 35 mm (c).

Note that in Figure 19, the return-level estimates are generally increasing with the threshold. Most of the 100-year return levels from the 25-mm threshold analysis range from around 240 mm to 350 mm, while they range from 260 mm to 475 mm in the 35-mm threshold analysis. The researcher also notes that the spread of the model returns increases with the threshold. The results lead the researcher to believe that the 25-mm threshold may have a slight negative bias, based on examining the model diagnostic plots (specifically, the return level plots in Appendix B, pages 119 - 127). Note that higher variance within the individual models due to low numbers of threshold exceedances results in larger spread of the estimates for the 35-mm threshold (Figure 19c). Although there is greater spread, the researcher is not discounting the estimates from the 35-mm threshold analysis. The quality-of-fit diagnostic plots show that at many grid points, the empirical data supports the estimates (e.g., grid locations 10F, 9I, 6C, 4F, 3B in Appendix B, pages 137 - 144). It is also very possible that rainfall return levels at individual grid points are naturally variable due to the geographically diverse domain. Overall, the researcher believes that the estimates from the 30-mm threshold analysis are most probable because an appropriate threshold balance is met and the return levels appear to be reasonable based on the quality-of-fit diagnostic plots (located in Appendix B) and longer-period Titusville estimates in Figure 15.

Another way to examine the statistical model results over the gridded domain is by calculating the model means and standard deviations for thresholds of u = 25, 30, and 35 mm (Table 3). The researcher believes that the 30-mm threshold models and 30-mm consensus strongly reflect the 24-hour regional return level based on the quality-of-fit diagnostic plots in Appendix B, strong model grouping in Figure 19b, consistency with the Titusville return-level estimates from the 45-mm threshold (Figure 15), and with NOAA Atlas 14 (2013) 100-year return-level estimates (335 mm at Titusville). However, one could expect some parts of the region to have higher return levels and others to have lower return levels.

Table 3

Consensus and Standard Deviations of 100-Year Return Level Estimates of 24-hour Rainfall Data from Gridded Locations

Threshold (mm)	100-year estimate consensus (mean; mm)	100-year estimate standard deviation (mm)
25	286.24	35.31
30	315.20	39.38
35	346.53	62.88

Titusville 72-hour Duration Rainfall

Figure 20 shows the resulting return levels from the analysis of the 72-hour data at Titusville for thresholds of u = 70, 80, 90, and 100 mm. The 100-year return level estimates were 339, 366, 350, and 361 mm, respectively. Figure 21 displays the uncertainty around the 100-year return level estimates, and shows that the 95% confidence interval ranges vary from between 184 and 495 mm for the 70-mm threshold, to between 130 and 592 mm for the 100-mm threshold. Figure 22 displays quality-of-fit diagnostic plots, which describe how well the estimated models fit the empirical data.

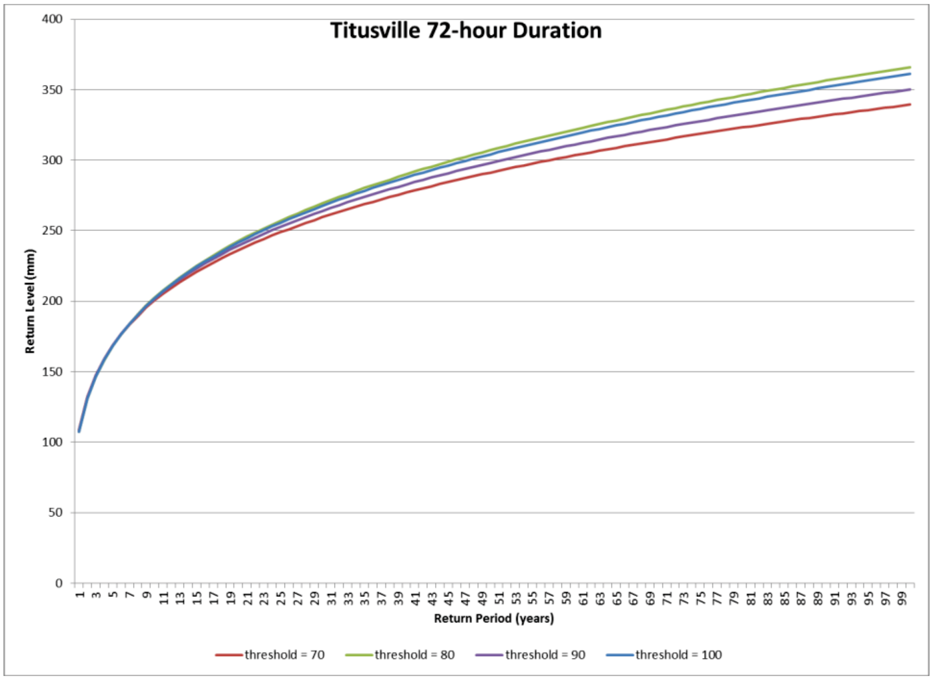

Figure 20. Titusville 72-hour-duration return-level estimates plotted for thresholds of 70 mm, 80 mm, 90 mm, and 100 mm.

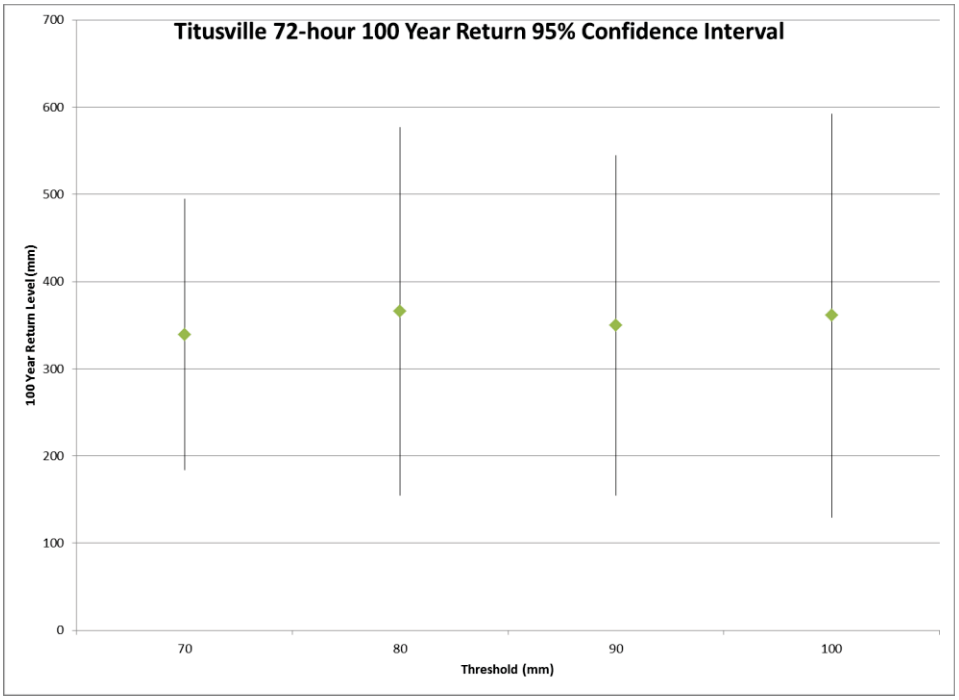

Figure 21. Titusville 72-hour 100-year return-level estimates and 95% confidence intervals plotted for thresholds of 70 mm, 80 mm, 90 mm, and 100 mm.

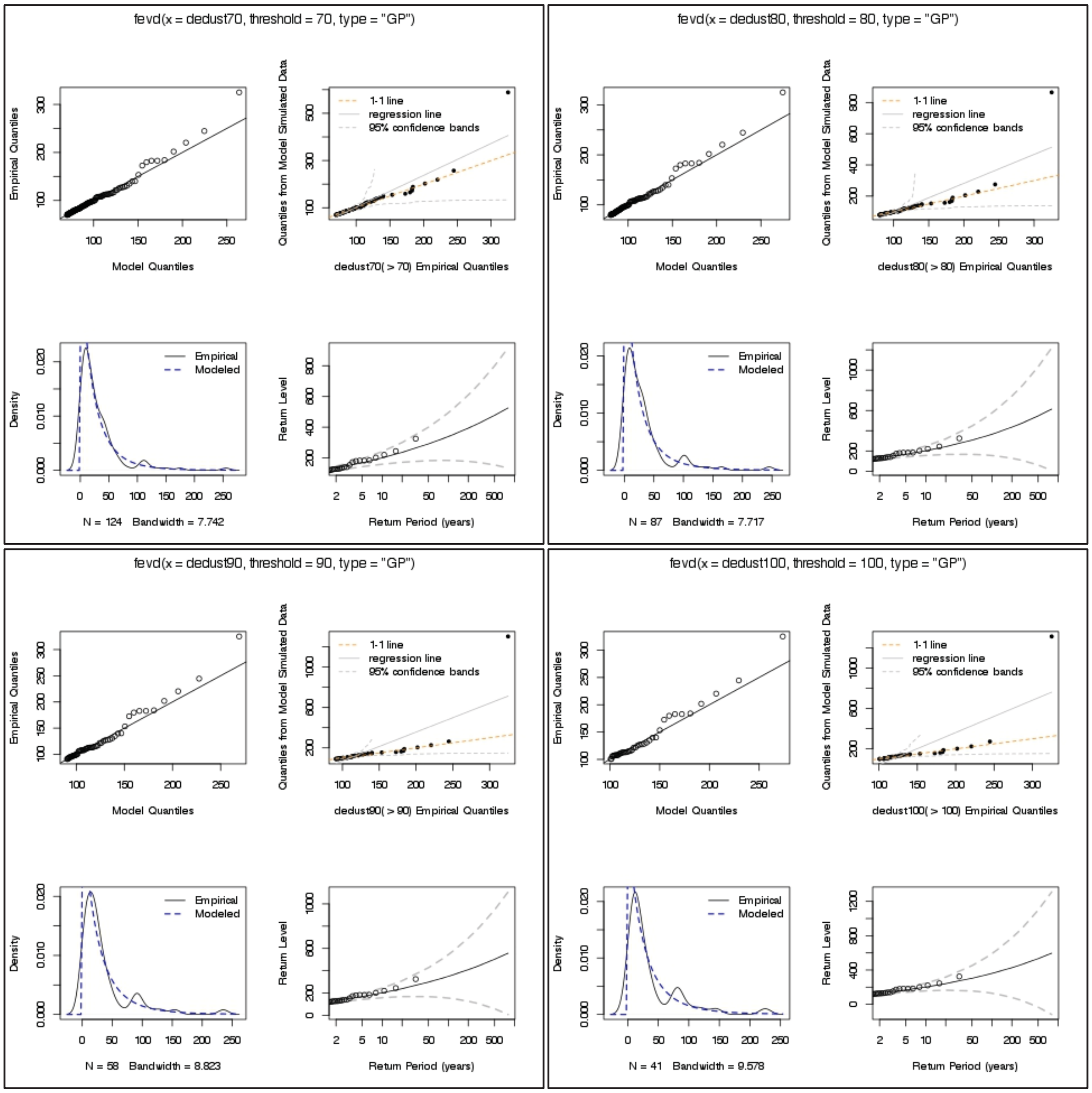

Figure 22. Diagnostic plots of GPD fit of Titusville 72-hour precipitation data for thresholds of 70 mm (top left panel), 80 mm (top right panel), 90 mm (bottom left panel), and 100 mm (bottom right panel). *Note.* Each diagnostic plot panel contains a quantile plot (top left), probability plot (top right), density plot (bottom left), and return-level plot (bottom right).

The researcher observed that the model estimates using 70-, 80-, 90-, and 100-mm thresholds are all relatively close, with a mean value of 354 mm. The diagnostic plots in Figure 22 suggest that the models fit the observed data well and the return-level plots do not show strong bias in the model for long return periods. The return-level estimates appear to be realistic and are close to, although slightly lower than the 100-year return-level estimate from NOAA Atlas 14 (409 mm at Titusville). Figure 23 displays the shape parameter estimates and their 95% confidence intervals. The shape estimates and confidence intervals from all three threshold models suggest that the most probable shape parameter is around 0.2. This means the distribution has a thick tail (Fréchet type) which is consistent with the 24-hour duration results. The higher threshold models (90, 100 mm) suggest there is a small chance the shape parameter could be around 0 due to the larger confidence intervals. This is due to high variance within the models. If one examines a trace of the negative log-likelihood over the shape parameter (not shown), the negative log-likelihood rapidly increases as the estimate approaches and passes 0. Therefore, it is highly unlikely that the frequency distribution has a light tail ($\xi = 0$).

All of the thresholds used were appropriate and produced similar results. Again, the entire 95% confidence intervals do not appear to be realistic. The lower ends of the confidence intervals (< 200 mm) are not realistic estimates of the expected 100-year 72-hour duration event, however, the upper ends of the confidence intervals (around 500 mm) are not unrealistic estimates for the expected 100-year event.

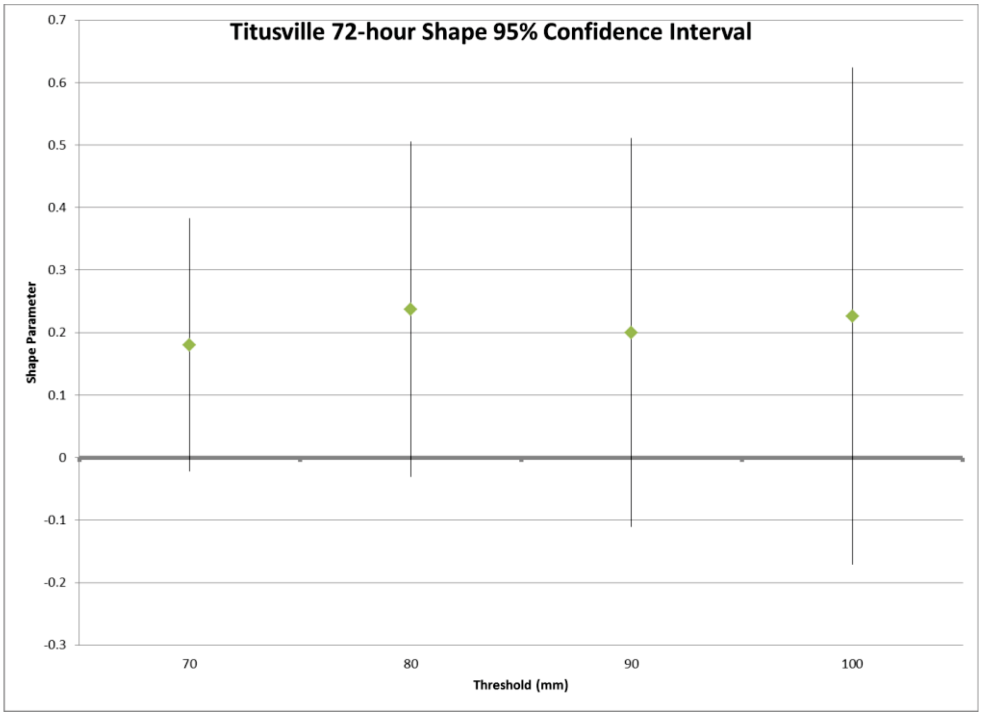

Figure 23. Titusville 72-hour shape estimates and 95% confidence intervals plotted for thresholds of 70 mm, 80 mm, 90 mm, and 100 mm.

Gridded 72-hour Duration Rainfall

Figure 24 shows the resulting return levels from the analysis of the 72-hour data at each of 36 grid locations for thresholds of u = 40, 45, and 50 mm, respectively.

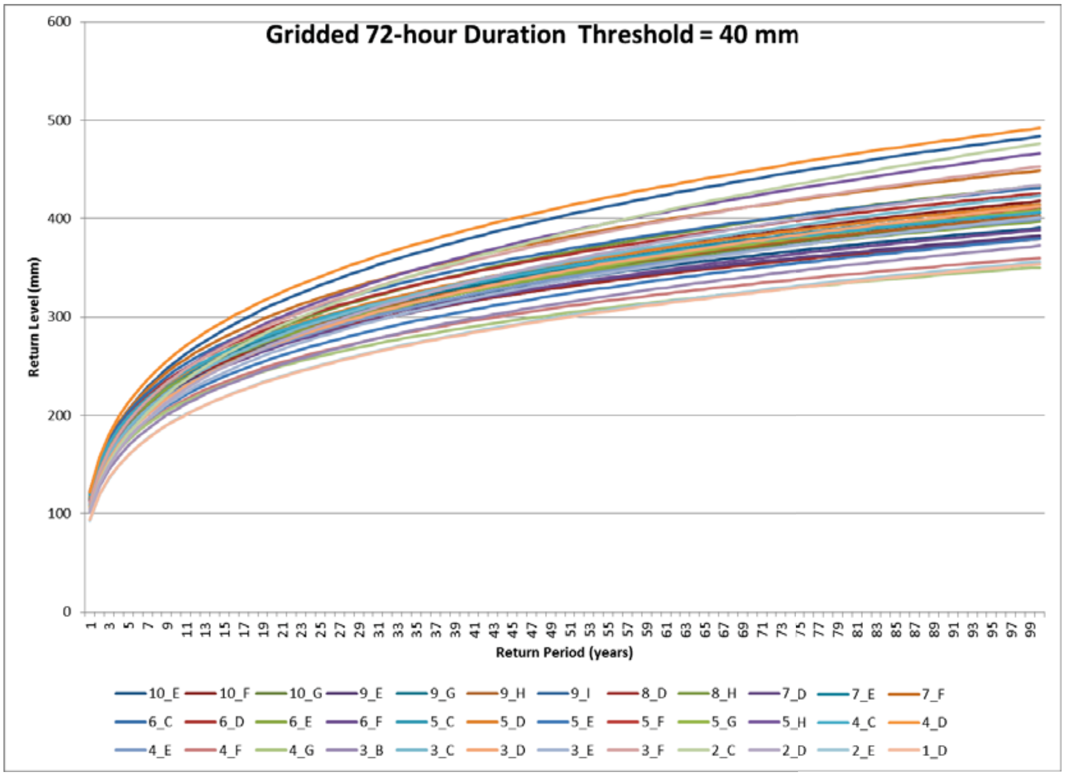
Gridded 72-hour Duration Threshold = 40 mm
Return Level (mm)
Return Period (years)
10_E
10_F
10_G
9_E
9_G
9_H
9_I
8_D
8_H
7_D
7_E
7_F
6_C
6_D
6_E
6_F
5_C
5_D
5_E
5_F
5_G
5_H
4_C
4_D
4_E
4_F
4_G
3_B
3_C
3_D
3_E
3_F
2_C
2_D
2_E
1_D

a

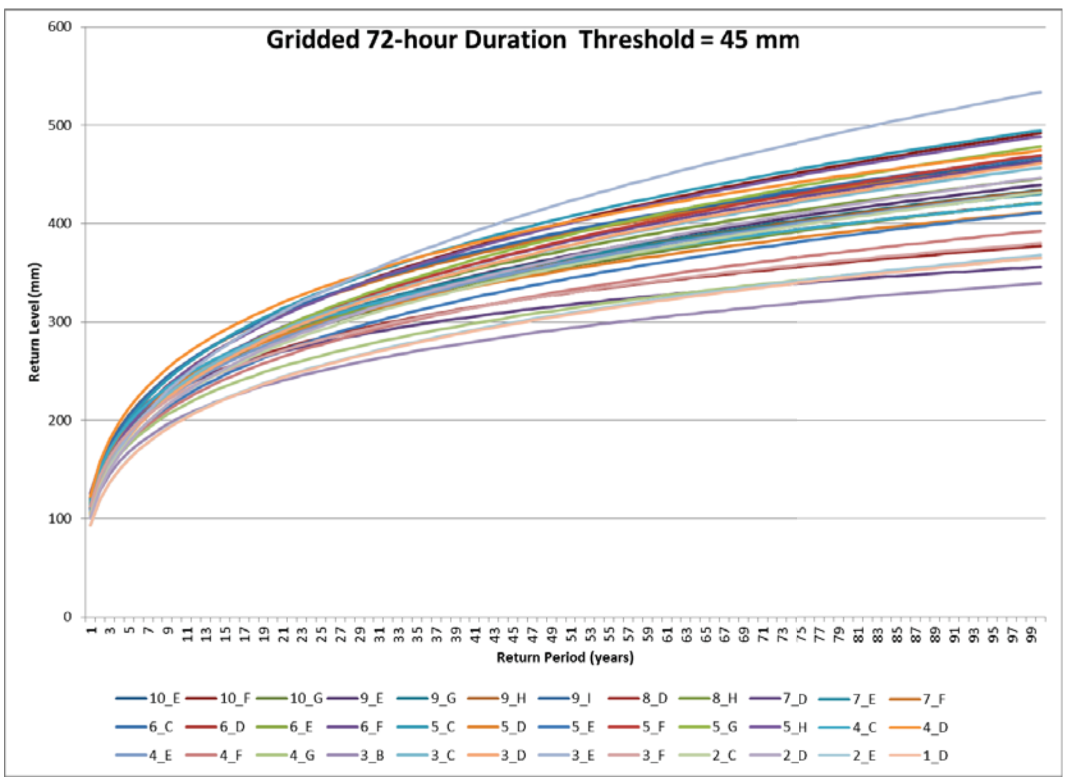
Gridded 72-hour Duration Threshold = 45 mm
Return Level (mm)
Return Period (years)
10_E
10_F
10_G
9_E
9_G
9_H
9_I
8_D
8_H
7_D
7_E
7_F
6_C
6_D
6_E
6_F
5_C
5_D
5_E
5_F
5_G
5_H
4_C
4_D
4_E
4_F
4_G
3_B
3_C
3_D
3_E
3_F
2_C
2_D
2_E
1_D

b

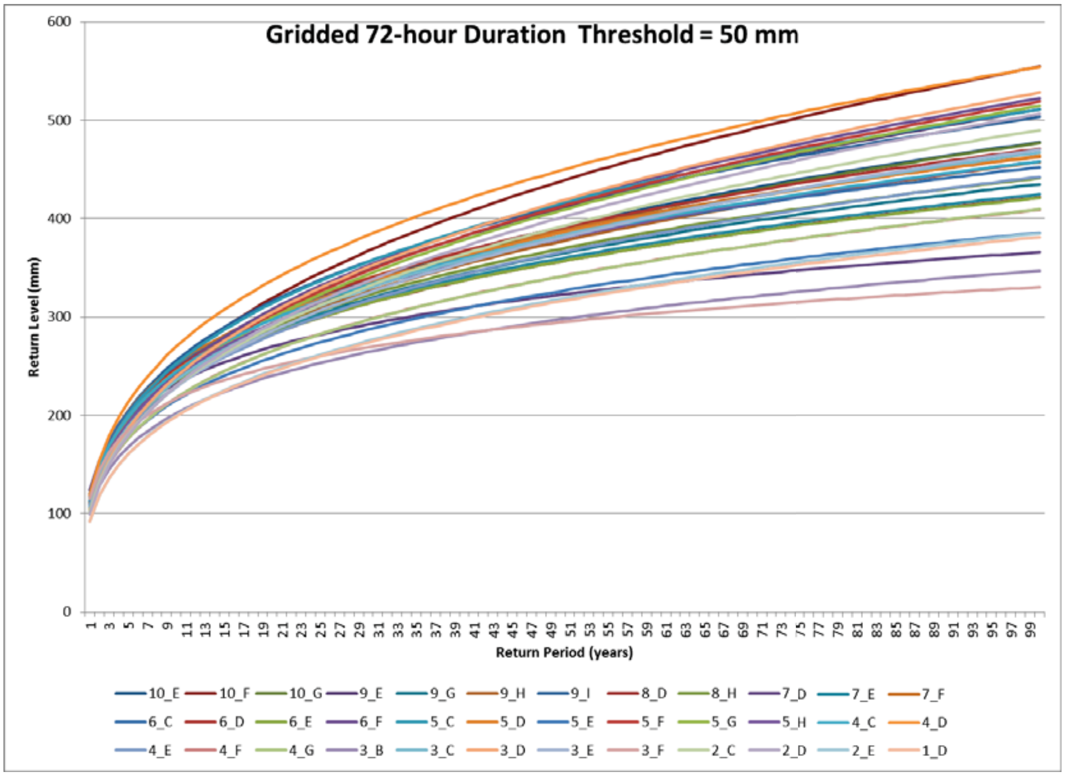

c

Figure 24. Gridded 72-hour duration return level estimates plotted from all relevant grid locations for thresholds of 40 mm (a), 45 mm (b), and 50 mm (c).

Return-level estimates appear to be very similar across the three thresholds used with 100-year return levels ranging from 350 to 490 mm for the 40-mm threshold, to 320 to 550 mm for the 50-mm threshold. The researcher has strong confidence that the return-level estimates are appropriate and relatively stable. The range and variance of return-level estimates increase with threshold, which is expected. The higher threshold models are more sensitive to individual extremes and are more likely to reveal spatial variations in extremes. In many cases, the 50-mm threshold model does a better job fitting the empirical data according to the diagnostic and return-level plots (shown in Appendix B).

As was done with the 24-hour duration data, the model means and standard deviations for threshold values used in the EVA are presented in Table 4. The diagnostic plots (in Appendix B) suggest that many of the models may have a negative bias when it comes to longer return periods, and the 45-mm and 50-mm threshold models (Figures 24b, c) do the best job according to the empirical data. These findings are consistent with NOAA Atlas 14 (2013) 100-year return level estimates (409 mm for Titusville), although higher than the Titusville return-level estimates in Figure 20. The quality-of-fit diagnostic plots (return-level plots in Appendix B, pages 145 - 168) suggest that the statistical model may be underestimating return levels at long return periods, therefore a range of return-level estimates should be considered at long return periods. The researcher noted that the rainfall amounts associated with Tropical Storm Fay in 2008 (24-hour amount of 371 mm; 72-hour amount of 626 mm) were beyond the return-level amounts produced from this EVA. According to the model estimates, Fay's return period is over 100 years. The EVA results and Tropical Storm Fay's observed rainfall suggest there is much larger uncertainty around the longer period and higher level return estimates.

Table 4

Consensus and Standard Deviations of 100-Year Return Level Estimates of 72-Hour Rainfall Data from Gridded Locations

Threshold (mm)	100-year estimate consensus (mean; mm)	100-year estimate standard deviation (mm)
40	410.88	35.38
45	433.71	44.40
50	456.37	56.30

Titusville 72-hour Duration Rainfall (Dry Season)

Figure 25 shows the resulting return levels from the analysis of the 72-hour data at Titusville for thresholds of u = 25, 30, and 35 mm during the dry season. The 100-year return-level estimates were 242, 272, and 275 mm, respectively. Figure 26 displays the uncertainty around the 100-year return-level estimates, and shows that for the 35-mm threshold, the 95% confidence interval of the 100-year return-level ranges from 134 mm to 416 mm. Figure 27 shows quality-of-fit diagnostic plots, which describe how well the estimated models fit the empirical data.

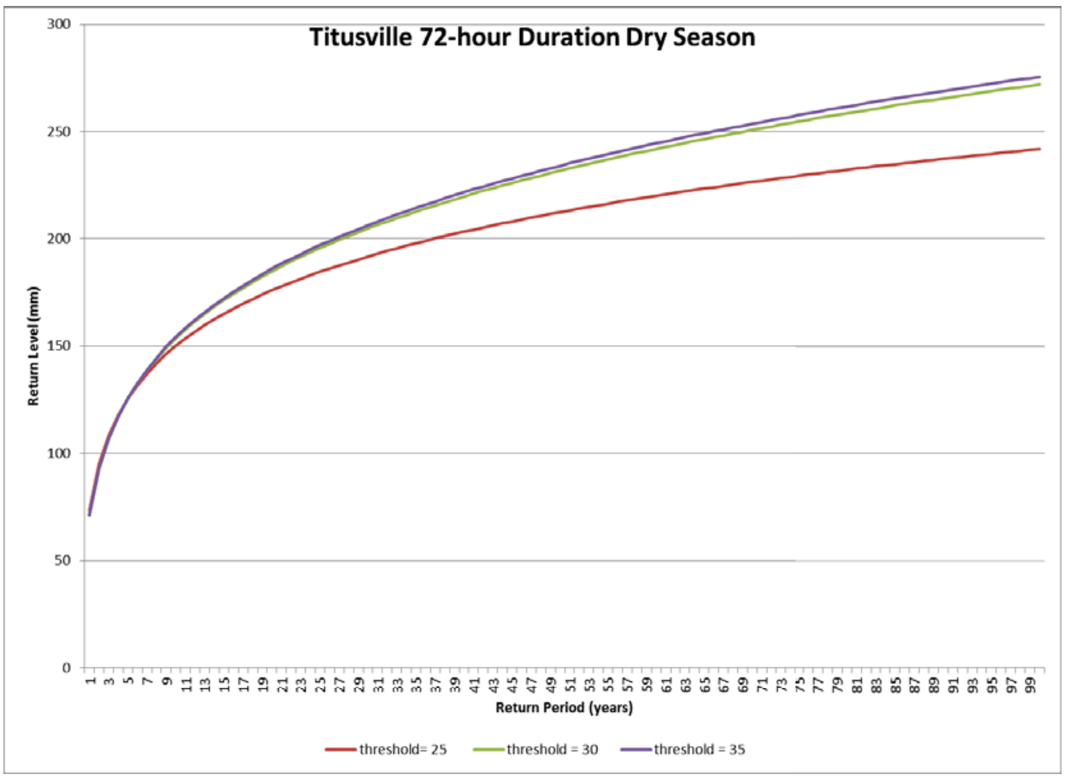

Figure 25. Titusville 72-hour duration dry season return-level estimates plotted for thresholds of 25 mm, 30 mm, and 35 mm.

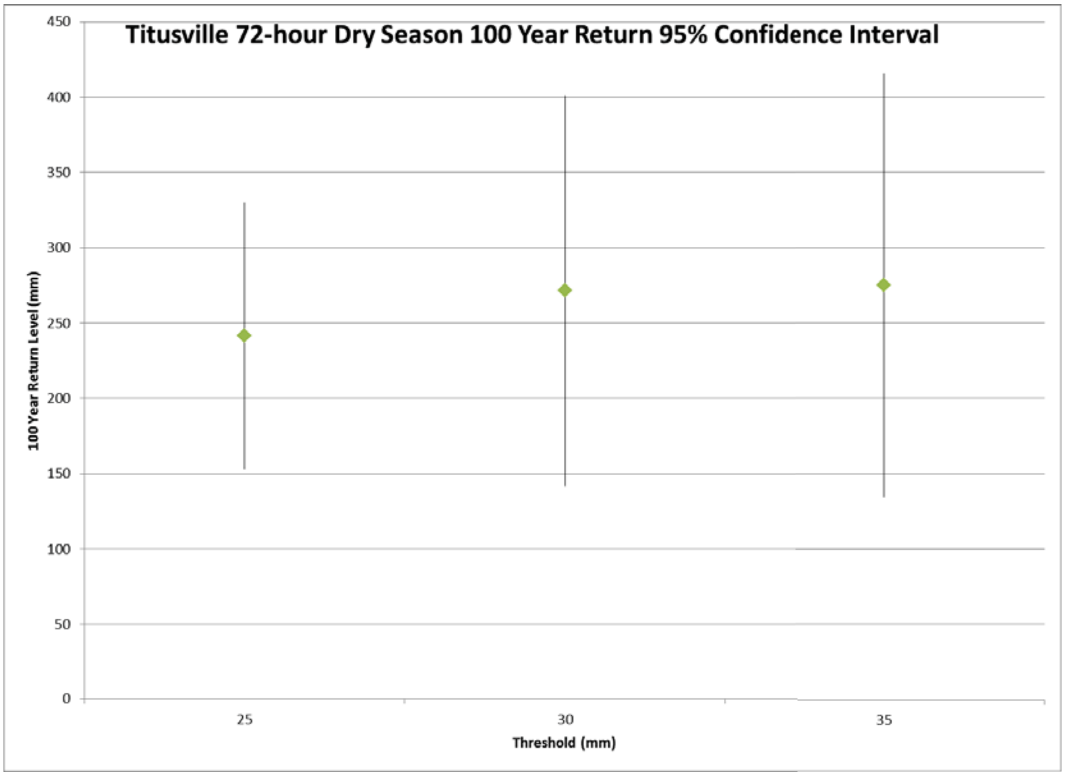

Figure 26. Titusville 72-hour 100-year dry season return level estimates and 95% confidence intervals plotted for thresholds of 25 mm, 30 mm, and 35 mm.

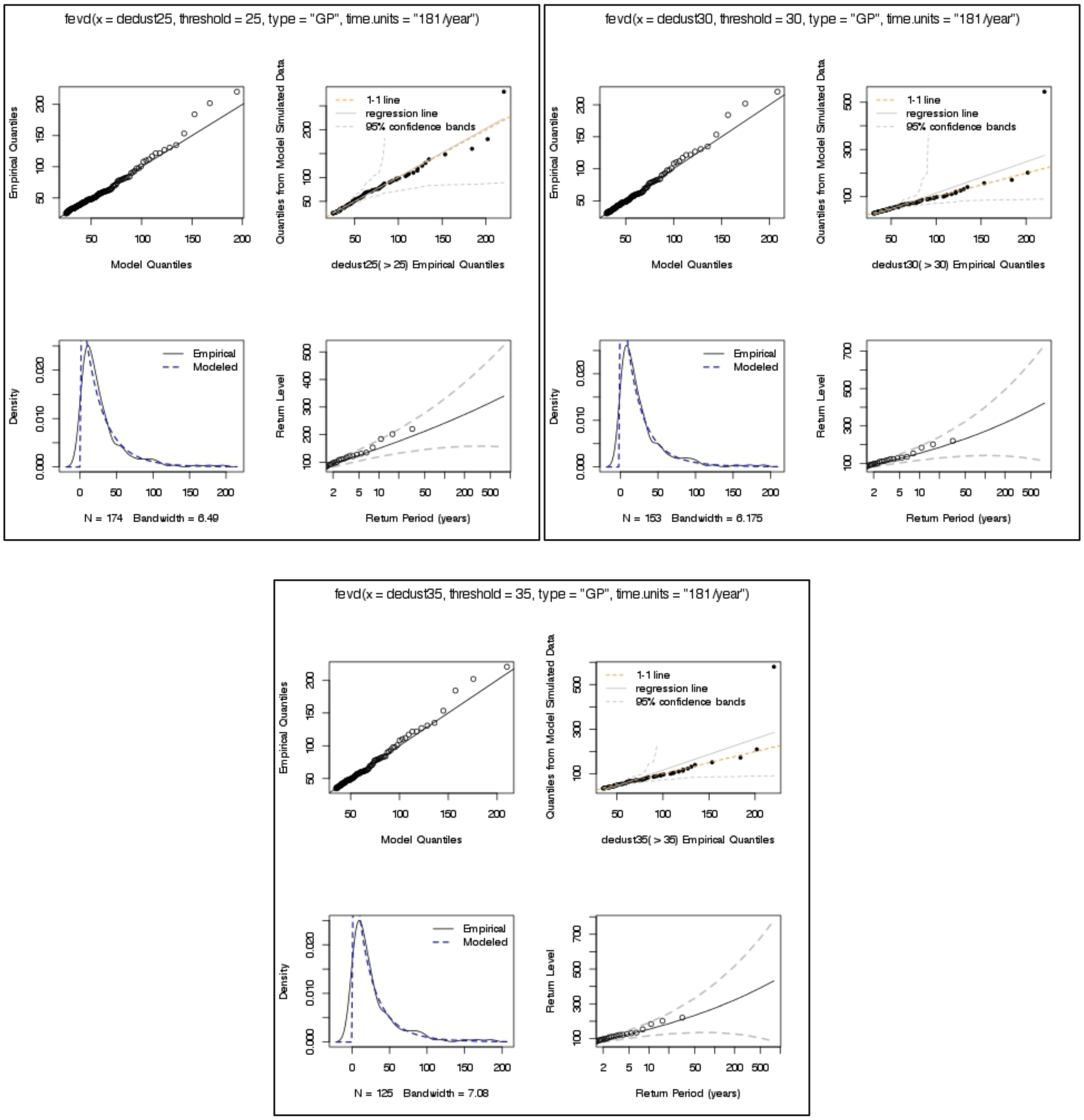

Figure 27. Diagnostic plots for GPD fit of Titusville dry-season 72-hour precipitation data for thresholds of 25 mm (top left panel), 30 mm (top right panel), and 35 mm (bottom panel). *Note.* Each diagnostic plot panel contains a quantile plot (top left), probability plot (top right), density plot (bottom left), and return-level plot (bottom right).

According to the diagnostic plots, it appears that the model may be underestimating the longer-period return levels at the 25-mm threshold. Note that the model estimate performs better for longer return periods in the return-level plots for thresholds of 30 and 35 mm. This suggests the estimates from these models may be more accurate for longer return periods, and that the range of values in the 95% confidence interval plot for these thresholds may be very realistic.

Gridded 72-hour Duration Rainfall (Dry Season)

Figure 28 shows the resulting return levels from the analysis of the 72-hour data at each of 36 grid locations during the dry season for thresholds of u = 20, 25, and 30 mm, respectively.

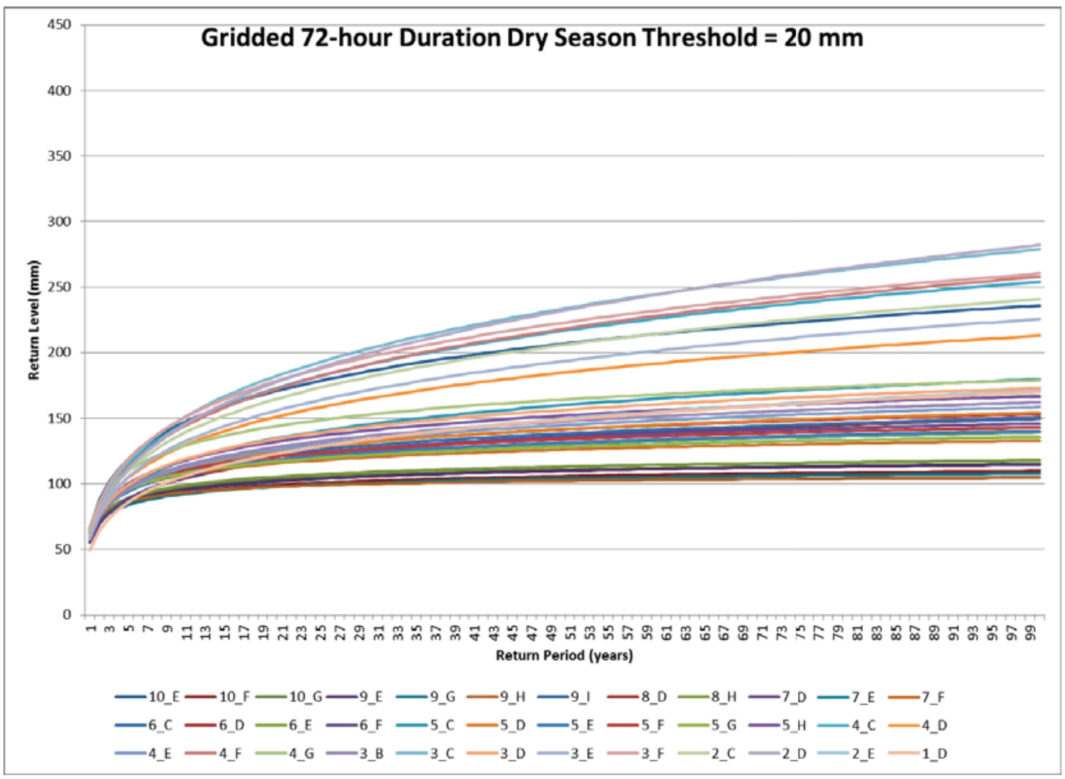

a

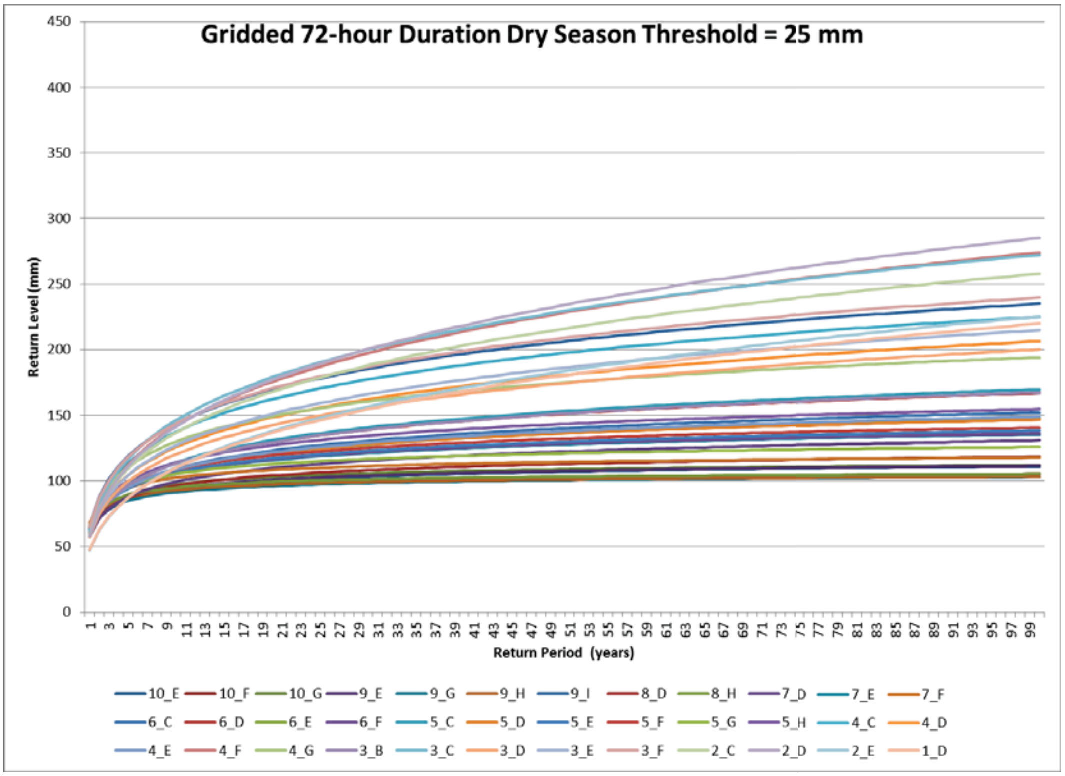

b

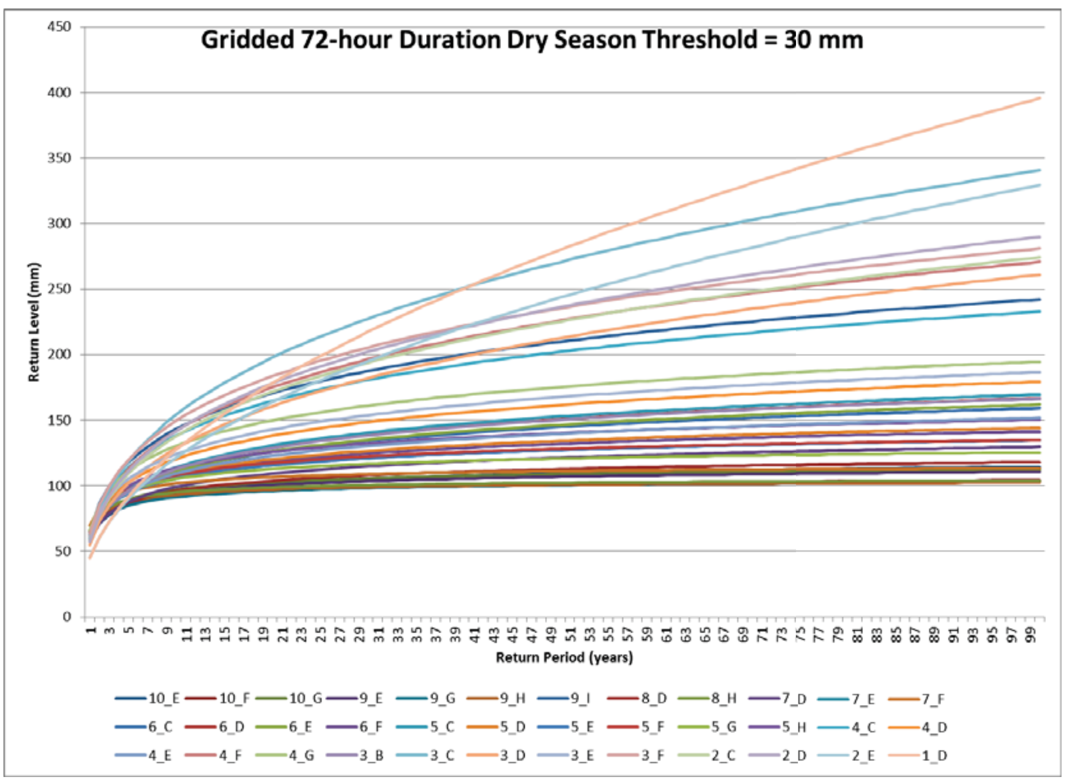

c

Figure 28. Gridded 72-hour duration dry-season return-level estimates plotted for thresholds of 20 mm (a), 25 mm (b), 30 mm (c).

Many return-level estimates from the grid points in the dry-season data show that the tail of the distribution is very light or bounded because the return levels increase very slowly across the return periods above 50 years. For example, in the 25-mm threshold analyses (Figure 28b), it appears as if half the grid point frequency distributions have the expected heavier tail, while the other half are indicating a bounded tail. As stated earlier, the bounded shape is not usually a characteristic of rainfall frequency distributions. The researcher also investigated how the return levels are geographically distributed. The 100-year return-level estimates from the 25-mm threshold analysis were mapped and are displayed in Figure 29. The lower return levels are grouped in the southern part of the domain. Lower return levels are expected during the dry season, however, the low return levels associated with the bounded-tail estimates may be misleading for longer return periods. These estimates and tail shape are not consistent with the analyses of the longer period dry-season 72-hour data from Titusville shown in Figure 25. The quality-of-fit diagnostic plots do suggest that the statistical models adequately fit the empirical data. The bounded shape parameters may be an artifact of the short time frame used for the analysis (only “dry seasons” between 1998 and 2012).

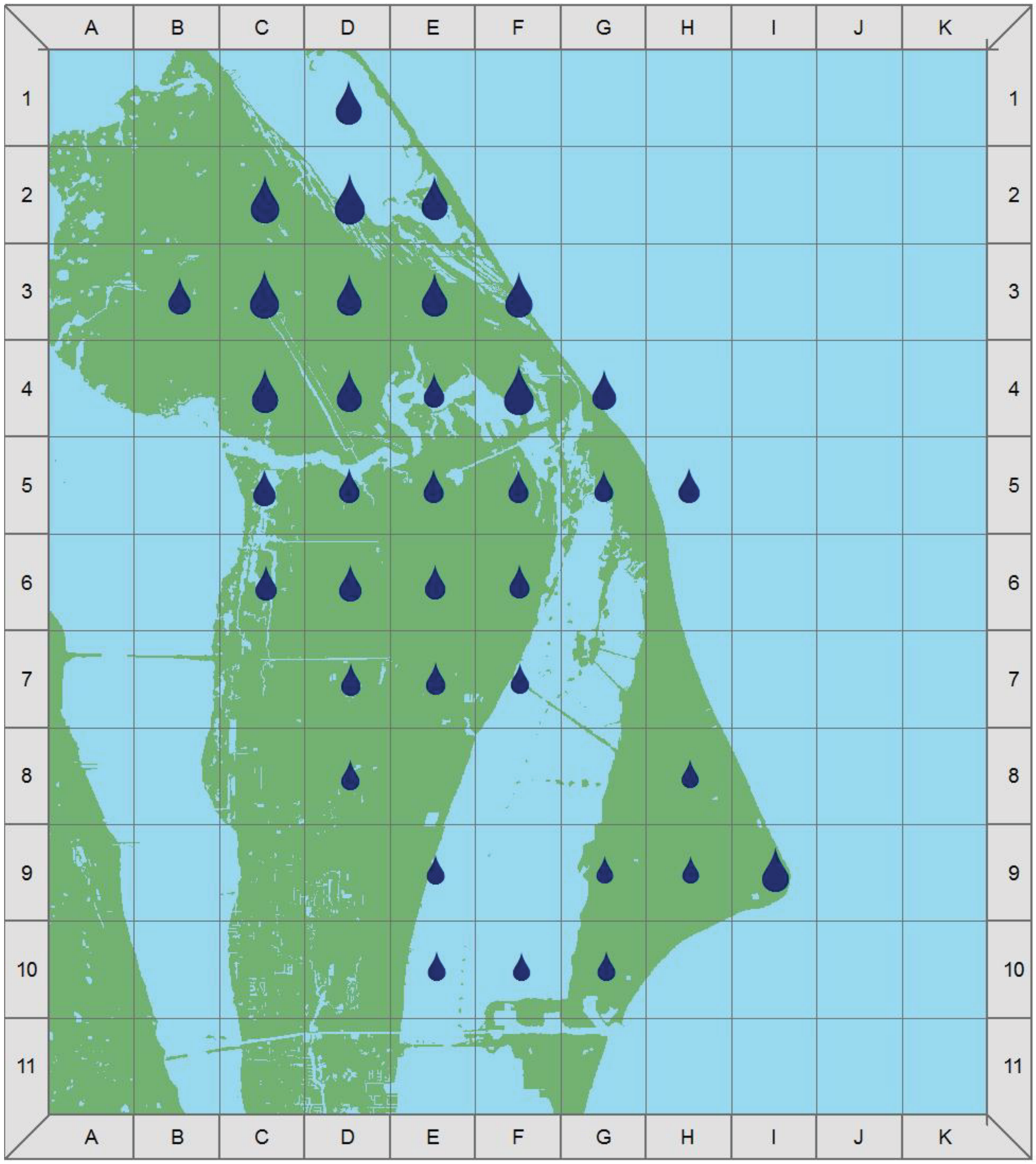

Figure 29. Rainfall Analysis domain; blue droplets are proportional to the 100-year return level from the 25-mm threshold dry-season analysis. *Note.* The largest and smallest drops represent 286 and 103 mm, respectively.

As was done previously, the model means and standard deviations for threshold values used in the EVA are presented in Table 5. Table 5 indicates there is very high variance and return-level range in the 100-year estimates for the 30-mm threshold analyses. Examining the return-level plots (Figure 28) and the bounded shape associated with many of the grid points makes the researcher skeptical of the consensus estimates in Table 5. One would expect the frequency distribution to have a lighter tail during the dry season, however, many models are suggesting the frequency distribution is bounded, and in many cases, the 50-year return event is the same as the 100-year return event. These models are most likely not accurately estimating return levels due to the small number of extreme events actually observed during the 15 dry seasons in the POR. The Titusville dry-season estimates using the longer POR (Figure 25) appear to be more realistic for the dry season than many of the gridded estimates.

Table 5

Consensus and Standard Deviations of 100-Year Return-Level Estimates of 72-Hour Rainfall Data from Gridded Locations during the Dry Season

Threshold (mm)	100-year estimate consensus (mean; mm)	100-year estimate standard deviation (mm)
20	170.67	52.13
25	169.82	55.77
30	182.00	78.06

Titusville 72-hour Duration Rainfall (Wet Season)

Figure 30 shows the resulting return levels from the analysis of the 72-hour data at Titusville for thresholds of u = 70, 80, 90, and 100 mm during the wet season. The 100-year return level estimates were 315, 332, 342 and 364 mm, respectively. Figure 31 displays the uncertainty around the 100-year return-level estimates, and shows that for the 100-mm threshold, the 95% confidence interval of the 100-year return level ranges from 62 mm to 665 mm. Figure 32 shows quality-of-fit diagnostic plots, which describe how well the estimated models fit the empirical data.

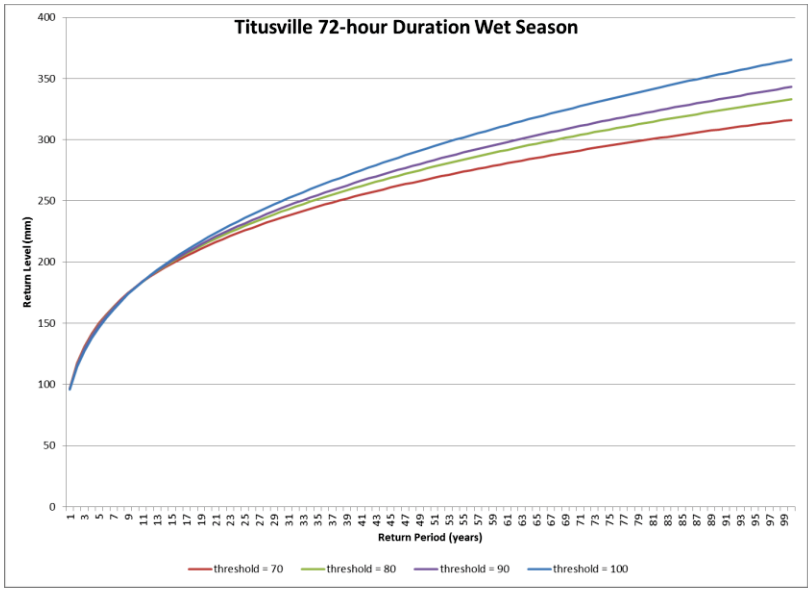

Figure 30. Titusville 72-hour duration wet-season return-level estimates plotted for thresholds of 70 mm, 80 mm, 90 mm, and 100 mm.

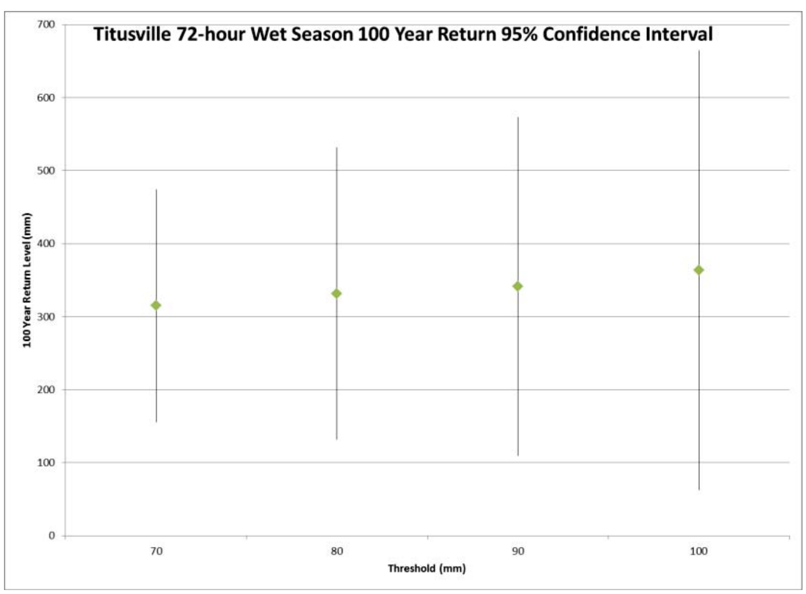

Figure 31. Titusville 72-hour 100 year wet-season return-level estimates and 95% confidence intervals plotted for thresholds of 70 mm, 80 mm, 90 mm, and 100 mm.

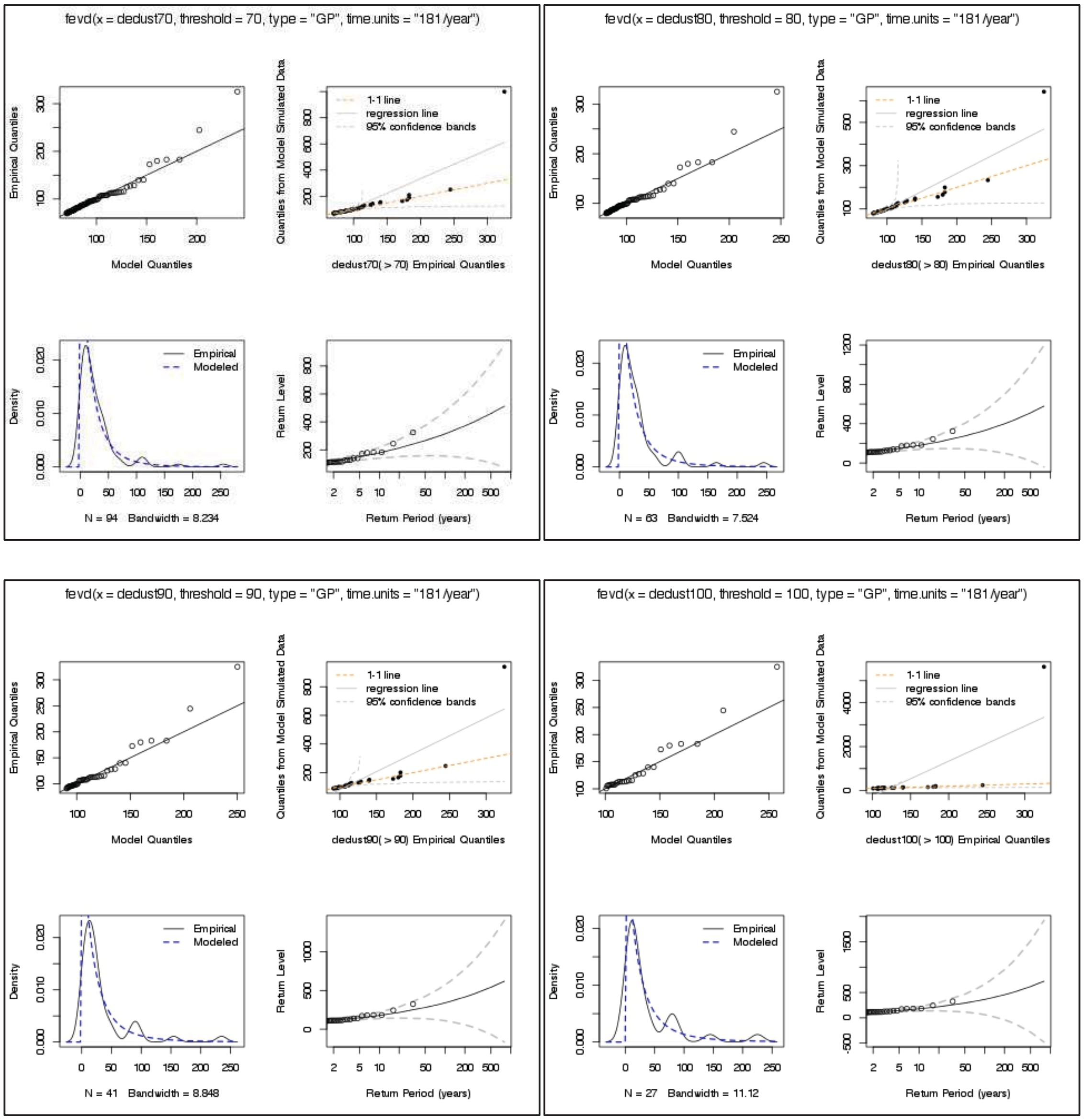

Figure 32. Diagnostic plots of GPD fit of Titusville wet-season 72-hour precipitation data for thresholds of 70 mm (top left panel), 80 mm (top right panel), 90 mm (bottom left panel), and 100 mm (bottom right panel). *Note.* Each diagnostic plot panel contains a quantile plot (top left), probability plot (top right), density plot (bottom left), and return-level plot (bottom right).

According to the diagnostic plots, it appears that the model may be underestimating the longer period return levels for thresholds of 70 and 80 mm. The longer period observations lie along the upper 95 percent confidence band (dashed lines in return-level plots in Figure 32). Note that the model estimate performs better for longer return periods in the return-level plots when the thresholds are 90 and 100 mm. The empirical data suggests the estimates from the 90-mm and 100-mm threshold models may be more accurate; however, the entire 95% confidence interval (Figure 31) does not appear to be realistic. The low-end estimates, 110 and 62 mm, respectively, are not realistic 100-year return levels; however, the upper-end estimates of 573 and 665 mm may not be unreasonable considering the 626 mm of rain from Tropical Storm Fay in 2008. There is larger uncertainty associated with the high-threshold models, but the empirical data suggests that the longer-period model estimates may be more accurate with the higher threshold models.

Gridded 72-hour Duration Rainfall (Wet Season)

Figure 33 shows the resulting return levels from the analysis of the 72-hour data at each of 36 grid locations during the wet season for thresholds of u = 40, 45, and 50 mm, respectively.

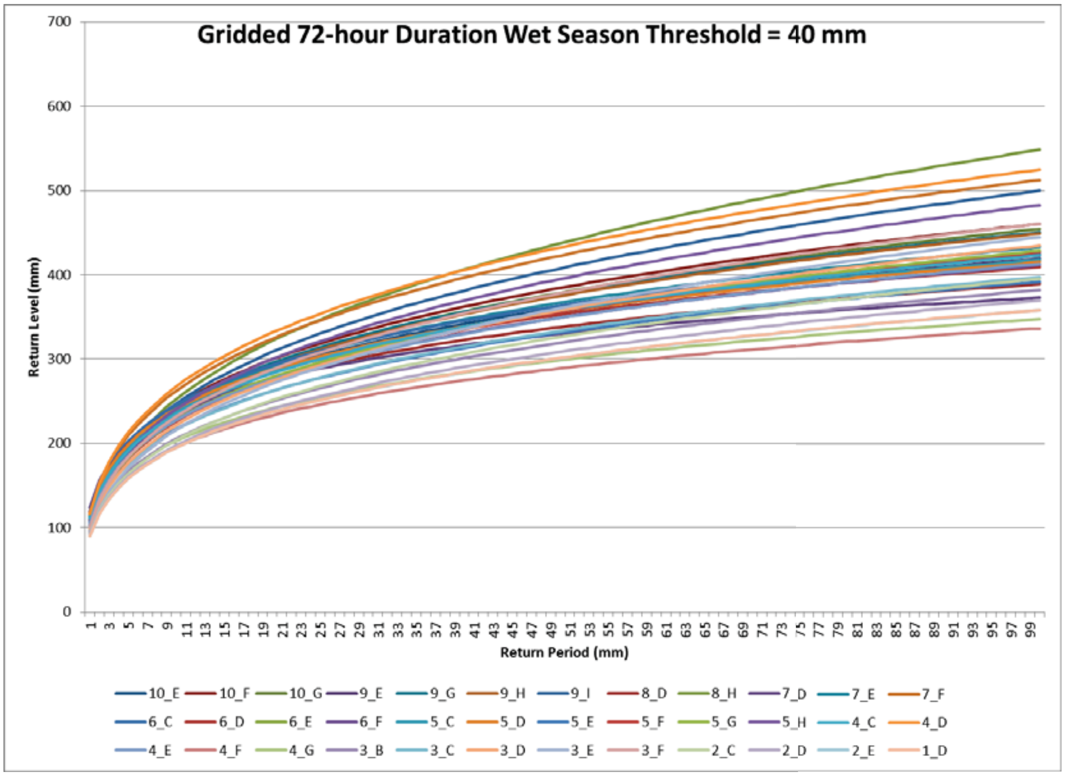

Gridded 72-hour Duration Wet Season Threshold = 40 mm
Return Level (mm)
Return Period (mm)
10_E 10_F 10_G 9_E 9_G 9_H 9_I 8_D 8_H 7_D 7_E 7_F
6_C 6_D 6_E 6_F 5_C 5_D 5_E 5_F 5_G 5_H 4_C 4_D
4_E 4_F 4_G 3_B 3_C 3_D 3_E 3_F 2_C 2_D 2_E 1_D

a

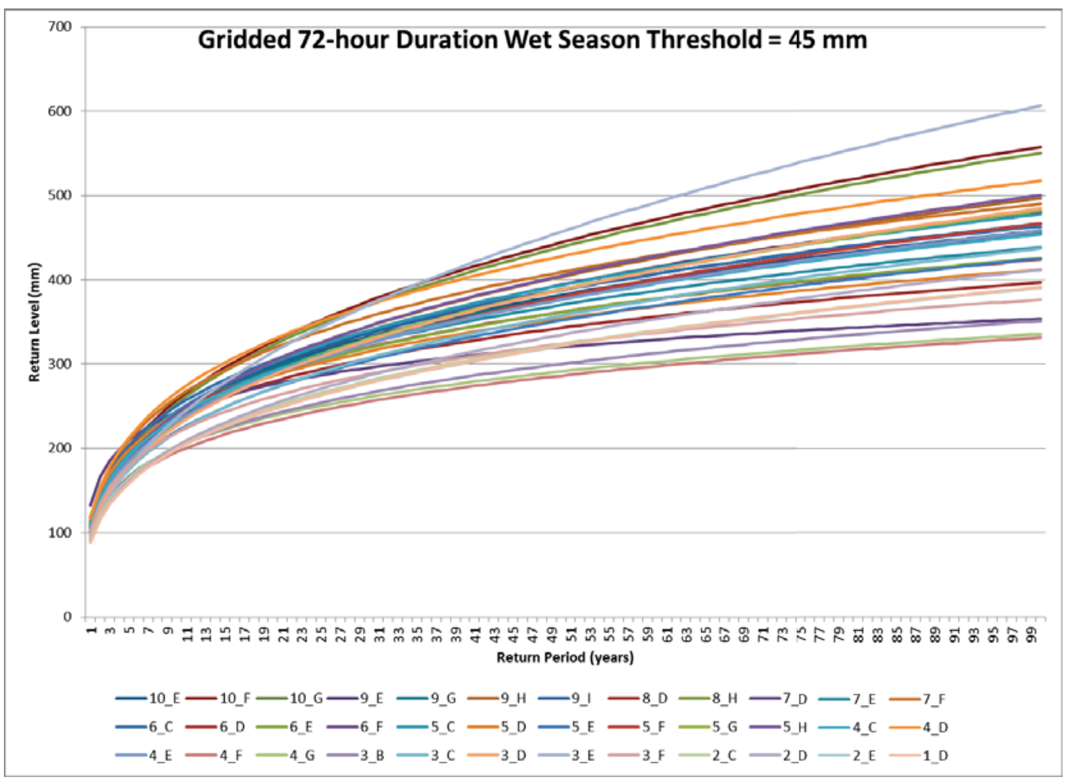

Gridded 72-hour Duration Wet Season Threshold = 45 mm
Return Level (mm)
Return Period (years)
10_E 10_F 10_G 9_E 9_G 9_H 9_I 8_D 8_H 7_D 7_E 7_F
6_C 6_D 6_E 6_F 5_C 5_D 5_E 5_F 5_G 5_H 4_C 4_D
4_E 4_F 4_G 3_B 3_C 3_D 3_E 3_F 2_C 2_D 2_E 1_D

b

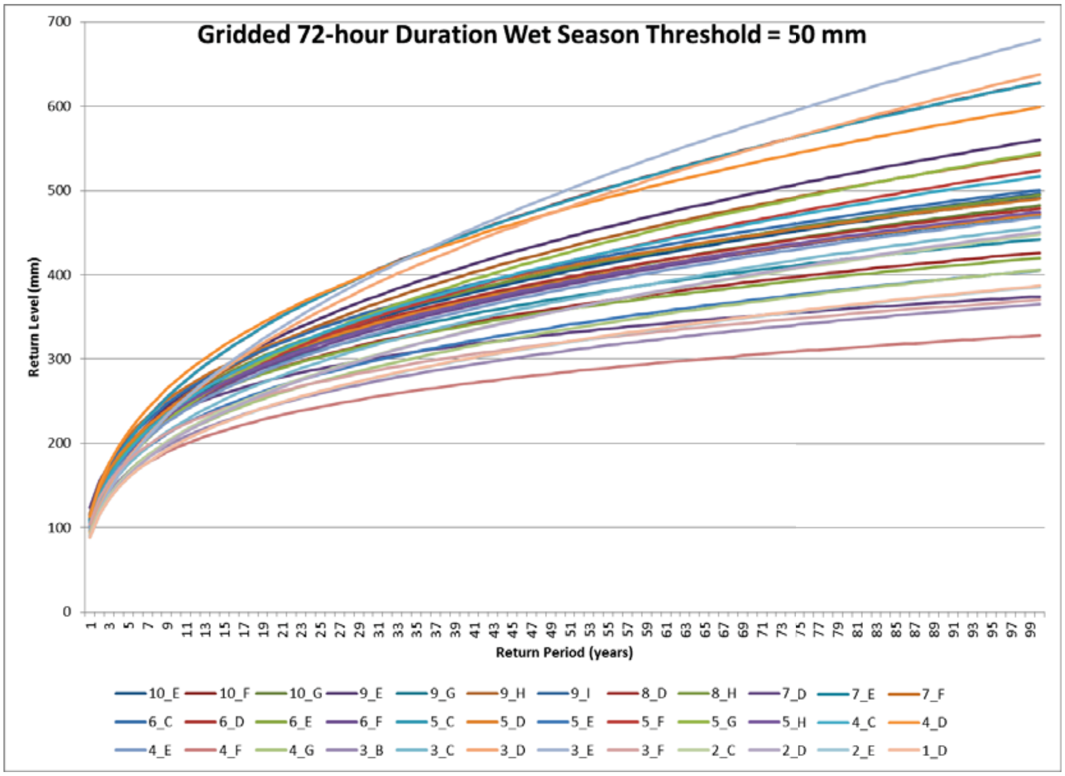

c

Figure 33. Gridded 72-hour duration wet-season return-level estimates were plotted for thresholds of 40 mm (a), 45 mm (b), 50 mm (c).

The return-level estimates over the gridded domain do not appear to be heavily biased for the 40-mm threshold estimates, and even though the spread of the 50-mm threshold models increased, most of them appear to be realistic, and diagnostic plots (return-level plots in Appendix B, pages 209 - 216) show the models fit the empirical data well. As stated earlier, there is greater uncertainty associated with high return-level estimates for longer return periods. Return levels for the wet season are very similar to the return levels for the whole year. This is because the majority of extreme events in any given year occur during the wet season. Recall that the researcher defined the wet season as May through October in order to include extreme events near the beginning and end of the season as defined by Lascody (2002). Table 6 displays the 100-year return estimate means and the standard deviations of the estimates. The consensus estimates from all the thresholds appear to be realistic and are consistent with NOAA Atlas 14 (2013) 72-hour 100-year return level (409 mm at Titusville) estimates for the whole year. The gridded estimate means are greater than the estimates from the 32-year Titusville record (recall Figure 30).

Table 6

Consensus and Standard Deviations of 100-Year Return-Level Estimates of 72-Hour Rainfall Data from Gridded Locations during the Wet Season

Threshold (mm)	100-year Estimate Consensus (mean; mm)	100-year Estimate Standard Deviation (mm)
40	424.42	38.25
45	426.75	77.56
50	480.99	115.79

The return levels from the 45-mm threshold analysis were mapped in order to examine spatial variations of expected return levels (Figure 34). There do not appear to be any obvious geographic variations; however, the results show that the highest expected return levels are around grid points 3E, 8H, and 10F.

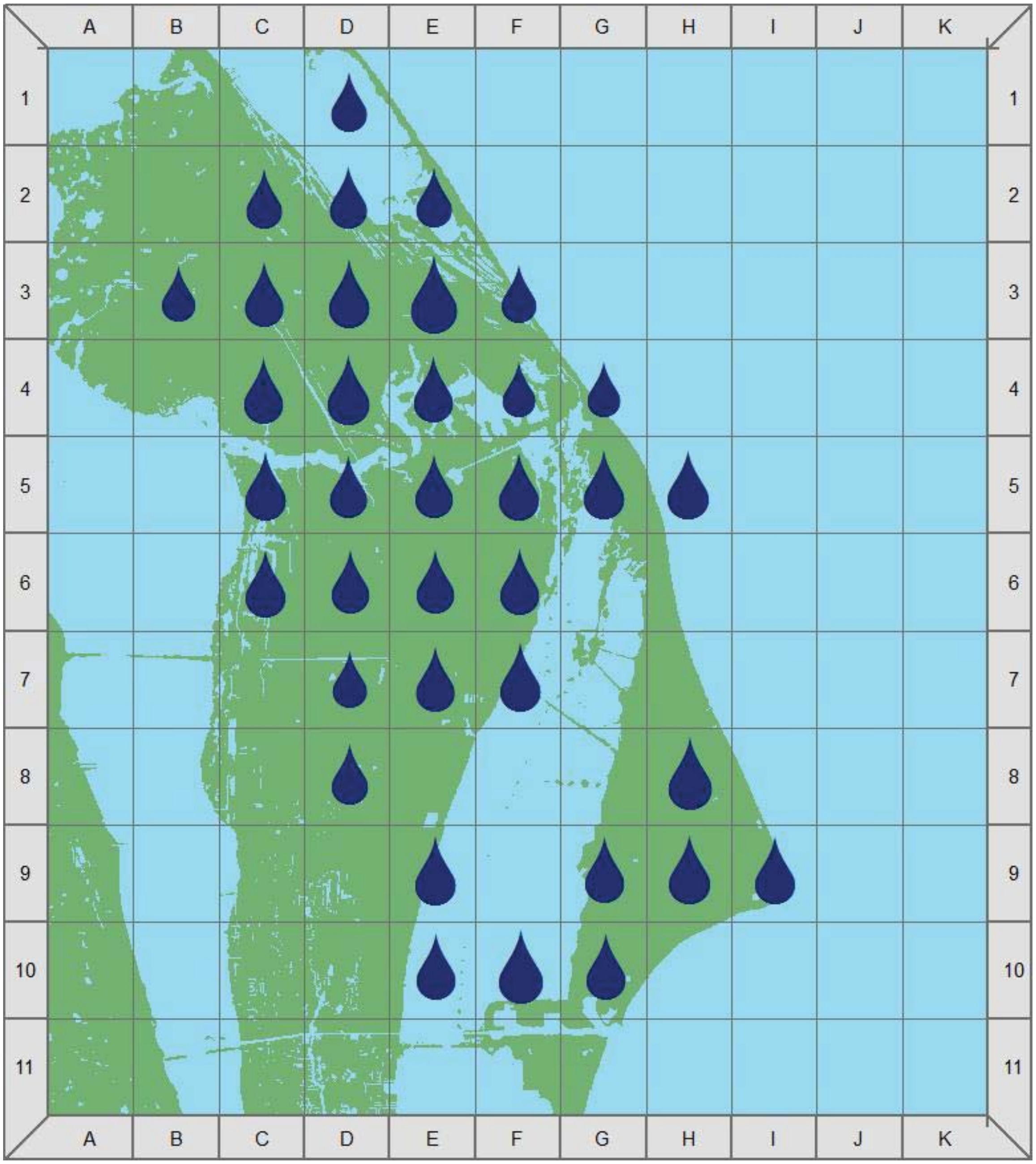

Figure 34. Rainfall Analysis domain; blue droplets are proportional to the 100-year return level from the 45-mm threshold wet-season analysis. *Note.* The largest and smallest drops represent 606 and 301 mm, respectively.

Chapter V

Conclusions and Recommendations

Conclusions

A total of 446 statistical models were produced for estimating 24- and 72-hour rainfall return levels across the KSC region. Thirty-seven rainfall time series from unique locations across the region were developed and examined (36 from individual grid locations and one from the Titusville ASOS). Multiple thresholds were used for modeling each series. The wet and dry seasons were also modeled separately. Together, these analyses assist with developing a climatic baseline of extreme rainfall for the KSC region.

Estimates produced at the gridded locations enhance the knowledge of the stochastic behavior of extreme rainfall in recent times. The density of the gauges from the network provided numerous unique observations across the region, which helps with understanding the stochastic behavior of extreme rainfall.

Significance of quality control. The raw daily rainfall data acquired from the TRMM website was not completely reliable; therefore a detailed quality control process was developed to minimize the biases of invalid or missing data on the EVA. An EVA is highly sensitive, and missing extremes can drastically affect the results.

The quality control process first removed invalid gauge observations based on surrounding gauge observations. The remaining unevenly spaced gauge observations were then transformed to an evenly spaced grid using a Barnes objective analysis (Koch et al., 1983). The objective analysis interpolates surrounding gauge observations to grid points, and therefore smooths the data and reduces the extreme values. The convergence parameter (gamma) controls the smoothing and the radius of influence at the grid point. A common range for gamma is 0.2 – 0.3, however, a gamma value of 0.03 was used for this gridded analysis in order to minimize how much the extremes were affected by smoothing. The quality control process was essential for ensuring that the EVA across the region was not biased by missing or invalid data.

It is important to remember that the extreme-value models are statistical estimates and their results are dependent upon the actual observed rainfall occurrences during the POR. Threshold models are also dependent on the threshold value used. This study used multiple locations and multiple threshold values to test how sensitive the models were to changes in the threshold, and how they varied across the region. Results should always be compared with empirical data, as was done in this study by using the Titusville ASOS and quality-of-fit diagnostic plots to ensure that return-level estimates appear realistic and that the model fits the empirical data. There will be greater uncertainty with the longer period return levels, and a longer POR will generally do better with estimating longer period return levels. There was less uncertainty about the Titusville estimates at long return periods, however, it is not clear whether a single longer POR analysis will perform better than the consensus of multiple shorter POR estimates.

Summary of results. The 24-hour duration gridded results appear to be realistic and fit the empirical data relatively well; however, there appears to be a slight negative bias in the 25-mm threshold models. The expected 24-hour 100-year return level for the region is around 315 mm (30-mm-threshold model consensus; recall Table 3 and Figure 19).

The 72-hour gridded results appear to be realistic and fit the empirical data relatively well. The empirical data suggests that there may be a negative bias in the models for longer return periods. The expected 72-hour 100-year return level for the region is around 433 mm (45-mm-threshold model consensus; recall Table 4 and Figure 24).

The 72-hour gridded results from the dry season appear to be highly variable across the region. Some of the gridded estimates in the southern half of the KSC domain have a bounded shape and suggest that expected return levels do not increase beyond 150 mm for any return periods. One could expect that the dry-season frequency distribution would be more lightly tailed than the rest of the year, however, it is difficult to believe that the rainfall frequency distribution is as bounded as some of the model estimates suggest. The researcher believes that the expected 72-hour duration 100-year return level during the dry season is greater than 170 mm (25-mm threshold model consensus; recall Table 5 and Figure 28). The Titusville estimates were better behaved and suggest the 72-hour duration 100-year return level during the dry season is around 250 mm. The Titusville estimates also suggest the frequency distribution has the expected thick tail (Fréchet) shape.

The 72-hour gridded results from the wet season appear to fit the empirical data relatively well and appear to be realistic. There is, however, larger uncertainty with the higher level and longer period return levels. Some diagnostic plots indicate there may be some negative bias in the long period return levels. The expected 72-hour duration event for the wet season is around 426 mm (45-mm-threshold model consensus; recall Table 6 and Figure 33). The 72-hour wet season return levels are similar to those for the whole year because most extreme rainfall events in a year occur during the wet season. Most of the model estimates suggest that the 626 mm of rain from Tropical Storm Fay in 2008 was rarer than the 100-year event.

Scope of the study. Return-level estimates produced from the gridded locations and Titusville ASOS complement the Titusville estimates from NOAA Atlas 14 (2013). NOAA Atlas 14 did not use as dense of a rainfall network as this study, and the closest location to KSC used by NOAA Atlas 14 was Titusville. NOAA Atlas 14 utilized longer periods and used yearly maxima (block maxima) instead of the POT approach used in this study. It should be noted that the present study is narrowly focused on the KSC region, whereas NOAA Atlas 14 covers the entire U.S.

This study produced return-level estimates at 36 individual locations across the KSC region. Previous rainfall return-level estimates for the region were generalized from the single-point Titusville estimates according to NOAA Atlas 14 (2013). Findings in this study show that there is variability in expected return estimates across the geographically diverse region, and that a single estimate for the region may not sufficiently convey the risk of extreme rainfall. Complex sea breeze interactions take place over the region, and influence extreme rainfall likelihoods over KSC, especially during the wet season. Although single estimates can be used to describe the region as a whole, a range of return levels should be considered for long-term planning. Having said this, the researcher does not recommend applying extreme rainfall estimates from a single location for applications because of larger uncertainty associated with using a single short POR (15 years). Instead, when planning for the 24-hour duration 100-year event, it would be wise to examine the return levels from multiple locations across multiple thresholds. For example, by examining the gridded 24-hour duration estimates (Figure 19) it appears that the most probable 100-year event is between 250 and 450 mm.

The gridded consensus (Tables 3, 4, 5, and 6) and Titusville return-level estimates (Figures 16, 20, 25, and 30) are most likely good estimates of the return levels of events that can be expected to impact the majority of the studied region, while the higher return-level estimates from individual grid locations are likely good estimates of the return levels which can be expected to impact localized parts of the studied region. The 72-hour maximum observed in the region during the POR, from Tropical Storm Fay (626 mm at gauge 34, near grid point 9H) would be an example of a localized extreme occurrence. The surrounding gauges 28, 29, and 32 observed 542, 512, and 551 mm, respectively, over the same time period. Gauge 30 had its daily observation removed by quality control when it reported a 0 within the same 72-hour time period. By contrast, the 72-hour maximum averaged across all the gridded locations (378 mm) would be an example of the average rainfall across the region during an extreme event. Return levels produced should be considered best estimates of what to expect. It is important to remember that actual extreme rainfall occurrence frequencies can vary greatly from what is expected.

Rainfall return levels in a warmer climate. One could utilize results from this study in conjunction with climate model projections to estimate changes from the current climate. Downscaled climate projections may allow researchers to produce future return-level estimates on smaller scales. Climate models still lack adequate resolution for identifying the small-scale features that drive localized precipitation, especially in the Florida Peninsula and over the KSC region. Statistical techniques and improved knowledge of the stochastic behavior of past rainfall could help improve intensity-duration-frequency estimates in the future. Statistically downscaled climate projections may allow researchers to produce realistic future return-level estimates on smaller scales (Palazi, 2013).

The IPCC AR5 has analyzed the literature and has stated that it is likely that precipitation extremes over land are increasing in the majority of locations. Studies also show that the large modern floods are comparable or surpass the large historical floods (pre-1900) in magnitude or frequency for central North America. It is most likely that extreme precipitation events over most mid-latitude locations and wet tropical regions will increase in intensity and frequency. The probable increase in extreme rainfall events can be attributed to warmer temperatures, higher saturation vapor pressures, and greater tropospheric precipitable water (IPCC, 2013).

Recommendations

Short duration return-levels. Twenty-four-hour and 72-hour duration return levels are useful when applications demand best estimates of events with longer durations. However, some applications, such as storm water management, demand estimates of shorter duration return levels, including 1-hour, 3-hour, and 6-hour events. For instance, the Florida Department of Transportation (DOT) uses rainfall return levels for calculating peak runoff rates. They use the peak runoff rates for designing drainage systems and planning roadways (Florida DOT, 2012). Future work could combine the methodologies used in this study with shorter duration sample data to estimate return levels of these short-duration events.

Examining shorter duration return-level estimates will provide additional information as to how variable the expected rainfall return levels may be. The researcher believes that shorter duration extreme rainfall events would be more useful for identifying the locations that most frequently receive heavy rainfall from deep moist convection forced by small-scale boundary interactions.

Classify rainfall by event type. Future work could involve categorizing rainfall events by event type (i.e., tropical systems, local convection, and extratropical systems). Categorizing the data by event type will allow one to ask questions such as "What is the likelihood that the most extreme rainfall event in any given year will be from local convection?" Another type of question could be "What are the rainfall return levels that can be expected from tropical systems?" Answers to the second question may be used as an analog for winds associated with heavy rainfall in tropical systems. Wind-driven rain into wind-damaged structures can cause costly water damage, as documented in KSC (2004). Estimating the potential for tropical events with heavy rainfall and high winds would assist with longer-range planning scenarios.

Introduce additional data sources. Introducing additional data sources with longer periods and increasing the size of the sample would improve the rainfall return-level estimate certainty. Fifteen years of data is too short a period to reveal changes in extreme rainfall reoccurrence frequencies. NOAA Atlas 14 (2013) does note that a positive statistically significant trend in maximum annual 1-hour precipitation exists at the closest site to the KSC Complex (Melbourne, closest site with hourly precipitation). NOAA Atlas 14 did not detect a statistically significant trend in maximum annual 24-hour precipitation at Titusville.

Introduce covariates. Covariate methods could reveal relationships between extreme rainfall events over KSC and large-scale climate oscillations such as El Niño Southern Oscillation. For example, La Niña tends to shift the highest probability of heavy rain events (> 1 inch) to earlier in the wet season (Florida Climate Center, n.d.). Hagemeyer (2006) showed that El Niño affects dry season storminess in Florida. El Niño could also affect the probability of extreme events during the dry and wet seasons. Covariate methods and extreme-value analyses could provide further insight into the likelihood of extreme weather events in the geographically complex environment of KSC.

References

Bodini, A., & Antonio, C. Q. (2008). Analysis of precipitation trends during the 2nd half of the 20th century in an area of Sardina (Italy) at high hydrological risk. Retrieved March 3, 2014, from http://www.mi.imati.cnr.it/iami/papers/08-11.pdf

Byers, H. R., & Rodebush, H. R. (1948). Causes of thunderstorms of the Florida peninsula. *Journal of Meteorology*, 5, 275-280.

Cheatle, J. (2006). Katrina's national security impacts. *World Watch*, 19, 23-25.

Coles, S. (2001). *An introduction to statistical modeling of extreme values.* London: Springer.

Dilumie, A. S., Gilleland, E., Bronaugh, D., & Wong, P. (2009). Extreme wind regime responses to climate variability and change in the inner south coast of British Columbia, Canada. *Atmosphere-Ocean*, 47, 41-62.

DOHS. (2006). The federal response to Hurricane Katrina lessons learned, Retrieved November 20, 2013, from http://library.stmarytx.edu/acadlib/edocs/katrinawh.pdf

DuMouchel, W. H. (1983). Estimating the stable index a in order to measure tail thickness: A critique. *The Annals of Statistics*, 11, 1019-1031.

Florida. (n.d.). Florida automated weather network. Retrieved March 3, 2014, from http://fawn.ifas.ufl.edu/

Florida Climate Center. (n.d.). Big rain events in the southeast. Retrieved April 13, 2014, from http://climatecenter.fsu.edu/climate-data-access-tools/big-rain

Florida DOT. (2012) Drainage handbook hydrology. Retrieved April 12, 2014, from http://www.dot.state.fl.us/rddesign/Hydraulics/files/HydrologyHB.pdf

Frank, N. L., Moore, P. L., & Fisher, G. E. (1967). Summer shower distribution over the florida peninsula as deduced from digitized radar data. *Journal of Applied Meteorology*, 6, 309-316.

Gentry, R. C., & Moore, P. L. (1954). Relation of local and general wind interaction near the sea coast to time and location of air-mass showers. *Journal of Meteorology*, 11, 507-511.

Gilleland, E., & Katz, R. W. (2011). New software to analyze how extremes change over time. *Eos*, 92(2), 13-14.

Gilleland, E., & Katz, R. W. (2006). Analyzing seasonal to interanual extreme weather and climate variability with the extremes toolkit. *18th Conference on Climate Variability and Change* (P. 2.15). Atlanta: 86th American Meteorological Society Annual Meeting.

Hagemeyer, B.C. (2006). ENSO, PNA, and NAO scenarios for extreme storminess, rainfall and temperature variability during the Florida dry season. *18th Conference on Climate Variability and Change* (P. 2.4). Atlanta: 86th American Meteorological Society Annual Meeting.

Hershfield, D.M. (1961), *Technical Paper No. 40, Rainfall Frequency Atlas of the United States for durations from 30 Minutes to 24 Hours and Return Periods from 1 to 100 Years*, U.S. Weather Bureau, [Available online at http://www.erh.noaa.gov/Tp40s.htm]

Institute for the Study of Society and Environment. (n.d.). Retrieved November 14, 2013, from Extreme Weather and Climate: http://www.isse.ucar.edu/extremevalues/evtk.html

IPCC. (2013). *Fifth Assesment Report (AR5)*. Retrieved November 20, 2013, from http://www.ipcc.ch/report/ar5/#.UpOVRsRDVjJ

Katz, R. W. (n.d). Statistics of Weather and Climate Extremes. Background [Available online at http://www.isse.ucar.edu/extremevalues/back.html

Katz, R. W., Brush, G. S., & Parlange, M. B. (2005). Statistics of extremes: Modeling ecological disturbances. *Ecology*, 86, 1124-1134.

Koch, S. E., desJardin, M., & Kocin, P.J. (1983). An interactive Barnes objective map analysis scheme for use with satellite and conventional data. *Journal of Climate and Applied Meteorology*, 22, 1487-1503

KSC. (2004). Hurricane recovery report *2004.*

Lascody, R. (2002) The Onset of the Wet and Dry Seasons in East Central Florida - A Subtropical Wet-Dry Climate [Available online at http://www.srh.noaa.gov/mlb/?n=wetdryseason]

NOAA Atlas 14, Volume 9 (2013) [Available online at http://www.nws.noaa.gov/oh/hdsc/relevant_publications.html#1_section]

Pallazi, E., Hardenburg J., & Von, Provenzale, A. (2013). Stochastic rainfall downscaling of climate models, *Journal of Hydrometeorology*, 15, 830-843

Richards, G. (1927). The rainfall of Florida. *Monthly Weather Review*, 55, 80-81.

Rosenzweig, C., & Horton, R. (2011, December 22). *NASA's CASI Building Climate-Reliant NASA Centers.* Retrieved October 25, 2013, from Center for a Better Life: http://livebettermagazine.com/article/nasas-casi-building-climate-resilient-nasa-centers/#thur

Rosenzweig, C., Horton, R. et al. (2014). Enhancing climate resilience at NASA centers: The climate adaptation investigator (CASI) workgroup for science and stewardship. *Bulletin of the American Meteorological Society*, 95, 1351–1363.

Scarrott, C., & MacDonald, A. (2012). A review of extreme value threshold estimation and uncertainty quantification. *Revstata Statistical Journal*, 10, 33-60.

Tannert, C., Elvers, H.-D., & Burkhard, J. (2007). The ethics of uncertainty. In the light of possible dangers research becomes a duty. *EMBO Rep*,8 , 892-896.

TRMM GV Gauge Quick Look Products. (n.d.). Retrieved October 1, 2012, from http://trmm-fc.gsfc.nasa.gov/trmm_gv/gauge/index.html

Wang, J., & Wolff, D. B. (2009). Evaluation of TRMM ground-validation radar-rain errors using rain gauge measurements. *Journal of Applied Meteorology and Climatology*, 49, 310-324.

Wang, J., & Wolff, D. B. (2011). Evaluation of TRMM rain estimates using ground measurements over Central Florida. *Journal of Applied Meteorology and Climatology*, 51, 926-940.

Appendix A

EVA Results

The EVA results presented in Appendix A include

- analysis threshold (mm)
- scale and shape parameter estimates
- 95% shape parameter confidence intervals
- number of threshold exceedances
- 100-year return level estimates and 95% confidence intervals (mm)
- exceedance rate (average number of points that exceeded the threshold per year)
- probability of threshold exceedance (probability of a 24-hour or 72-hour period exceeding the threshold)

Titusville 24-hour Duration

location	Titusville	Titusville	Titusville
threshold	35	40	45
scale	15.69	16.41	14.04
shape	0.176	0.181	0.291
shape 95% lower CI	0.051	0.039	0.102
shape 95% upper CI	0.300	0.323	0.481
exceedances	286	210	166
95% lower CI (mm)	153	149	133
100-year return level (mm)	240	243	294
95% upper CI (mm)	327	336	456
Exceedance rate ($year^{-1}$)	8.94	6.56	5.19
P (threshold exceedance)	0.024	0.018	0.014

Titusville 72-hour Duration

location	Titusville	Titusville	Titusville	Titusville
threshold	70	80	90	100
scale	25.17	24.39	28.45	29.57
shape	0.180	0.237	0.200	0.226
shape 95% lower CI	-0.022	-0.030	-0.111	-0.171
shape 95% upper CI	0.383	0.505	0.511	0.624
exceedances	124	87	58	41
95% lower CI (mm)	184	155	155	130
100-year return level (mm)	339	366	350	361
95% upper CI (mm)	495	577	545	592
Exceedance rate ($year^{-1}$)	3.88	2.72	1.81	1.28
P (threshold exceedance)	0.011	0.007	0.005	0.004

Titusville Dry Season 72-hour Duration

location	Titusville	Titusville	Titusville
threshold	25	30	35
scale	26.67	23.25	23.66
shape	0.078	0.157	0.165
shape 95% lower CI	-0.074	-0.030	-0.047
shape 95% upper CI	0.229	0.344	0.377
exceedances	174	153	125
95% lower CI (mm)	153	142	134
100-year return level (mm)	242	272	275
95% upper CI (mm)	330	401	416
Exceedance rate ($year^{-1}$)	5.44	4.78	3.91
P (threshold exceedance)	0.015	0.013	0.011

Titusville Wet Season 72-hour Duration

location	Titusville	Titusville	Titusville	Titusville
threshold	70	80	90	100
scale	21.92	21.85	23.57	24.93
shape	0.218	0.266	0.293	0.350
shape 95% lower CI	-0.014	-0.032	-0.083	-0.161
shape 95% upper CI	0.449	0.565	0.669	0.862
exceedances	94	63	41	27
95% lower CI (mm)	156	132	110	62
100-year return level (mm)	315	332	342	364
95% upper CI (mm)	474	531	573	665
exceedance rate ($year^{-1}$)	2.94	1.97	1.28	0.84
P (threshold exceedance)	0.008	0.005	0.004	0.002

Gridded 24-hour Duration

location	10_E	10_F	10_G	9_E	9_G	9_H	9_I	8_D	8_H	7_D
threshold	25	25	25	25	25	25	25	25	25	25
scale	17.90	18.43	18.47	18.61	17.42	18.56	18.64	19.53	19.48	20.08
shape	0.157	0.175	0.159	0.134	0.192	0.177	0.204	0.137	0.165	0.138
shape 95% lower CI	0.008	0.011	-0.003	0.001	0.017	0.010	0.028	-0.004	-0.002	-0.015
shape 95% upper CI	0.306	0.339	0.320	0.267	0.367	0.344	0.379	0.278	0.332	0.290
exceedances	164	155	162	173	166	159	160	174	148	176
95% lower CI	133.3	130.2	129.0	141.6	120.6	129.4	129.4	143.8	131.1	139.8
100-year return level	253.3	275.3	261.4	243.7	282.9	280.3	312.5	257.7	275.8	265.4
95% upper CI	373.2	420.4	393.9	345.8	445.3	431.1	495.6	371.7	420.5	390.9
exceedance rate ($year^{-1}$)	10.93	10.33	10.80	11.53	11.07	10.60	10.67	11.60	9.87	11.73
P (threshold exceedance)	0.030	0.028	0.030	0.032	0.030	0.029	0.029	0.032	0.027	0.032

location	7_E	7_F	6_C	6_D	6_E	6_F	5_C	5_D	5_E	5_F
threshold	25	25	25	25	25	25	25	25	25	25
scale	18.30	18.61	21.21	21.21	18.27	18.43	19.65	20.30	19.17	17.02
shape	0.190	0.204	0.134	0.122	0.191	0.174	0.155	0.154	0.127	0.216
shape 95% lower CI	0.035	0.050	-0.012	-0.012	0.031	0.015	0.003	0.008	-0.030	0.035
shape 95% upper CI	0.345	0.359	0.280	0.255	0.350	0.333	0.307	0.301	0.285	0.397
exceedances	178	180	170	176	172	165	169	180	156	162
95% lower CI	142.5	149.4	148.9	153.7	138.2	134.3	141.9	150.9	127.6	118.0
100-year return level	298.9	322.4	272.8	262.9	297.0	277.7	275.7	287.0	239.5	302.9
95% upper CI	455.4	495.4	396.7	372.1	455.8	421.0	409.5	423.0	351.4	487.9
exceedance rate ($year^{-1}$)	11.87	12.00	11.33	11.73	11.47	11.00	11.27	12.00	10.40	10.80
P (threshold exceedance)	0.032	0.033	0.031	0.032	0.031	0.030	0.031	0.033	0.028	0.030

Gridded 24-hour Duration

location	5_G	5_H	4_C	4_D	4_E	4_F	4_G	3_B	3_C	3_D
threshold	25	25	25	25	25	25	25	25	25	25
scale	17.88	18.87	22.01	19.69	20.88	19.10	21.39	15.21	17.55	16.81
shape	0.202	0.189	0.176	0.273	0.159	0.185	0.102	0.241	0.246	0.215
shape 95% lower CI	0.020	0.007	0.018	0.078	-0.028	-0.035	-0.087	0.053	0.064	0.031
shape 95% upper CI	0.384	0.372	0.335	0.469	0.346	0.404	0.291	0.429	0.429	0.399
exceedances	152	148	153	163	144	129	144	156	155	155
95% lower CI	118.7	121.4	155.5	124.2	122.6	94.0	114.4	105.9	124.5	113.9
100-year return level	295.1	293.5	324.0	440.5	285.1	282.5	237.8	299.3	348.3	295.6
95% upper CI	471.5	465.6	492.6	756.8	447.7	470.9	361.1	492.6	572.2	477.2
exceedance rate ($year^{-1}$)	10.13	9.87	10.20	10.87	9.60	8.60	9.60	10.40	10.33	10.33
P (threshold exceedance)	0.028	0.027	0.028	0.030	0.026	0.024	0.026	0.028	0.028	0.028

location	3_E	3_F	2_C	2_D	2_E	1_D
threshold	25	25	25	25	25	25
scale	17.55	21.01	18.00	17.16	17.51	17.59
shape	0.189	0.158	0.178	0.210	0.195	0.193
shape 95% lower CI	0.007	-0.046	0.011	0.030	0.004	0.003
shape 95% upper CI	0.372	0.362	0.345	0.390	0.386	0.384
exceedances	149	149	149	145	122	122
95% lower CI	114.5	110.4	125.9	117.5	108.1	108.5
100-year return level	275.2	288.2	270.2	289.8	267.5	266.8
95% upper CI	435.8	465.9	414.5	462.1	426.9	425.2
exceedance rate ($year^{-1}$)	9.93	9.93	9.93	9.67	8.13	8.13
P (threshold exceedance)	0.027	0.027	0.027	0.026	0.022	0.022

Gridded 24-hour Duration

location	10_E	10_F	10_G	9_E	9_G	9_H	9_I	8_D	8_H	7_D
threshold	30	30	30	30	30	30	30	30	30	30
scale	16.44	17.03	18.76	15.53	19.57	18.69	18.13	16.62	17.70	18.31
shape	0.212	0.233	0.173	0.218	0.159	0.192	0.244	0.219	0.229	0.196
shape 95% lower CI	0.031	0.035	-0.012	0.049	-0.023	0.003	0.036	0.041	0.023	0.010
shape 95% upper CI	0.394	0.432	0.358	0.387	0.341	0.380	0.451	0.398	0.435	0.382
exceedances	132	125	125	148	123	125	127	150	122	146
95% lower CI	117.0	109.1	120.2	123.4	123.6	120.1	107.3	122.6	106.0	122.0
100-year return level	279.8	308.4	269.0	279.4	264.9	287.2	340.7	299.3	311.9	296.8
95% upper CI	442.6	507.7	417.8	435.4	406.2	454.3	574.1	475.9	517.8	471.6
exceedance rate (year^{-1})	8.800	8.333	8.333	9.867	8.200	8.333	8.467	10.000	8.133	9.733
P (threshold exceedance)	0.024	0.023	0.023	0.027	0.022	0.023	0.023	0.027	0.022	0.027

location	7_E	7_F	6_C	6_D	6_E	6_F	5_C	5_D	5_E	5_F
threshold	30	30	30	30	30	30	30	30	30	30
scale	18.08	19.37	17.29	18.59	16.50	17.29	15.99	17.73	19.25	18.36
shape	0.219	0.212	0.238	0.189	0.263	0.226	0.277	0.234	0.139	0.210
shape 95% lower CI	0.039	0.040	0.049	0.023	0.064	0.030	0.067	0.049	-0.037	0.006
shape 95% upper CI	0.398	0.383	0.428	0.354	0.462	0.423	0.486	0.419	0.315	0.415
exceedances	140	139	150	150	140	132	144	152	123	121
95% lower CI	128.9	141.6	120.0	138.1	109.0	112.1	96.7	125.5	122.1	108.9
100-year return level	316.5	327.7	334.4	294.7	346.8	308.6	359.3	337.6	244.0	299.9
95% upper CI	504.2	513.8	548.8	451.3	584.6	505.2	622.0	549.7	365.9	490.8
exceedance rate (year^{-1})	9.333	9.267	10.000	10.000	9.333	8.800	9.600	10.133	8.200	8.067
P (threshold exceedance)	0.026	0.025	0.027	0.027	0.026	0.024	0.026	0.028	0.022	0.022

Gridded 24-hour Duration

location	5_G	5_H	4_C	4_D	4_E	4_F	4_G	3_B	3_C	3_D
threshold	30	30	30	30	30	30	30	30	30	30
scale	19.29	21.23	21.38	20.72	18.80	19.44	21.81	15.32	17.78	15.45
shape	0.191	0.158	0.206	0.274	0.240	0.202	0.099	0.271	0.269	0.293
shape 95% lower CI	-0.008	-0.030	0.026	0.058	-0.001	-0.062	-0.112	0.049	0.061	0.060
shape 95% upper CI	0.391	0.345	0.386	0.489	0.480	0.466	0.310	0.492	0.477	0.526
exceedances	115	111	126	130	119	101	116	118	121	122
95% lower CI	114.3	126.4	142.7	109.5	80.6	70.0	108.5	84.5	106.4	71.7
100-year return level	288.9	277.3	342.0	437.6	340.7	292.9	235.8	318.1	364.8	353.8
95% upper CI	463.4	428.1	541.3	765.6	600.7	515.9	363.0	551.7	623.1	635.9
exceedance rate (year^{-1})	7.667	7.400	8.400	8.667	7.933	6.733	7.733	7.867	8.067	8.133
P (threshold exceedance)	0.021	0.020	0.023	0.024	0.022	0.018	0.021	0.022	0.022	0.022

location	3_E	3_F	2_C	2_D	2_E	1_D
threshold	30	30	30	30	30	30
scale	18.03	20.39	15.85	15.07	14.43	14.57
shape	0.202	0.201	0.265	0.308	0.325	0.320
shape 95% lower CI	-0.008	-0.051	0.049	0.075	0.059	0.055
shape 95% upper CI	0.412	0.453	0.482	0.541	0.591	0.585
exceedances	114	120	121	116	100	100
95% lower CI	102.8	77.9	90.5	69.7	36.8	39.5
100-year return level	282.1	317.6	323.8	361.5	353.8	350.0
95% upper CI	461.4	557.3	557.1	653.3	670.7	660.4
exceedance rate (year^{-1})	7.600	8.000	8.067	7.733	6.667	6.667
P (threshold exceedance)	0.021	0.022	0.022	0.021	0.018	0.018

Gridded 24-hour Duration

location	10_E	10_F	10_G	9_E	9_G	9_H	9_I	8_D	8_H	7_D
threshold	35	35	35	35	35	35	35	35	35	35
scale	15.31	16.54	17.60	14.13	18.80	17.08	15.77	17.63	19.99	18.43
shape	0.272	0.282	0.227	0.298	0.201	0.258	0.353	0.218	0.205	0.219
shape 95% lower CI	0.052	0.042	0.001	0.080	-0.020	0.024	0.082	0.022	-0.019	0.001
shape 95% upper CI	0.492	0.523	0.454	0.516	0.422	0.492	0.624	0.414	0.429	0.436
exceedances	104	97	100	114	98	102	105	113	90	115
95% lower CI	90.8	78.1	95.2	87.6	103.1	86.6	23.3	117.0	105.3	104.5
100-year return level	312.9	341.5	297.5	330.5	285.9	325.0	442.2	297.7	299.9	311.3
95% upper CI	535.0	604.9	499.8	573.4	468.7	563.4	861.0	478.3	494.5	518.0
exceedance rate ($year^{-1}$)	6.933	6.467	6.667	7.600	6.533	6.800	7.000	7.533	6.000	7.667
P (threshold exceedance)	0.019	0.018	0.018	0.021	0.018	0.019	0.019	0.021	0.016	0.021

location	7_E	7_F	6_C	6_D	6_E	6_F	5_C	5_D	5_E	5_F
threshold	35	35	35	35	35	35	35	35	35	35
scale	17.25	16.40	14.61	17.22	16.37	16.83	16.96	19.11	17.58	18.83
shape	0.265	0.315	0.379	0.243	0.305	0.272	0.287	0.225	0.194	0.221
shape 95% lower CI	0.053	0.087	0.105	0.046	0.065	0.032	0.041	0.024	-0.016	-0.009
shape 95% upper CI	0.476	0.543	0.653	0.439	0.544	0.512	0.532	0.426	0.405	0.451
exceedances	112	117	120	122	108	103	108	116	101	95
95% lower CI	105.5	83.0	-1.4	117.9	73.8	79.2	71.9	121.1	104.9	97.3
100-year return level	345.9	408.6	483.1	325.4	380.7	339.6	366.9	329.8	265.5	304.6
95% upper CI	586.3	734.3	967.6	533.0	687.5	600.1	661.8	538.5	426.2	511.9
exceedance rate ($year^{-1}$)	7.467	7.800	8.000	8.133	7.200	6.867	7.200	7.733	6.733	6.333
P (threshold exceedance)	0.020	0.021	0.022	0.022	0.020	0.019	0.020	0.021	0.018	0.017

Gridded 24-hour Duration

location	5_G	5_H	4_C	4_D	4_E	4_F	4_G	3_B	3_C	3_D
threshold	35	35	35	35	35	35	35	35	35	35
scale	19.05	23.06	20.83	24.05	19.99	20.40	24.04	14.85	15.30	15.16
shape	0.219	0.136	0.240	0.235	0.233	0.195	0.062	0.329	0.378	0.352
shape 95% lower CI	-0.014	-0.054	0.033	0.003	-0.041	-0.108	-0.170	0.059	0.113	0.060
shape 95% upper CI	0.452	0.326	0.446	0.467	0.507	0.498	0.294	0.598	0.642	0.643
exceedances	92	87	103	99	93	80	89	90	100	93
95% lower CI	96.0	131.7	123.9	111.9	65.6	56.6	108.2	40.8	23.5	7.3
100-year return level	303.4	268.7	364.9	404.2	333.9	286.6	223.8	360.8	467.7	406.5
95% upper CI	510.8	405.7	605.8	696.6	602.2	516.5	339.3	680.7	911.9	805.6
exceedance rate ($year^{-1}$)	6.133	5.800	6.867	6.600	6.200	5.333	5.933	6.000	6.667	6.200
P (threshold exceedance)	0.017	0.016	0.019	0.018	0.017	0.015	0.016	0.016	0.018	0.017

location	3_E	3_F	2_C	2_D	2_E	1_D
threshold	35	35	35	35	35	35
scale	16.54	23.96	15.87	13.66	15.02	14.58
shape	0.271	0.130	0.305	0.421	0.378	0.394
shape 95% lower CI	0.018	-0.159	0.044	0.108	0.013	0.022
shape 95% upper CI	0.523	0.420	0.566	0.734	0.743	0.766
exceedances	92	91	92	89	72	73
95% lower CI	70.1	77.8	55.3	-57.4	-69.2	-90.5
100-year return level	321.9	275.2	352.0	481.6	406.4	423.1
95% upper CI	573.7	472.5	648.7	1020.5	881.9	936.6
exceedance rate ($year^{-1}$)	6.133	6.067	6.133	5.933	4.800	4.867
P (threshold exceedance)	0.017	0.017	0.017	0.016	0.013	0.013

Gridded 72-hour Duration

location	10_E	10_F	10_G	9_E	9_G	9_H	9_I	8_D	8_H	7_D
threshold	40	40	40	40	40	40	40	40	40	40
scale	31.11	28.01	28.75	29.42	30.22	29.38	28.74	30.90	28.93	33.19
shape	0.142	0.186	0.169	0.145	0.162	0.165	0.221	0.129	0.197	0.114
shape 95% lower CI	-0.018	0.016	0.006	-0.007	-0.001	0.015	0.027	-0.030	0.000	-0.060
shape 95% upper CI	0.301	0.357	0.333	0.296	0.324	0.316	0.415	0.287	0.395	0.288
exceedances	126	127	127	138	123	126	124	141	111	135
95% lower CI	204.3	192.7	197.8	206.1	203.7	211.8	177.8	202.6	169.6	194.3
100-year return level	391.1	418.5	402.5	383.0	406.8	403.9	484.6	380.0	434.3	381.2
95% upper CI	577.9	644.2	607.1	559.8	609.8	596.0	791.3	557.4	699.0	568.0
exceedance rate ($year^{-1}$)	8.400	8.467	8.467	9.200	8.200	8.400	8.267	9.400	7.400	9.000
P (threshold exceedance)	0.023	0.023	0.023	0.025	0.022	0.023	0.023	0.026	0.020	0.025

location	7_E	7_F	6_C	6_D	6_E	6_F	5_C	5_D	5_E	5_F
threshold	40	40	40	40	40	40	40	40	40	40
scale	28.84	29.81	30.75	29.08	30.21	28.12	29.61	29.10	25.84	25.84
shape	0.169	0.186	0.170	0.177	0.153	0.164	0.169	0.170	0.181	0.203
shape 95% lower CI	-0.002	0.025	-0.018	-0.004	-0.023	-0.005	-0.016	-0.006	-0.014	0.020
shape 95% upper CI	0.341	0.347	0.357	0.358	0.329	0.333	0.355	0.347	0.375	0.387
exceedances	138	137	132	138	129	130	129	137	125	123
95% lower CI	192.7	214.2	185.0	186.4	188.8	188.6	181.1	188.7	156.9	171.5
100-year return level	411.3	449.7	432.0	426.6	398.0	389.1	415.1	415.2	380.1	410.7
95% upper CI	629.9	685.2	679.0	666.8	607.2	589.6	649.1	641.7	603.3	649.9
exceedance rate ($year^{-1}$)	9.200	9.133	8.800	9.200	8.600	8.667	8.600	9.133	8.333	8.200
P (threshold exceedance)	0.025	0.025	0.024	0.025	0.024	0.024	0.024	0.025	0.023	0.022

Gridded 72-hour Duration

location	5_G	5_H	4_C	4_D	4_E	4_F	4_G	3_B	3_C	3_D
threshold	40	40	40	40	40	40	40	40	40	40
scale	26.42	26.42	31.36	30.63	28.53	29.99	28.51	23.56	25.98	26.18
shape	0.199	0.236	0.149	0.209	0.178	0.143	0.139	0.201	0.208	0.207
shape 95% lower CI	0.021	0.033	-0.015	0.018	-0.017	-0.079	-0.071	-0.014	0.022	-0.004
shape 95% upper CI	0.378	0.439	0.313	0.401	0.372	0.365	0.349	0.415	0.394	0.417
exceedances	119	116	130	125	112	97	114	121	127	114
95% lower CI	178.1	157.7	205.2	187.6	167.0	144.1	148.3	130.7	171.1	145.2
100-year return level	409.5	467.4	407.1	493.0	400.2	360.5	350.9	373.1	423.9	413.3
95% upper CI	641.0	777.1	609.0	798.4	633.4	576.9	553.5	615.5	676.8	681.3
exceedance rate (year^{-1})	7.933	7.733	8.667	8.333	7.467	6.467	7.600	8.067	8.467	7.600
P (threshold exceedance)	0.022	0.021	0.024	0.023	0.020	0.018	0.021	0.022	0.023	0.021

location	3_E	3_F	2_C	2_D	2_E	1_D
threshold	40	40	40	40	40	40
scale	25.09	27.72	21.22	22.63	24.69	24.85
shape	0.209	0.217	0.288	0.254	0.196	0.192
shape 95% lower CI	-0.012	-0.047	0.065	0.037	-0.037	-0.039
shape 95% upper CI	0.430	0.481	0.510	0.470	0.428	0.423
exceedances	115	115	124	117	91	91
95% lower CI	130.8	89.8	112.2	126.6	119.7	121.3
100-year return level	402.1	453.8	477.0	435.1	356.7	354.5
95% upper CI	673.3	817.8	841.9	743.5	593.7	587.7
exceedance rate (year^{-1})	7.667	7.667	8.267	7.800	6.067	6.067
P (threshold exceedance)	0.021	0.021	0.023	0.021	0.017	0.017

Gridded 72-hour Duration

location	10_E	10_F	10_G	9_E	9_G	9_H	9_I	8_D	8_H	7_D
threshold	45	45	45	45	45	45	45	45	45	45
scale	27.12	23.84	26.74	24.45	27.31	26.19	30.53	31.78	28.64	37.39
shape	0.206	0.272	0.204	0.229	0.208	0.217	0.202	0.125	0.215	0.067
shape 95% lower CI	0.012	0.060	0.021	0.040	0.020	0.038	0.009	-0.040	-0.001	-0.096
shape 95% upper CI	0.400	0.485	0.388	0.417	0.396	0.396	0.396	0.289	0.431	0.229
exceedances	116	115	114	129	112	114	107	120	96	112
95% lower CI	171.9	142.1	180.0	170.2	178.8	185.0	186.0	201.8	154.1	208.8
100-year return level	432.8	493.2	422.2	440.2	434.9	434.3	465.2	377.6	446.8	356.4
95% upper CI	693.6	844.3	664.5	710.3	691.0	683.5	744.5	553.3	739.4	504.0
exceedance rate ($year^{-1}$)	7.733	7.667	7.600	8.600	7.467	7.600	7.133	8.000	6.400	7.467
P (threshold exceedance)	0.021	0.021	0.021	0.024	0.020	0.021	0.020	0.022	0.018	0.020

location	7_E	7_F	6_C	6_D	6_E	6_F	5_C	5_D	5_E	5_F
threshold	45	45	45	45	45	45	45	45	45	45
scale	27.65	29.27	28.88	29.77	28.58	23.74	25.39	29.80	23.89	22.84
shape	0.198	0.204	0.212	0.174	0.187	0.256	0.257	0.168	0.227	0.275
shape 95% lower CI	0.006	0.028	-0.001	-0.014	-0.012	0.039	0.032	-0.017	0.002	0.053
shape 95% upper CI	0.389	0.380	0.424	0.363	0.387	0.473	0.482	0.354	0.452	0.496
exceedances	121	119	117	119	114	118	118	118	111	109
95% lower CI	175.6	202.0	159.1	184.0	169.3	135.1	130.9	185.3	128.1	126.9
100-year return level	431.0	462.5	468.2	421.9	422.0	464.1	495.8	412.5	412.3	470.7
95% upper CI	686.4	723.1	777.3	659.7	674.7	793.1	860.6	639.7	696.5	814.6
exceedance rate ($year^{-1}$)	8.067	7.933	7.800	7.933	7.600	7.867	7.867	7.867	7.400	7.267
P (threshold exceedance)	0.022	0.022	0.021	0.022	0.021	0.022	0.022	0.022	0.020	0.020

Gridded 72-hour Duration

location	5_G	5_H	4_C	4_D	4_E	4_F	4_G	3_B	3_C	3_D
threshold	45	45	45	45	45	45	45	45	45	45
scale	21.96	25.50	30.36	32.97	26.28	28.01	27.46	26.84	24.51	24.06
shape	0.287	0.264	0.172	0.190	0.224	0.193	0.165	0.151	0.250	0.264
shape 95% lower CI	0.069	0.039	-0.008	-0.005	0.002	-0.065	-0.068	-0.065	0.038	0.022
shape 95% upper CI	0.506	0.489	0.352	0.385	0.446	0.450	0.398	0.367	0.461	0.506
exceedances	111	102	114	105	101	85	100	97	110	100
95% lower CI	126.5	132.9	193.9	192.8	140.0	113.6	133.0	143.3	145.3	108.2
100-year return level	479.7	489.8	421.7	475.2	432.9	393.4	365.7	340.1	457.8	461.9
95% upper CI	832.9	846.7	649.5	757.6	725.8	673.1	598.5	536.9	770.4	815.6
exceedance rate ($year^{-1}$)	7.400	6.800	7.600	7.000	6.733	5.667	6.667	6.467	7.333	6.667
P (threshold exceedance)	0.020	0.019	0.021	0.019	0.018	0.016	0.018	0.018	0.020	0.018

location	3_E	3_F	2_C	2_D	2_E	1_D
threshold	45	45	45	45	45	45
scale	21.06	33.07	24.55	23.60	25.28	25.42
shape	0.332	0.133	0.243	0.265	0.210	0.207
shape 95% lower CI	0.045	-0.144	0.014	0.020	-0.056	-0.057
shape 95% upper CI	0.620	0.410	0.473	0.510	0.477	0.471
exceedances	101	92	97	94	74	74
95% lower CI	18.4	113.7	125.7	104.1	99.7	102.1
100-year return level	535.1	380.5	432.4	447.8	368.6	366.2
95% upper CI	1051.8	647.3	739.0	791.5	637.6	630.3
exceedance rate ($year^{-1}$)	6.733	6.133	6.467	6.267	4.933	4.933
P (threshold exceedance)	0.018	0.017	0.018	0.017	0.014	0.014

Gridded 72-hour Duration

location	10_E	10_F	10_G	9_E	9_G	9_H	9_I	8_D	8_H	7_D
threshold	50	50	50	50	50	50	50	50	50	50
scale	24.76	22.07	23.04	21.80	27.69	24.65	28.16	27.36	29.89	35.42
shape	0.261	0.330	0.278	0.302	0.213	0.252	0.250	0.197	0.210	0.091
shape 95% lower CI	0.032	0.082	0.057	0.072	0.016	0.051	0.026	-0.005	-0.015	-0.088
shape 95% upper CI	0.491	0.578	0.498	0.531	0.411	0.452	0.474	0.399	0.435	0.271
exceedances	103	100	104	113	96	102	96	111	81	102
95% lower CI	129.6	85.0	133.3	114.8	173.9	162.7	148.9	168.0	153.5	198.8
100-year return level	478.8	556.0	478.1	512.2	435.9	458.7	504.2	422.4	442.3	366.3
95% upper CI	828.0	1027.0	823.0	909.6	697.8	754.6	859.5	676.8	731.0	533.8
exceedance rate (year^{-1})	6.867	6.667	6.933	7.533	6.400	6.800	6.400	7.400	5.400	6.800
P (threshold exceedance)	0.019	0.018	0.019	0.021	0.018	0.019	0.018	0.020	0.015	0.019

location	7_E	7_F	6_C	6_D	6_E	6_F	5_C	5_D	5_E	5_F
threshold	50	50	50	50	50	50	50	50	50	50
scale	29.00	29.56	30.58	26.77	29.20	22.24	26.03	26.91	26.57	22.11
shape	0.191	0.209	0.197	0.236	0.189	0.312	0.271	0.232	0.194	0.320
shape 95% lower CI	-0.009	0.025	-0.025	0.014	-0.022	0.051	0.018	0.010	-0.034	0.057
shape 95% upper CI	0.391	0.393	0.419	0.457	0.401	0.572	0.525	0.454	0.422	0.582
exceedances	101	103	99	107	97	101	98	105	89	92
95% lower CI	174.8	197.2	159.8	147.0	164.4	72.9	101.7	146.9	139.5	71.8
100-year return level	425.4	463.9	453.2	472.0	421.7	523.7	512.3	464.9	386.3	520.3
95% upper CI	676.1	730.6	746.7	797.0	679.1	974.5	923.0	782.8	633.1	968.8
exceedance rate (year^{-1})	6.733	6.867	6.600	7.133	6.467	6.733	6.533	7.000	5.933	6.133
P (threshold exceedance)	0.018	0.019	0.018	0.020	0.018	0.018	0.018	0.019	0.016	0.017

Gridded 72-hour Duration

location	5_G	5_H	4_C	4_D	4_E	4_F	4_G	3_B	3_C	3_D
threshold	50	50	50	50	50	50	50	50	50	50
scale	21.59	28.93	27.71	27.99	26.23	27.31	25.02	27.03	25.43	22.82
shape	0.323	0.228	0.223	0.275	0.240	0.218	0.228	0.163	0.259	0.325
shape 95% lower CI	0.073	0.006	0.015	0.043	-0.001	-0.068	-0.045	-0.076	0.026	0.036
shape 95% upper CI	0.573	0.451	0.431	0.508	0.481	0.505	0.501	0.403	0.493	0.613
exceedances	92	82	102	98	86	74	88	81	90	84
95% lower CI	85.8	153.3	165.0	135.0	125.2	89.9	91.5	131.8	128.9	38.1
100-year return level	516.1	458.9	459.0	555.5	443.5	409.9	410.4	347.6	468.4	529.6
95% upper CI	946.4	764.5	753.0	975.9	761.8	729.9	729.2	563.5	807.9	1021.2
exceedance rate ($year^{-1}$)	6.133	5.467	6.800	6.533	5.733	4.933	5.867	5.400	6.000	5.600
P (threshold exceedance)	0.017	0.015	0.019	0.018	0.016	0.014	0.016	0.015	0.016	0.015

location	3_E	3_F	2_C	2_D	2_E	1_D
threshold	50	50	50	50	50	50
scale	24.38	38.43	22.72	22.35	25.04	25.22
shape	0.281	0.049	0.307	0.324	0.237	0.232
shape 95% lower CI	-0.028	-0.221	0.037	0.034	-0.067	-0.069
shape 95% upper CI	0.591	0.319	0.577	0.613	0.541	0.533
exceedances	80	77	83	79	62	62
95% lower CI	37.5	143.1	70.8	41.2	71.8	76.2
100-year return level	471.4	330.6	491.4	507.8	385.9	382.2
95% upper CI	905.4	518.1	912.0	974.4	700.0	688.1
exceedance rate ($year^{-1}$)	5.333	5.133	5.533	5.267	4.133	4.133
P (threshold exceedance)	0.015	0.014	0.015	0.014	0.011	0.011

Gridded 72-hour Duration Dry Season

location	10_E	10_F	10_G	9_E	9_G	9_H	9_I	8_D	8_H	7_D
threshold	20	20	20	20	20	20	20	20	20	20
scale	28.18	30.66	32.42	29.12	30.68	36.54	28.01	20.40	31.50	20.65
shape	-0.222	-0.282	-0.280	-0.240	-0.293	-0.393	0.071	0.000	-0.257	0.000
shape 95% lower CI	-0.472	-0.521	-0.488	-0.459	-0.533	-0.605	-0.141	-0.279	-0.566	-0.253
shape 95% upper CI	0.028	-0.042	-0.072	-0.021	-0.054	-0.181	0.283	0.279	0.053	0.253
exceedances	78	74	71	82	76	74	70	86	76	84
95% lower CI	72.7	62.0	66.5	74.0	58.4	9.0	113.7	64.7	64.8	71.9
100-year return level	115.4	109.9	115.2	114.7	107.9	104.9	236.6	149.9	118.0	151.0
95% upper CI	158.1	157.9	163.9	155.5	157.4	200.8	359.6	235.0	171.2	230.1
exceedance rate ($year^{-1}$)	5.200	4.933	4.733	5.467	5.067	4.933	4.667	5.733	5.067	5.600
P (threshold exceedance)	0.014	0.014	0.013	0.015	0.014	0.014	0.013	0.016	0.014	0.015

location	7_E	7_F	6_C	6_D	6_E	6_F	5_C	5_D	5_E	5_F
threshold	20	20	20	20	20	20	20	20	20	20
scale	27.63	30.21	26.88	26.27	28.13	26.33	22.20	24.70	28.35	28.44
shape	-0.128	-0.185	-0.084	-0.071	-0.133	-0.093	0.045	-0.049	-0.132	-0.128
shape 95% lower CI	-0.366	-0.457	-0.340	-0.314	-0.363	-0.345	-0.244	-0.294	-0.388	-0.360
shape 95% upper CI	0.109	0.088	0.171	0.172	0.097	0.159	0.333	0.196	0.124	0.104
exceedances	81	86	73	81	80	84	77	84	76	82
95% lower CI	86.1	79.3	84.4	86.6	88.2	83.2	67.3	83.8	83.9	89.2
100-year return level	139.4	133.0	149.9	153.5	140.0	146.1	180.2	154.6	140.5	143.3
95% upper CI	192.8	186.7	215.4	220.4	191.7	209.1	293.2	225.4	197.2	197.4
exceedance rate ($year^{-1}$)	5.400	5.733	4.867	5.400	5.333	5.600	5.133	5.600	5.067	5.467
P (threshold exceedance)	0.015	0.016	0.013	0.015	0.015	0.015	0.014	0.015	0.014	0.015

Gridded 72-hour Duration Dry Season

location	5_G	5_H	4_C	4_D	4_E	4_F	4_G	3_B	3_C	3_D
threshold	20	20	20	20	20	20	20	20	20	20
scale	30.19	25.44	23.51	21.10	24.76	23.09	30.95	24.71	22.07	25.24
shape	-0.173	-0.028	0.143	0.111	-0.035	0.159	-0.063	-0.026	0.187	-0.006
shape 95% lower CI	-0.413	-0.282	-0.178	-0.183	-0.320	-0.111	-0.308	-0.292	-0.096	-0.250
shape 95% upper CI	0.067	0.227	0.465	0.404	0.251	0.429	0.182	0.240	0.470	0.238
exceedances	80	81	73	83	76	67	74	76	75	72
95% lower CI	86.2	84.3	46.3	58.8	74.3	73.3	98.6	79.6	59.4	88.1
100-year return level	135.9	167.3	254.9	213.6	158.9	258.9	179.3	162.5	280.0	173.4
95% upper CI	185.6	250.3	463.6	368.3	243.6	444.4	260.0	245.5	500.5	258.7
exceedance rate ($year^{-1}$)	5.333	5.400	4.867	5.533	5.067	4.467	4.933	5.067	5.000	4.800
P (threshold exceedance)	0.015	0.015	0.013	0.015	0.014	0.012	0.014	0.014	0.014	0.013

location	3_E	3_F	2_C	2_D	2_E	1_D
threshold	20	20	20	20	20	20
scale	20.96	24.52	21.86	18.96	18.29	18.51
shape	0.135	0.137	0.145	0.227	0.095	0.089
shape 95% lower CI	-0.174	-0.163	-0.081	-0.040	-0.191	-0.196
shape 95% upper CI	0.445	0.438	0.371	0.495	0.381	0.374
exceedances	77	75	76	78	67	67
95% lower CI	49.6	60.0	92.9	57.5	59.3	60.2
100-year return level	226.3	261.4	241.9	283.3	171.8	170.6
95% upper CI	403.0	462.8	391.0	509.1	284.3	281.1
exceedance rate ($year^{-1}$)	5.133	5.000	5.067	5.200	4.467	4.467
P (threshold exceedance)	0.014	0.014	0.014	0.014	0.012	0.012

Gridded 72-hour Duration Dry Season

location	10_E	10_F	10_G	9_E	9_G	9_H	9_I	8_D	8_H	7_D
threshold	25	25	25	25	25	25	25	25	25	25
scale	29.31	34.39	36.26	30.25	34.96	37.76	28.40	27.90	39.69	24.78
shape	-0.275	-0.385	-0.371	-0.290	-0.409	-0.451	0.069	-0.220	-0.464	-0.122
shape 95% lower CI	-0.543	-0.596	-0.561	-0.524	-0.619	-0.662	-0.153	-0.476	-0.733	-0.402
shape 95% upper CI	-0.007	-0.174	-0.181	-0.055	-0.200	-0.241	0.291	0.036	-0.194	0.157
exceedances	63	58	56	66	59	62	59	64	59	63
95% lower CI	63.9	16.8	25.7	62.8	-0.1	-39.2	113.8	75.8	-56.3	77.6
100-year return level	111.4	105.4	112.0	111.6	103.1	103.2	235.7	118.5	105.3	131.0
95% upper CI	158.8	193.9	198.3	160.4	206.2	245.6	357.6	161.1	266.9	184.4
exceedance rate (year^{-1})	4.200	3.867	3.733	4.400	3.933	4.133	3.933	4.267	3.933	4.200
P (threshold exceedance)	0.011	0.011	0.010	0.012	0.011	0.011	0.011	0.012	0.011	0.011

location	7_E	7_F	6_C	6_D	6_E	6_F	5_C	5_D	5_E	5_F
threshold	25	25	25	25	25	25	25	25	25	25
scale	28.39	37.00	25.88	23.23	25.19	28.72	24.09	26.26	28.36	28.60
shape	-0.160	-0.352	-0.070	0.000	-0.079	-0.163	0.000	-0.095	-0.148	-0.146
shape 95% lower CI	-0.424	-0.618	-0.369	-0.299	-0.355	-0.435	-0.335	-0.359	-0.438	-0.403
shape 95% upper CI	0.104	-0.087	0.230	0.299	0.197	0.110	0.335	0.169	0.142	0.111
exceedances	66	67	61	68	69	67	61	67	63	68
95% lower CI	84.6	38.2	78.4	72.5	81.3	83.7	65.1	85.3	81.4	87.7
100-year return level	135.7	117.8	152.3	167.4	147.8	136.3	170.1	146.9	138.5	140.9
95% upper CI	186.7	197.4	226.3	262.4	214.2	188.9	275.0	208.5	195.5	194.1
exceedance rate (year^{-1})	4.400	4.467	4.067	4.533	4.600	4.467	4.067	4.467	4.200	4.533
P (threshold exceedance)	0.012	0.012	0.011	0.012	0.013	0.012	0.011	0.012	0.011	0.012

Gridded 72-hour Duration Dry Season

location	5_G	5_H	4_C	4_D	4_E	4_F	4_G	3_B	3_C	3_D
threshold	25	25	25	25	25	25	25	25	25	25
scale	34.81	28.02	27.13	22.59	26.74	22.02	27.86	23.60	23.40	20.95
shape	-0.283	-0.094	0.070	0.089	-0.090	0.199	0.000	0.000	0.174	0.103
shape 95% lower CI	-0.529	-0.352	-0.306	-0.285	-0.425	-0.114	-0.270	-0.306	-0.139	-0.208
shape 95% upper CI	-0.037	0.164	0.447	0.464	0.246	0.512	0.270	0.306	0.488	0.413
exceedances	63	65	57	64	60	56	65	63	60	63
95% lower CI	70.0	90.6	48.8	39.4	72.3	49.3	88.3	70.8	54.2	60.9
100-year return level	125.9	154.9	225.6	207.1	149.2	275.2	194.6	167.9	273.4	200.8
95% upper CI	181.8	219.2	402.4	374.8	226.1	501.0	300.9	264.9	492.5	340.8
exceedance rate ($year^{-1}$)	4.200	4.333	3.800	4.267	4.000	3.733	4.333	4.200	4.000	4.200
P (threshold exceedance)	0.011	0.012	0.010	0.012	0.011	0.010	0.012	0.011	0.011	0.011

location	3_E	3_F	2_C	2_D	2_E	1_D
threshold	25	25	25	25	25	25
scale	22.29	27.22	20.50	19.73	14.18	14.52
shape	0.110	0.088	0.191	0.235	0.261	0.247
shape 95% lower CI	-0.251	-0.251	-0.081	-0.069	-0.113	-0.123
shape 95% upper CI	0.471	0.426	0.463	0.538	0.635	0.616
exceedances	61	60	63	61	56	56
95% lower CI	42.1	61.2	69.3	43.5	0.8	7.0
100-year return level	215.5	240.4	258.9	286.4	226.3	220.8
95% upper CI	388.9	419.5	448.5	529.2	451.9	434.6
exceedance rate ($year^{-1}$)	4.067	4.000	4.200	4.067	3.733	3.733
P (threshold exceedance)	0.011	0.011	0.011	0.011	0.010	0.010

Gridded 72-hour Duration Dry Season

location	10_E	10_F	10_G	9_E	9_G	9_H	9_I	8_D	8_H	7_D
threshold	30	30	30	30	30	30	30	30	30	30
scale	25.62	35.81	33.83	29.57	32.91	37.10	26.77	26.96	39.98	24.57
shape	-0.220	-0.445	-0.361	-0.307	-0.409	-0.481	0.101	-0.223	-0.513	-0.133
shape 95% lower CI	-0.548	-0.663	-0.569	-0.566	-0.638	-0.704	-0.155	-0.517	-0.798	-0.457
shape 95% upper CI	0.109	-0.226	-0.153	-0.047	-0.181	-0.257	0.356	0.071	-0.227	0.191
exceedances	56	47	49	55	51	53	51	53	50	51
95% lower CI	69.4	-27.6	34.2	57.8	4.2	-64.8	100.6	74.0	-113.6	74.9
100-year return level	114.9	104.3	112.2	110.8	103.0	102.6	242.9	118.2	104.1	129.8
95% upper CI	160.5	236.3	190.1	163.7	201.9	270.0	385.3	162.5	321.7	184.8
exceedance rate (year^{-1})	3.733	3.133	3.267	3.667	3.400	3.533	3.400	3.533	3.333	3.400
P (threshold exceedance)	0.010	0.009	0.009	0.010	0.009	0.010	0.009	0.010	0.009	0.009

location	7_E	7_F	6_C	6_D	6_E	6_F	5_C	5_D	5_E	5_F
threshold	30	30	30	30	30	30	30	30	30	30
scale	27.76	40.17	24.08	23.18	22.14	25.99	24.12	26.84	28.88	30.80
shape	-0.164	-0.446	-0.029	0.000	0.000	-0.117	0.000	-0.117	-0.179	-0.206
shape 95% lower CI	-0.466	-0.723	-0.401	-0.341	-0.341	-0.438	-0.341	-0.418	-0.508	-0.489
shape 95% upper CI	0.138	-0.169	0.344	0.341	0.341	0.203	0.341	0.183	0.151	0.078
exceedances	55	55	51	55	58	58	49	54	52	54
95% lower CI	82.0	-34.8	64.6	65.9	64.2	78.5	60.7	83.6	78.9	84.6
100-year return level	135.3	113.6	159.5	167.2	162.3	141.6	170.0	144.3	135.0	135.2
95% upper CI	188.5	262.0	254.3	268.5	260.3	204.8	279.3	205.1	191.0	185.8
exceedance rate (year^{-1})	3.667	3.667	3.400	3.667	3.867	3.867	3.267	3.600	3.467	3.600
P (threshold exceedance)	0.010	0.010	0.009	0.010	0.011	0.011	0.009	0.010	0.009	0.010

Gridded 72-hour Duration Dry Season

location	5_G	5_H	4_C	4_D	4_E	4_F	4_G	3_B	3_C	3_D
threshold	30	30	30	30	30	30	30	30	30	30
scale	33.67	29.20	26.13	25.73	25.70	23.71	27.81	23.34	20.06	16.96
shape	-0.287	-0.129	0.097	-0.001	-0.073	0.188	0.000	0.000	0.294	0.256
shape 95% lower CI	-0.563	-0.404	-0.345	-0.447	-0.489	-0.163	-0.282	-0.365	-0.127	-0.179
shape 95% upper CI	-0.012	0.147	0.538	0.444	0.343	0.539	0.282	0.365	0.715	0.691
exceedances	54	53	49	51	50	44	56	52	51	53
95% lower CI	68.2	91.9	24.9	45.3	60.7	43.3	80.7	63.3	-52.2	-28.6
100-year return level	125.7	150.5	233.6	179.8	152.0	271.8	195.1	166.9	342.2	262.1
95% upper CI	183.1	209.2	442.3	314.2	243.3	500.3	309.6	270.6	736.7	552.7
exceedance rate (year^{-1})	3.600	3.533	3.267	3.400	3.333	2.933	3.733	3.467	3.400	3.533
P (threshold exceedance)	0.010	0.010	0.009	0.009	0.009	0.008	0.010	0.009	0.009	0.010

location	3_E	3_F	2_C	2_D	2_E	1_D
threshold	30	30	30	30	30	30
scale	27.15	23.97	19.85	20.51	12.30	11.10
shape	0.000	0.183	0.231	0.244	0.438	0.511
shape 95% lower CI	-0.542	-0.234	-0.094	-0.101	-0.159	-0.105
shape 95% upper CI	0.542	0.600	0.556	0.590	1.034	1.128
exceedances	48	52	51	48	41	42
95% lower CI	30.7	3.3	40.6	26.5	-228.5	-349.8
100-year return level	187.0	282.0	275.3	291.1	331.4	398.4
95% upper CI	343.3	560.8	510.0	555.7	891.4	1146.6
exceedance rate (year^{-1})	3.200	3.467	3.400	3.200	2.733	2.800
P (threshold exceedance)	0.009	0.009	0.009	0.009	0.007	0.008

Gridded 72-hour Duration Wet Season

location	10_E	10_F	10_G	9_E	9_G	9_H	9_I	8_D	8_H	7_D
threshold	40	40	40	40	40	40	40	40	40	40
scale	32.36	30.55	29.14	30.41	30.70	29.68	27.97	34.46	27.44	39.86
shape	0.167	0.207	0.213	0.175	0.200	0.207	0.254	0.120	0.294	0.071
shape 95% lower CI	-0.024	0.002	0.008	-0.007	0.001	0.021	0.020	-0.054	0.022	-0.109
shape 95% upper CI	0.358	0.412	0.418	0.358	0.398	0.393	0.488	0.294	0.566	0.250
exceedances	104	101	104	112	101	101	97	113	85	106
95% lower CI	184.8	169.0	163.7	187.0	175.4	184.9	125.7	199.1	67.7	202.3
100-year return level	423.9	460.3	454.4	419.4	450.4	448.9	499.6	388.8	548.1	372.8
95% upper CI	663.0	751.7	745.1	651.8	725.3	712.9	873.5	578.5	1028.6	543.2
exceedance rate ($year^{-1}$)	6.933	6.733	6.933	7.467	6.733	6.733	6.467	7.533	5.667	7.067
P (threshold exceedance)	0.019	0.018	0.019	0.020	0.018	0.018	0.018	0.021	0.016	0.019

location	7_E	7_F	6_C	6_D	6_E	6_F	5_C	5_D	5_E	5_F
threshold	40	40	40	40	40	40	40	40	40	40
scale	31.58	30.56	35.19	34.97	33.66	31.31	32.44	34.36	28.86	28.59
shape	0.177	0.232	0.145	0.136	0.156	0.172	0.163	0.146	0.182	0.210
shape 95% lower CI	-0.021	0.027	-0.056	-0.053	-0.050	-0.028	-0.041	-0.051	-0.042	-0.002
shape 95% upper CI	0.374	0.438	0.346	0.326	0.362	0.371	0.366	0.343	0.407	0.422
exceedances	108	106	104	104	98	97	103	103	92	91
95% lower CI	177.4	171.8	182.7	190.8	173.2	172.1	172.1	183.0	140.4	152.8
100-year return level	432.6	512.5	423.4	409.4	417.0	411.4	417.8	415.0	391.8	426.6
95% upper CI	687.8	853.3	664.0	628.1	660.9	650.8	663.4	646.9	643.2	700.4
exceedance rate ($year^{-1}$)	7.200	7.067	6.933	6.933	6.533	6.467	6.867	6.867	6.133	6.067
P (threshold exceedance)	0.020	0.019	0.019	0.019	0.018	0.018	0.019	0.019	0.017	0.017

Gridded 72-hour Duration Wet Season

location	5_G	5_H	4_C	4_D	4_E	4_F	4_G	3_B	3_C	3_D
threshold	40	40	40	40	40	40	40	40	40	40
scale	29.94	29.00	29.90	32.29	31.58	29.67	30.48	25.40	26.85	26.40
shape	0.204	0.245	0.184	0.230	0.179	0.141	0.140	0.208	0.200	0.237
shape 95% lower CI	-0.003	0.013	0.002	0.010	-0.043	-0.103	-0.100	-0.038	0.003	-0.005
shape 95% upper CI	0.411	0.476	0.367	0.450	0.400	0.386	0.379	0.454	0.396	0.479
exceedances	85	86	108	99	86	76	81	92	99	89
95% lower CI	161.2	133.6	186.1	159.7	152.3	126.3	132.4	110.3	160.0	115.1
100-year return level	428.4	482.5	423.1	524.5	412.9	336.3	347.5	381.8	397.2	434.5
95% upper CI	695.7	831.4	660.1	889.4	673.5	546.4	562.5	653.3	634.3	754.0
exceedance rate (year^{-1})	5.667	5.733	7.200	6.600	5.733	5.067	5.400	6.133	6.600	5.933
P (threshold exceedance)	0.016	0.016	0.020	0.018	0.016	0.014	0.015	0.017	0.018	0.016

location	3_E	3_F	2_C	2_D	2_E	1_D
threshold	40	40	40	40	40	40
scale	23.53	27.95	23.16	24.01	27.09	27.06
shape	0.272	0.241	0.238	0.215	0.189	0.189
shape 95% lower CI	0.014	-0.060	0.005	-0.016	-0.066	-0.065
shape 95% upper CI	0.530	0.543	0.472	0.445	0.443	0.444
exceedances	89	86	95	90	73	73
95% lower CI	85.1	52.5	113.2	119.4	110.9	110.7
100-year return level	444.8	460.6	395.1	369.7	357.7	358.0
95% upper CI	804.6	868.8	677.0	620.0	604.5	605.4
exceedance rate (year^{-1})	5.933	5.733	6.333	6.000	4.867	4.867
P (threshold exceedance)	0.016	0.016	0.017	0.016	0.013	0.013

Gridded 72-hour Duration Wet Season

location	10_E	10_F	10_G	9_E	9_G	9_H	9_I	8_D	8_H	7_D
threshold	45	45	45	45	45	45	45	45	45	45
scale	29.66	25.73	29.41	25.88	30.39	26.47	31.12	33.71	28.93	48.08
shape	0.215	0.304	0.217	0.255	0.211	0.268	0.218	0.136	0.295	0.000
shape 95% lower CI	-0.007	0.047	0.002	0.034	0.001	0.046	-0.010	-0.052	-0.004	-0.149
shape 95% upper CI	0.437	0.560	0.432	0.475	0.420	0.491	0.446	0.323	0.593	0.149
exceedances	94	93	91	104	89	91	82	100	71	92
95% lower CI	151.7	85.4	158.3	140.2	167.1	139.5	150.3	190.6	45.9	227.6
100-year return level	458.2	557.7	454.0	481.0	454.8	496.8	466.5	396.8	550.3	353.6
95% upper CI	764.7	1029.9	749.7	821.8	742.6	854.0	782.7	603.0	1054.8	479.6
exceedance rate (year^{-1})	6.267	6.200	6.067	6.933	5.933	6.067	5.467	6.667	4.733	6.133
P (threshold exceedance)	0.017	0.017	0.017	0.019	0.016	0.017	0.015	0.018	0.013	0.017

location	7_E	7_F	6_C	6_D	6_E	6_F	5_C	5_D	5_E	5_F
threshold	45	45	45	45	45	45	45	45	45	45
scale	31.27	33.77	31.51	33.14	33.35	28.23	27.77	34.92	26.23	26.08
shape	0.188	0.206	0.201	0.163	0.170	0.233	0.241	0.143	0.234	0.264
shape 95% lower CI	-0.022	0.004	-0.025	-0.041	-0.053	-0.007	0.007	-0.061	-0.023	0.021
shape 95% upper CI	0.399	0.407	0.426	0.368	0.393	0.474	0.475	0.347	0.491	0.508
exceedances	95	88	97	95	86	87	97	91	84	81
95% lower CI	168.2	188.3	154.3	178.0	161.6	127.2	131.8	181.8	105.4	114.6
100-year return level	438.6	490.1	463.4	424.1	425.8	457.7	477.9	411.7	425.4	466.7
95% upper CI	708.9	791.8	772.5	670.2	690.1	788.2	824.1	641.7	745.4	818.8
exceedance rate (year^{-1})	6.333	5.867	6.467	6.333	5.733	5.800	6.467	6.067	5.600	5.400
P (threshold exceedance)	0.017	0.016	0.018	0.017	0.016	0.016	0.018	0.017	0.015	0.015

Gridded 72-hour Duration Wet Season

location	5_G	5_H	4_C	4_D	4_E	4_F	4_G	3_B	3_C	3_D
threshold	45	45	45	45	45	45	45	45	45	45
scale	25.06	28.01	27.66	33.77	28.09	31.44	32.29	28.65	24.06	24.06
shape	0.283	0.270	0.229	0.224	0.242	0.128	0.118	0.161	0.260	0.297
shape 95% lower CI	0.041	0.018	0.022	-0.004	-0.013	-0.134	-0.129	-0.086	0.031	0.024
shape 95% upper CI	0.526	0.521	0.435	0.452	0.498	0.390	0.365	0.408	0.488	0.569
exceedances	81	77	96	85	79	63	69	75	88	79
95% lower CI	110.1	109.9	161.3	159.1	110.6	125.5	136.9	126.8	125.0	70.3
100-year return level	482.3	500.3	454.0	517.3	458.2	331.3	335.6	351.3	437.2	484.7
95% upper CI	854.5	890.8	746.6	875.5	805.8	537.2	534.2	575.8	749.4	899.1
exceedance rate (year^{-1})	5.400	5.133	6.400	5.667	5.267	4.200	4.600	5.000	5.867	5.267
P (threshold exceedance)	0.015	0.014	0.018	0.016	0.014	0.011	0.013	0.014	0.016	0.014

location	3_E	3_F	2_C	2_D	2_E	1_D
threshold	45	45	45	45	45	45
scale	19.45	34.82	24.34	22.47	25.77	25.72
shape	0.407	0.136	0.234	0.272	0.238	0.239
shape 95% lower CI	0.078	-0.171	-0.015	0.000	-0.065	-0.065
shape 95% upper CI	0.736	0.442	0.483	0.544	0.541	0.542
exceedances	78	68	78	76	62	62
95% lower CI	-77.8	101.0	108.6	78.0	68.7	68.0
100-year return level	606.6	376.7	390.7	411.9	390.5	391.2
95% upper CI	1291.0	652.4	672.7	745.8	712.2	714.3
exceedance rate (year^{-1})	5.200	4.533	5.200	5.067	4.133	4.133
P (threshold exceedance)	0.014	0.012	0.014	0.014	0.011	0.011

Gridded 72-hour Duration Wet Season

location	10_E	10_F	10_G	9_E	9_G	9_H	9_I	8_D	8_H	7_D
threshold	50	50	50	50	50	50	50	50	50	50
scale	28.06	24.01	27.26	23.46	29.35	24.71	29.36	30.68	33.94	38.89
shape	0.255	0.360	0.258	0.326	0.236	0.315	0.257	0.185	0.237	0.081
shape 95% lower CI	0.001	0.062	0.017	0.059	0.006	0.060	-0.003	-0.033	-0.049	-0.114
shape 95% upper CI	0.510	0.658	0.499	0.593	0.465	0.570	0.517	0.402	0.523	0.277
exceedances	83	82	82	91	79	82	73	91	58	87
95% lower CI	113.3	1.8	126.4	64.3	147.3	91.1	111.4	163.7	100.9	196.3
100-year return level	491.5	628.0	482.2	560.0	471.0	542.4	496.4	426.2	494.6	374.2
95% upper CI	869.8	1254.2	838.1	1055.7	794.6	993.6	881.5	688.8	888.2	552.1
exceedance rate (year^{-1})	5.533	5.467	5.467	6.067	5.267	5.467	4.867	6.067	3.867	5.800
P (threshold exceedance)	0.015	0.015	0.015	0.017	0.014	0.015	0.013	0.017	0.011	0.016

location	7_E	7_F	6_C	6_D	6_E	6_F	5_C	5_D	5_E	5_F
threshold	50	50	50	50	50	50	50	50	50	50
scale	31.66	33.96	29.58	28.81	34.69	27.61	23.17	29.73	28.66	23.85
shape	0.195	0.210	0.243	0.237	0.161	0.256	0.363	0.227	0.208	0.326
shape 95% lower CI	-0.029	0.002	-0.009	-0.004	-0.068	-0.007	0.065	-0.018	-0.055	0.039
shape 95% upper CI	0.418	0.419	0.495	0.477	0.391	0.518	0.660	0.472	0.471	0.612
exceedances	82	78	87	88	74	76	87	85	69	72
95% lower CI	161.0	184.7	121.2	133.3	163.4	105.0	-3.9	132.3	116.3	49.3
100-year return level	442.1	490.1	500.3	478.8	419.8	472.8	627.9	472.0	405.3	524.1
95% upper CI	723.2	795.5	879.4	824.2	676.2	840.5	1259.7	811.7	694.3	998.8
exceedance rate (year^{-1})	5.467	5.200	5.800	5.867	4.933	5.067	5.800	5.667	4.600	4.800
P (threshold exceedance)	0.015	0.014	0.016	0.016	0.014	0.014	0.016	0.016	0.013	0.013

Gridded 72-hour Duration Wet Season

location	5_G	5_H	4_C	4_D	4_E	4_F	4_G	3_B	3_C	3_D
threshold	50	50	50	50	50	50	50	50	50	50
scale	22.69	31.55	24.39	29.21	28.13	31.90	25.33	28.14	24.14	20.36
shape	0.350	0.237	0.301	0.304	0.257	0.124	0.245	0.186	0.283	0.420
shape 95% lower CI	0.066	-0.011	0.055	0.038	-0.018	-0.148	-0.054	-0.091	0.030	0.080
shape 95% upper CI	0.634	0.486	0.547	0.569	0.533	0.397	0.543	0.463	0.537	0.760
exceedances	71	63	86	79	68	55	66	64	73	69
95% lower CI	40.9	132.8	105.2	88.4	94.2	125.6	73.2	108.1	101.7	-94.4
100-year return level	544.6	474.6	516.8	598.7	468.4	328.0	406.0	365.4	456.5	637.5
95% upper CI	1048.4	816.3	928.3	1109.0	842.6	530.3	738.8	622.7	811.2	1369.3
exceedance rate (year^{-1})	4.733	4.200	5.733	5.267	4.533	3.667	4.400	4.267	4.867	4.600
P (threshold exceedance)	0.013	0.011	0.016	0.014	0.012	0.010	0.012	0.012	0.013	0.013

location	3_E	3_F	2_C	2_D	2_E	1_D
threshold	50	50	50	50	50	50
scale	19.78	35.71	22.01	21.76	27.37	27.30
shape	0.452	0.126	0.309	0.319	0.230	0.232
shape 95% lower CI	0.051	-0.203	0.012	0.005	-0.098	-0.097
shape 95% upper CI	0.853	0.456	0.606	0.634	0.558	0.561
exceedances	63	60	67	63	51	51
95% lower CI	-229.5	95.7	48.4	28.6	63.4	62.2
100-year return level	678.5	370.0	447.8	450.7	385.8	386.8
95% upper CI	1586.6	644.3	847.1	872.9	708.2	711.3
exceedance rate (year^{-1})	4.200	4.000	4.467	4.200	3.400	3.400
P (threshold exceedance)	0.011	0.011	0.012	0.011	0.009	0.009

Appendix B

Quality of Fit Diagnostic Plots

24-hour Gridded Diagnostic Plots Threshold = 25 mm

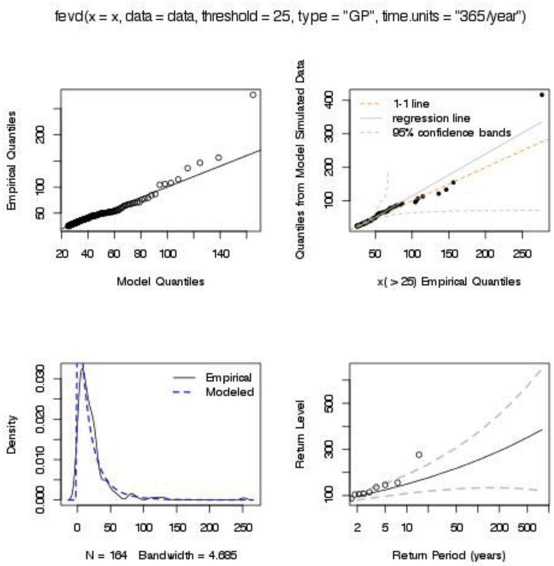

10E

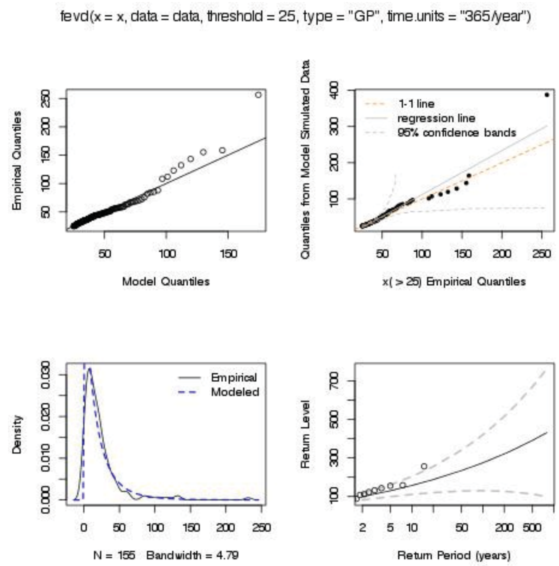

10F

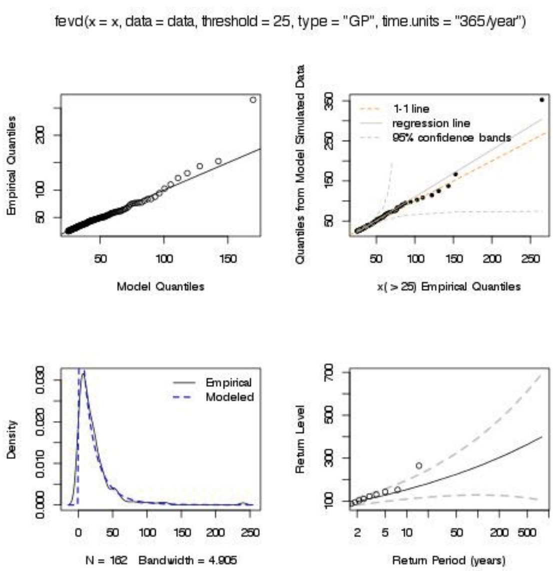

10G

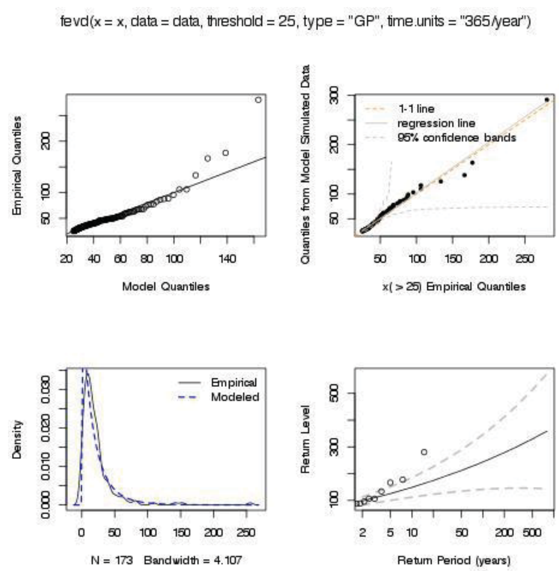

9E

24-hour Gridded Diagnostic Plots Threshold = 25 mm

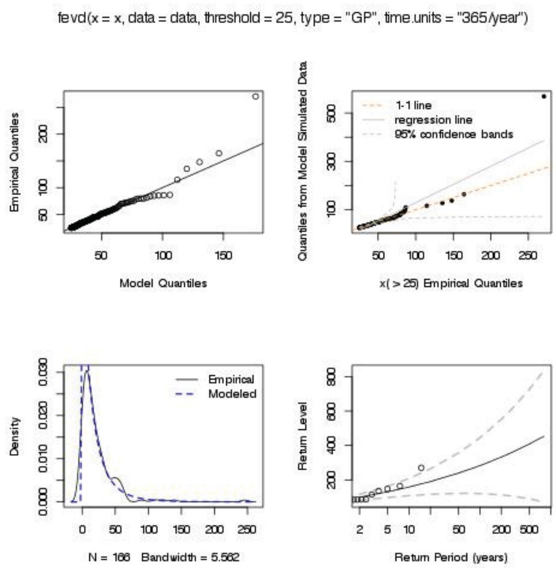

9G

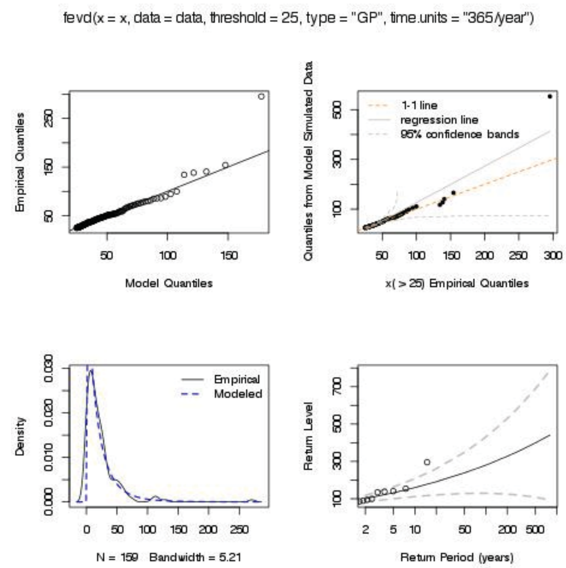

9H

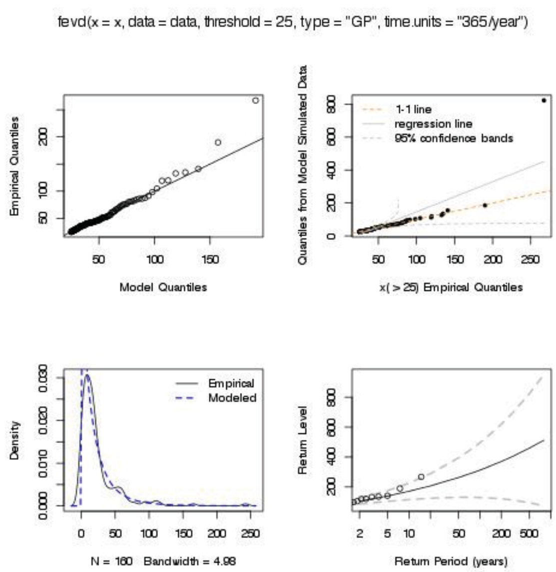

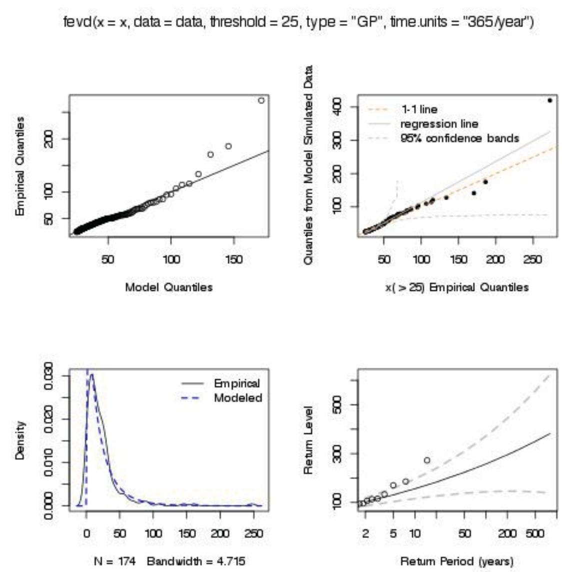

9I

8D

24-hour Gridded Diagnostic Plots Threshold = 25 mm

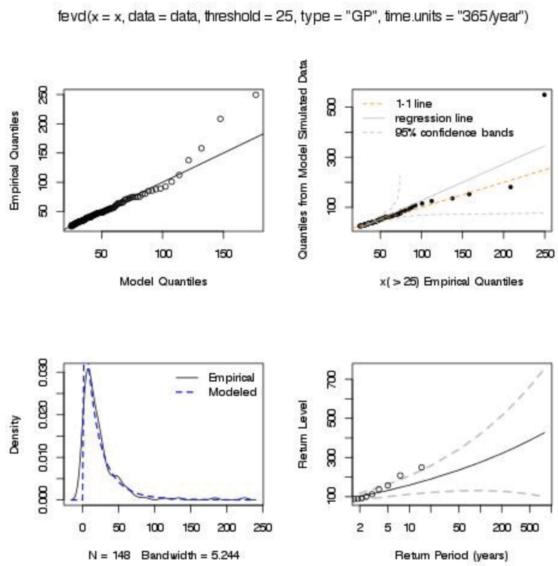

8H

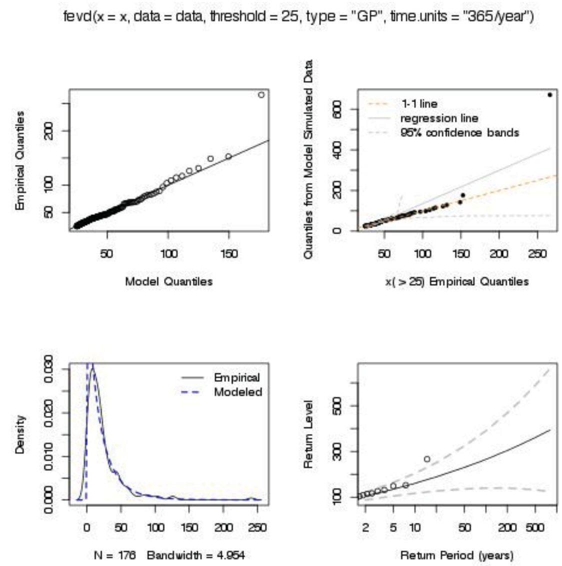

7D

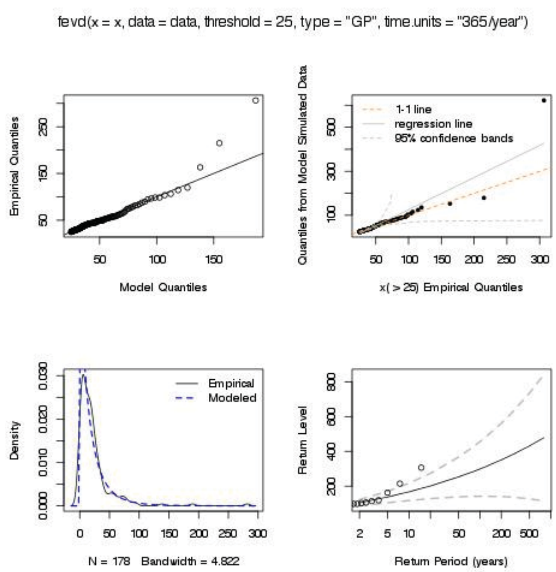

7E

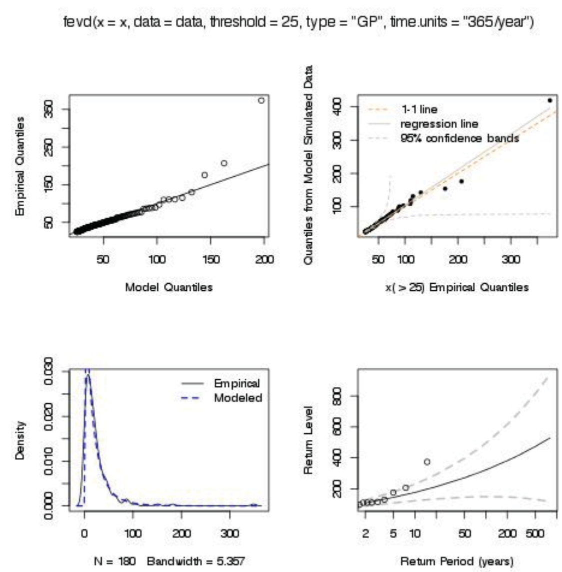

7F

24-hour Gridded Diagnostic Plots Threshold = 25 mm

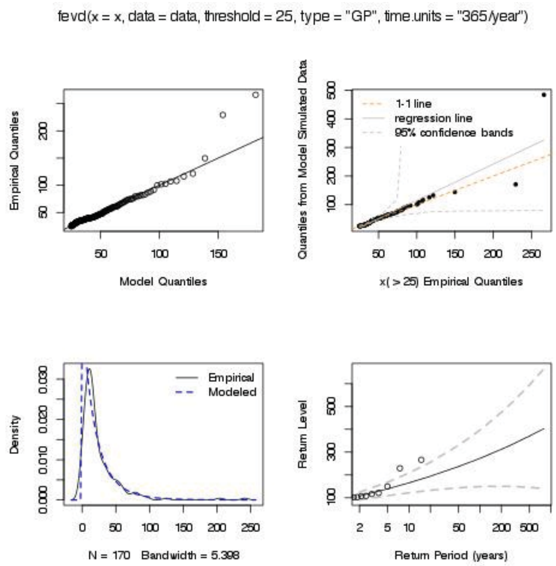

6C

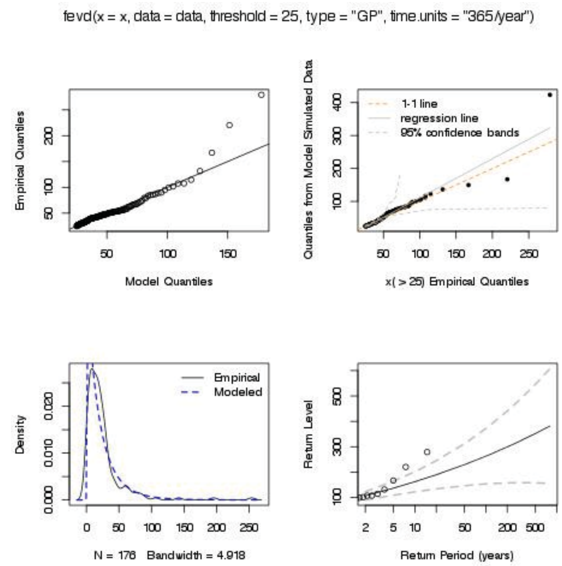

6D

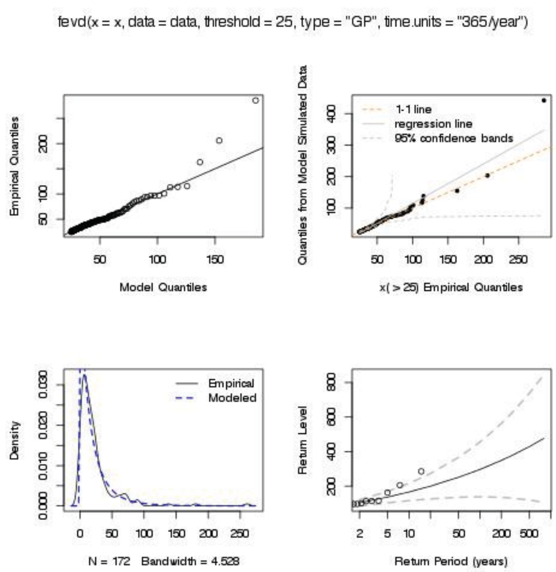

6E

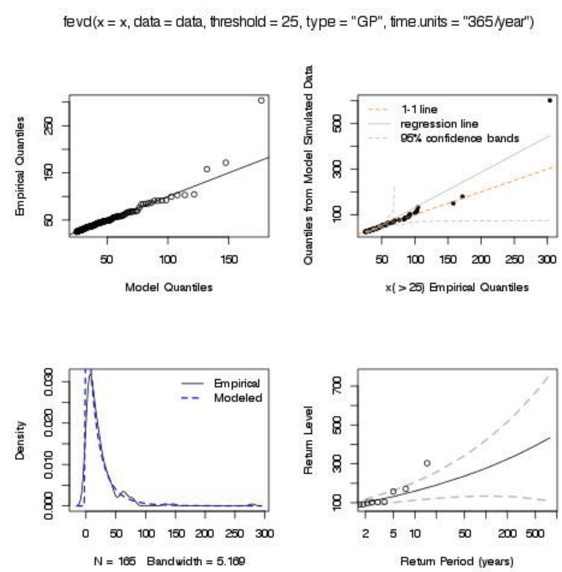

6F

24-hour Gridded Diagnostic Plots Threshold = 25 mm

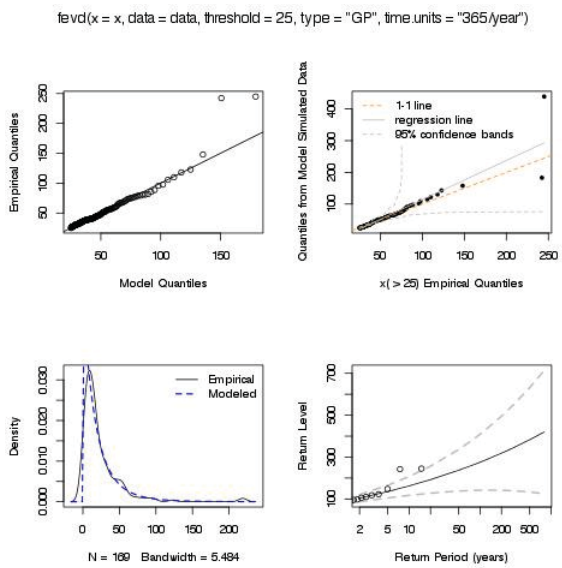

5C

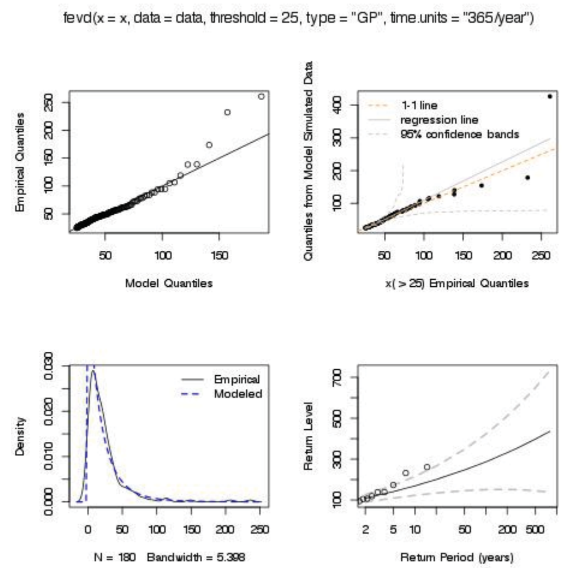

5D

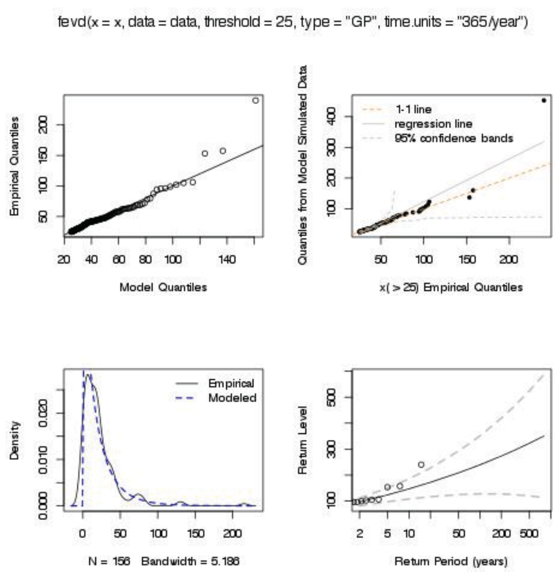

5E

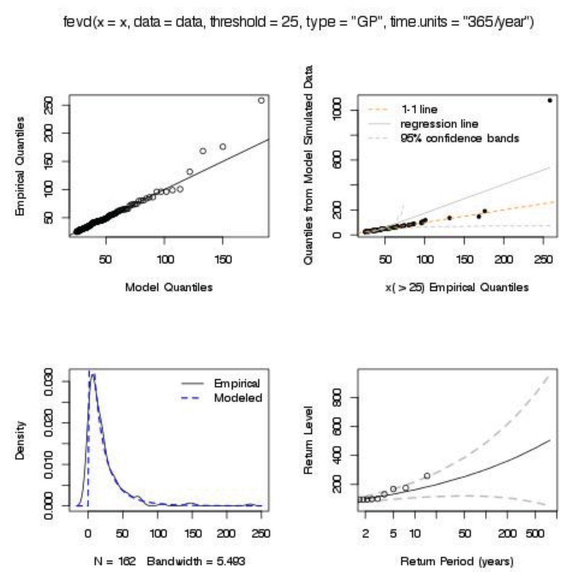

5F

24-hour Gridded Diagnostic Plots Threshold = 25 mm

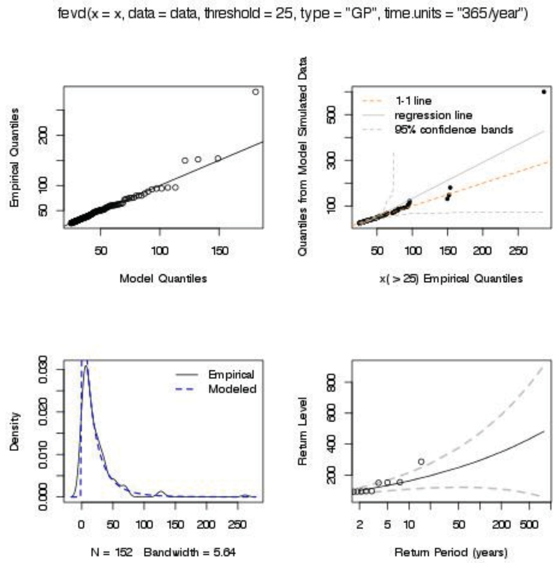

5G

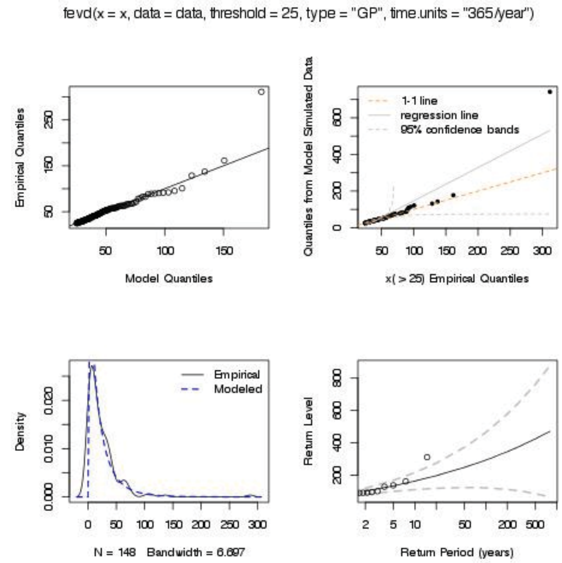

5H

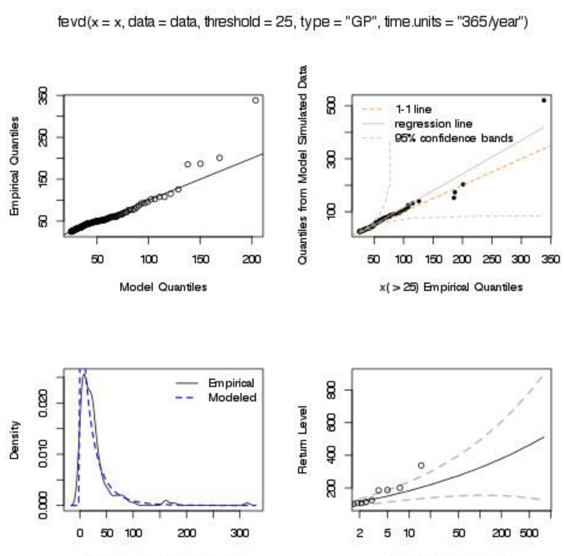

4C

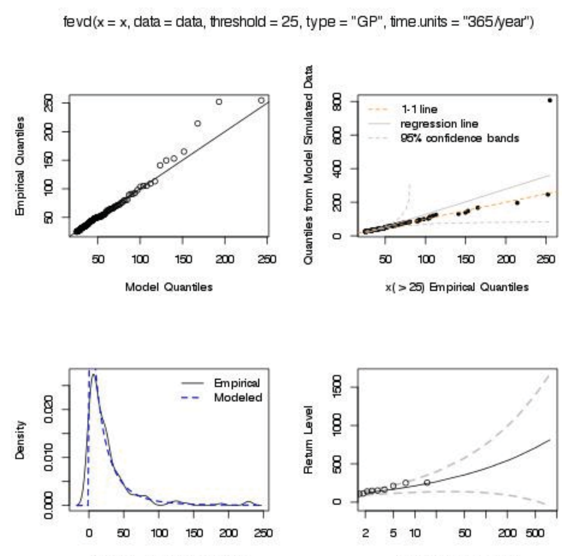

4D

24-hour Gridded Diagnostic Plots Threshold = 25 mm

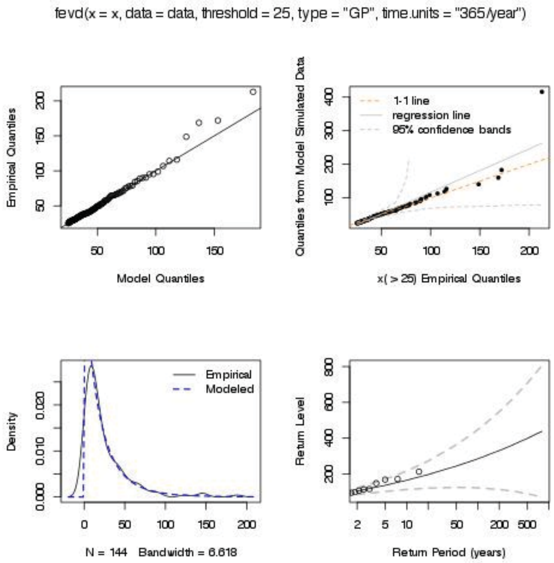

4E

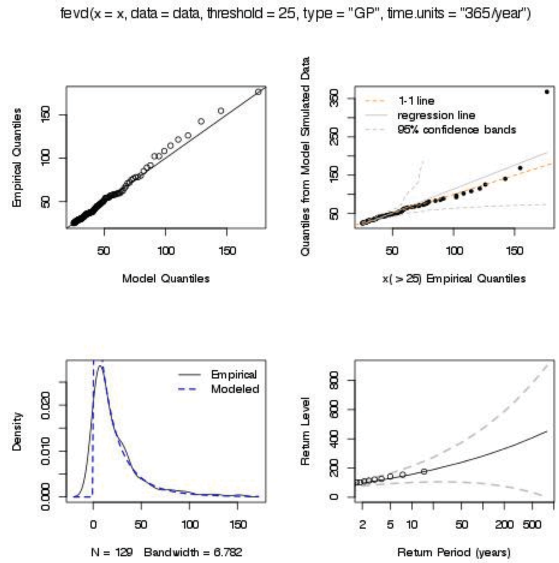

4F

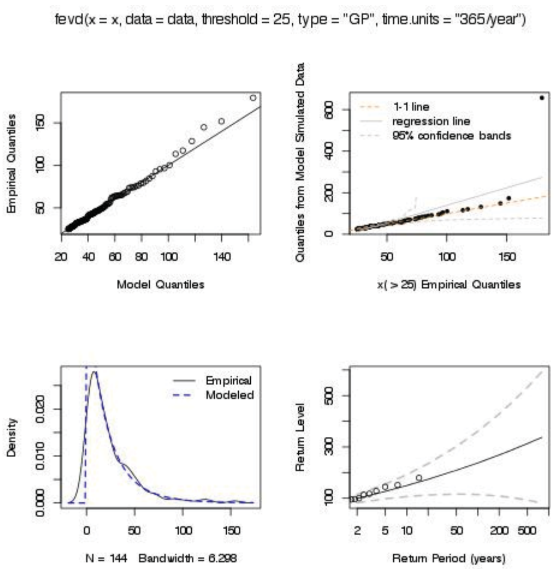

4G

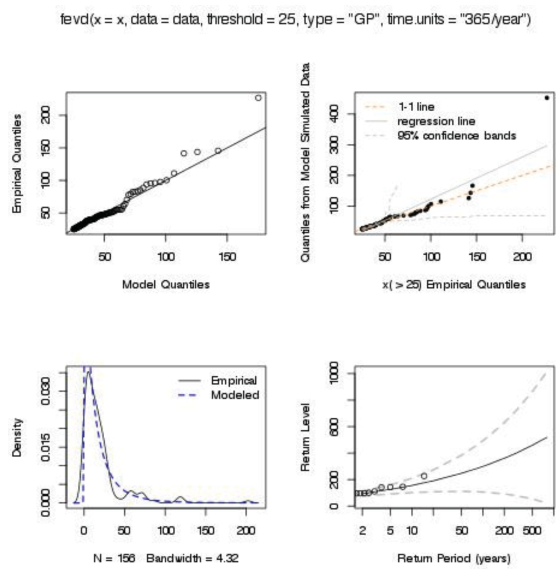

3B

24-hour Gridded Diagnostic Plots Threshold = 25 mm

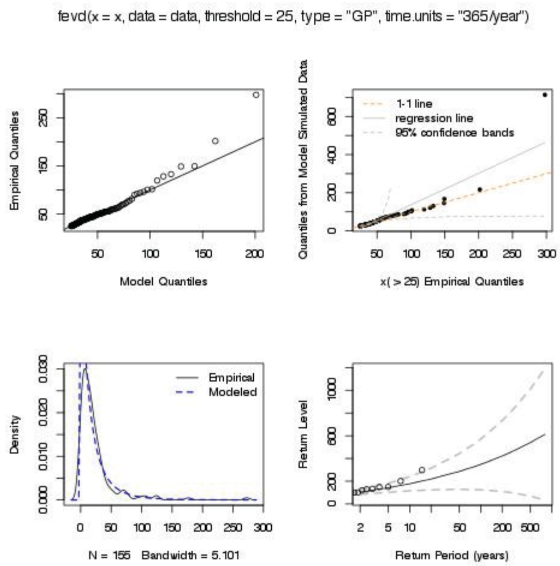

3C

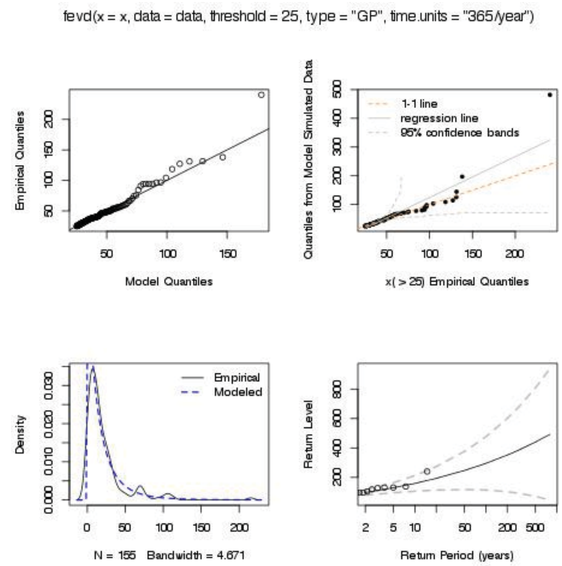

3D

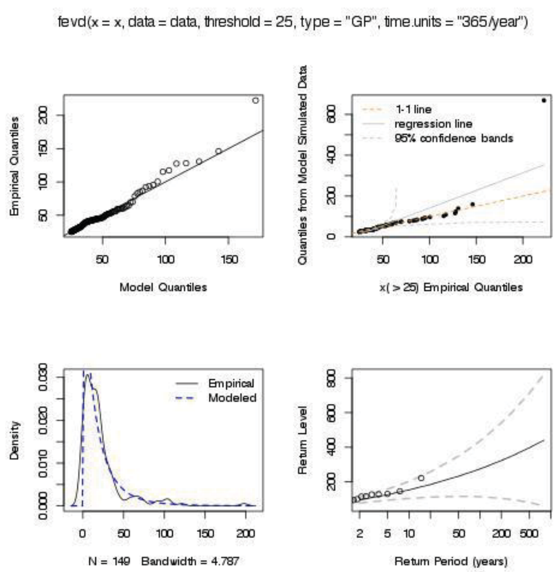

3E

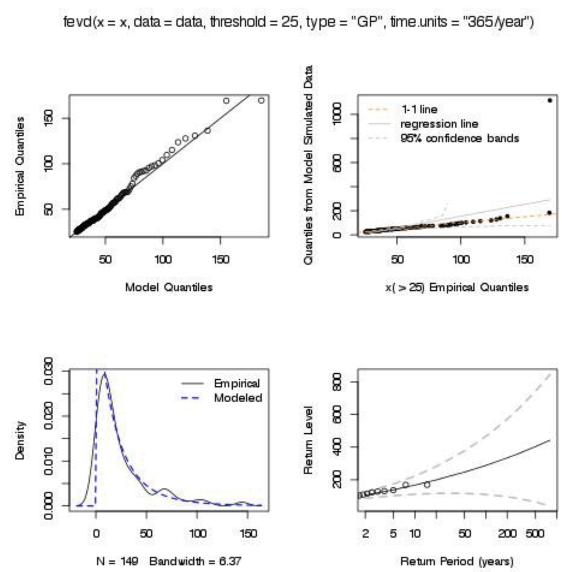

3F

24-hour Gridded Diagnostic Plots Threshold = 25 mm

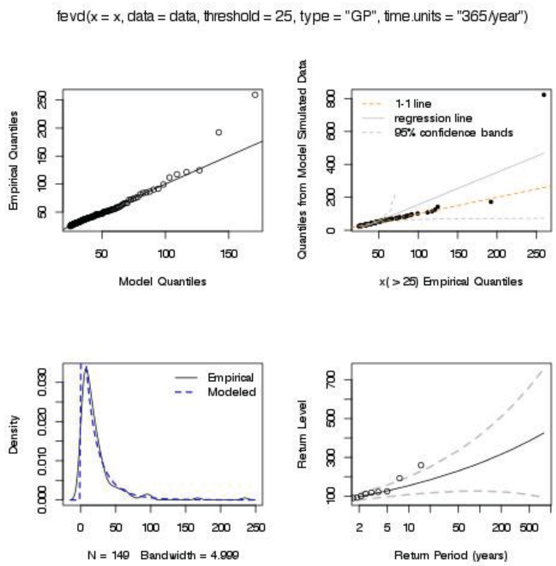

2C

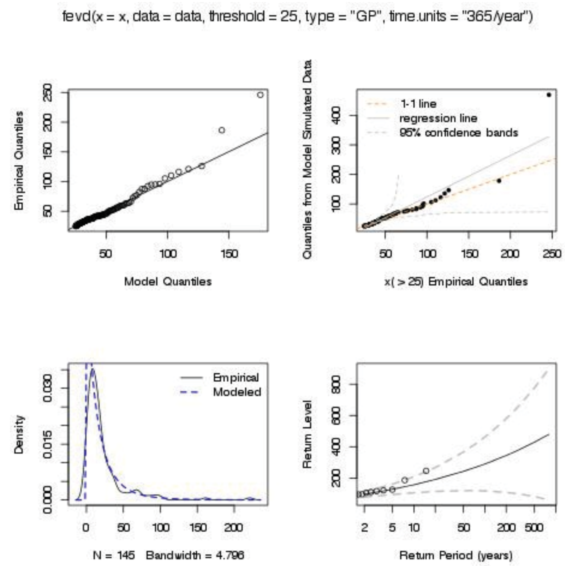

2D

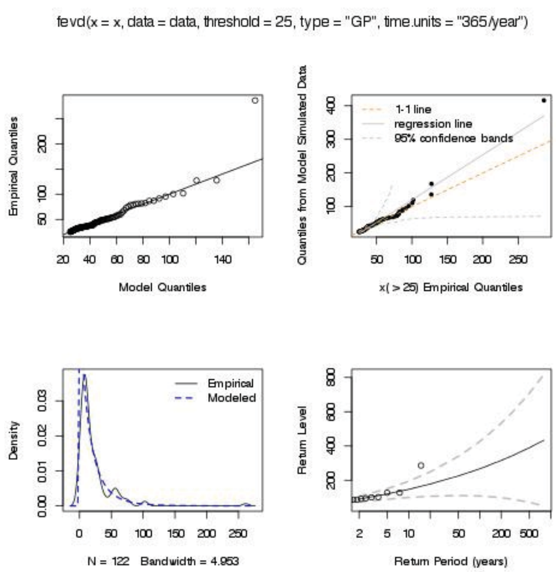

2E

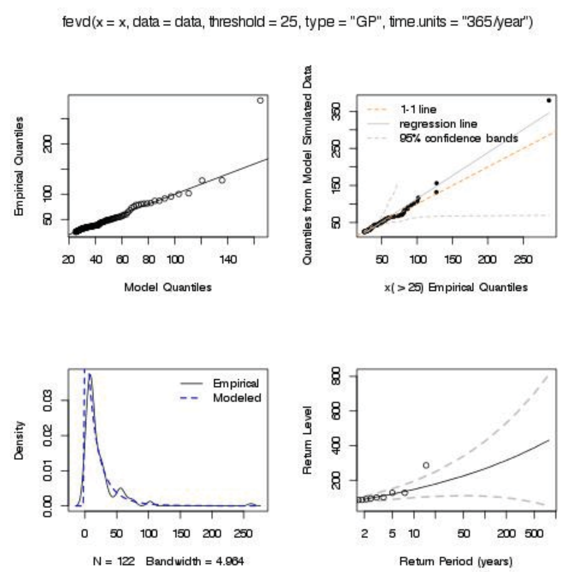

1D

24-hour Gridded Diagnostic Plots Threshold = 30 mm

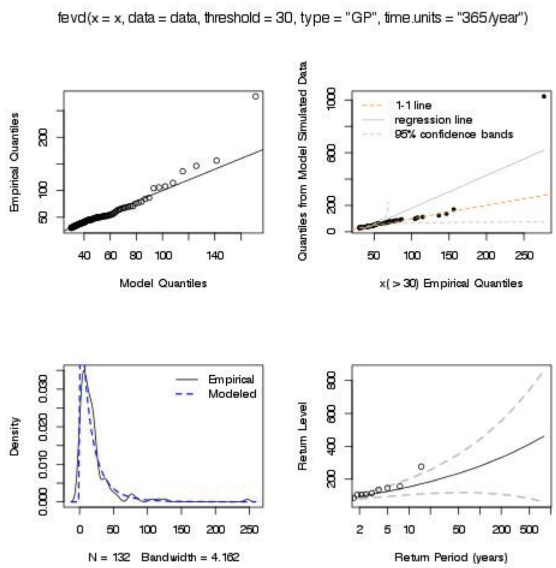

10E

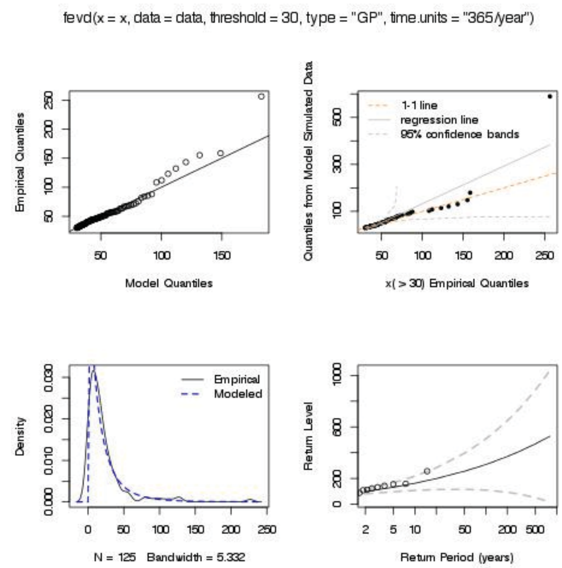

10F

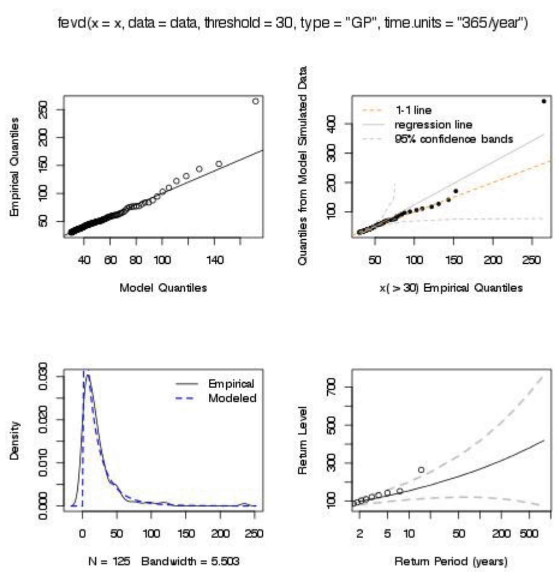

10G

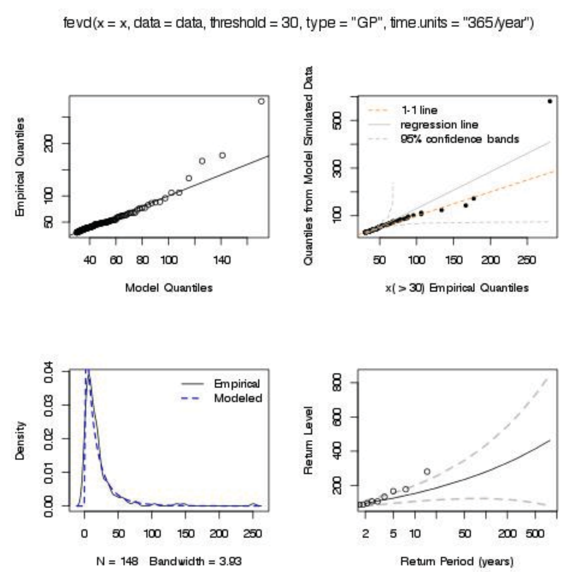

9E

24-hour Gridded Diagnostic Plots Threshold = 30 mm

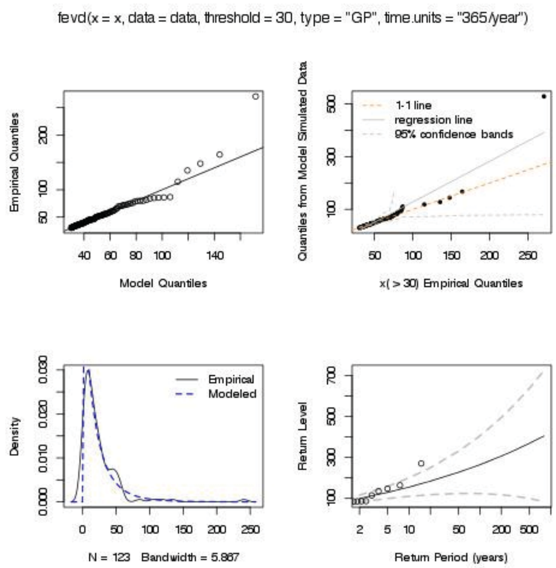

9G

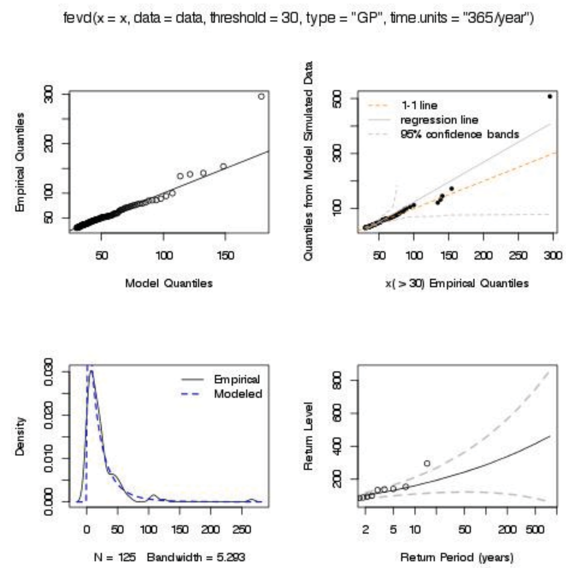

9H

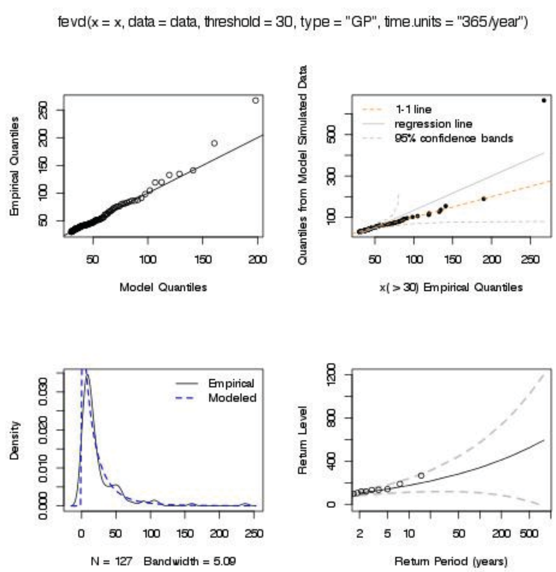

9I

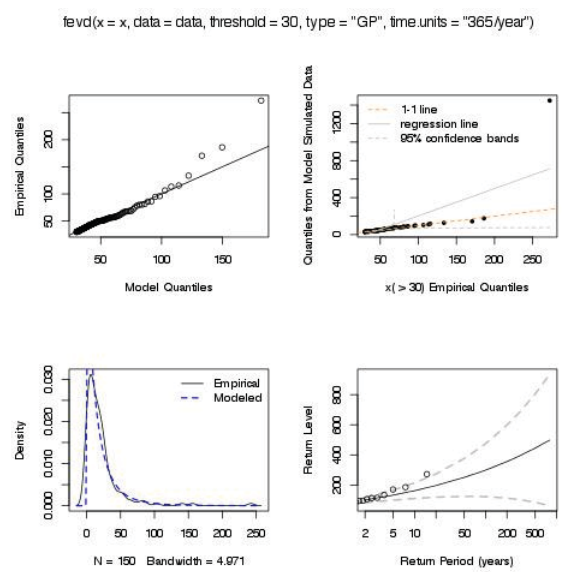

8D

24-hour Gridded Diagnostic Plots Threshold = 30 mm

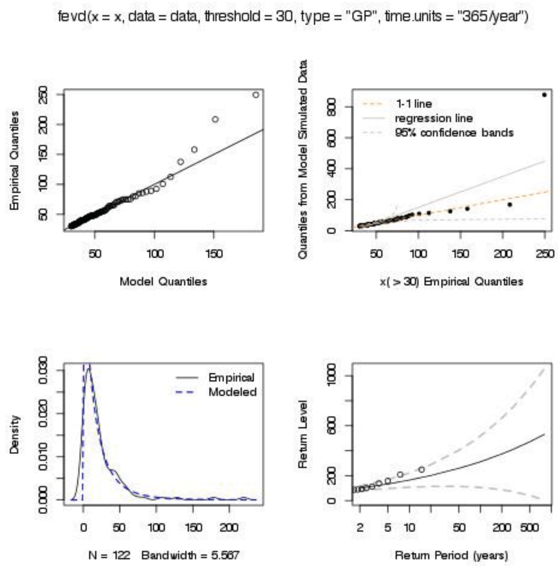

8H

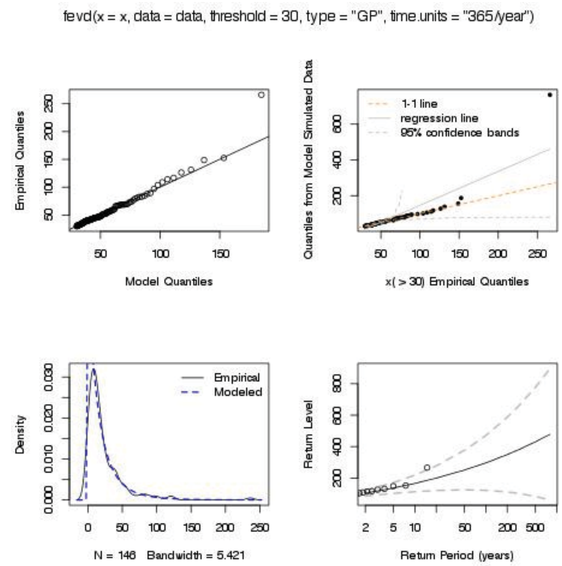

7D

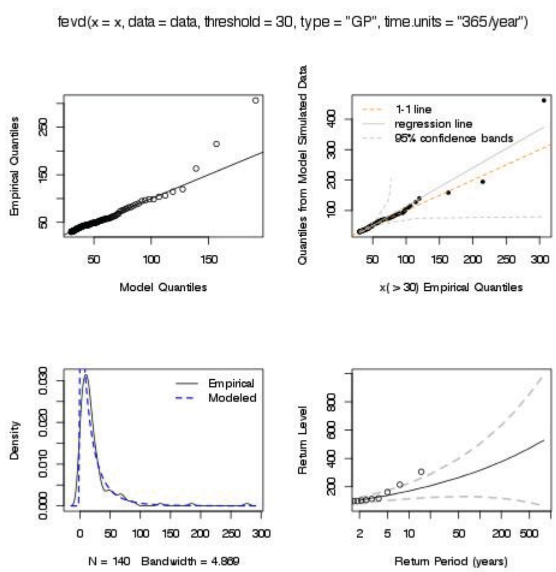

7E

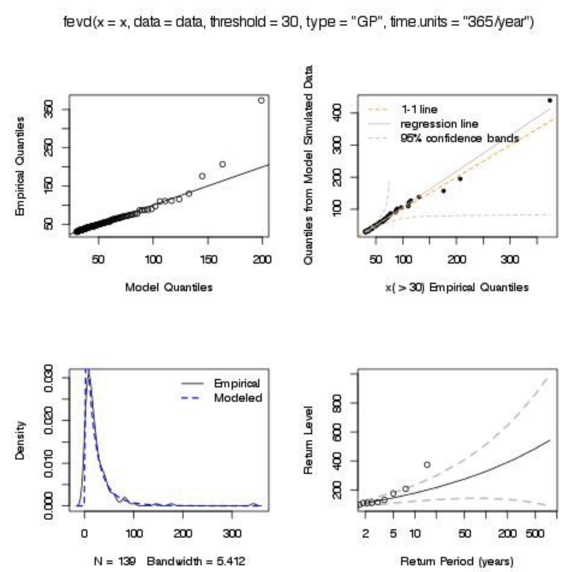

7F

24-hour Gridded Diagnostic Plots Threshold = 30 mm

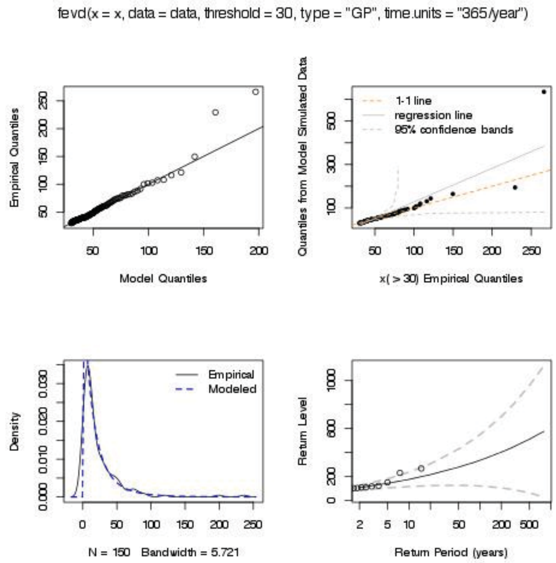

6C

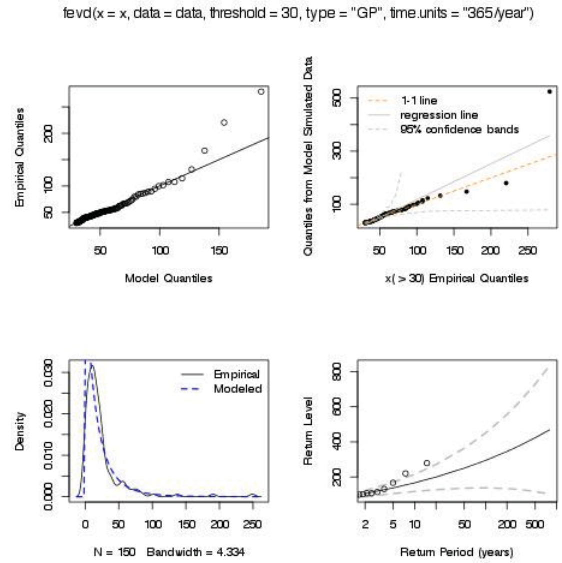

6D

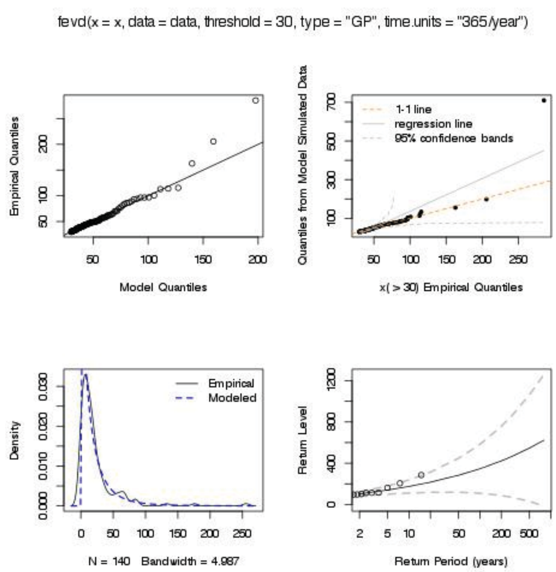

6E

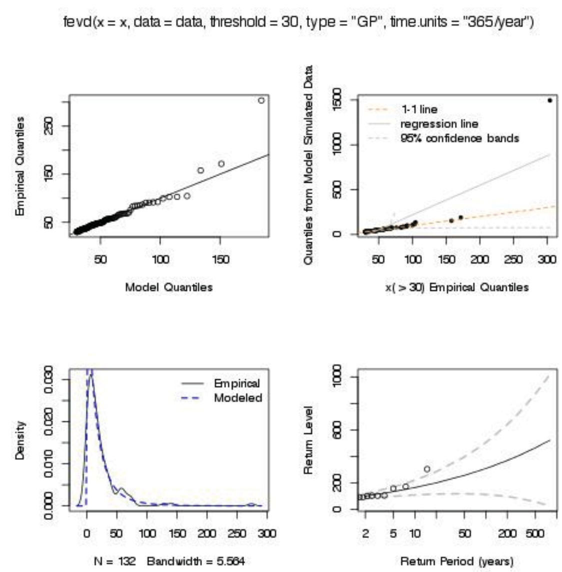

6F

24-hour Gridded Diagnostic Plots Threshold = 30 mm

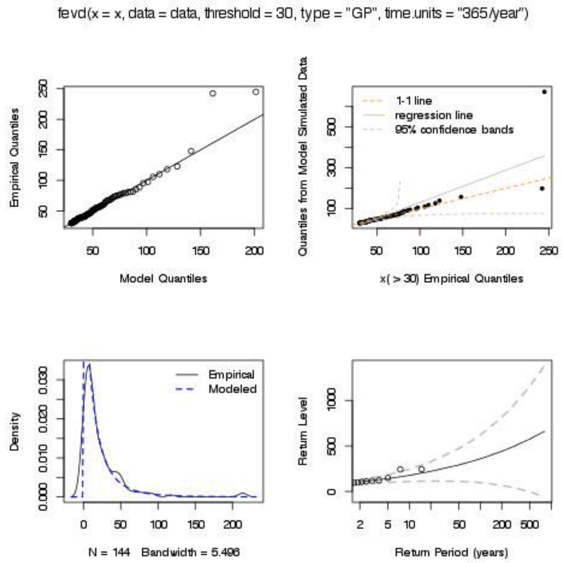

5C

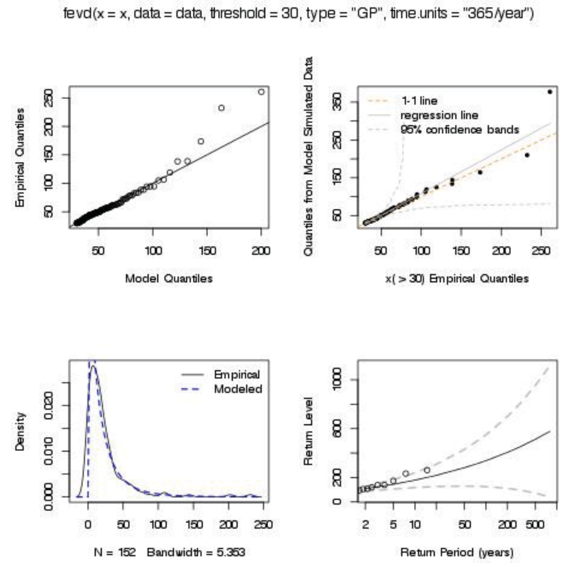

5D

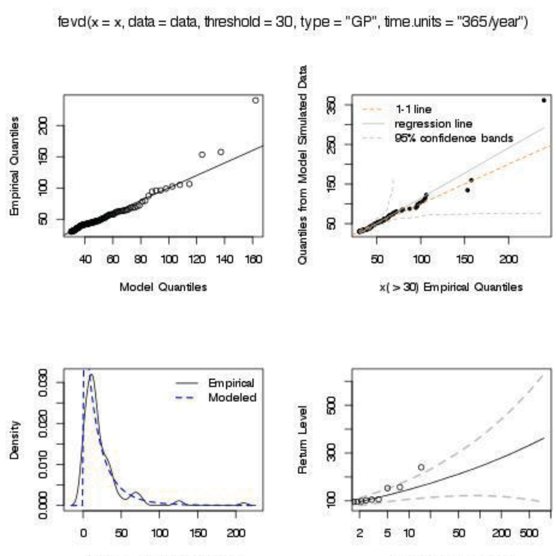

5E

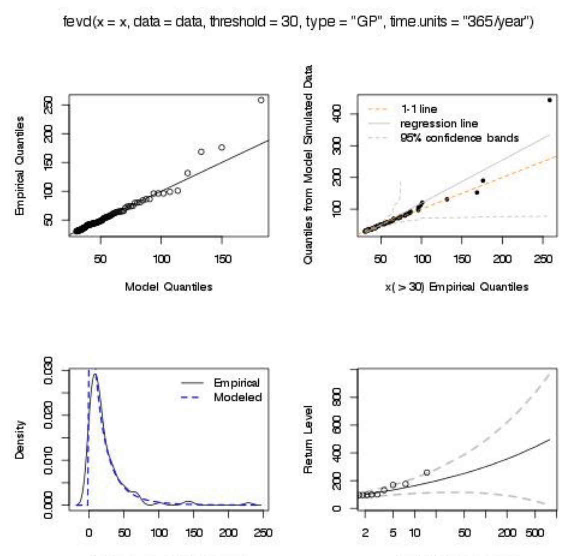

5F

24-hour Gridded Diagnostic Plots Threshold = 30 mm

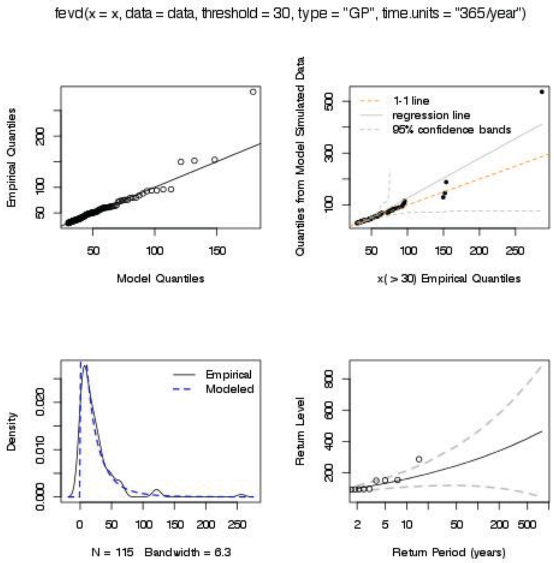

5G

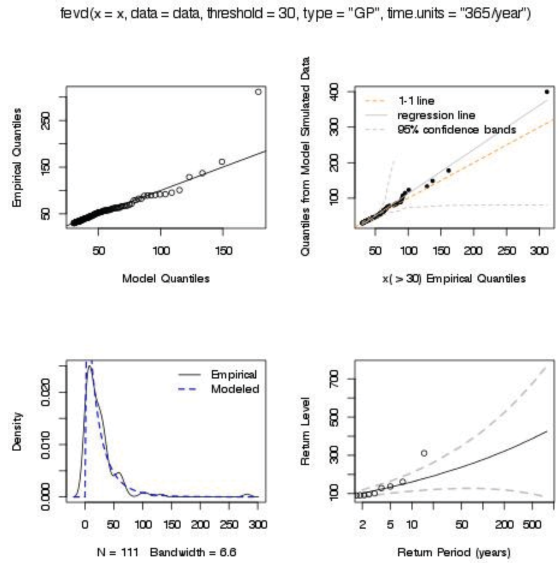

5H

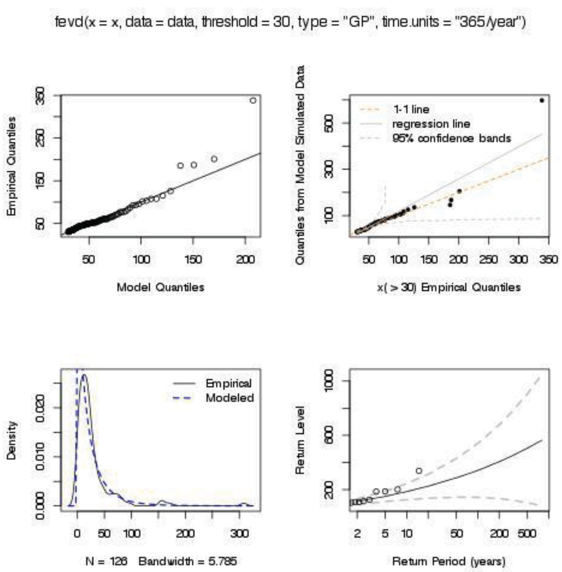

4C

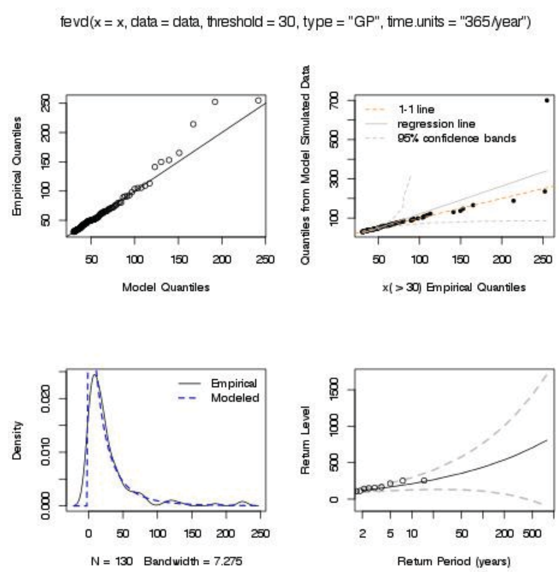

4D

24-hour Gridded Diagnostic Plots Threshold = 30 mm

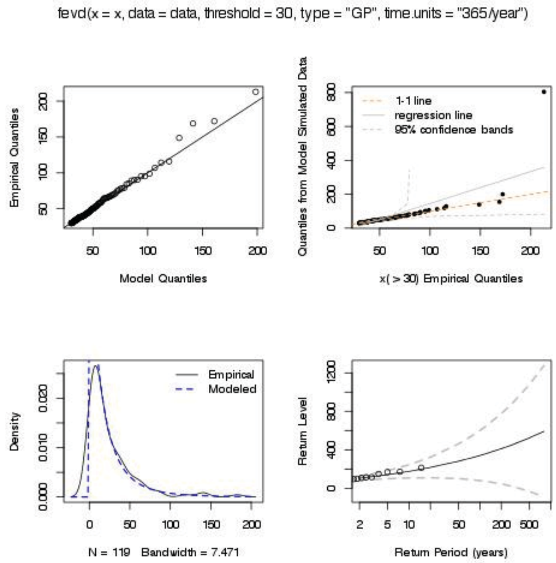

4E

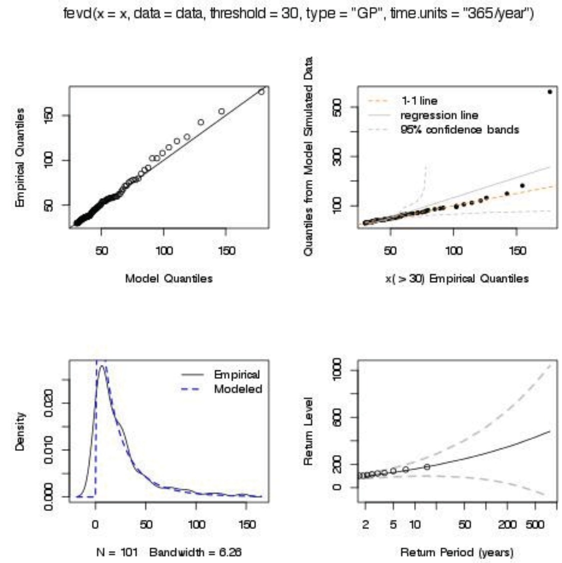

4F

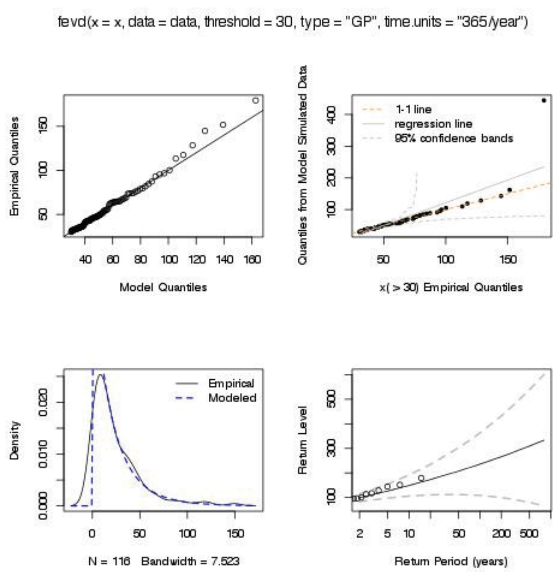

4G

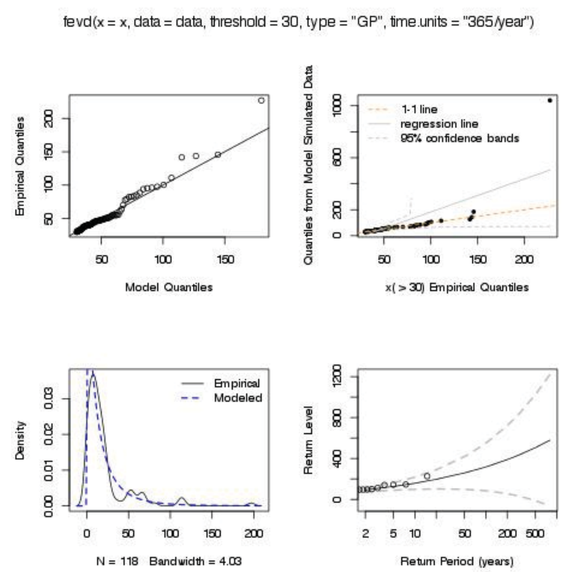

3B

24-hour Gridded Diagnostic Plots Threshold = 30 mm

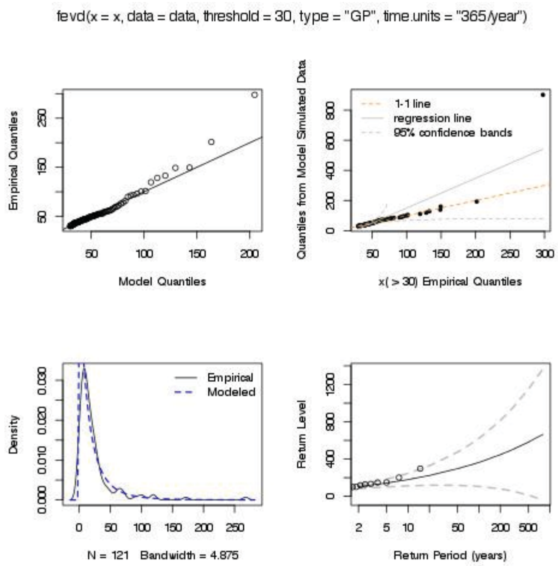

3C

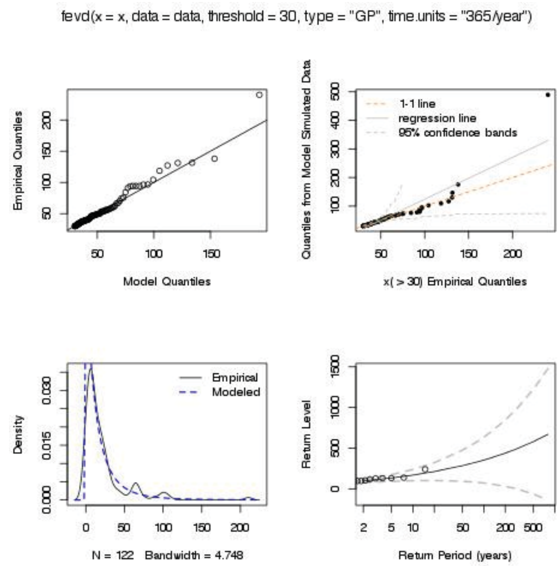

3D

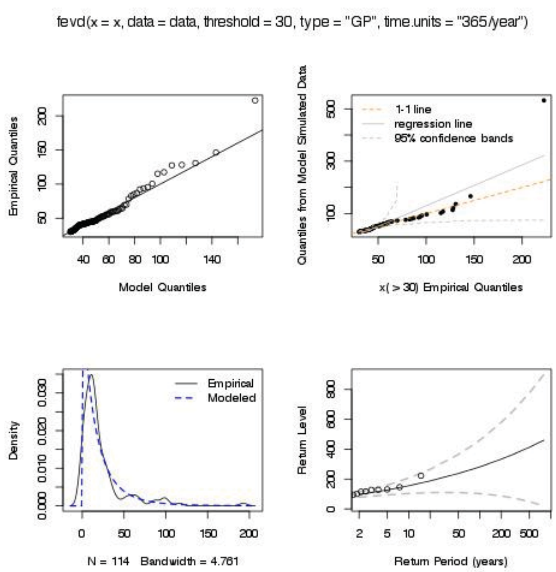

3E

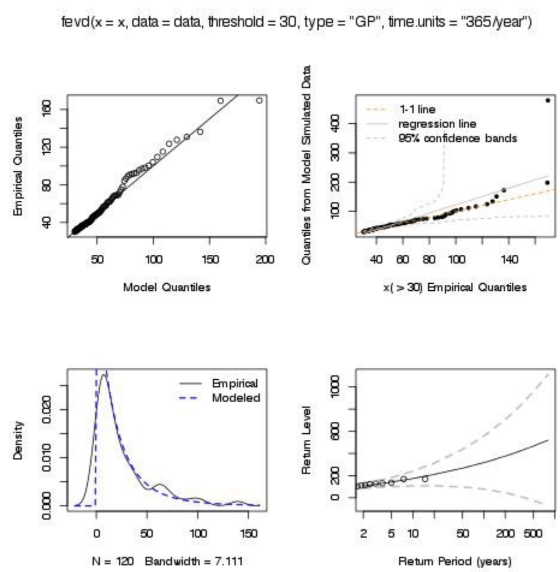

3F

24-hour Gridded Diagnostic Plots Threshold = 30 mm

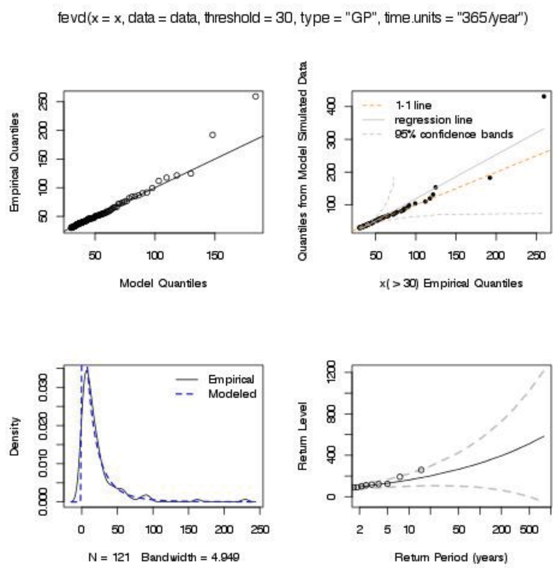

2C

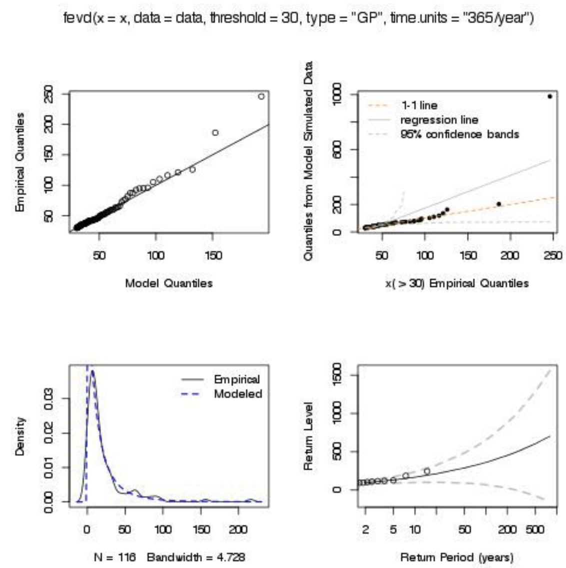

2D

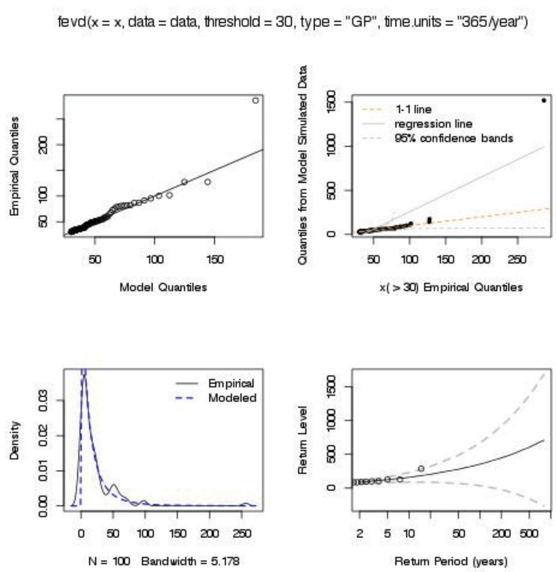

2E

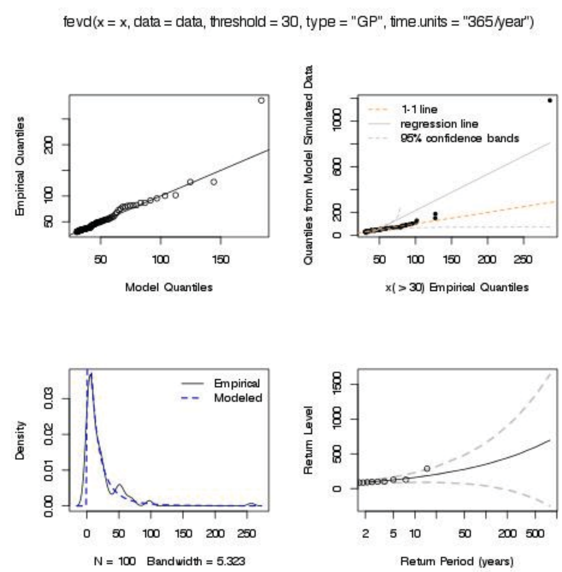

1D

24-hour Gridded Diagnostic Plots Threshold = 35 mm

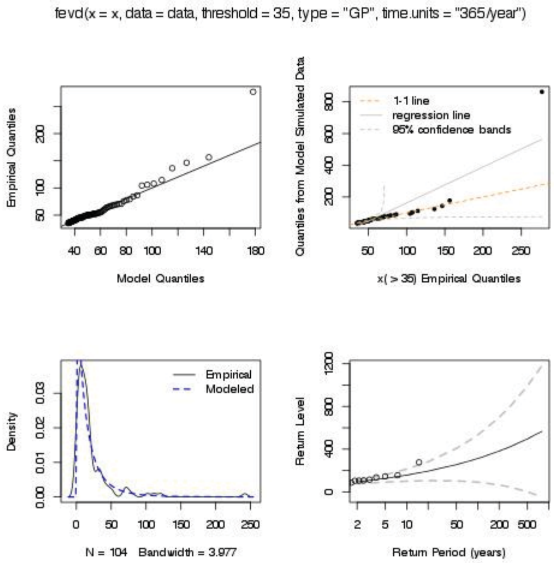

10E

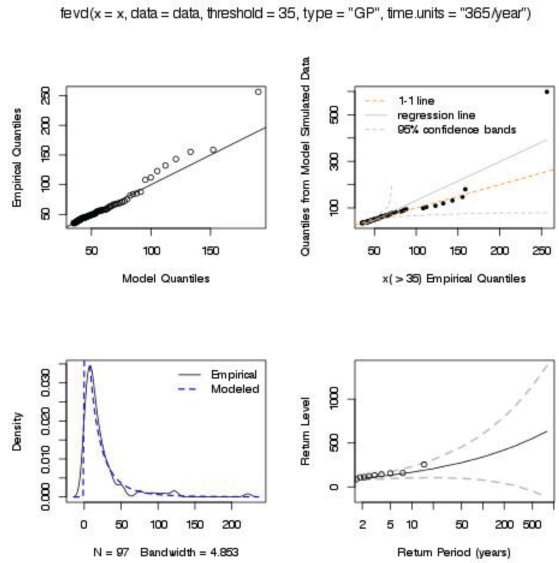

10F

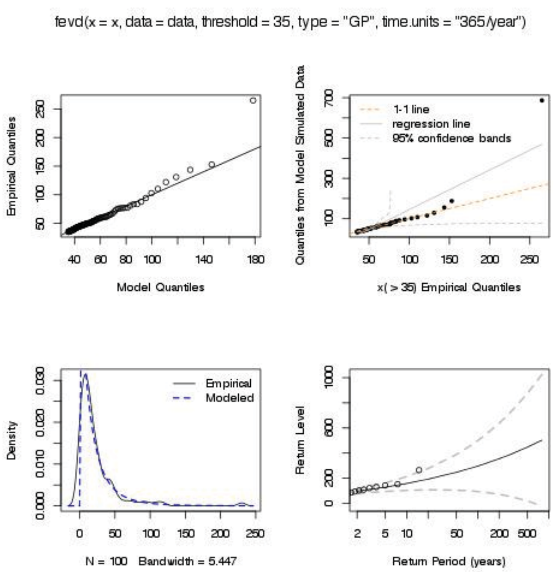

10G

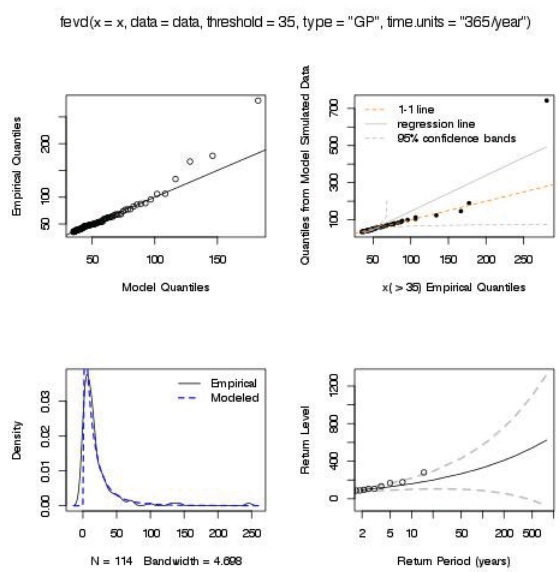

9E

24-hour Gridded Diagnostic Plots Threshold = 35 mm

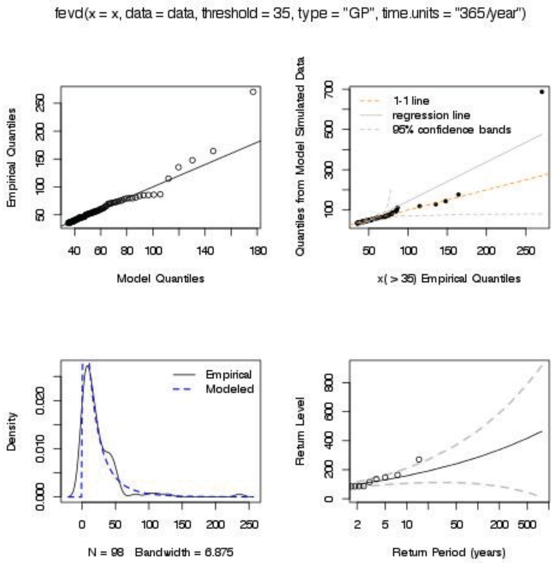

9G

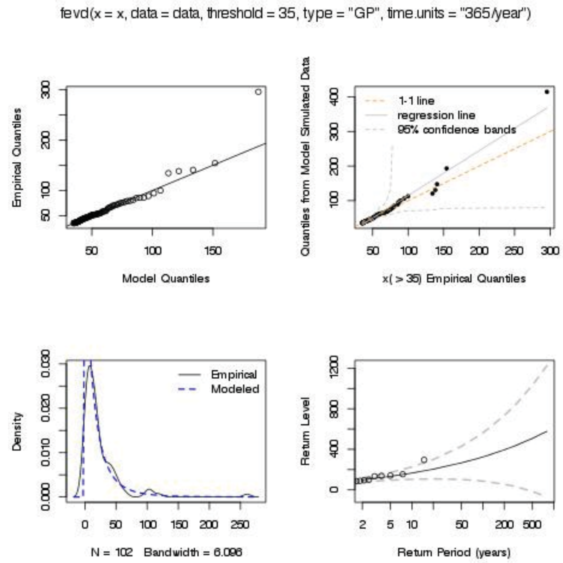

9H

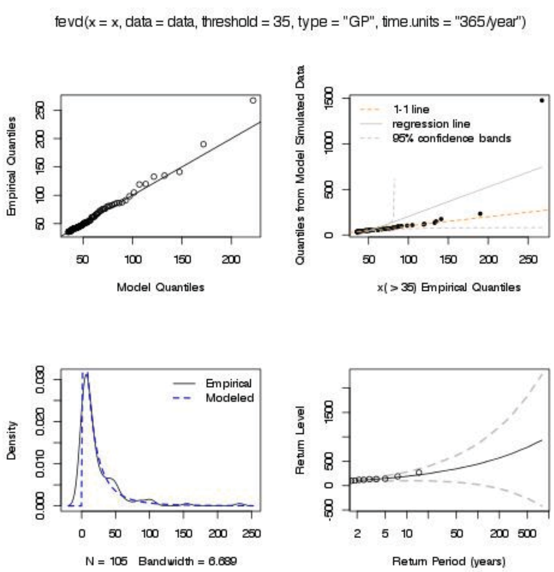

9I

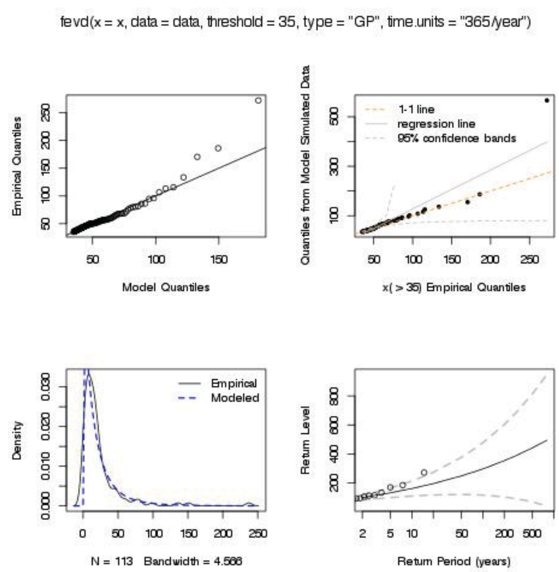

8D

24-hour Gridded Diagnostic Plots Threshold = 35 mm

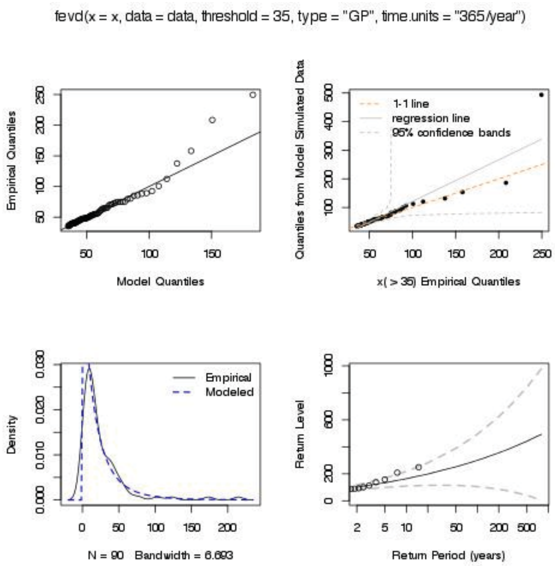

8H

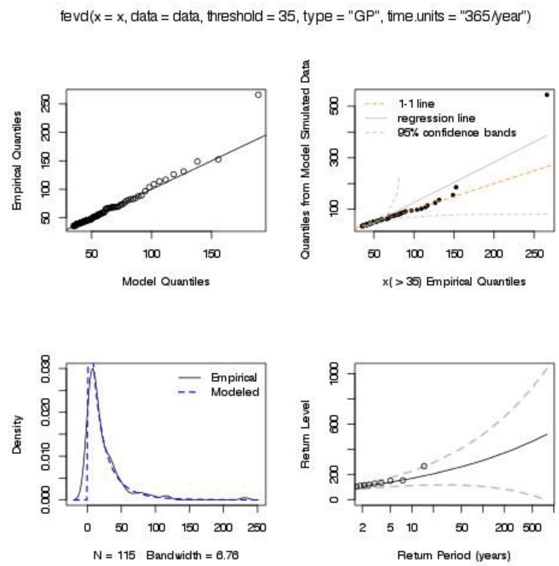

7D

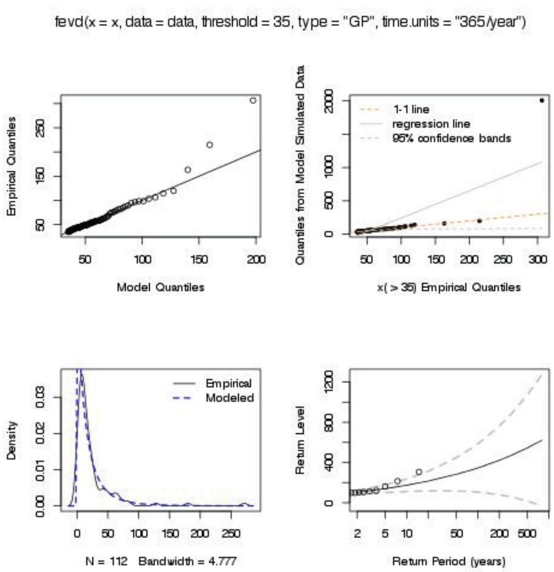

7E

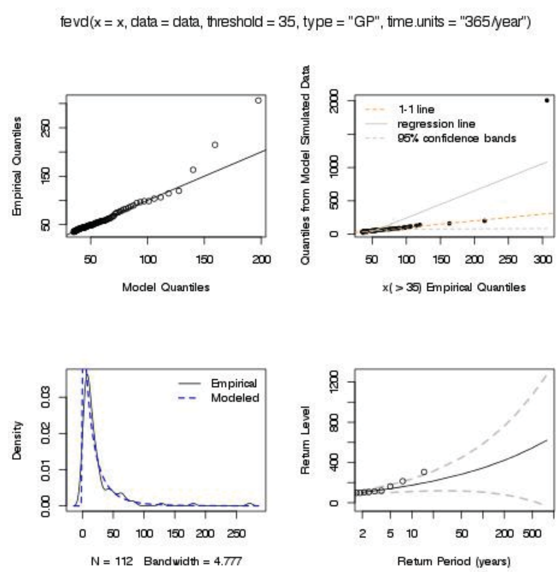

7F

24-hour Gridded Diagnostic Plots Threshold = 35 mm

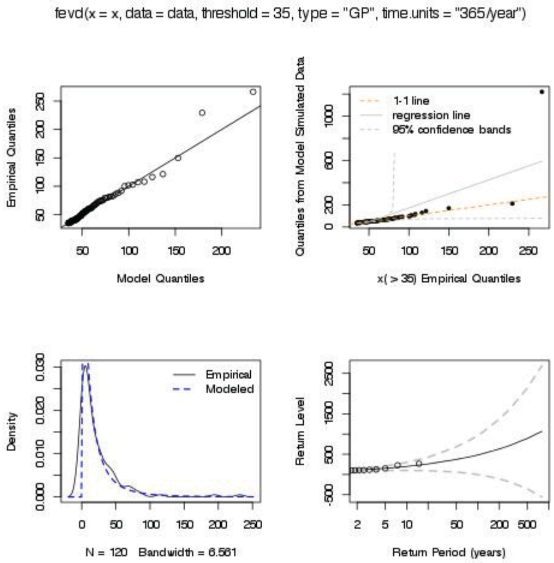

6C

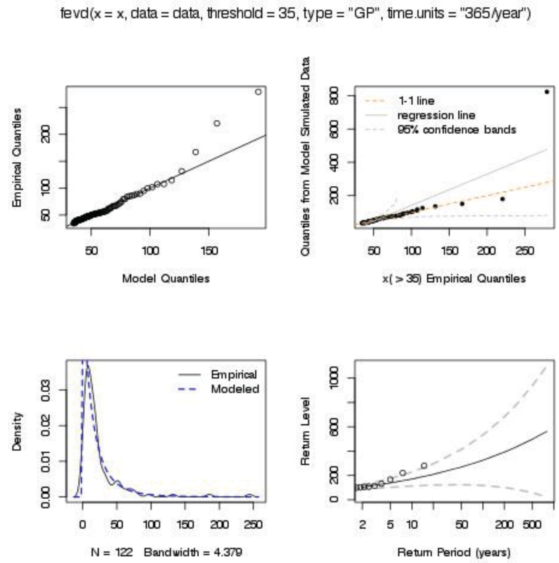

6D

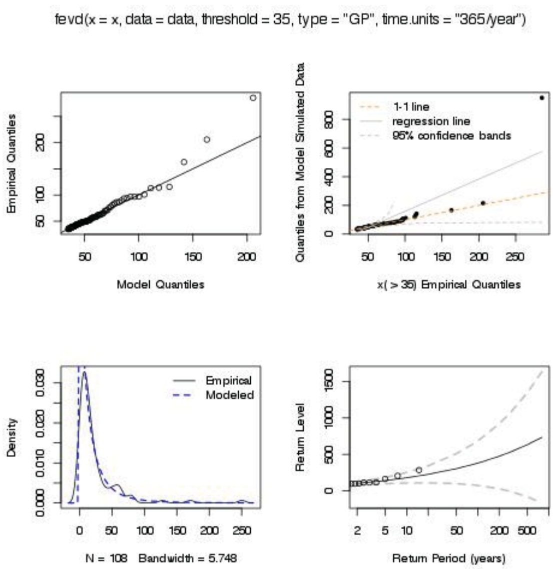

6E

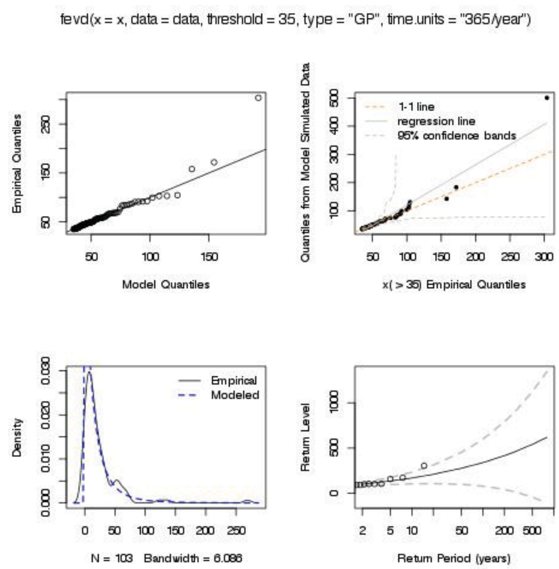

6F

24-hour Gridded Diagnostic Plots Threshold = 35 mm

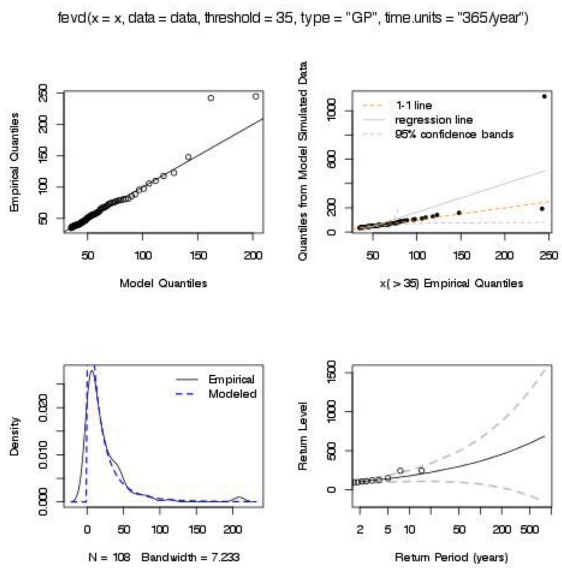

5C

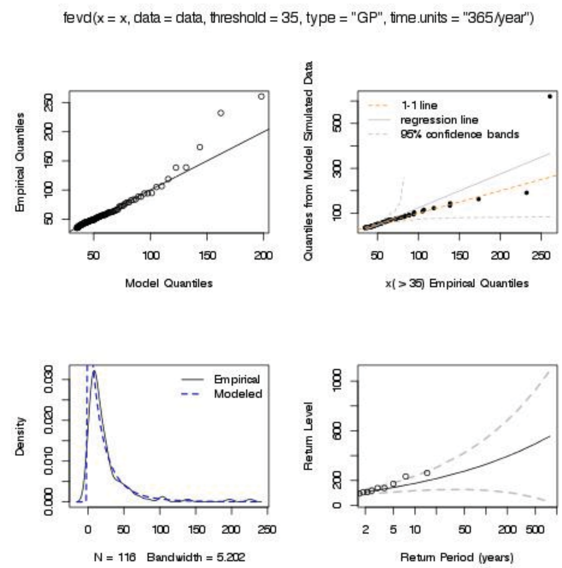

5D

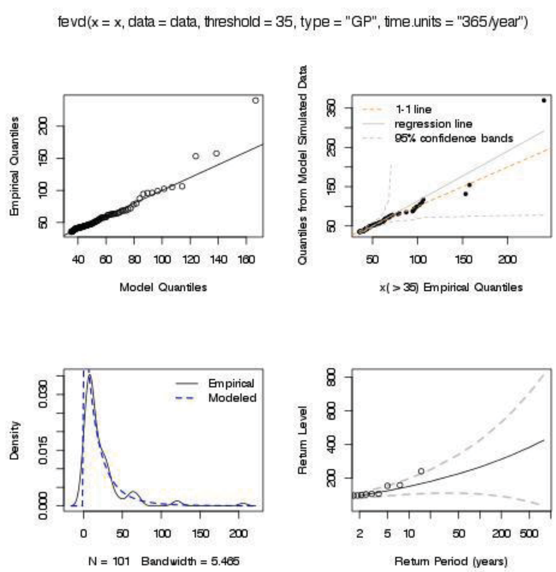

5E

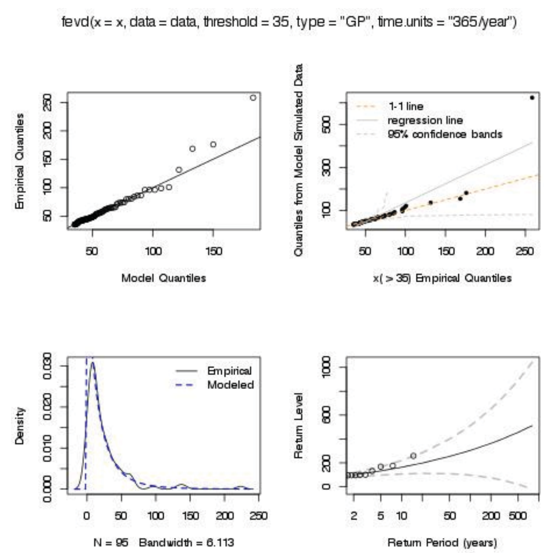

5F

24-hour Gridded Diagnostic Plots Threshold = 35 mm

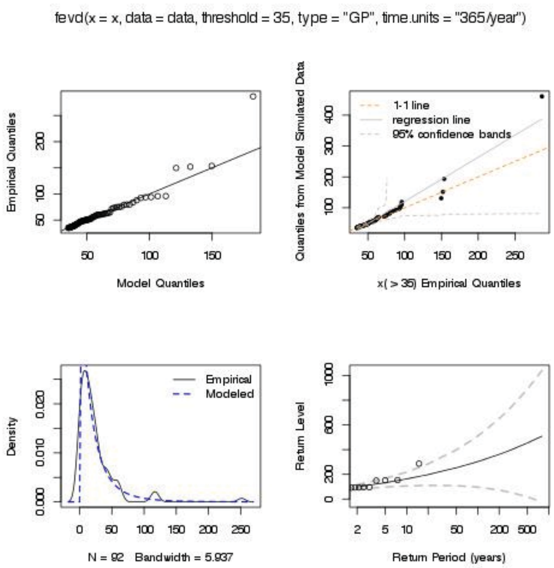

5G

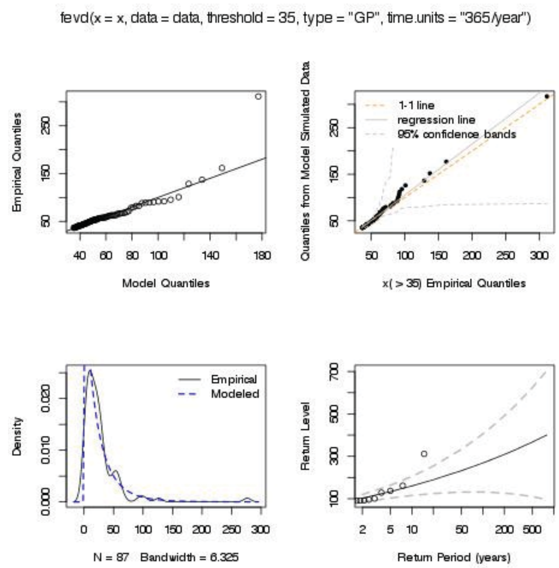

5H

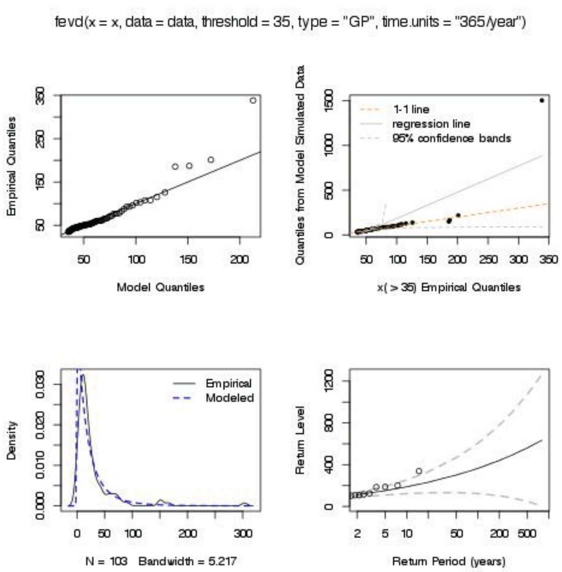

4C

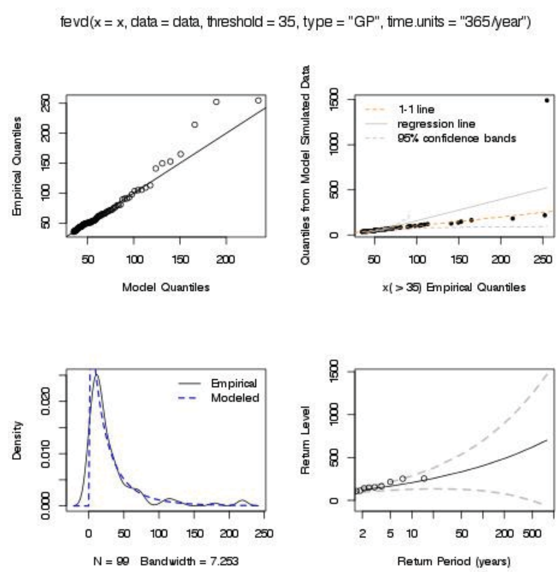

4D

24-hour Gridded Diagnostic Plots Threshold = 35 mm

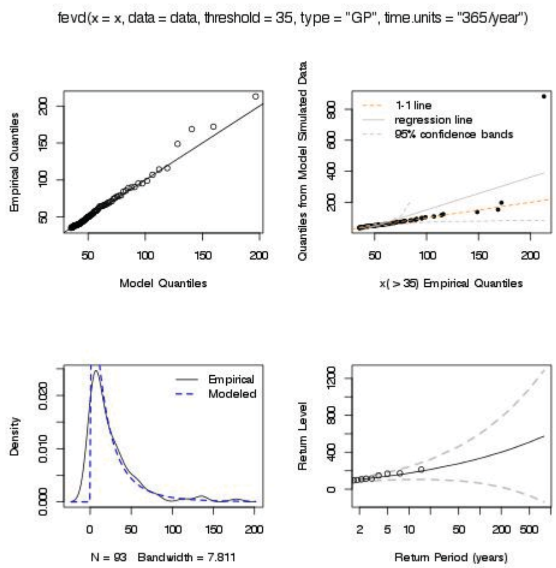

4E

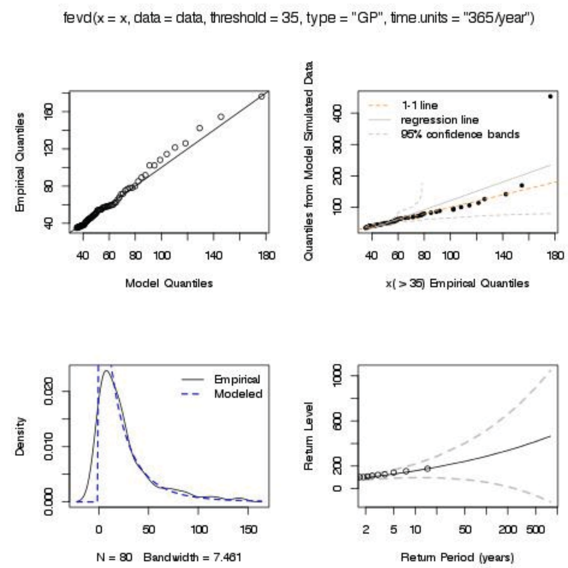

4F

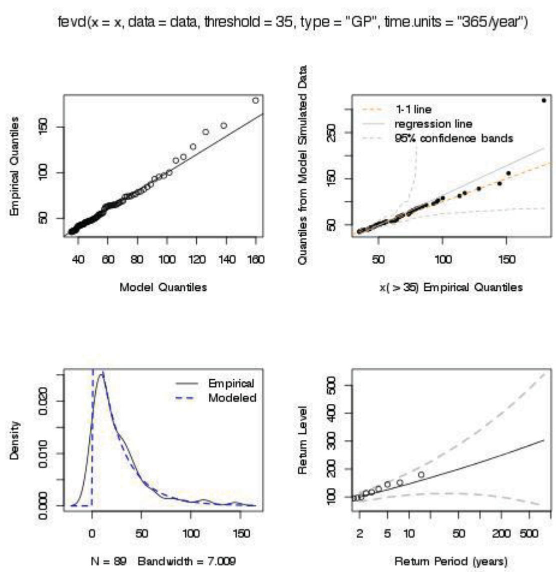

4G

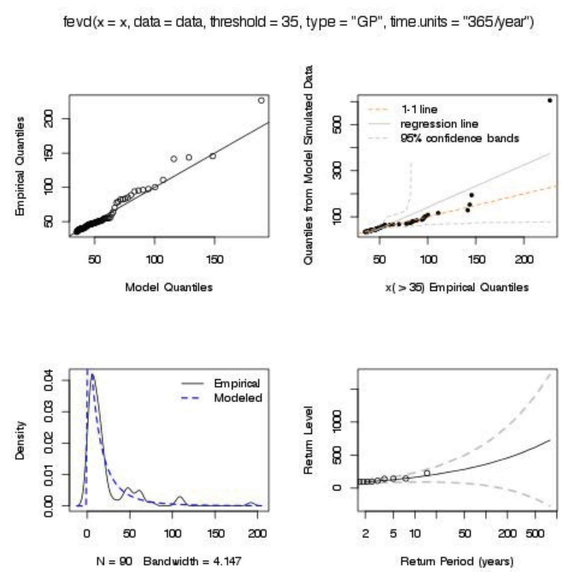

3B

24-hour Gridded Diagnostic Plots Threshold = 35 mm

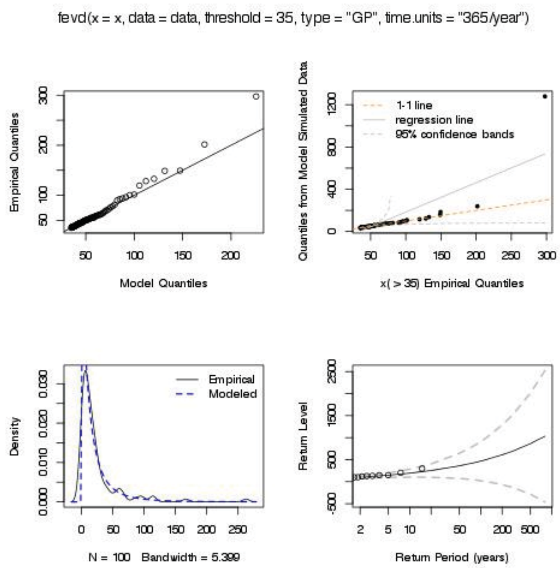

3C

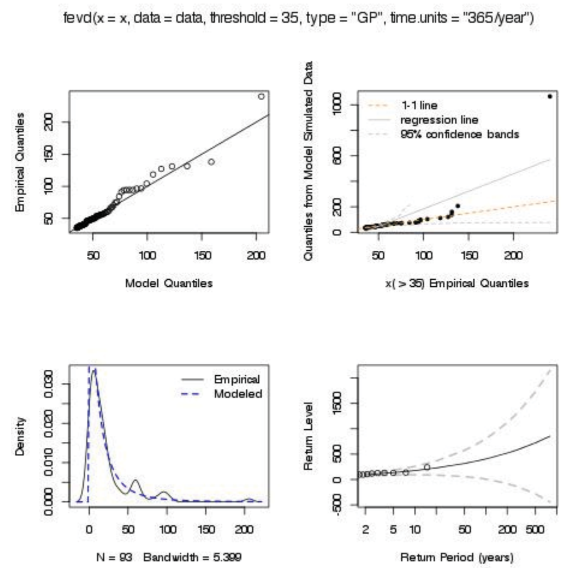

3D

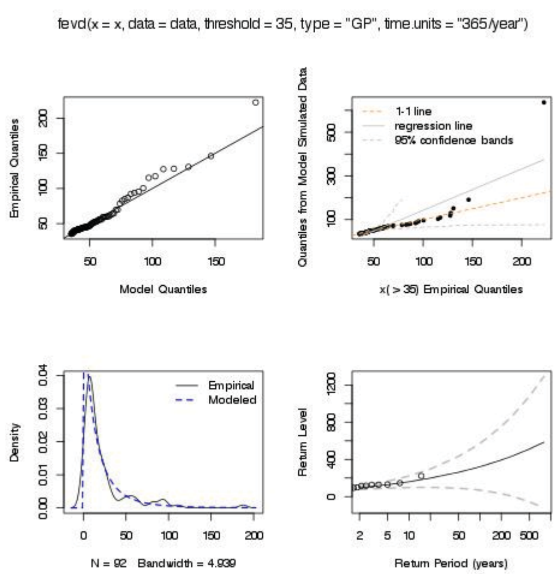

3E

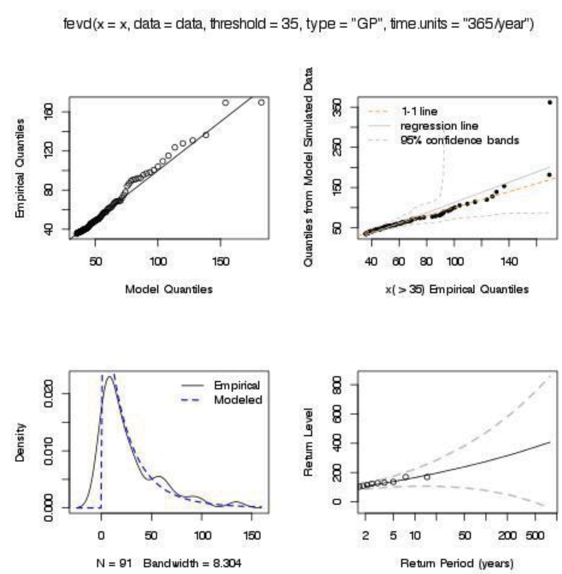

3F

24-hour Gridded Diagnostic Plots Threshold = 35 mm

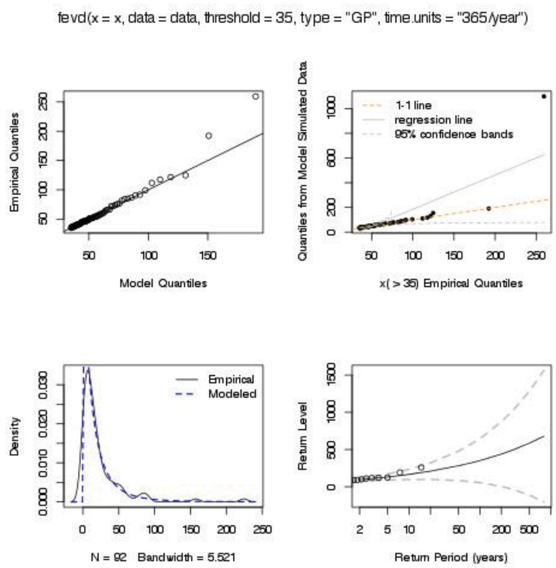

2C

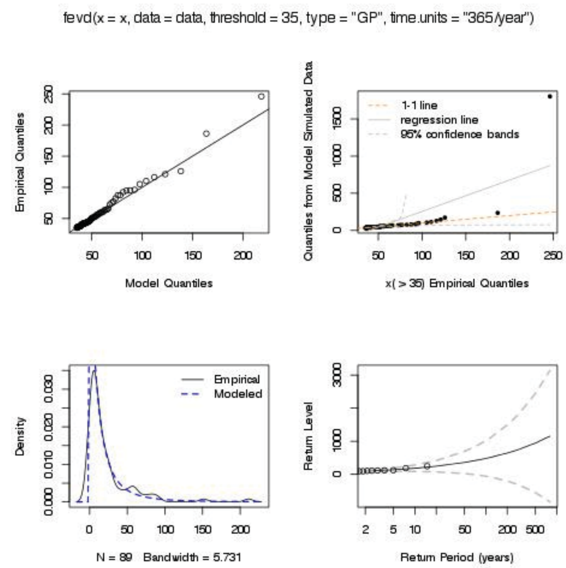

2D

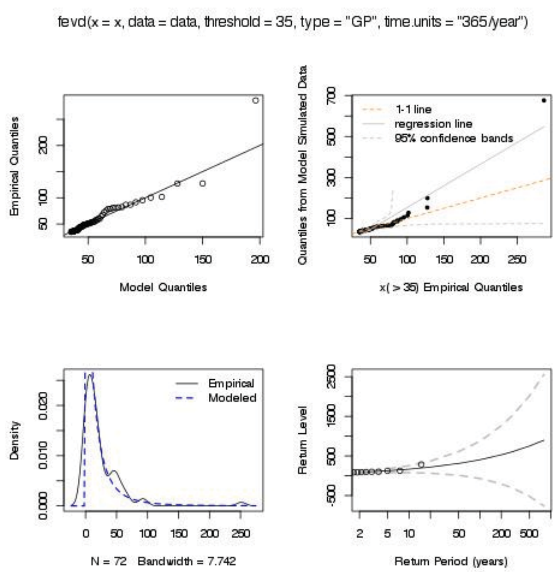

2E

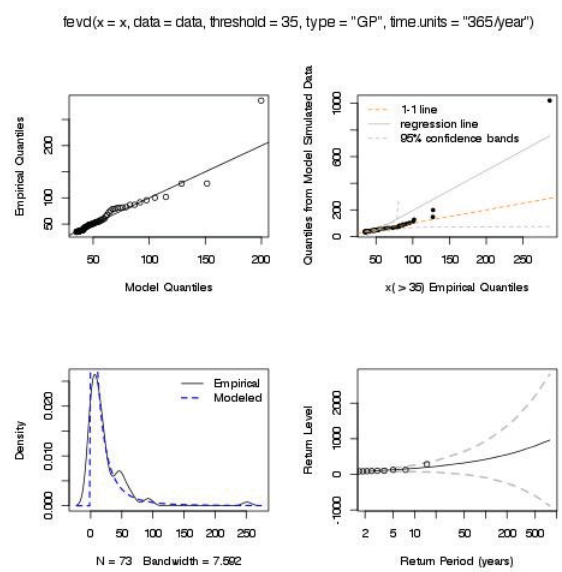

1D

72-hour Gridded Diagnostic Plots Threshold = 40 mm

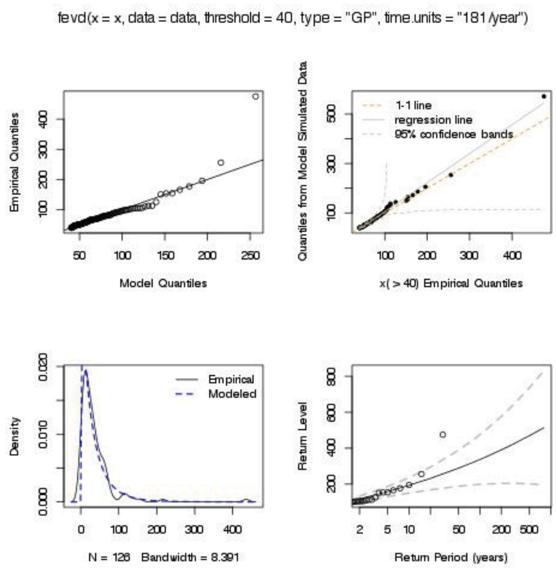

10E

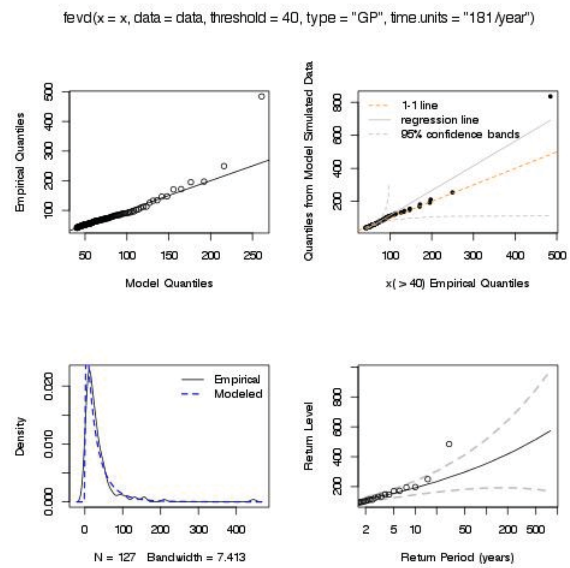

10F

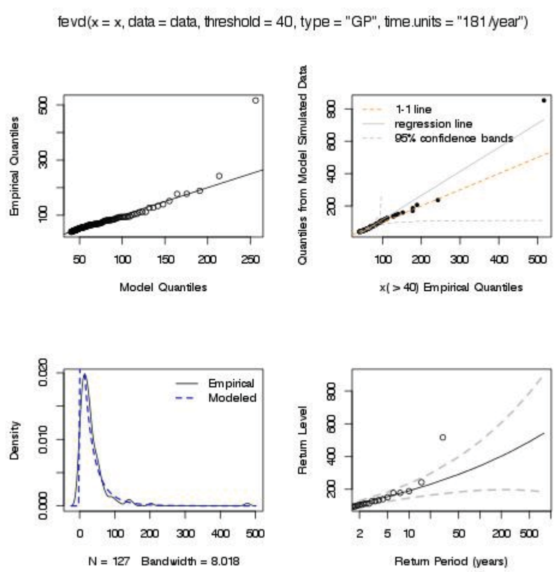

10G

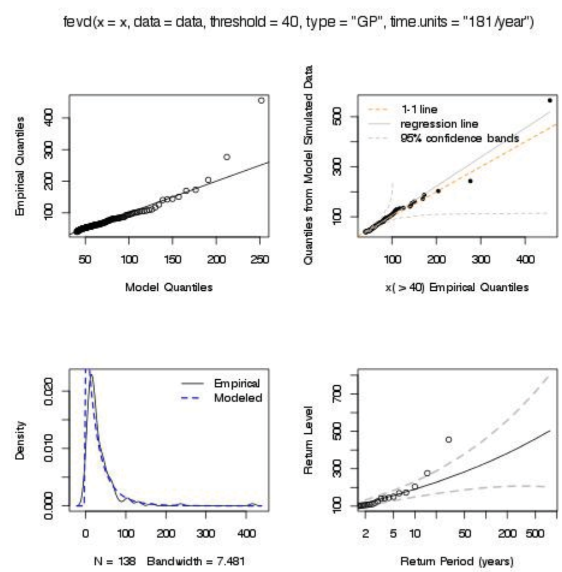

9E

72-hour Gridded Diagnostic Plots Threshold = 40 mm

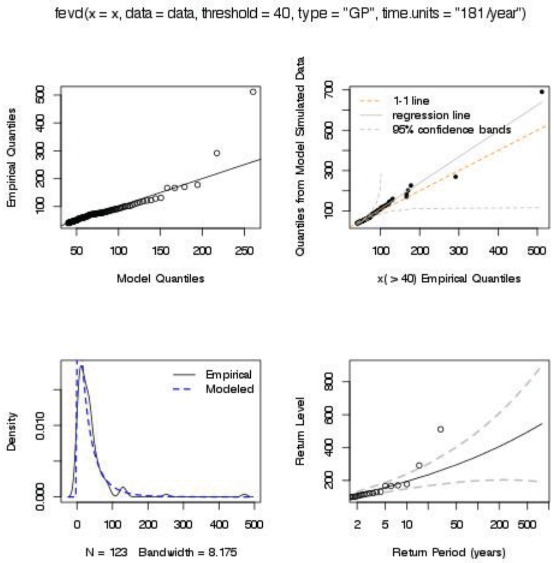

9G

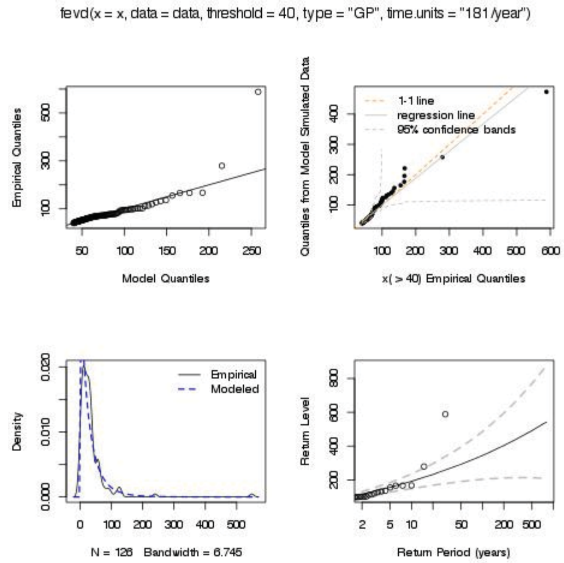

9H

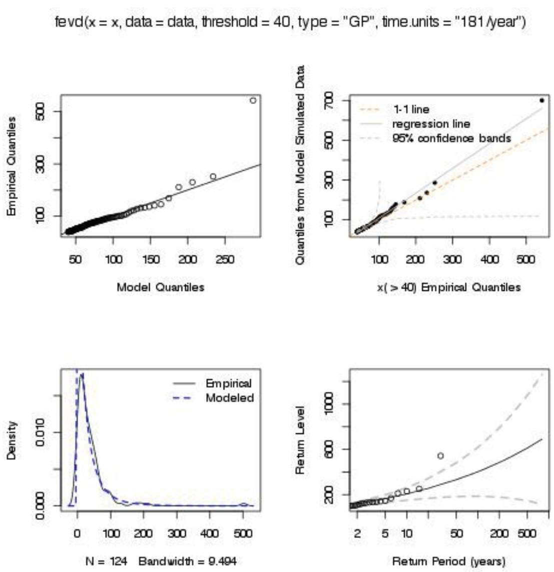

9I

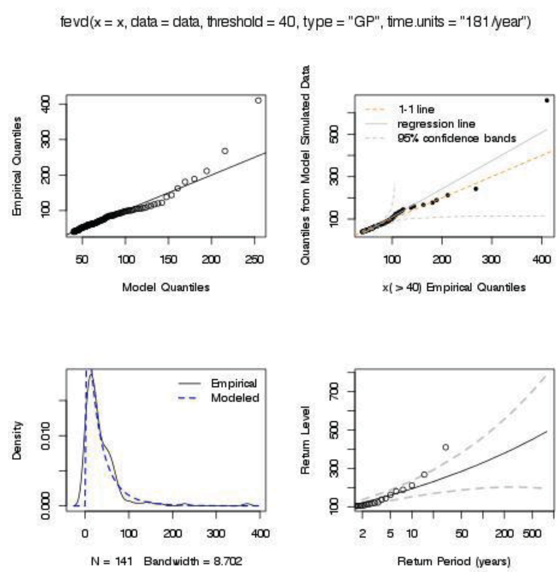

8D

72-hour Gridded Diagnostic Plots Threshold = 40 mm

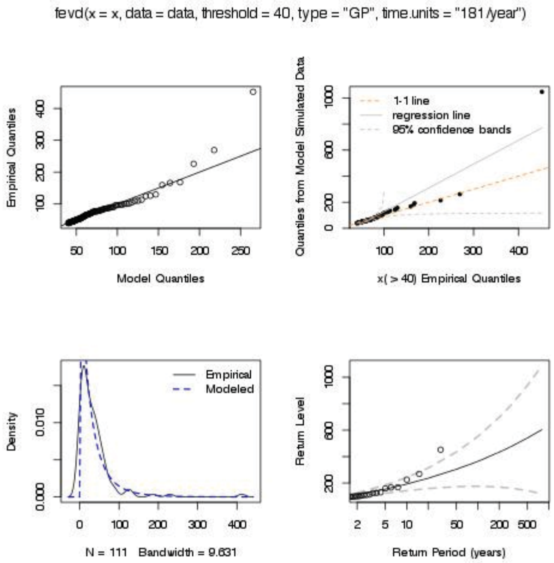

8H

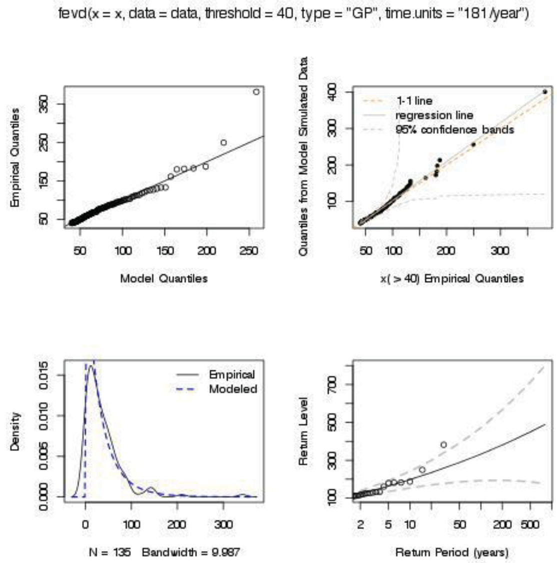

7D

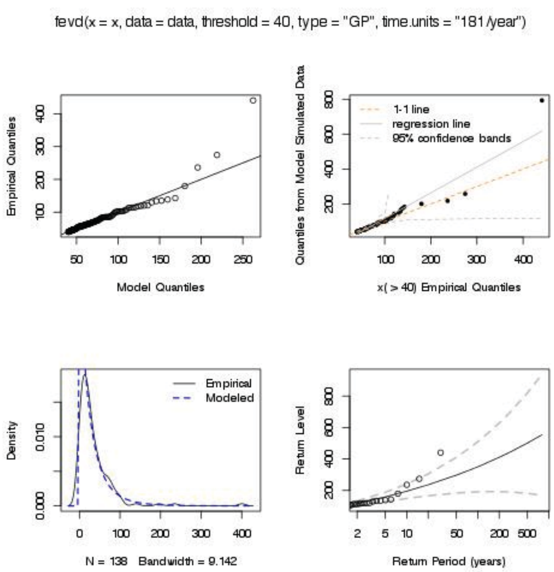

7E

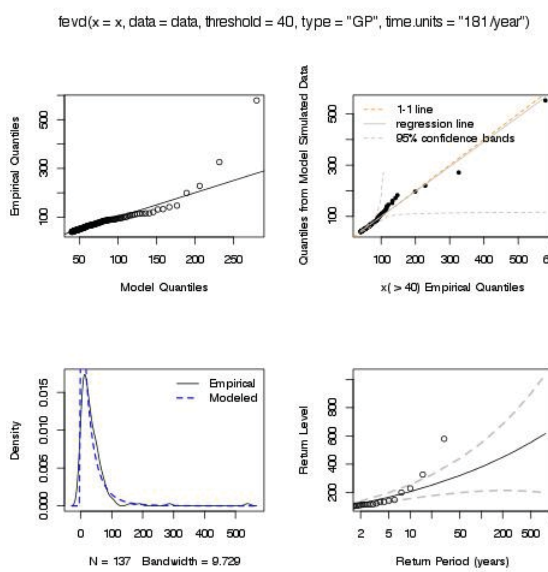

7F

72-hour Gridded Diagnostic Plots Threshold = 40 mm

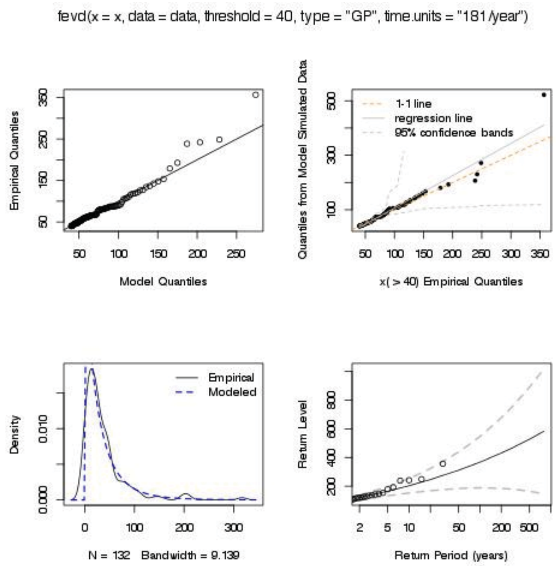

6C

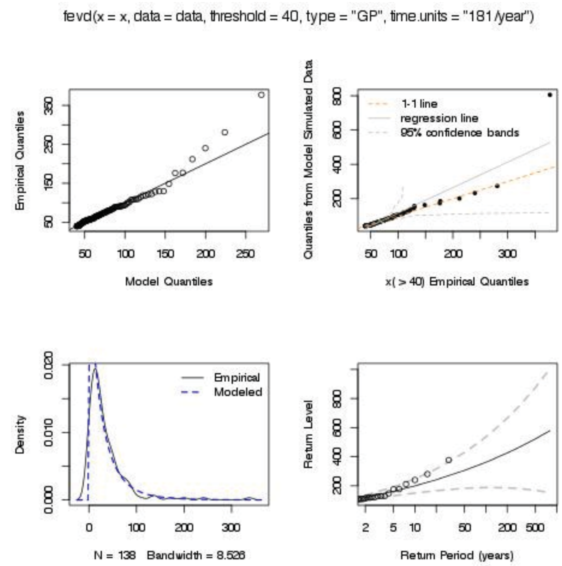

6D

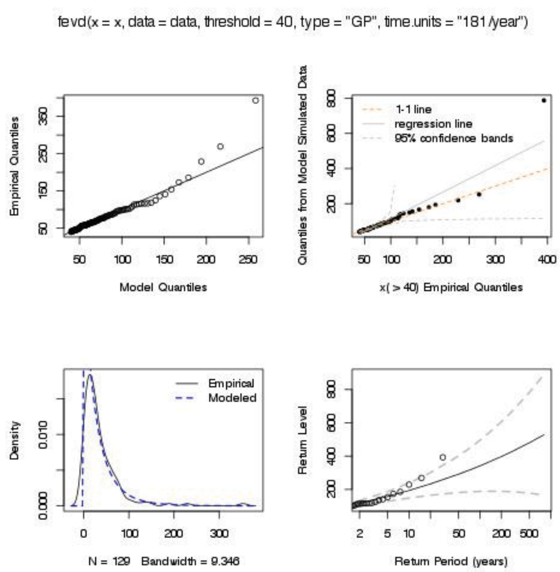

6E

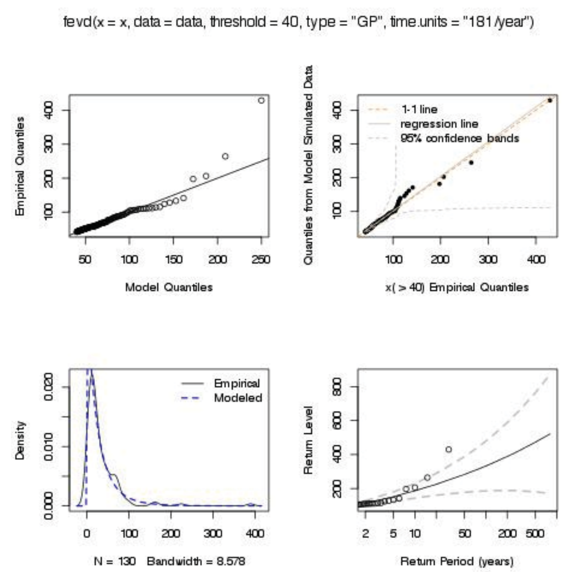

6F

72-hour Gridded Diagnostic Plots Threshold = 40 mm

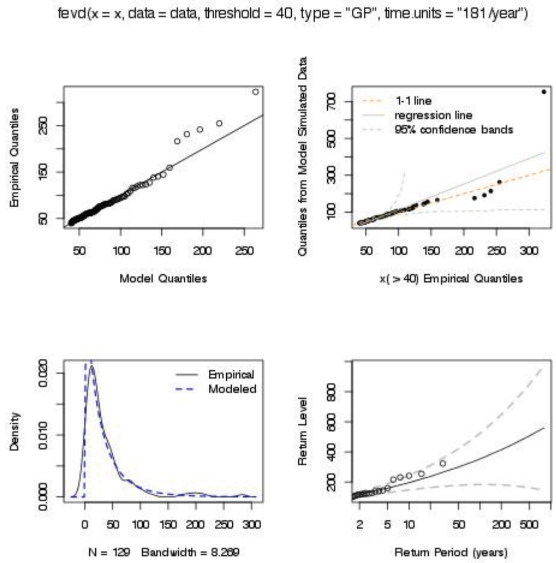

5C

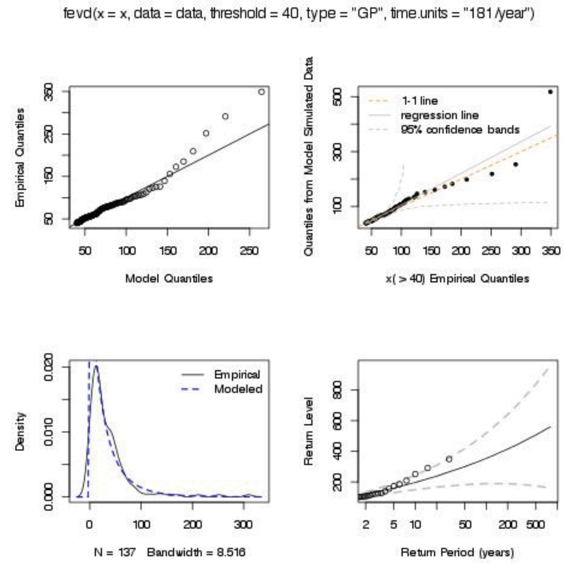

5D

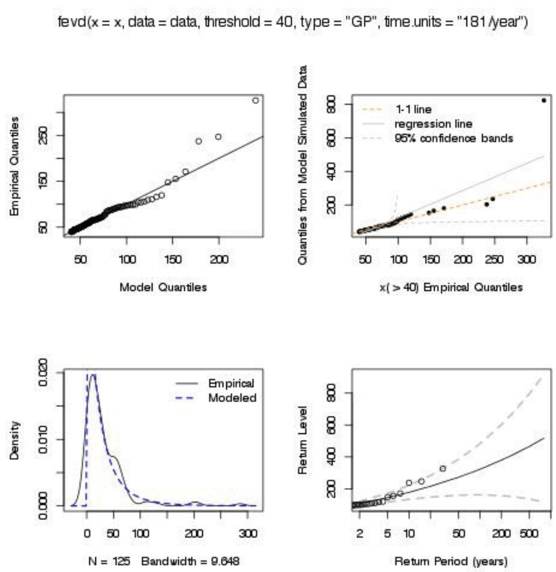

5E

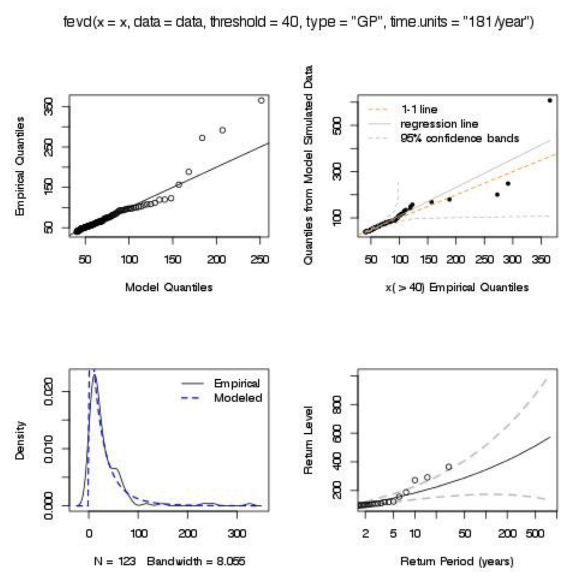

5F

72-hour Gridded Diagnostic Plots Threshold = 40 mm

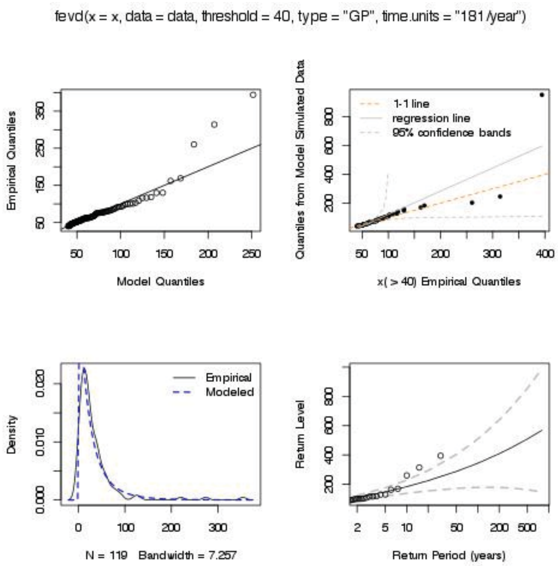

5G

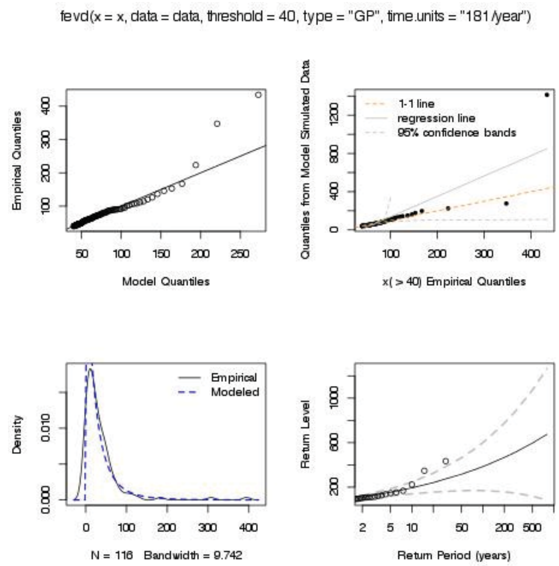

5H

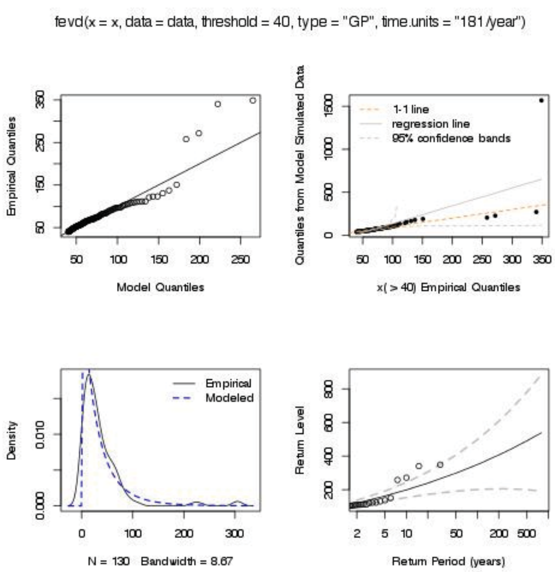

4C

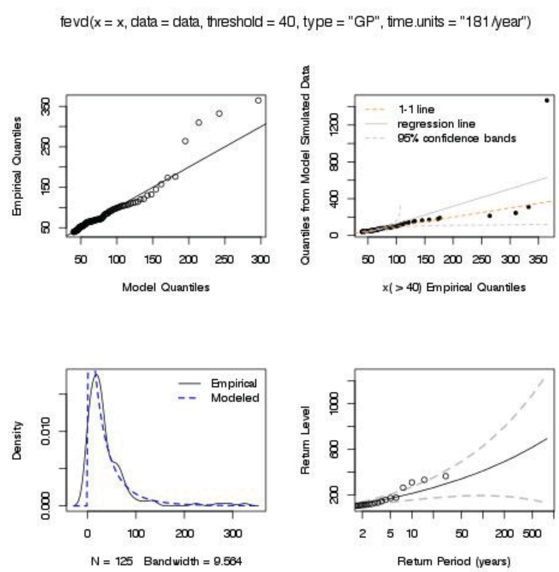

4D

72-hour Gridded Diagnostic Plots Threshold = 40 mm

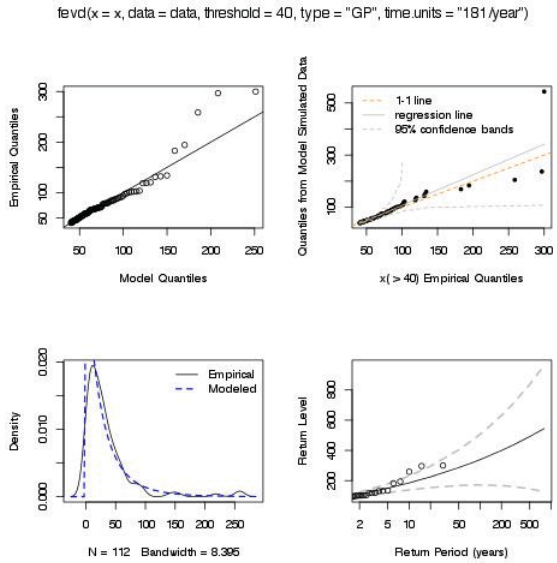

4E

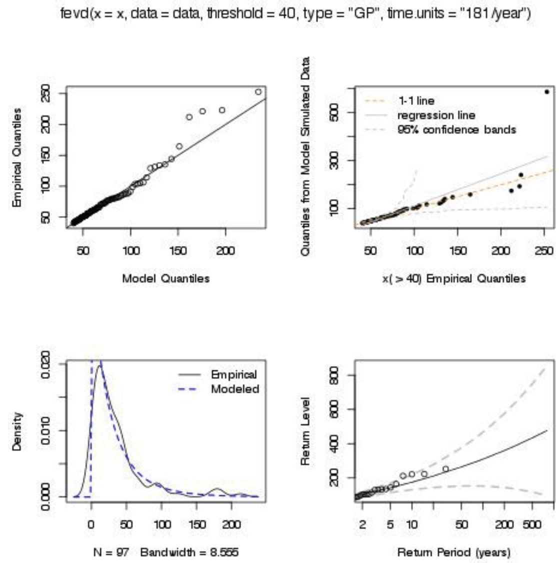

4F

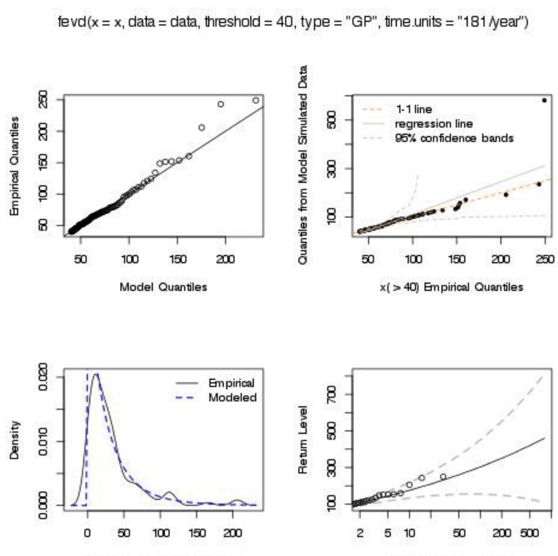

4G

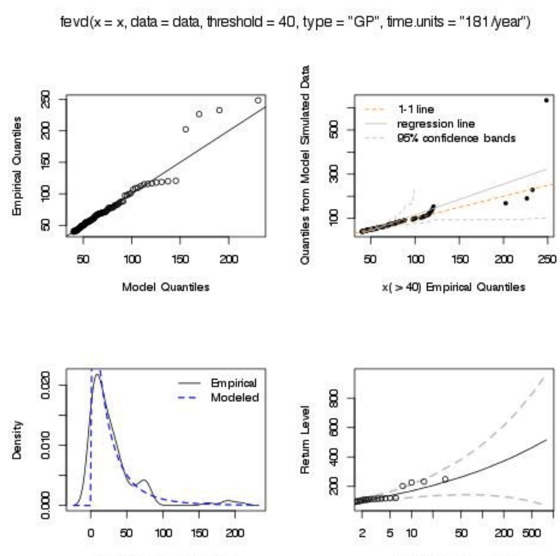

3B

72-hour Gridded Diagnostic Plots Threshold = 40 mm

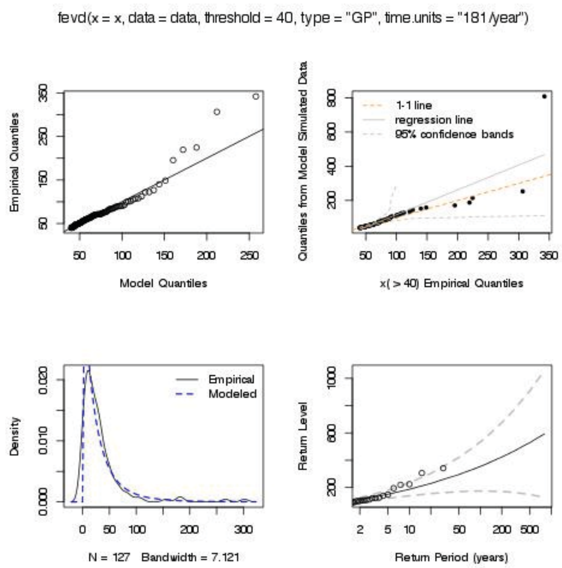

3C

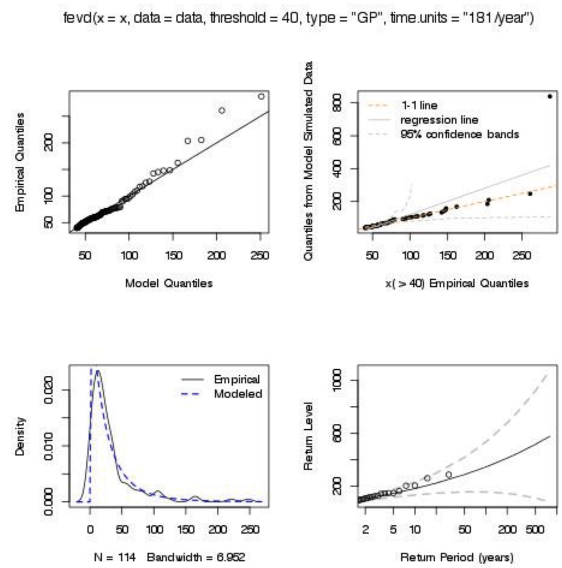

3D

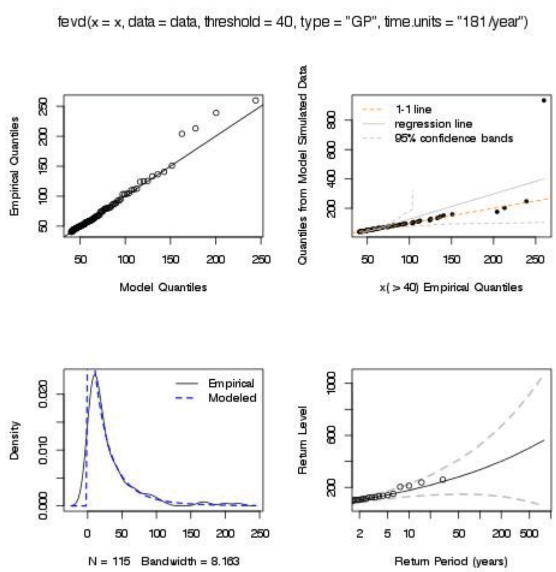

3E

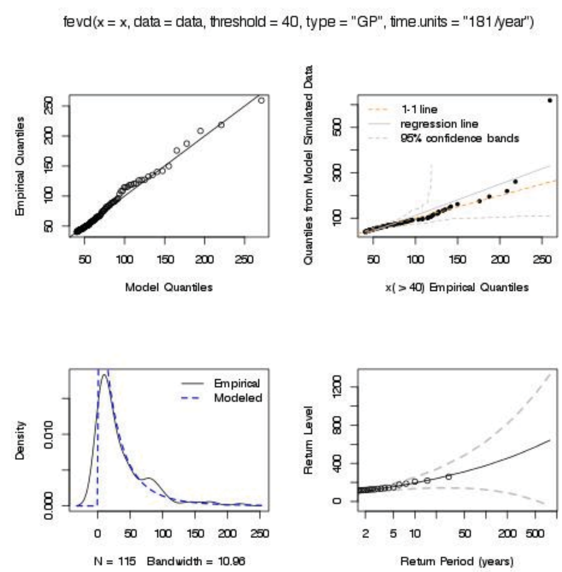

3F

72-hour Gridded Diagnostic Plots Threshold = 40 mm

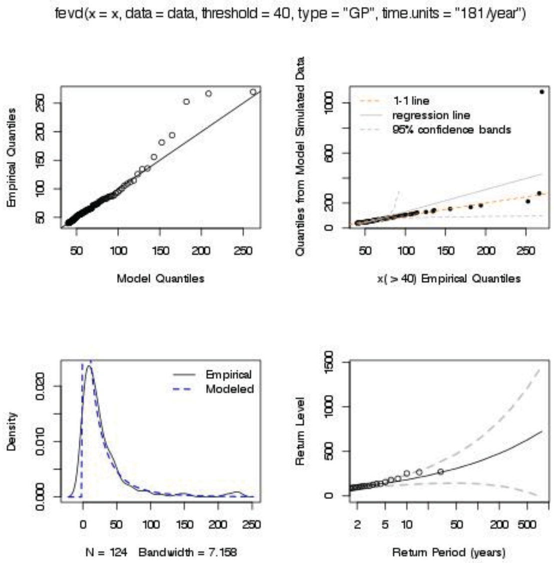

2C

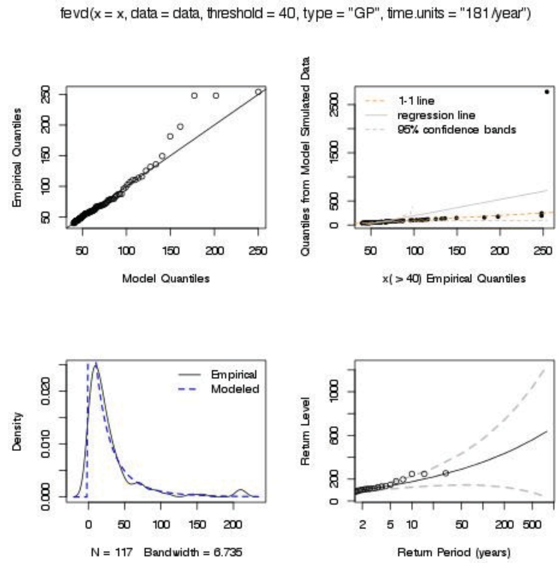

2D

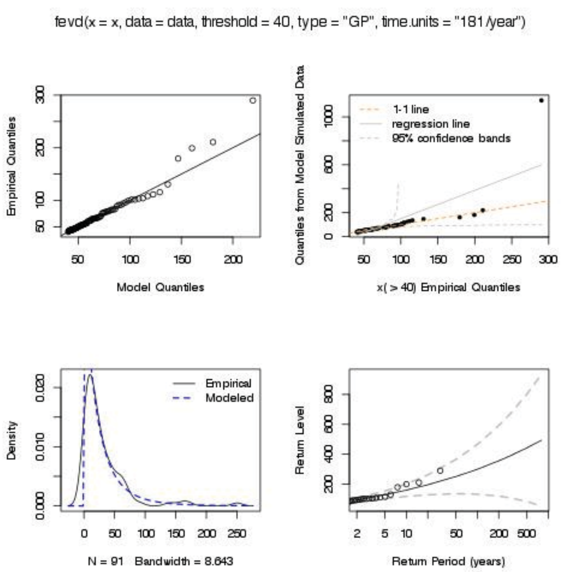

2E

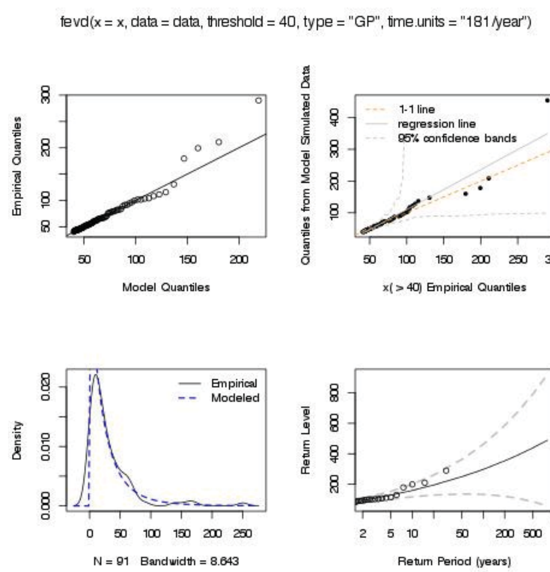

1D

72-hour Gridded Diagnostic Plots Threshold = 45 mm

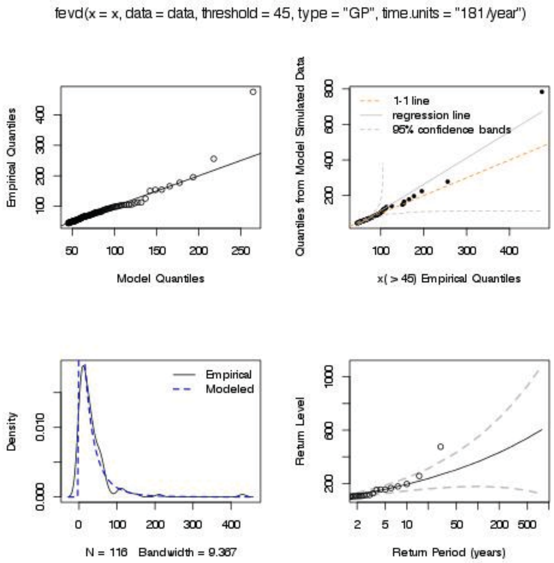

10E

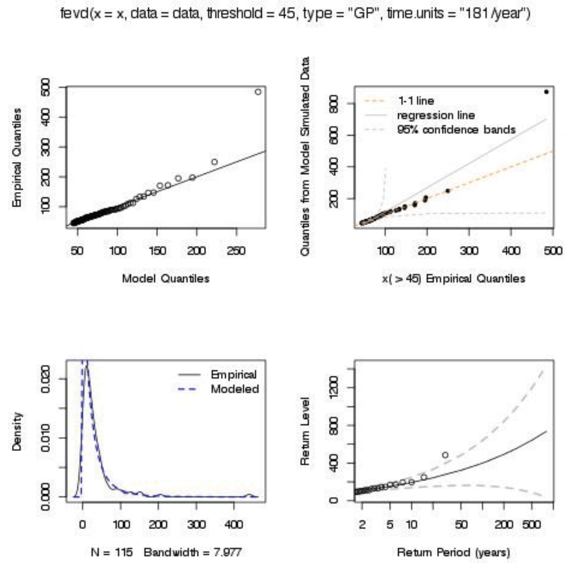

10F

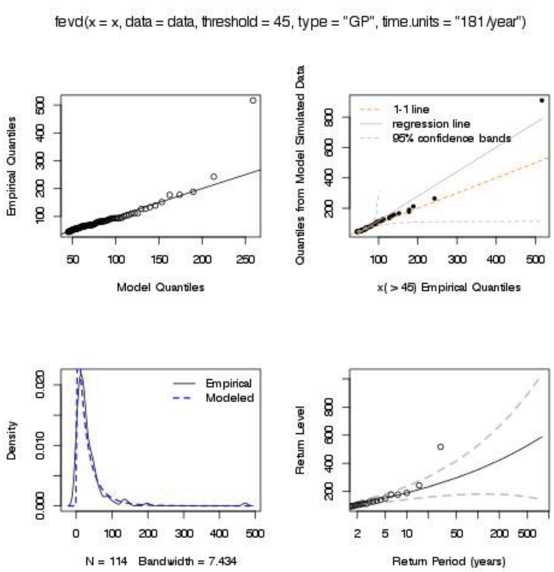

10G

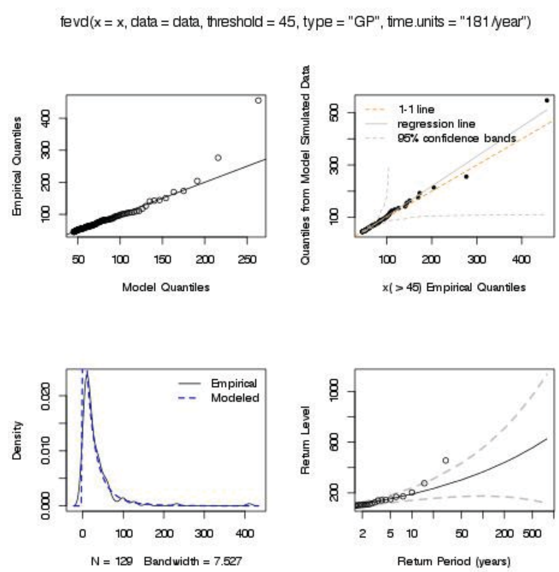

9E

72-hour Gridded Diagnostic Plots Threshold = 45 mm

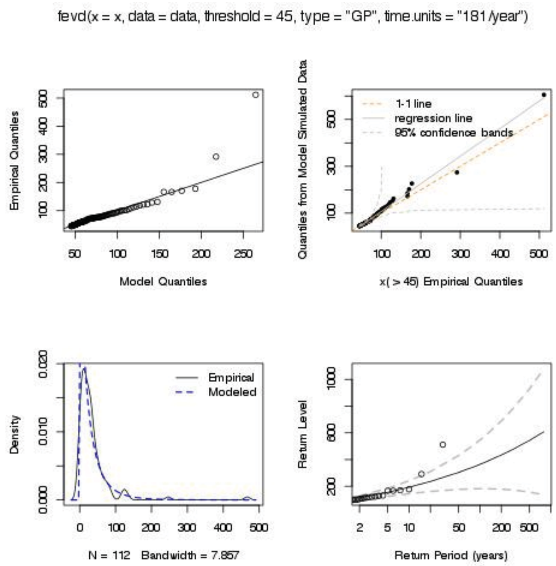

9G

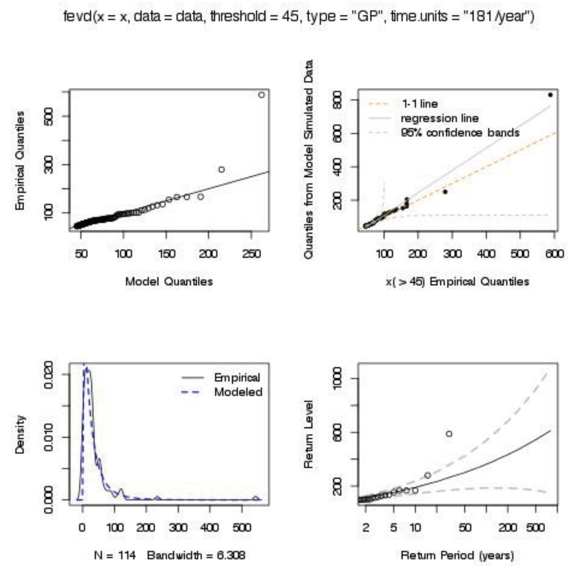

9H

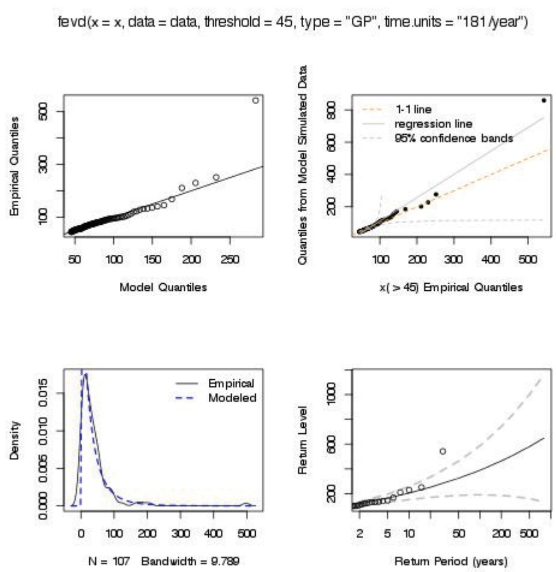

9I

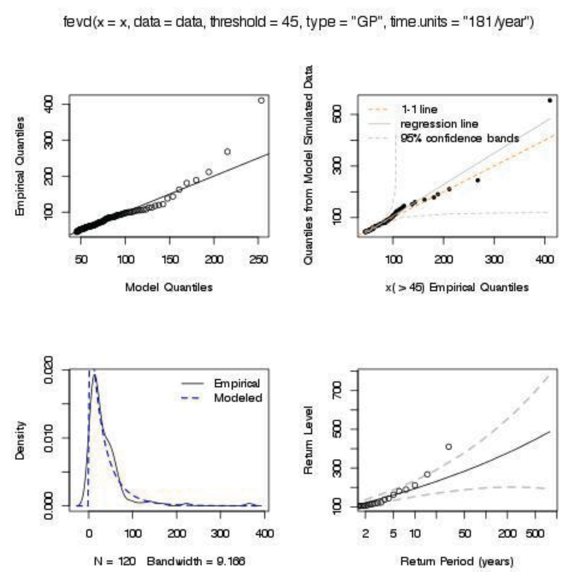

8D

72-hour Gridded Diagnostic Plots Threshold = 45 mm

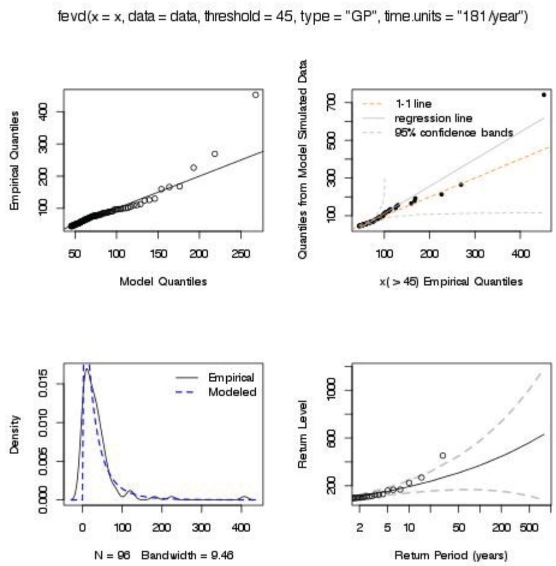

8H

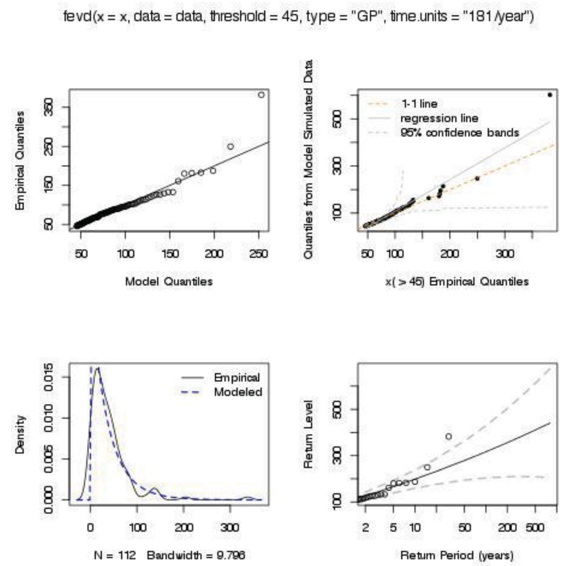

7D

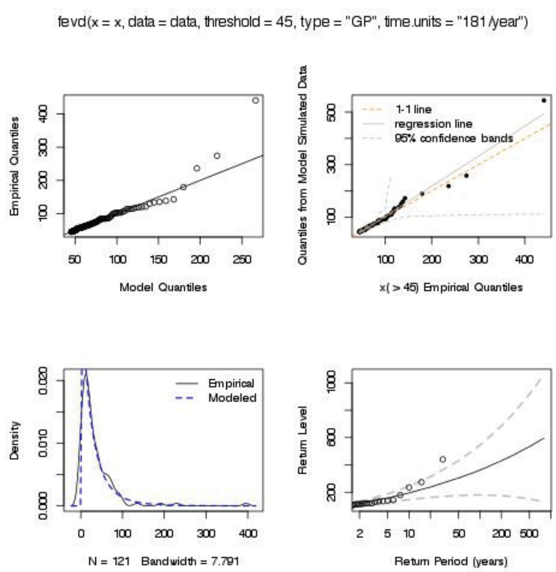

7E

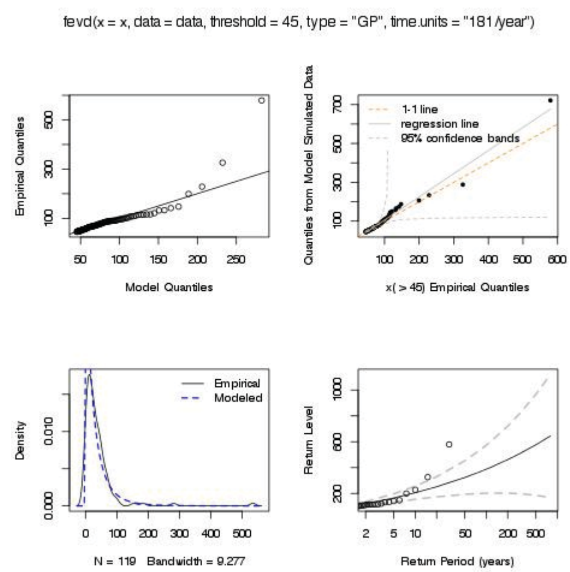

7F

72-hour Gridded Diagnostic Plots Threshold = 45 mm

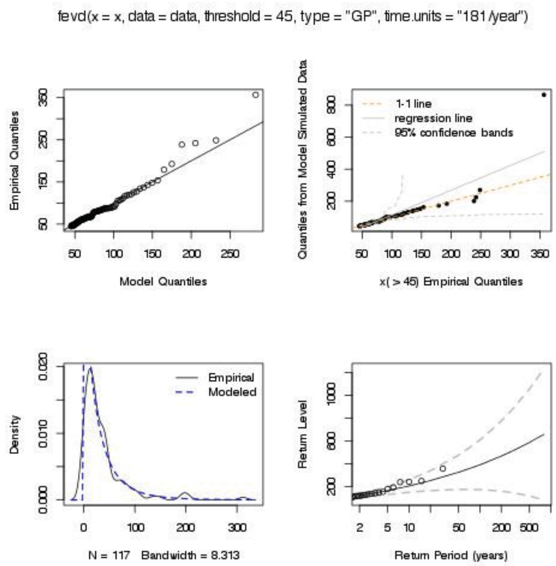

6C

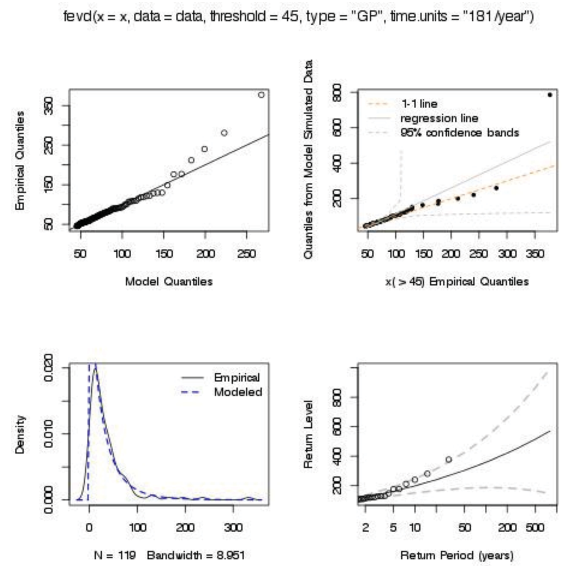

6D

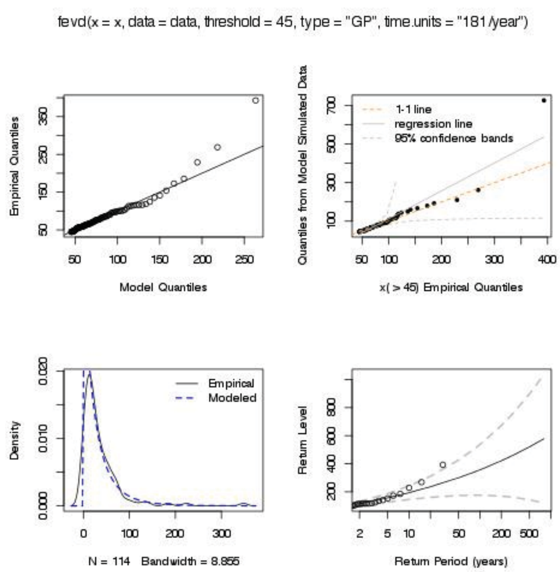

6E

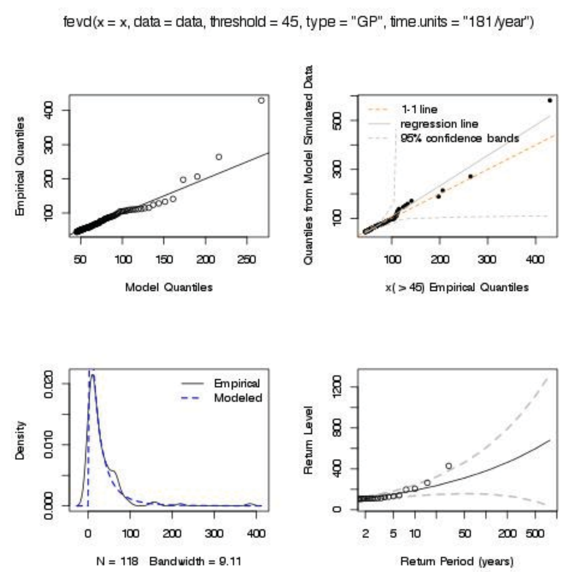

6F

72-hour Gridded Diagnostic Plots Threshold = 45 mm

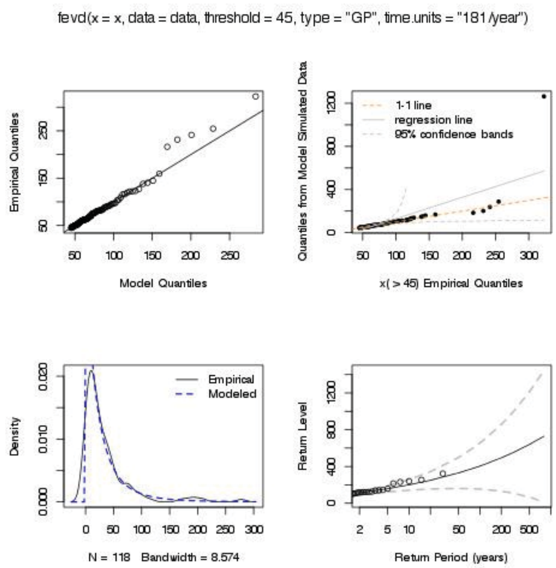

5C

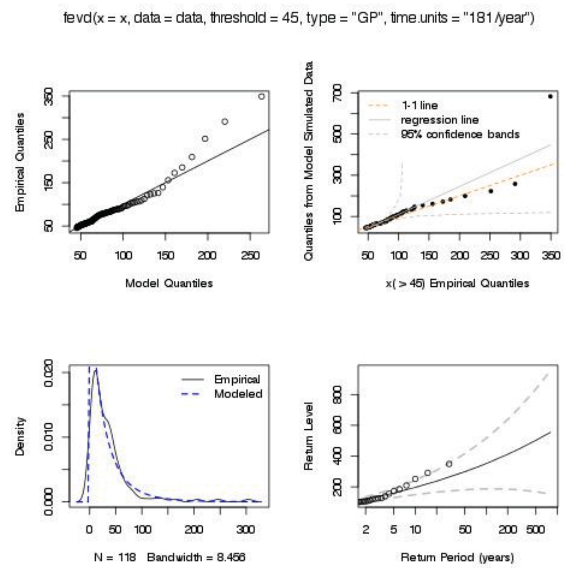

5D

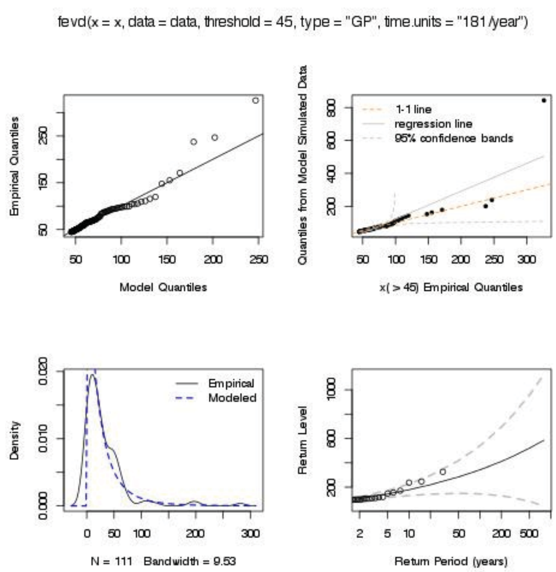

5E

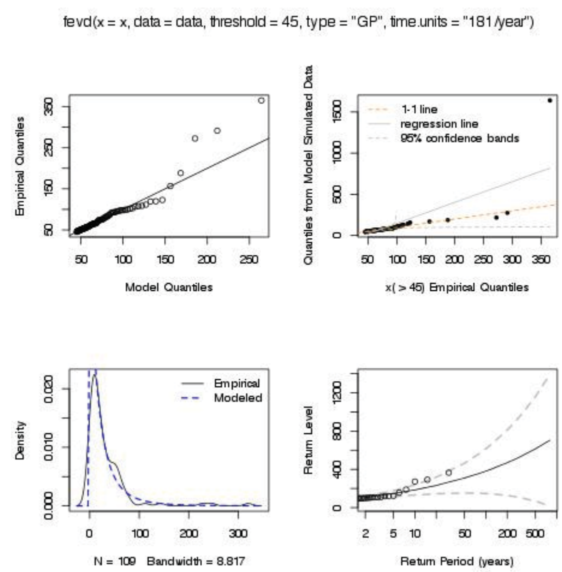

5F

72-hour Gridded Diagnostic Plots Threshold = 45 mm

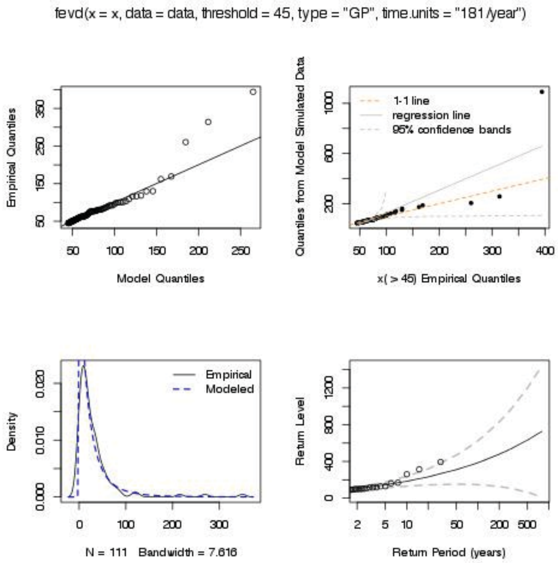

5G

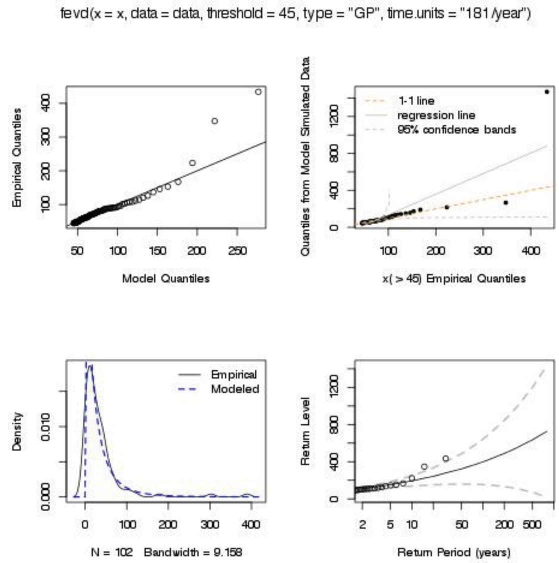

5H

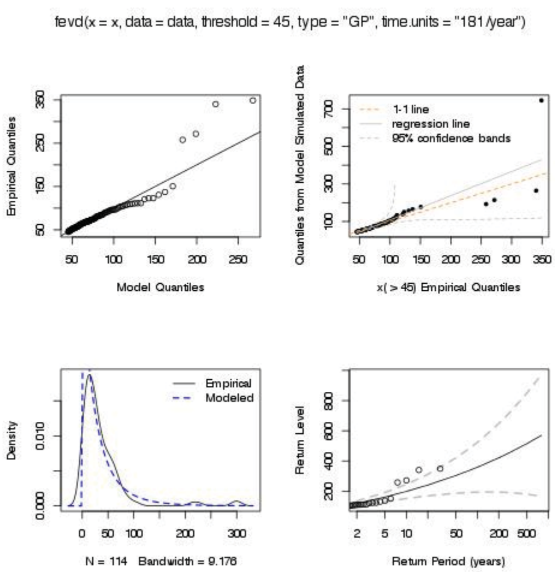

4C

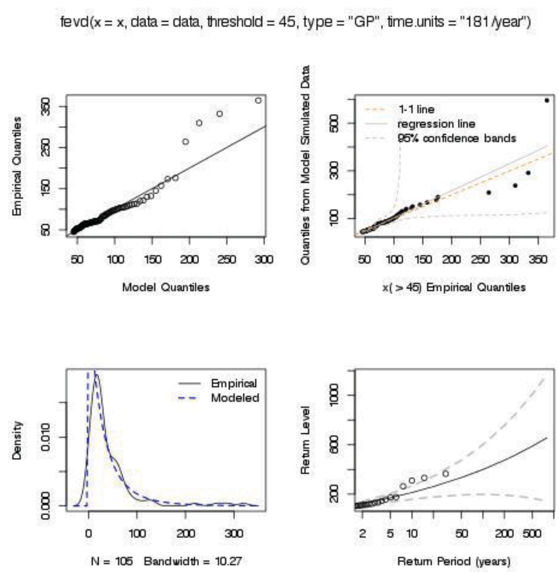

4D

72-hour Gridded Diagnostic Plots Threshold = 45 mm

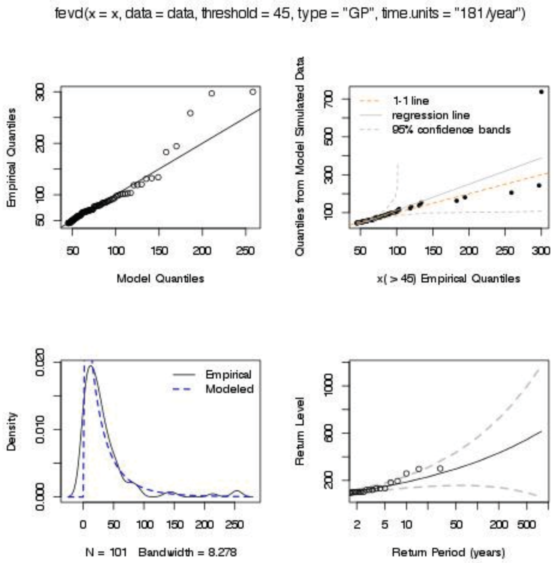

4E

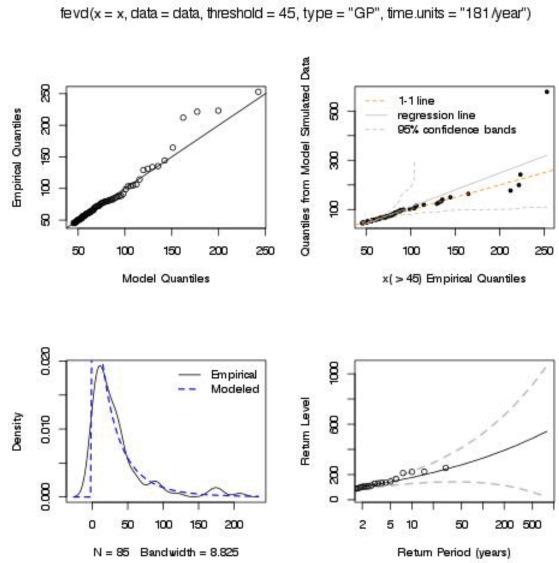

4F

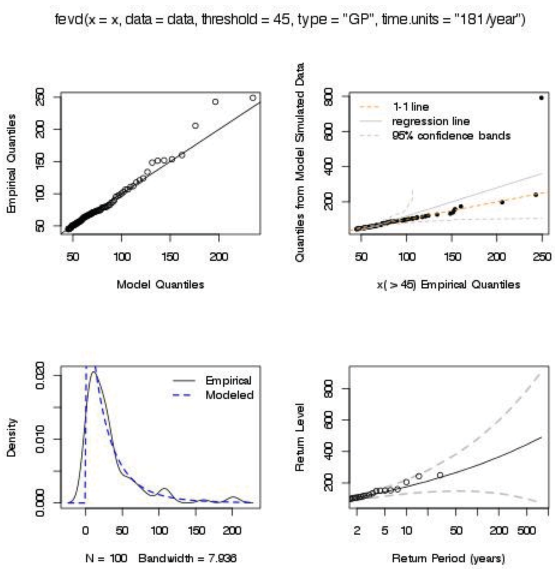

4G

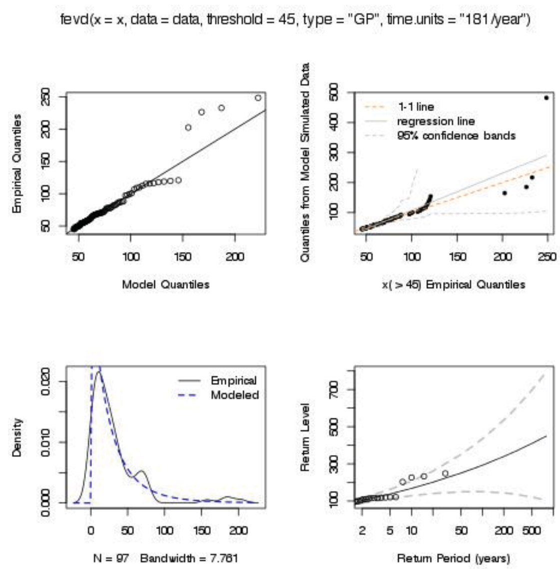

3B

72-hour Gridded Diagnostic Plots Threshold = 45 mm

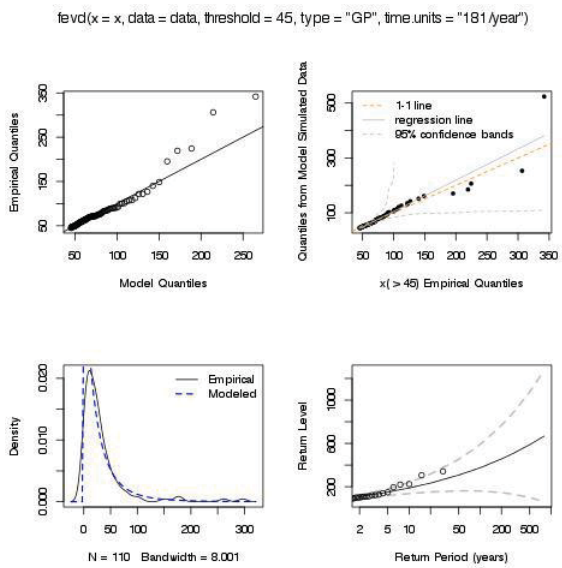

3C

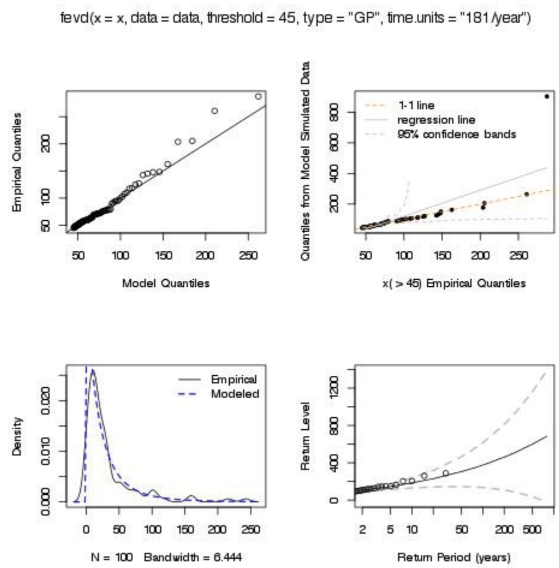

3D

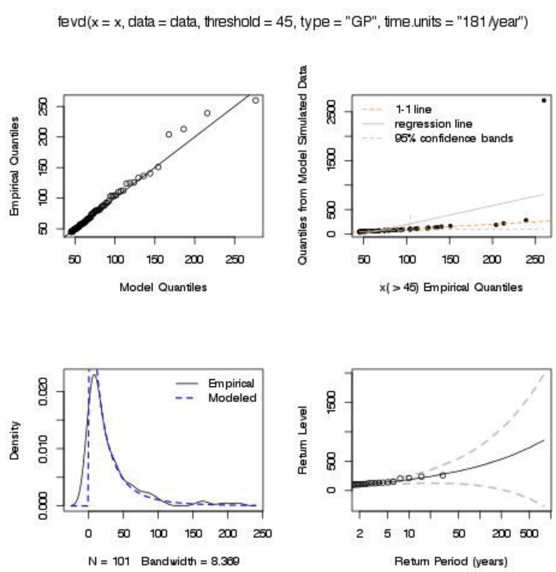

3E

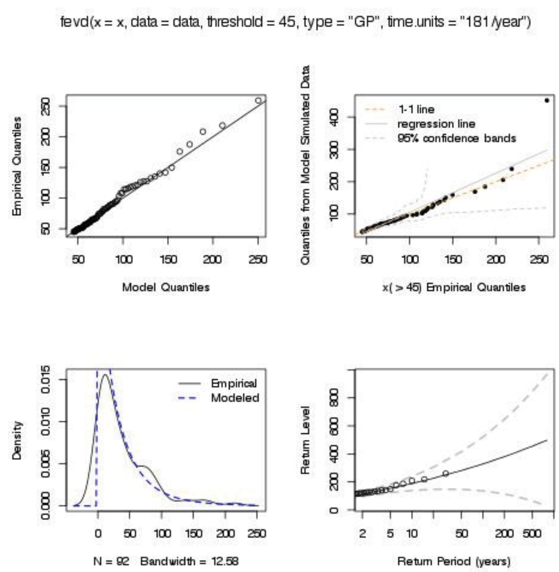

3F

72-hour Gridded Diagnostic Plots Threshold = 45 mm

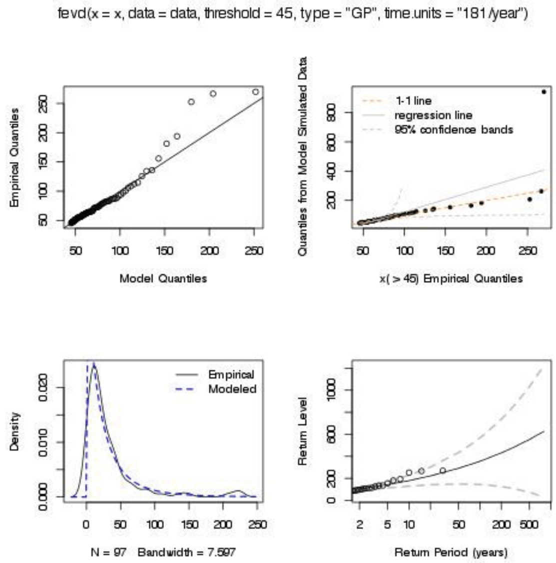

2C

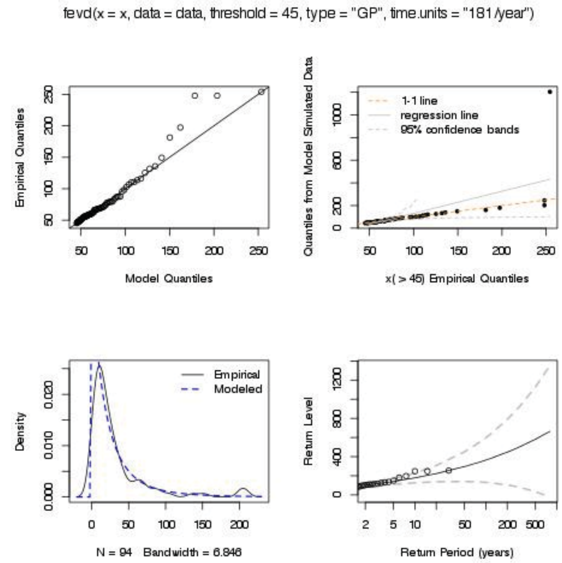

2D

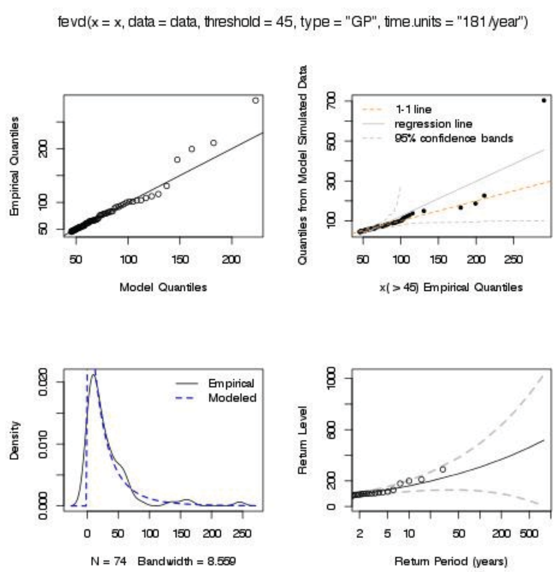

2E

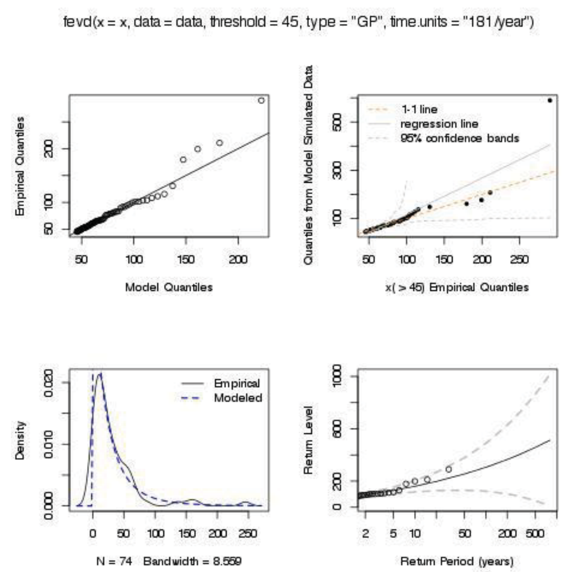

1D

72-hour Gridded Diagnostic Plots Threshold = 50 mm

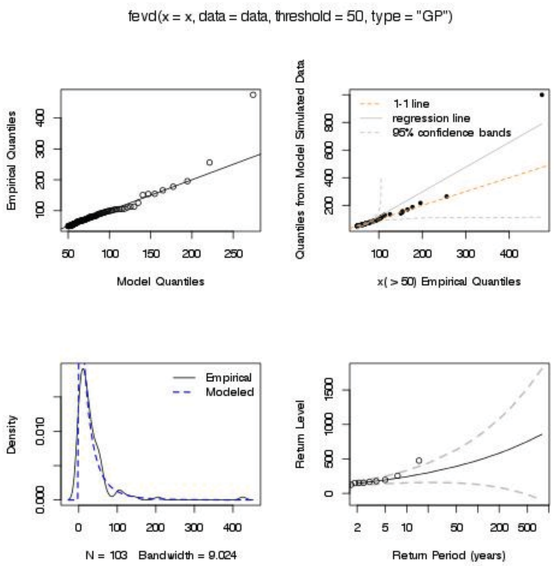

10E

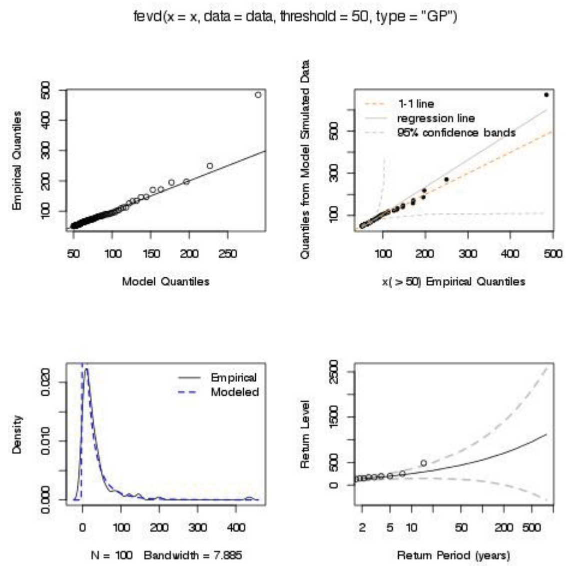

10F

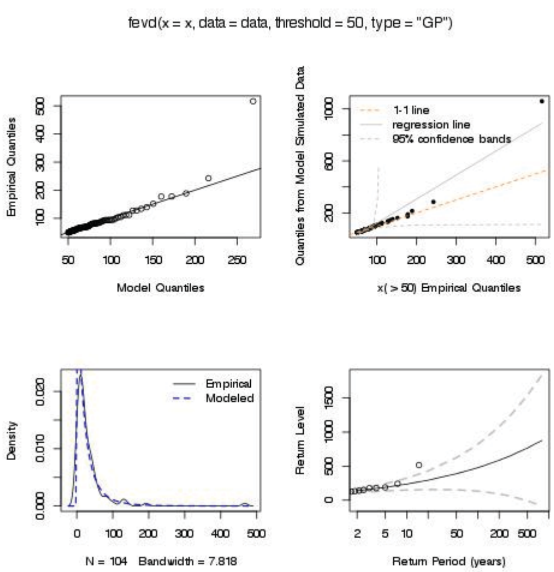

10G

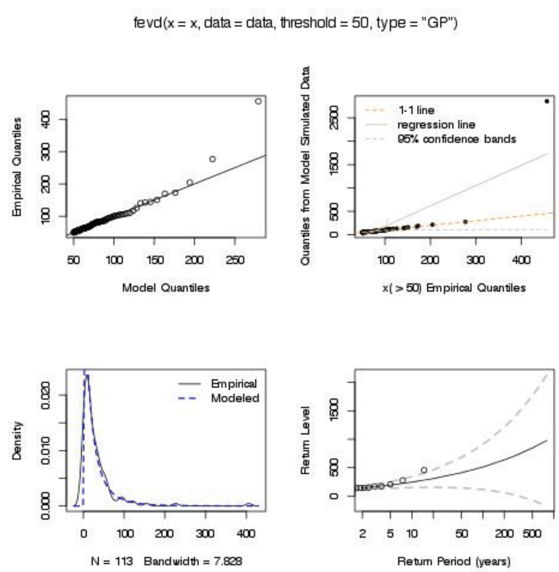

9E

72-hour Gridded Diagnostic Plots Threshold = 50 mm

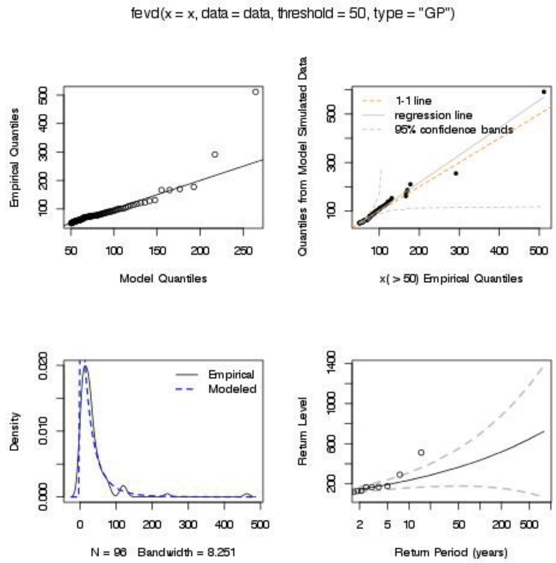

9G

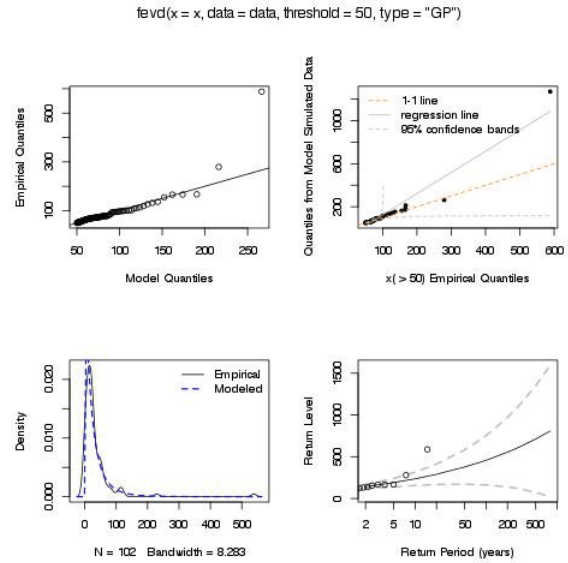

9H

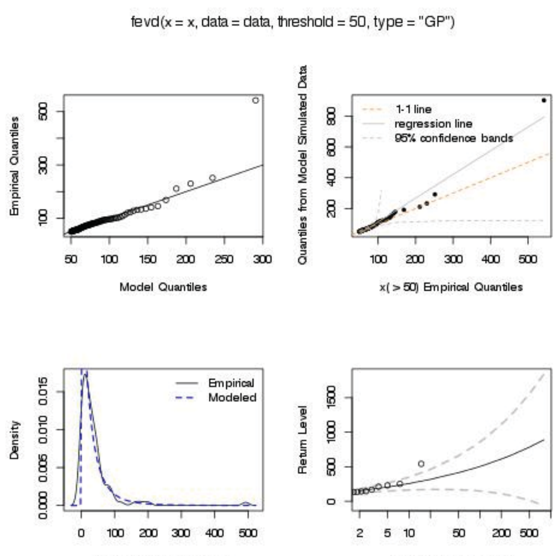

9I

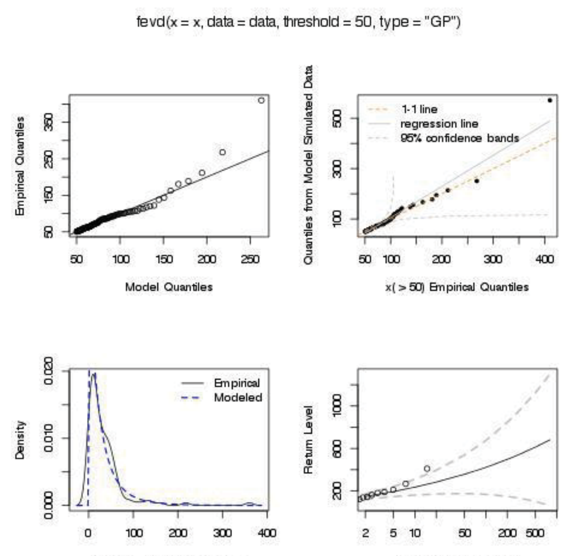

8D

72-hour Gridded Diagnostic Plots Threshold = 50 mm

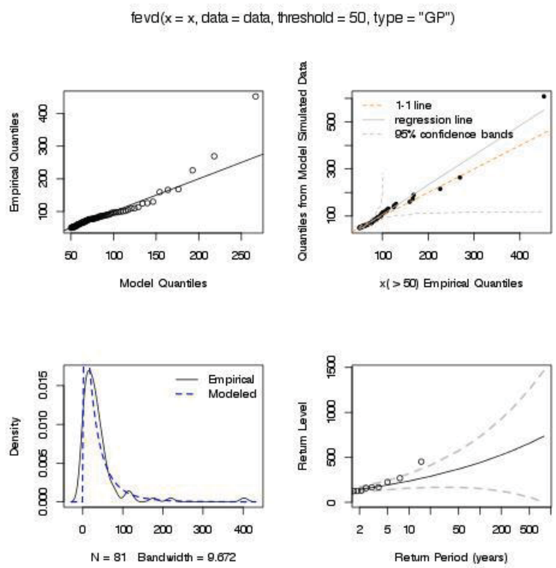

8H

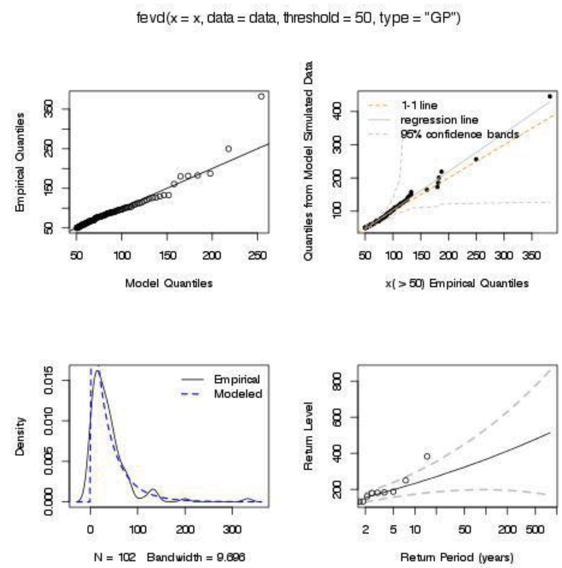

7D

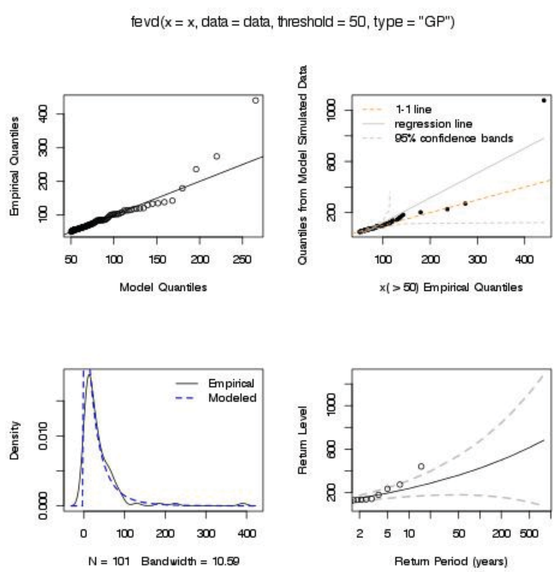

7E

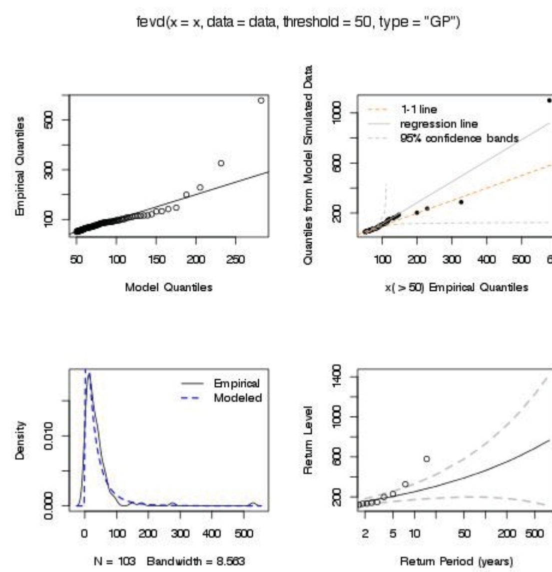

7F

72-hour Gridded Diagnostic Plots Threshold = 50 mm

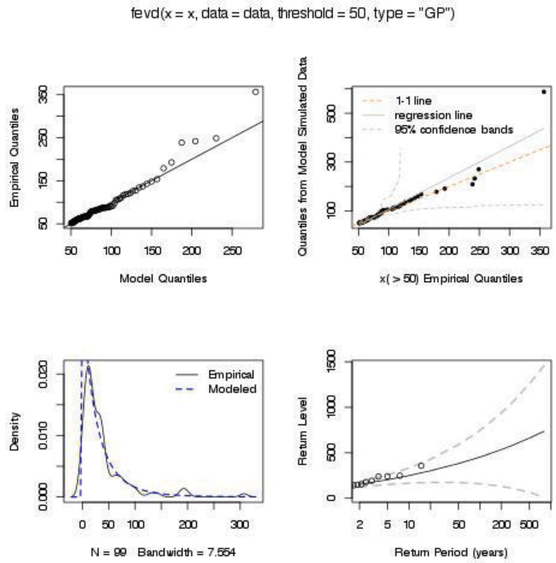

6C

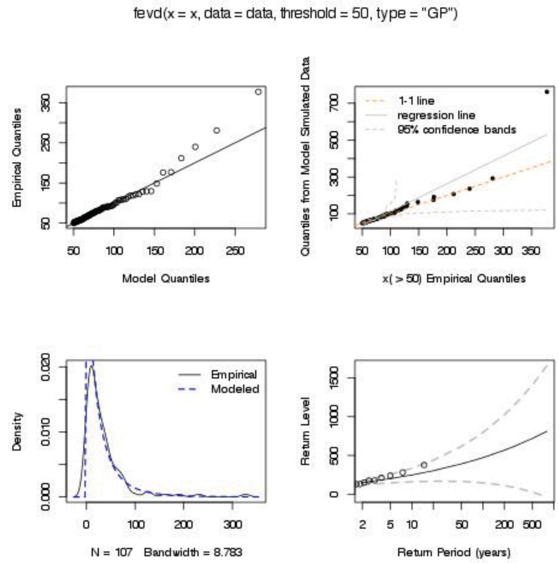

6D

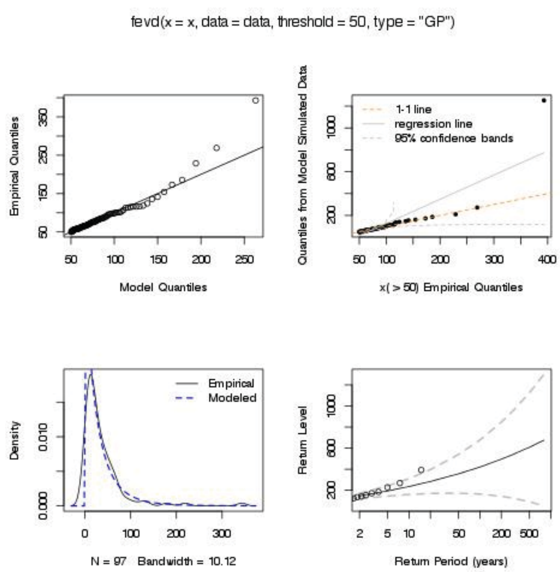

6E

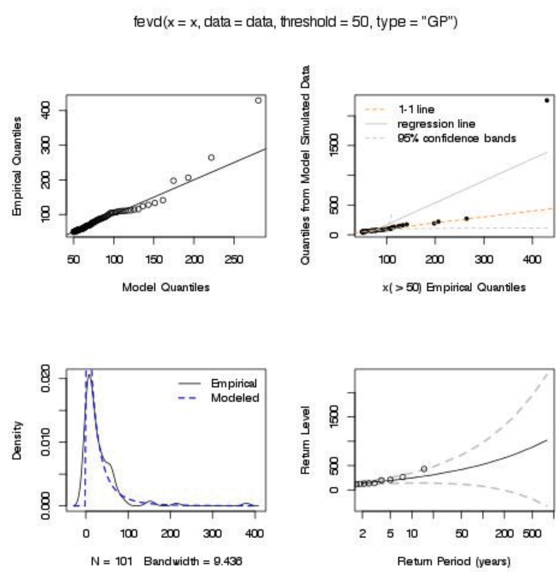

6F

72-hour Gridded Diagnostic Plots Threshold = 50 mm

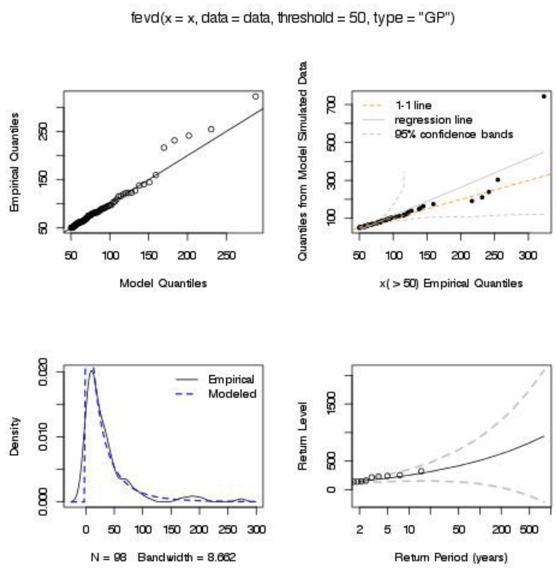

5C

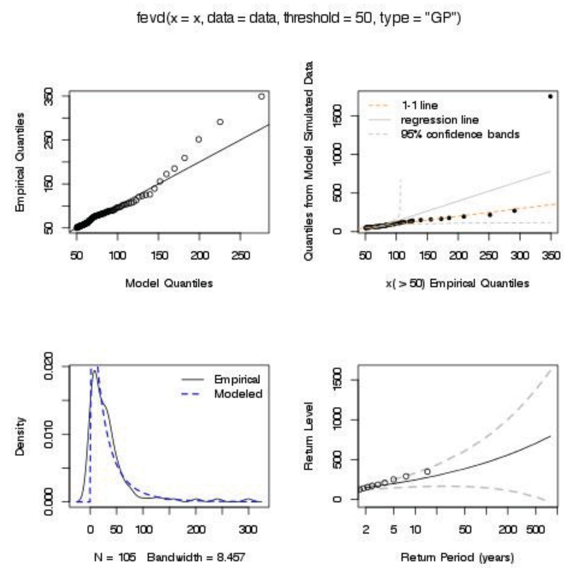

5D

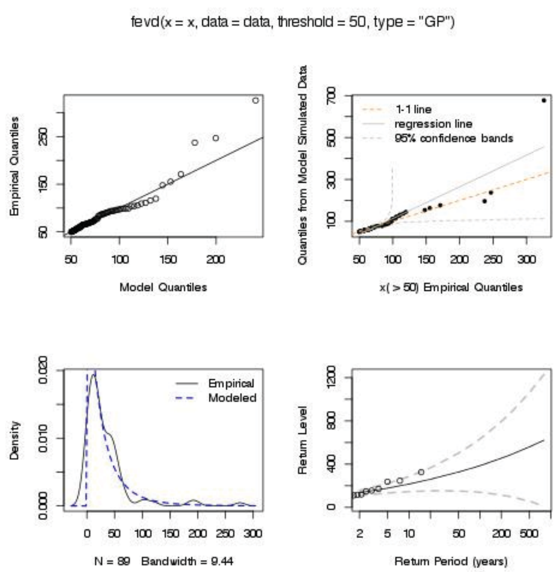

5E

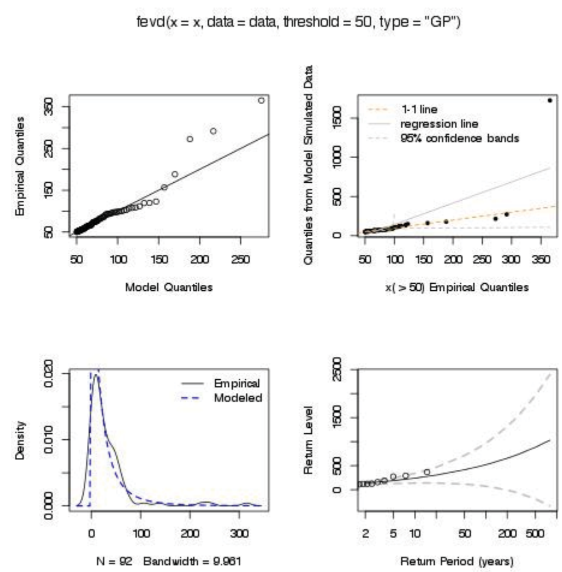

5F

72-hour Gridded Diagnostic Plots Threshold = 50 mm

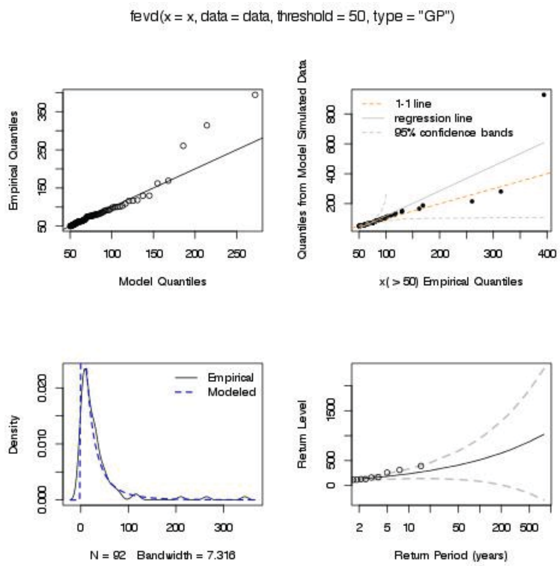

5G

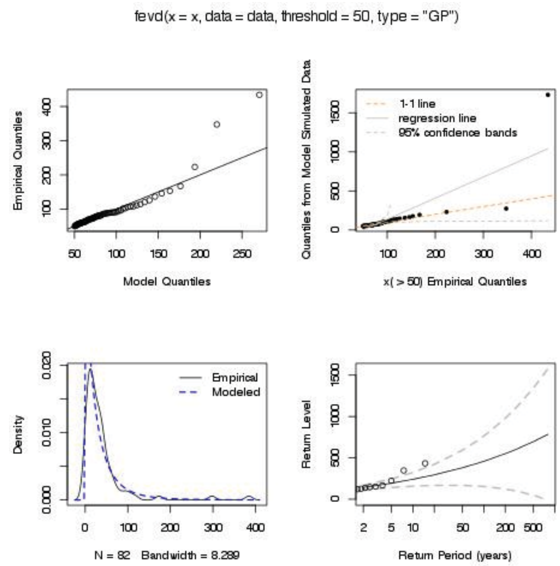

5H

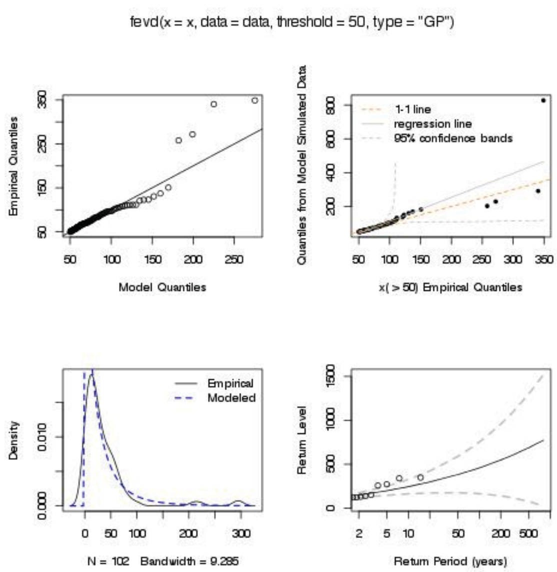

4C

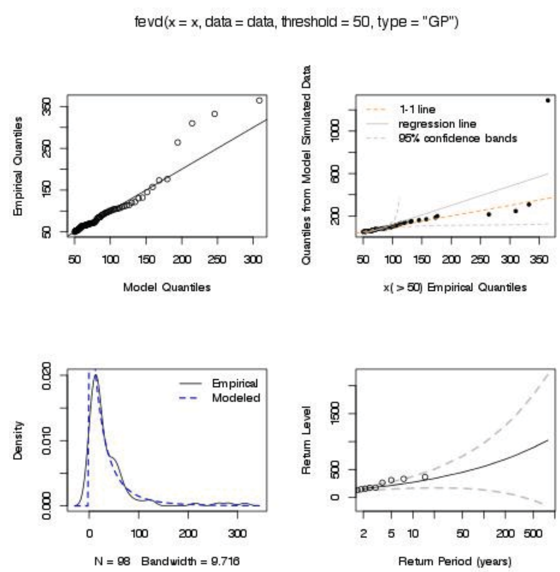

4D

72-hour Gridded Diagnostic Plots Threshold = 50 mm

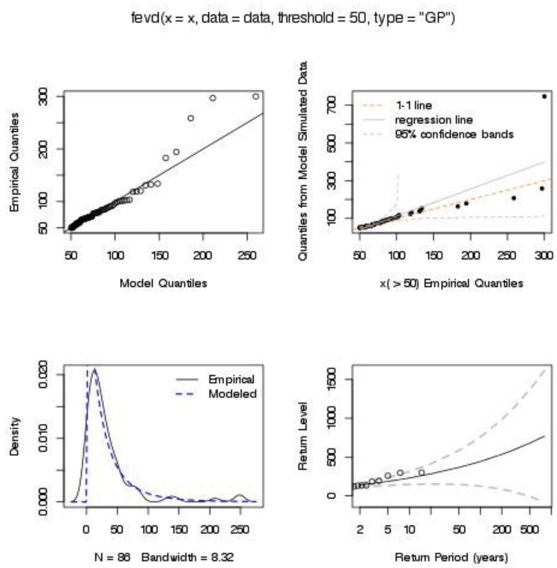

4E

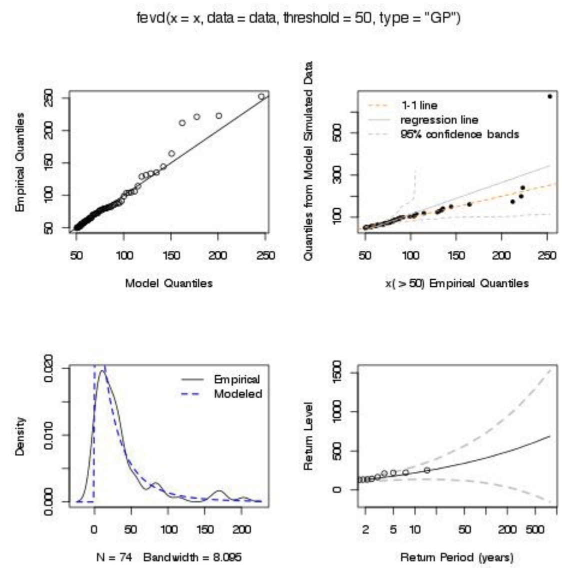

4F

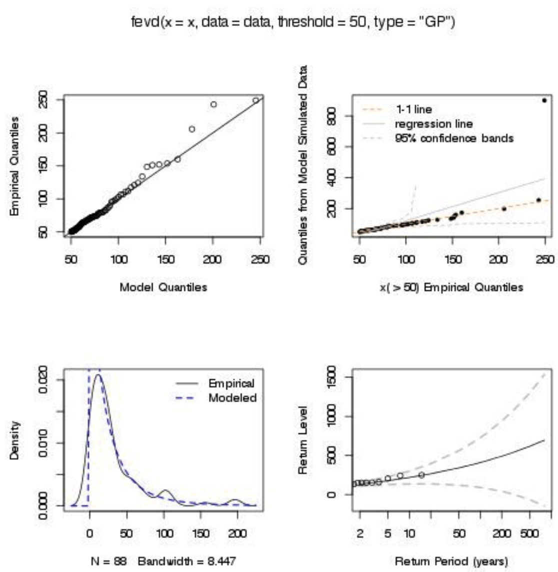

4G

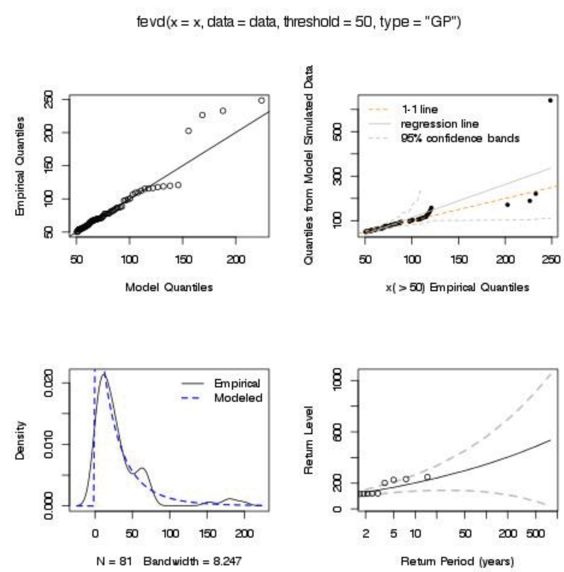

3B

72-hour Gridded Diagnostic Plots Threshold = 50 mm

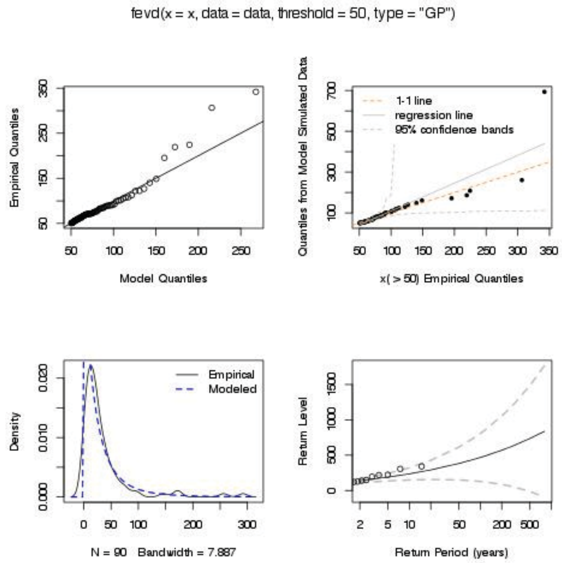

3C

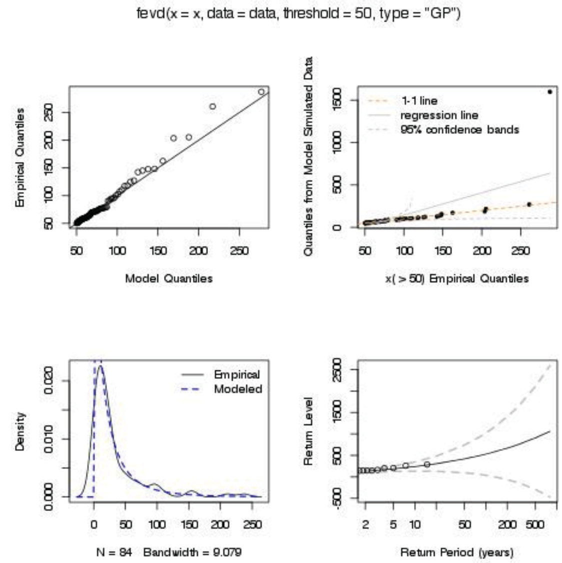

3D

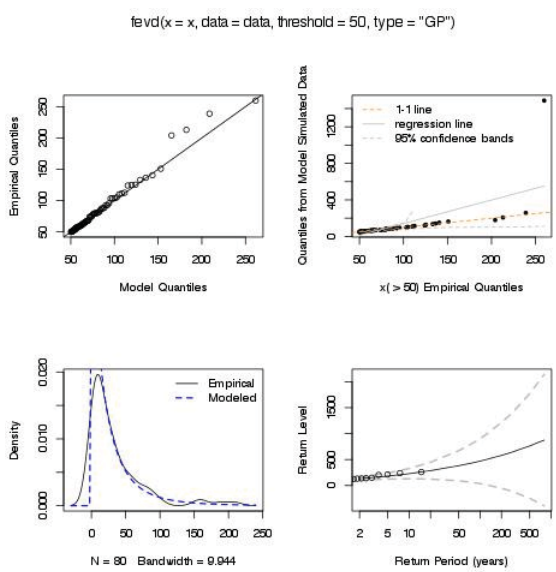

3E

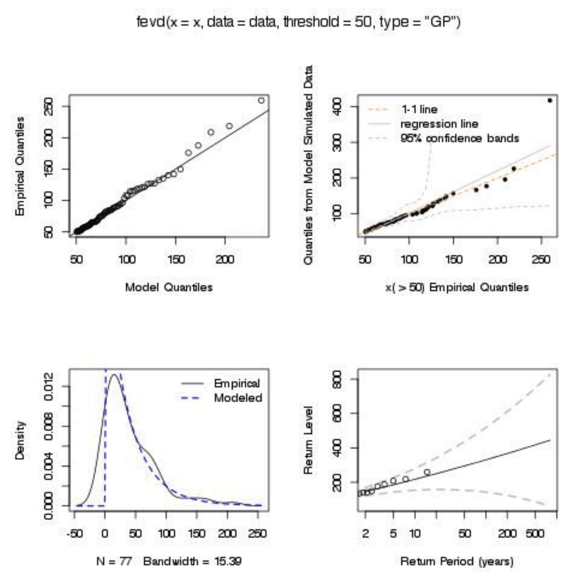

3F

72-hour Gridded Diagnostic Plots Threshold = 50 mm

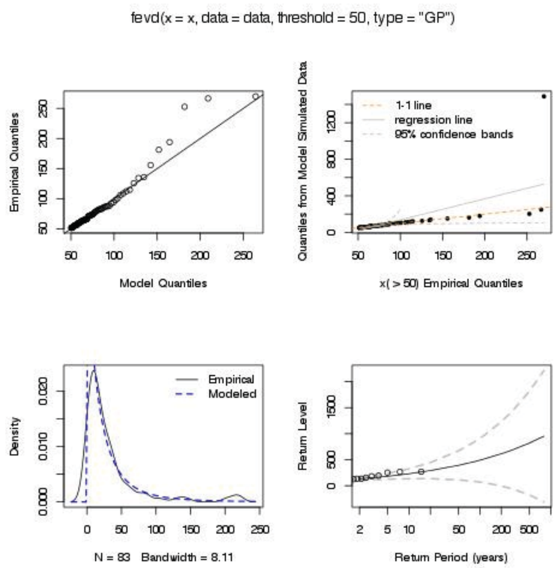

2C

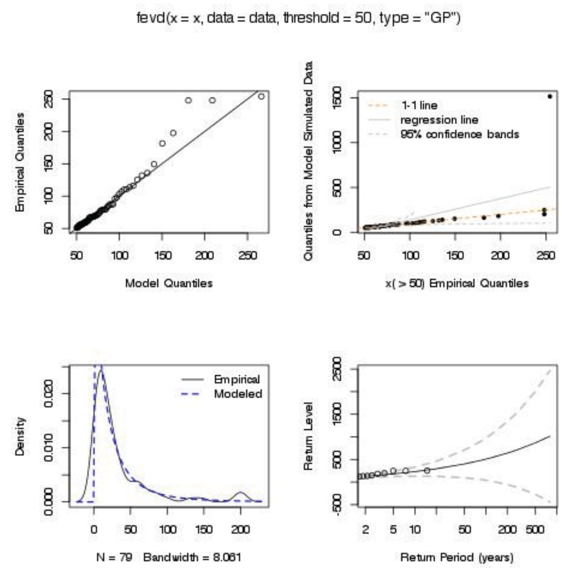

2D

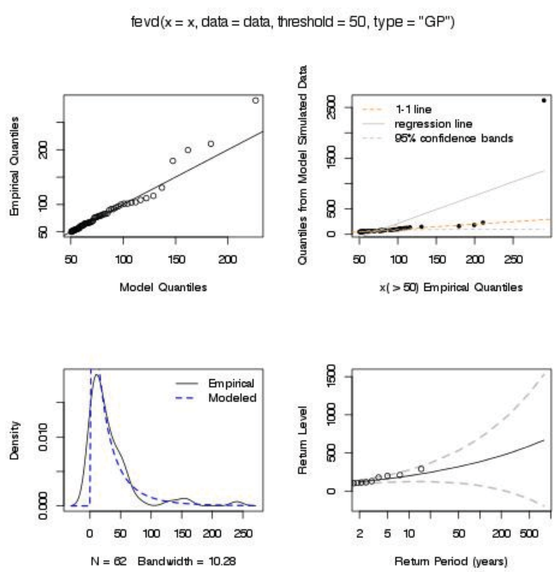

2E

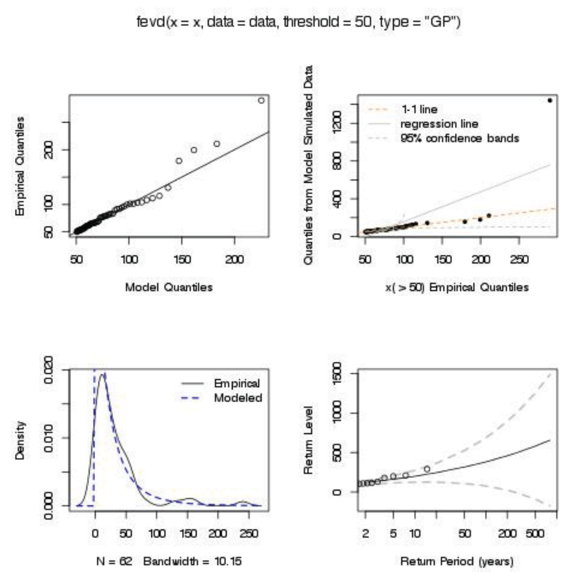

1D

72-hour Gridded Diagnostic Plots Dry Season Threshold = 20 mm

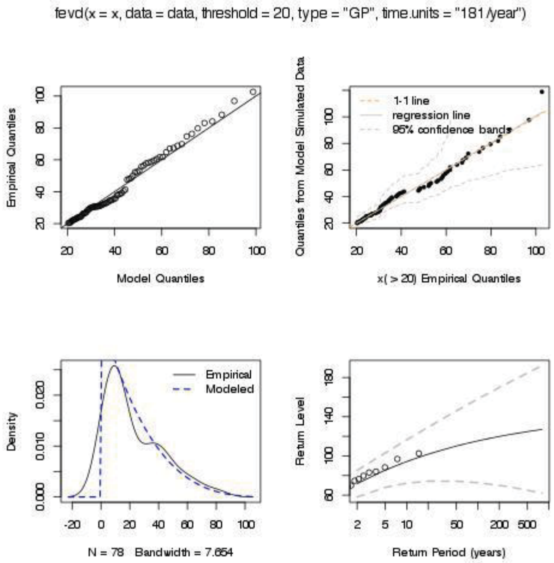

10E

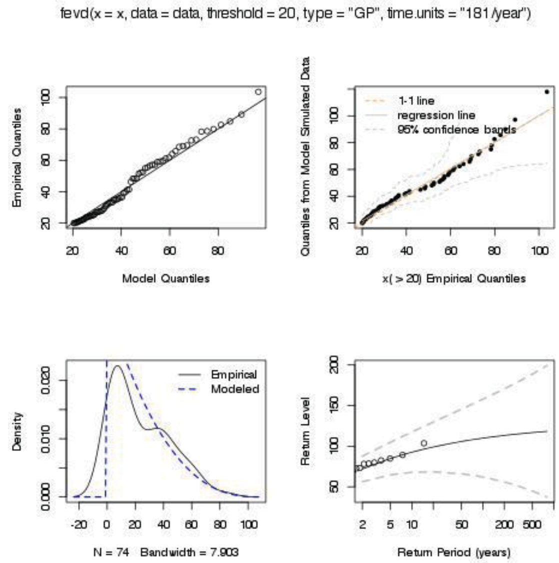

10F

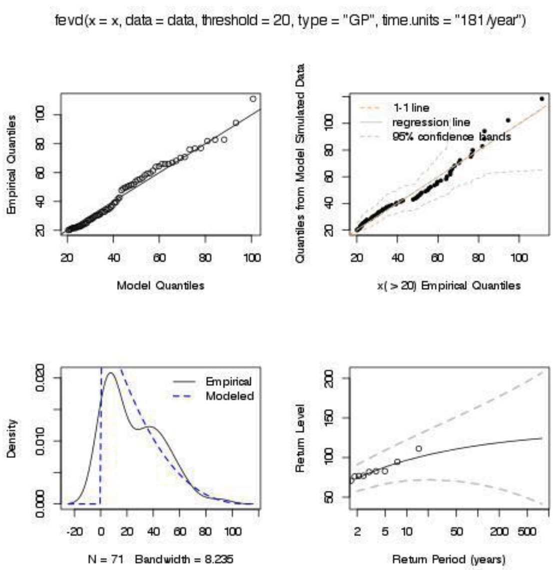

10G

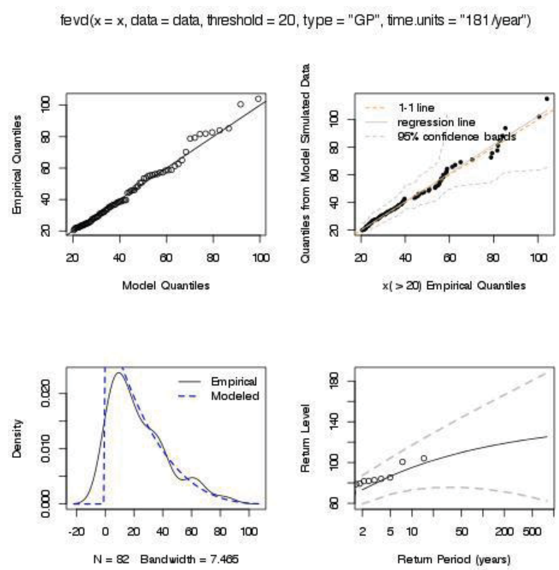

9E

72-hour Gridded Diagnostic Plots Dry Season Threshold = 20 mm

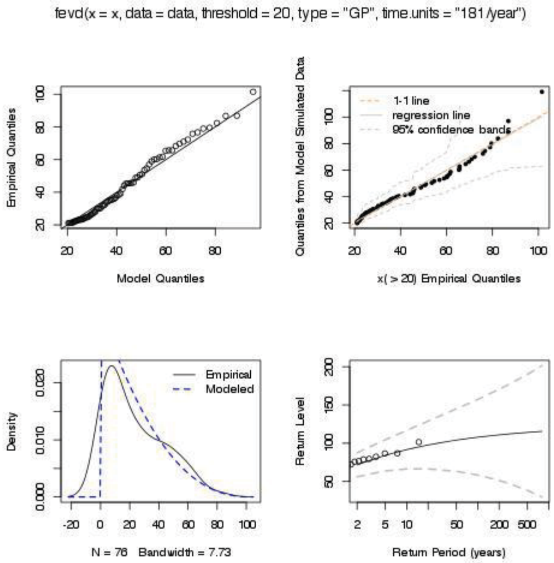

9G

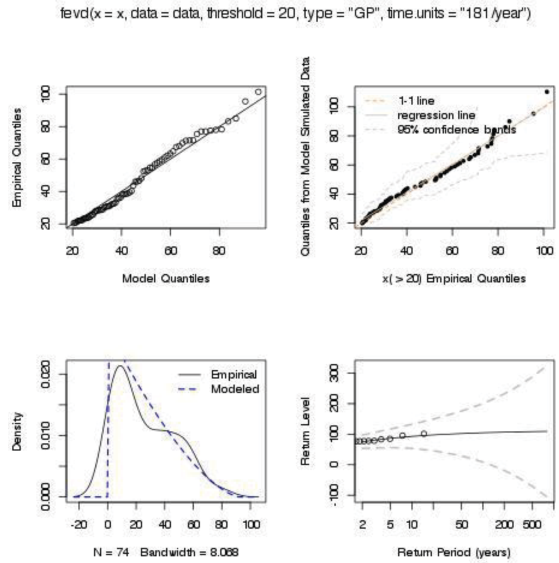

9H

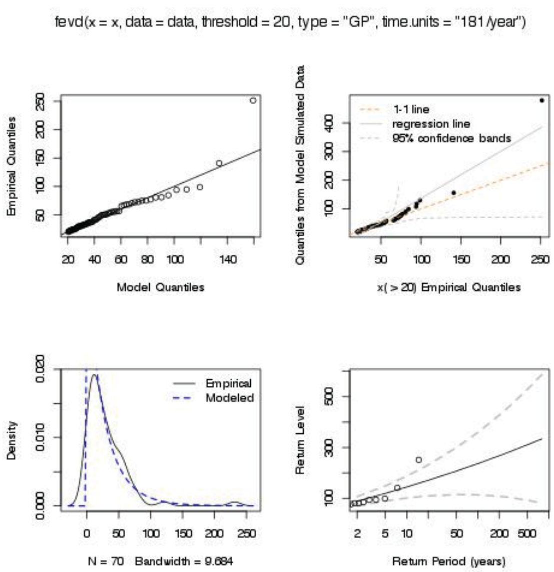

9I

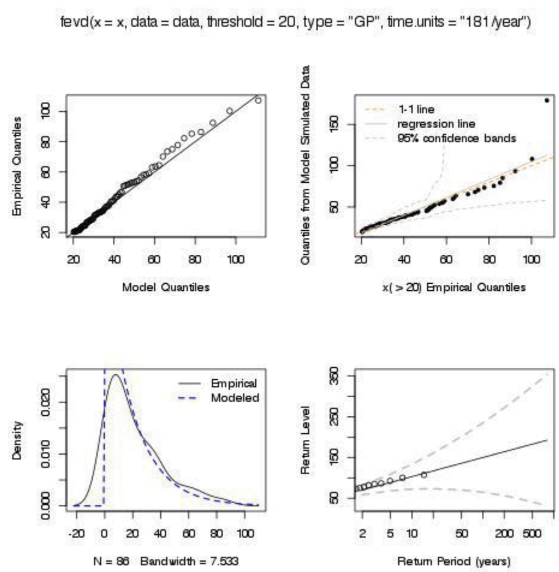

8D

72-hour Gridded Diagnostic Plots Dry Season Threshold = 20 mm

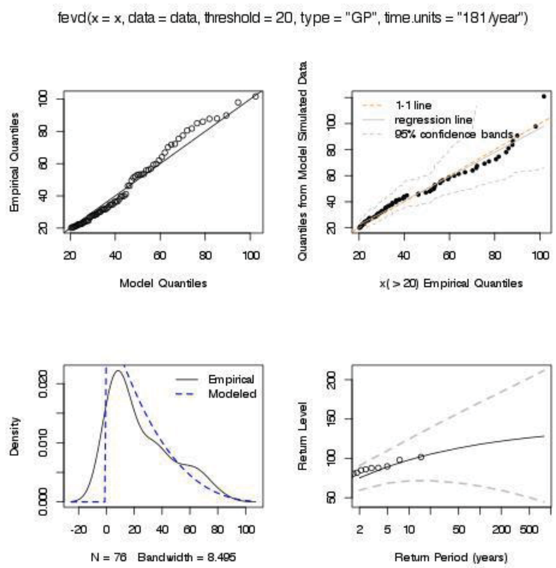

8H

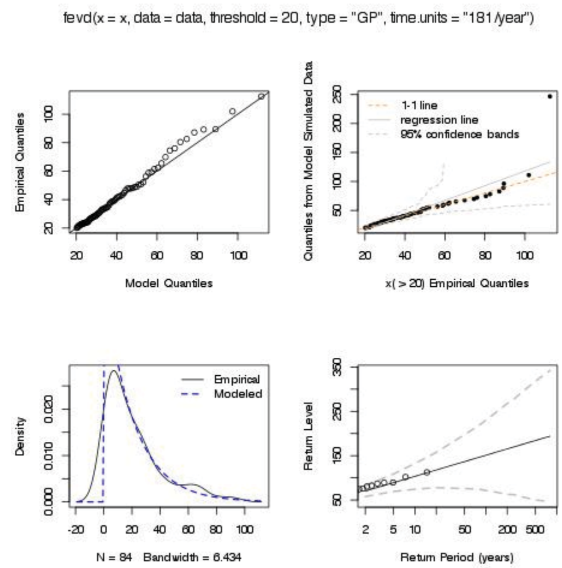

7D

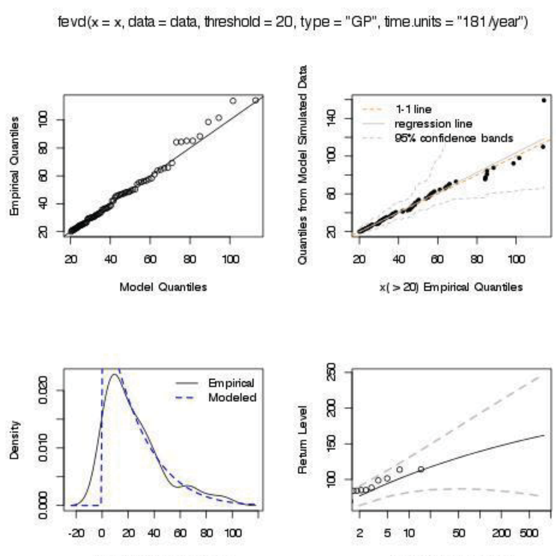

7E

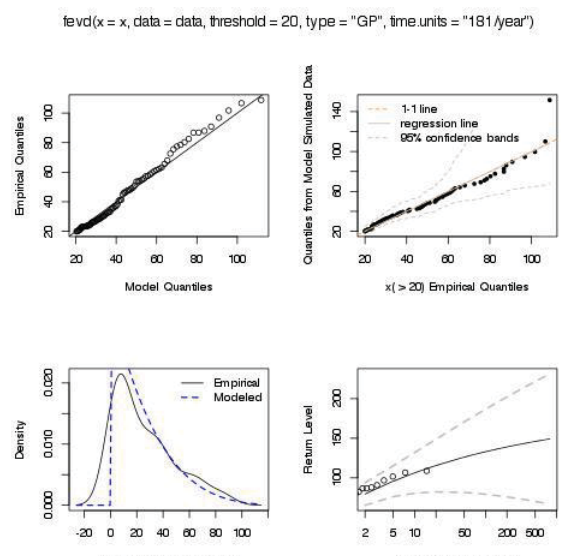

7F

72-hour Gridded Diagnostic Plots Dry Season Threshold = 20 mm

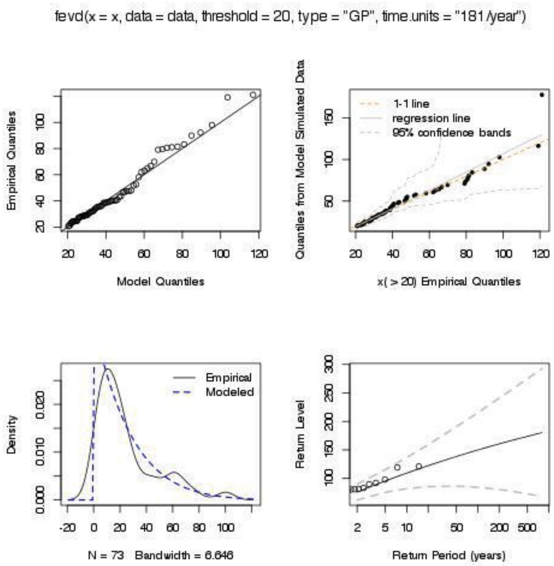

6C

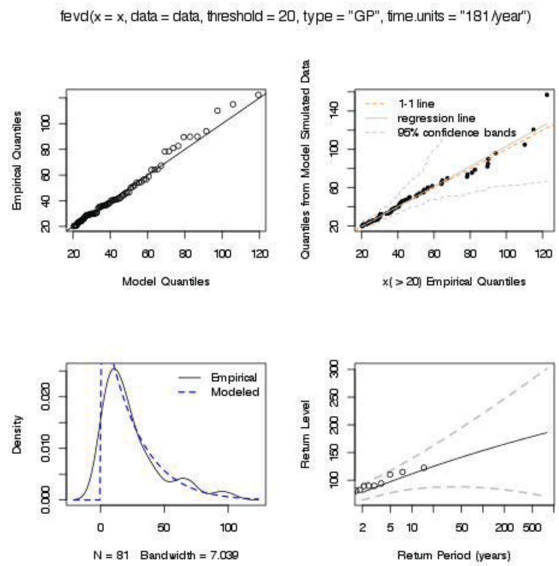

6D

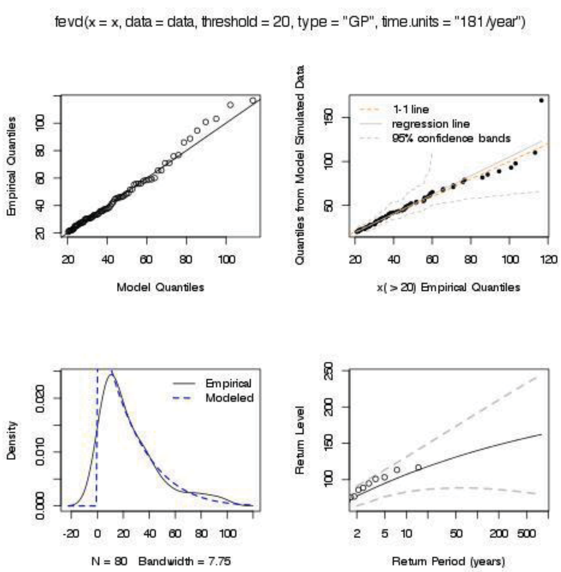

6E

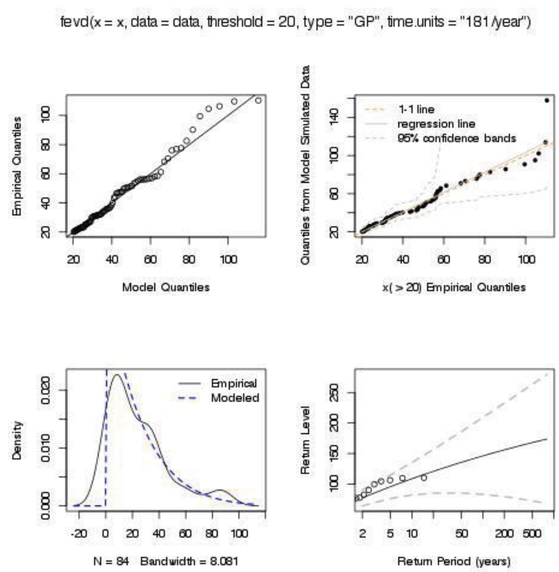

6F

72-hour Gridded Diagnostic Plots Dry Season Threshold = 20 mm

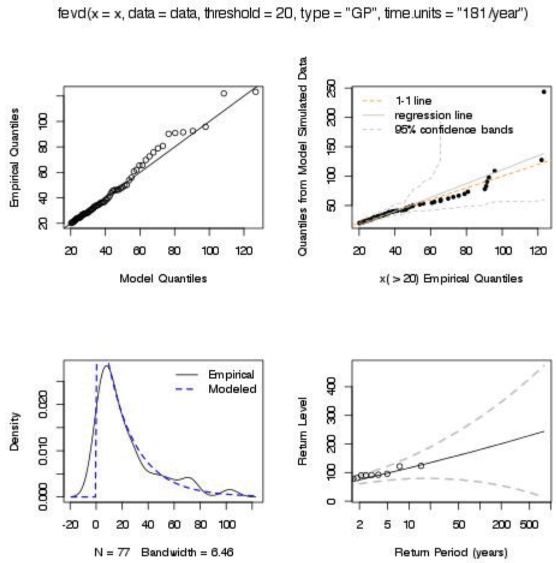

5C

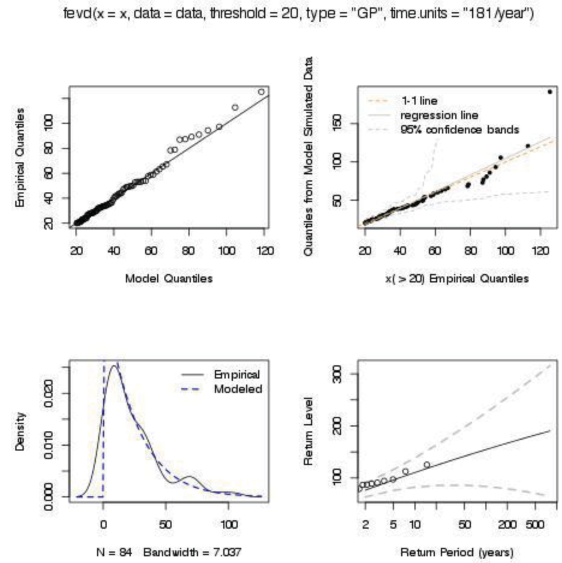

5D

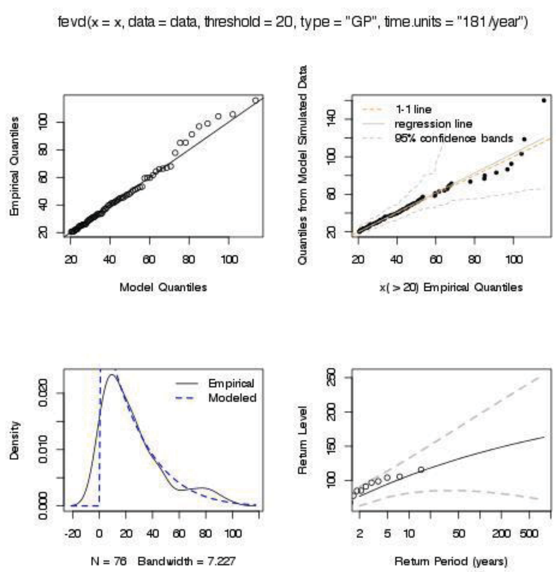

5E

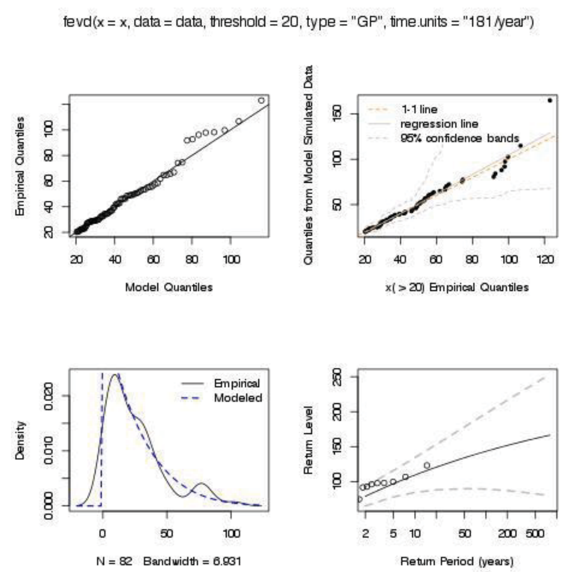

5F

72-hour Gridded Diagnostic Plots Dry Season Threshold = 20 mm

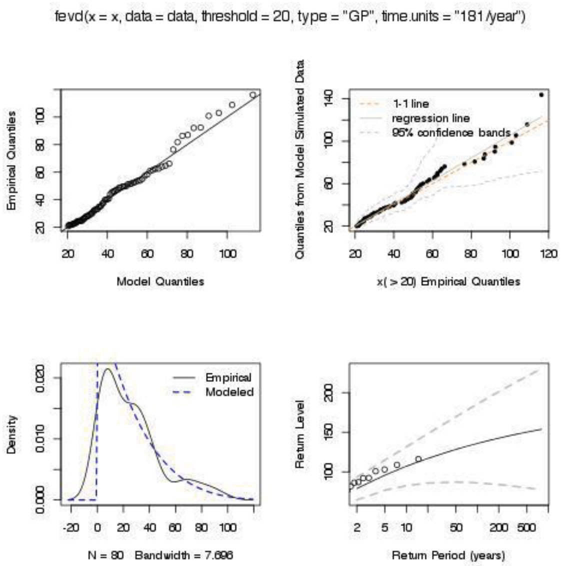

5G

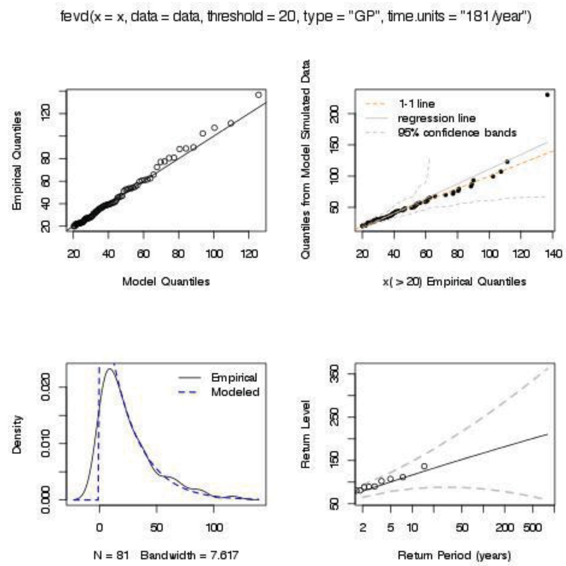

5H

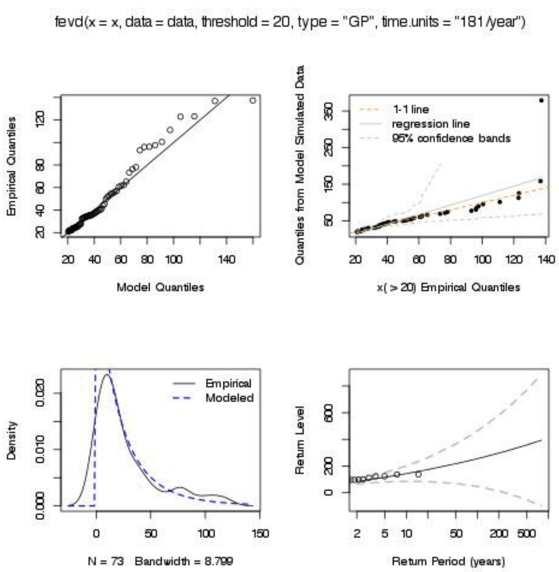

4C

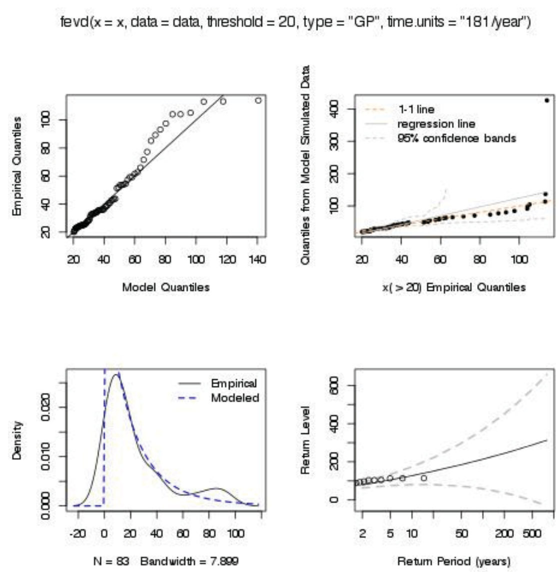

4D

72-hour Gridded Diagnostic Plots Dry Season Threshold = 20 mm

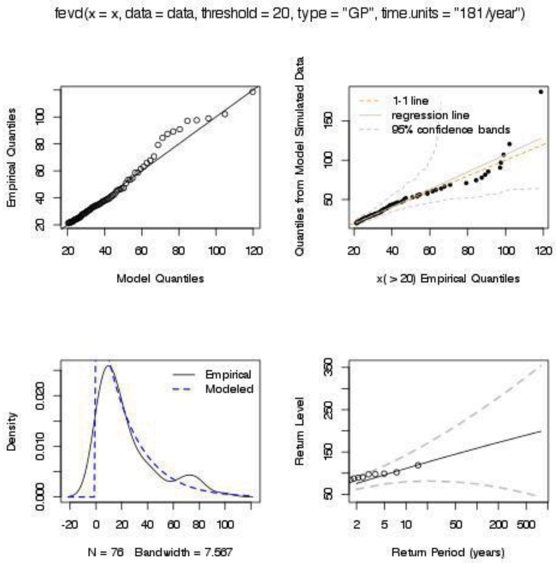

4E

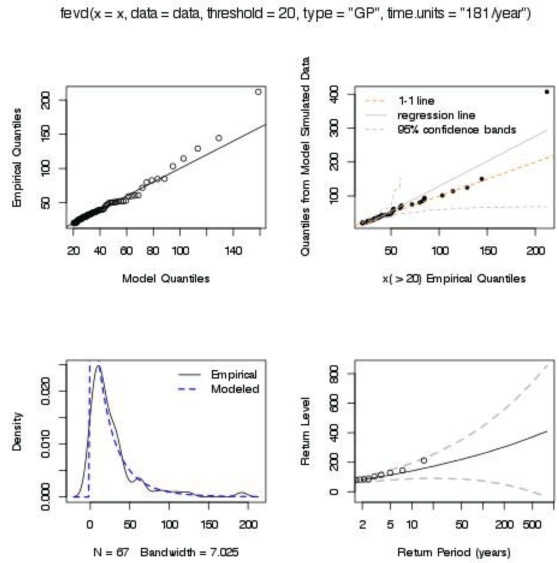

4F

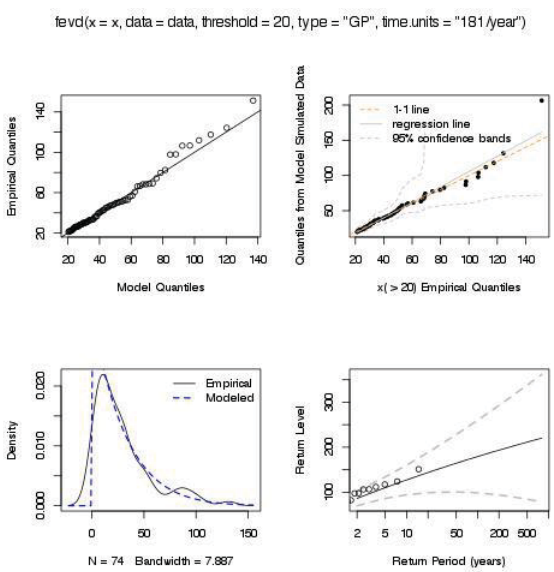

4G

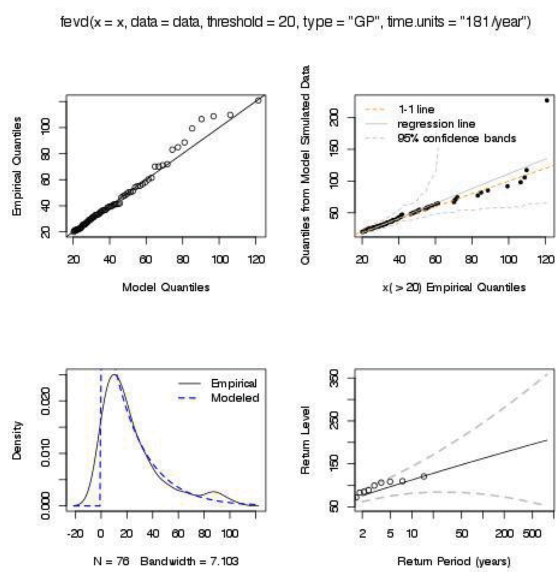

3B

72-hour Gridded Diagnostic Plots Dry Season Threshold = 20 mm

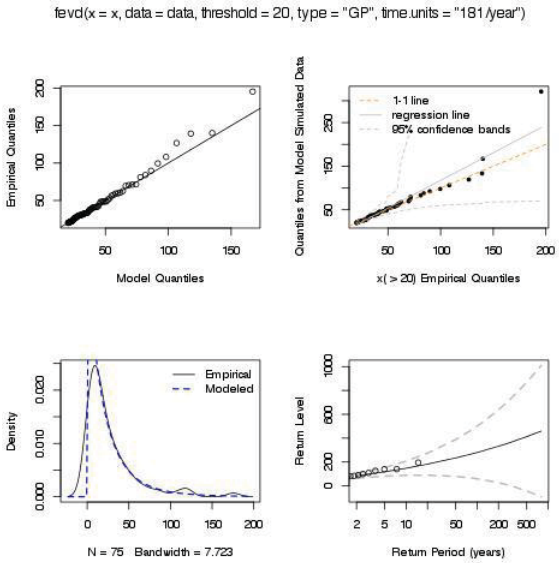

3C

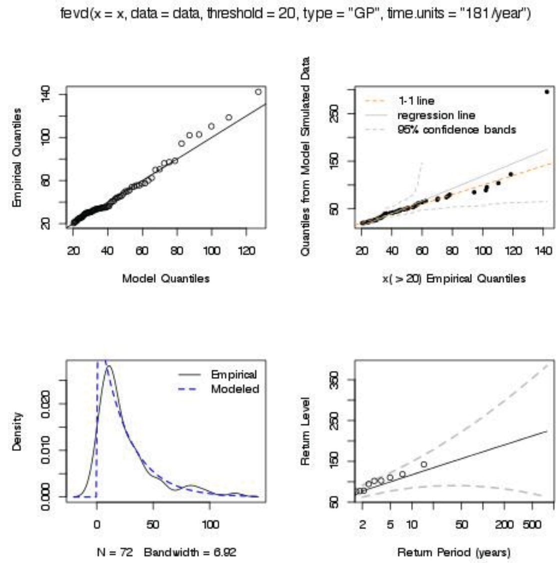

3D

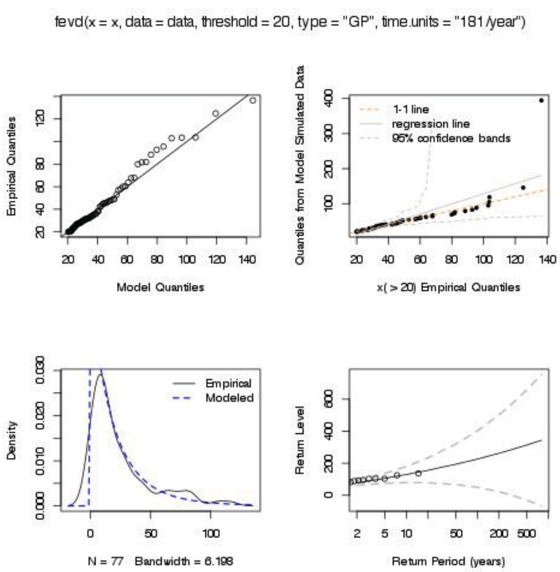

3E

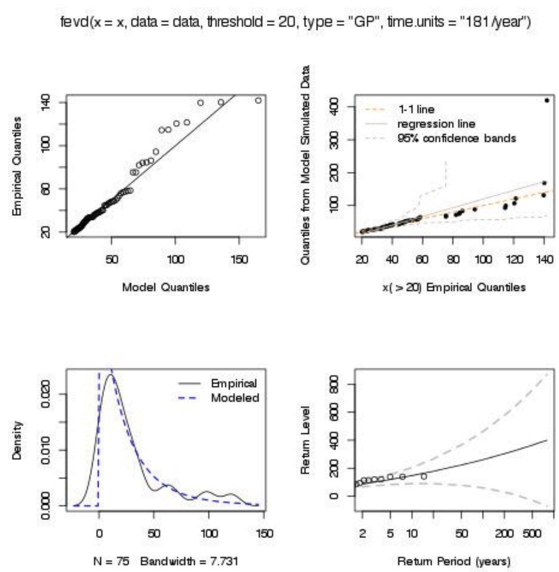

3F

72-hour Gridded Diagnostic Plots Dry Season Threshold = 20 mm

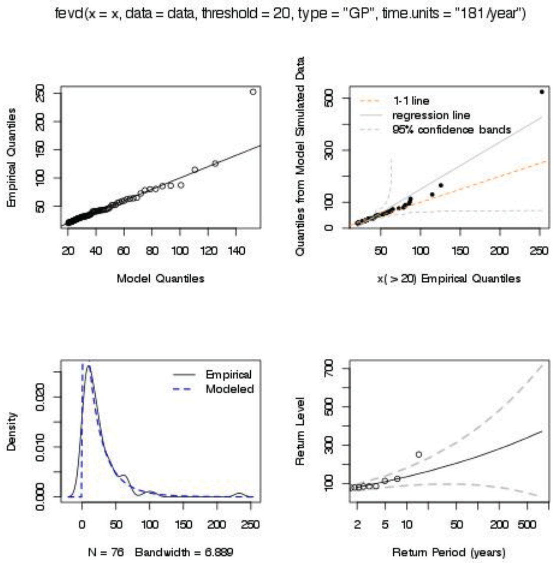

2C

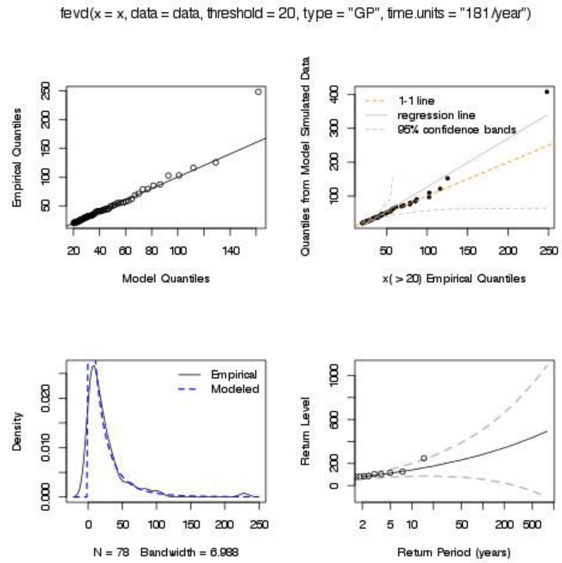

2D

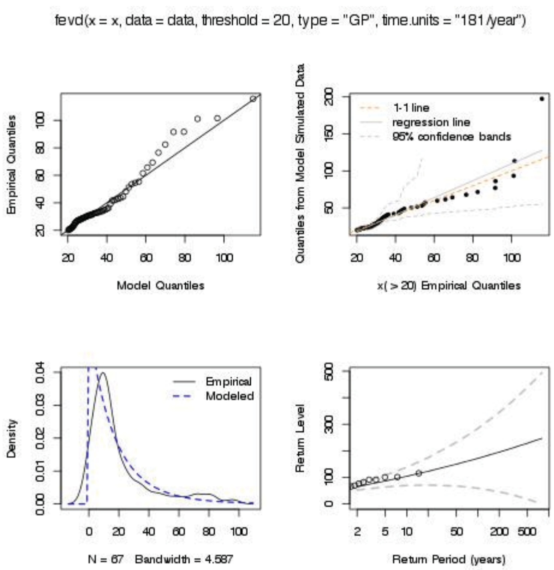

2E

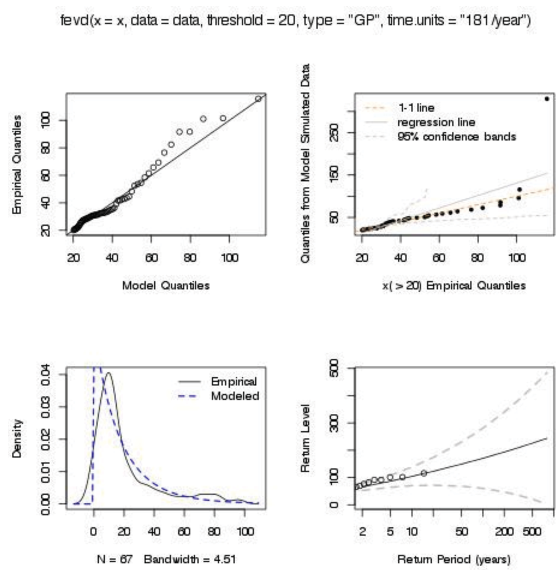

1D

72-hour Gridded Diagnostic Plots Dry Season Threshold = 25 mm

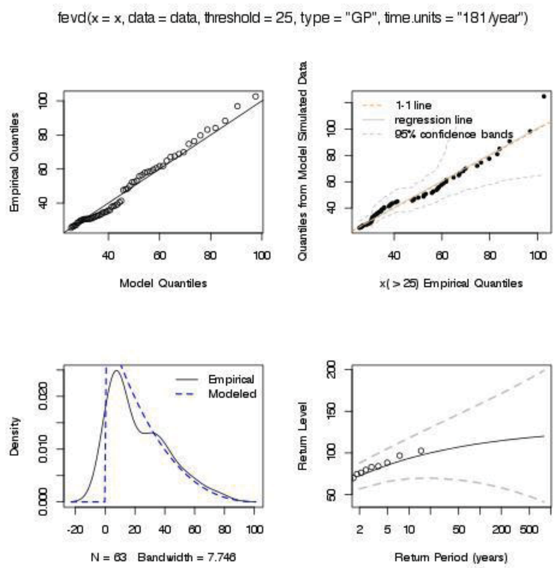

10E

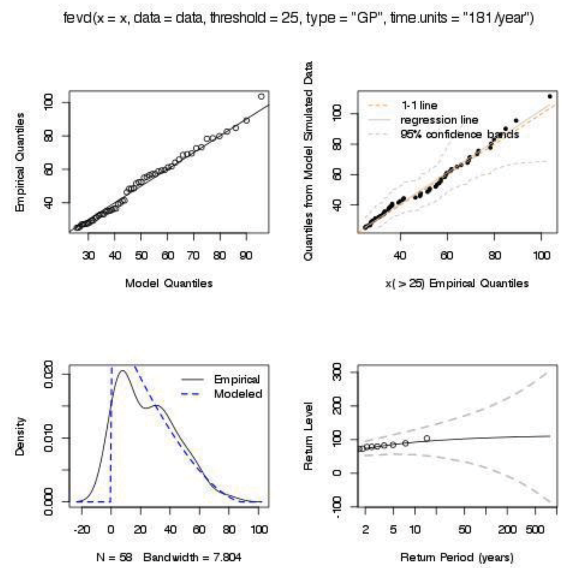

10F

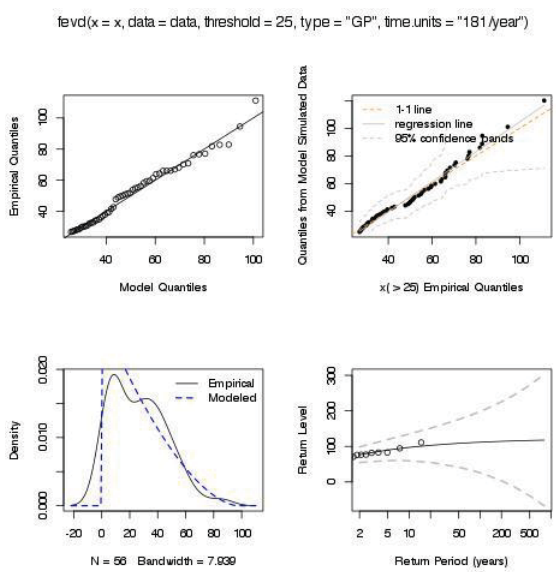

10G

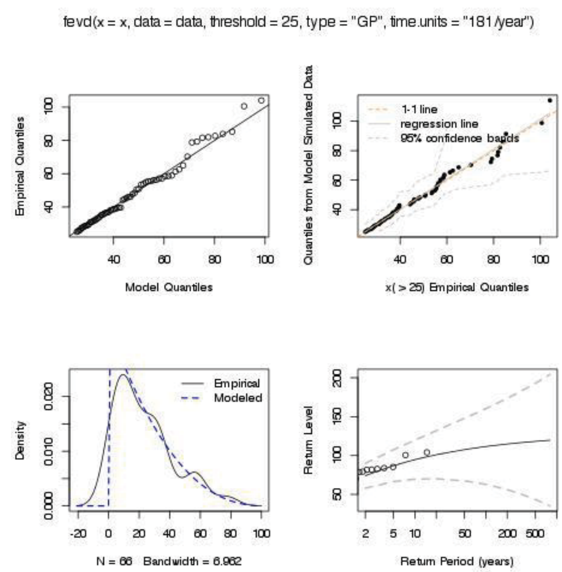

9E

72-hour Gridded Diagnostic Plots Dry Season Threshold = 25 mm

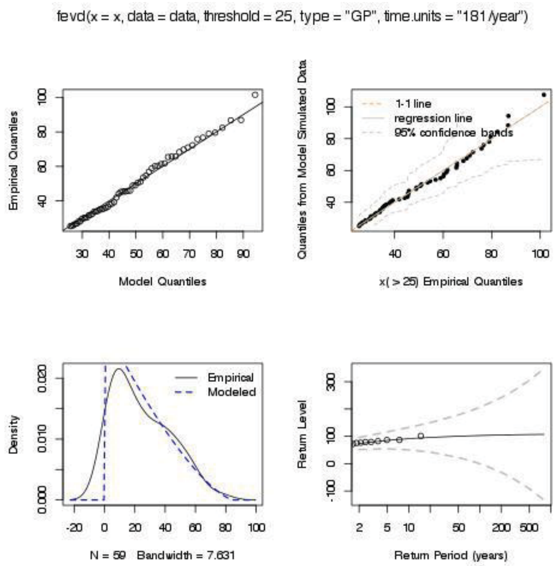

9G

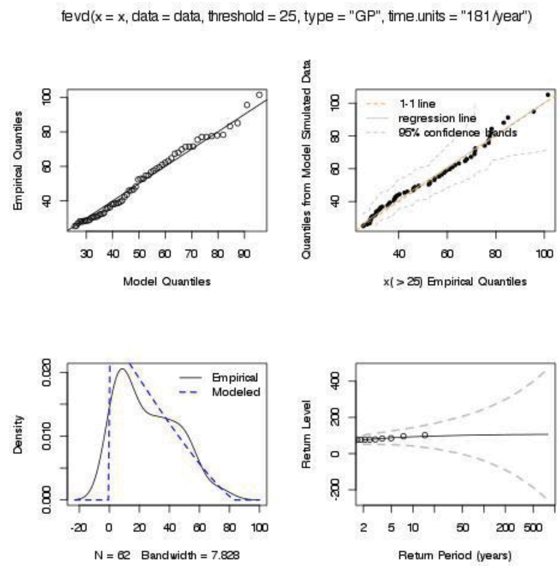

9H

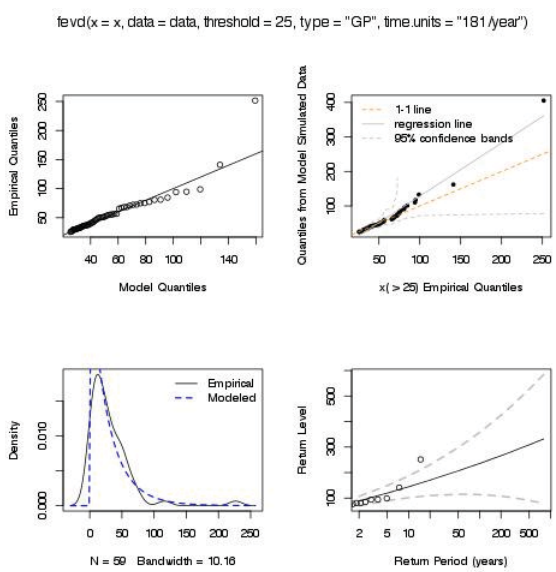

9I

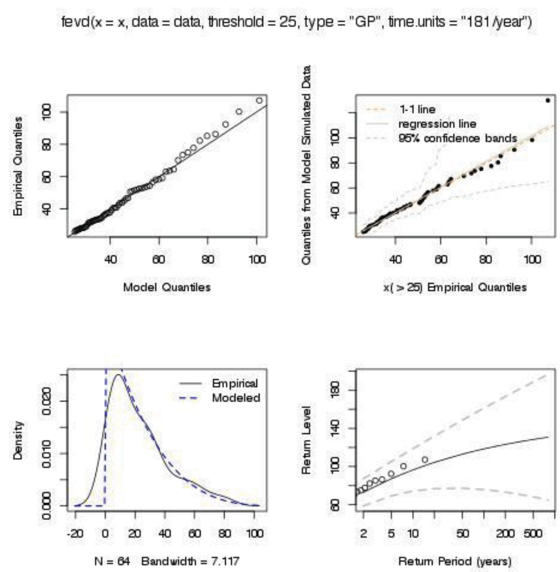

8D

72-hour Gridded Diagnostic Plots Dry Season Threshold = 25 mm

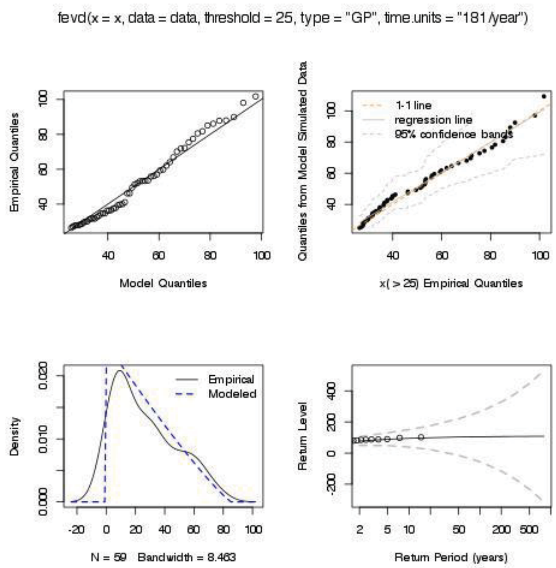

8H

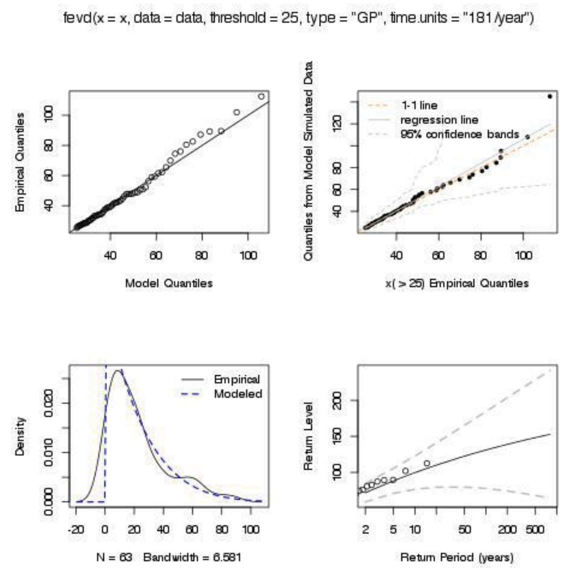

7D

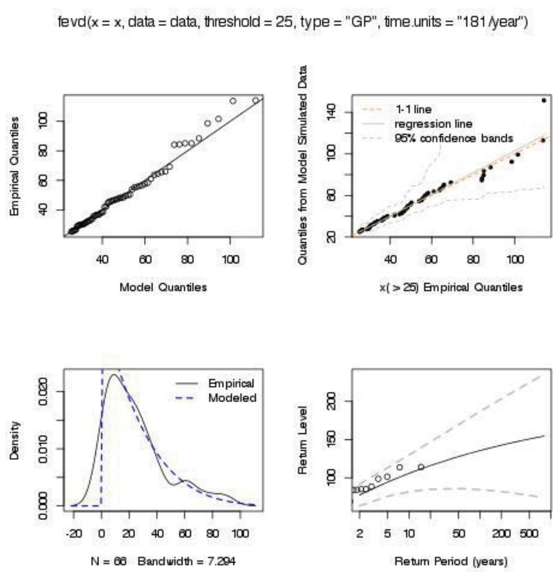

7E

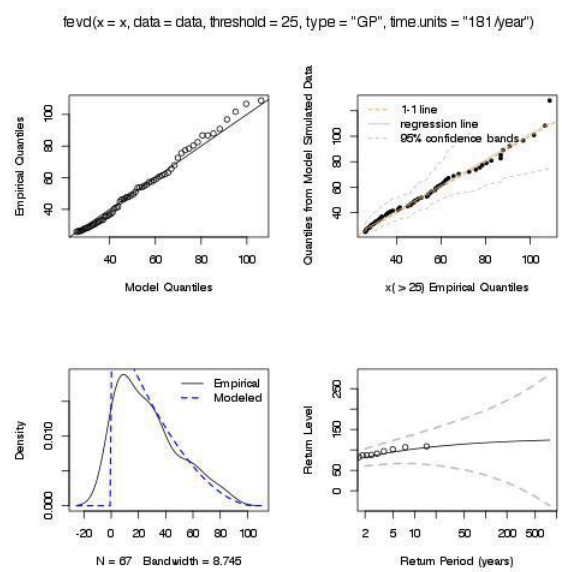

7F

72-hour Gridded Diagnostic Plots Dry Season Threshold = 25 mm

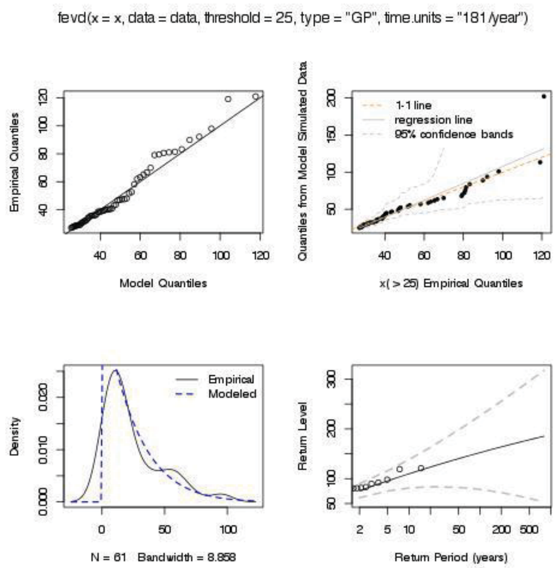

6C

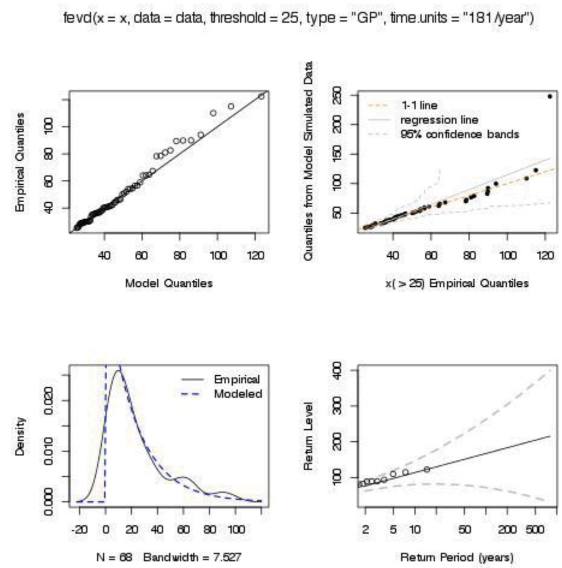

6D

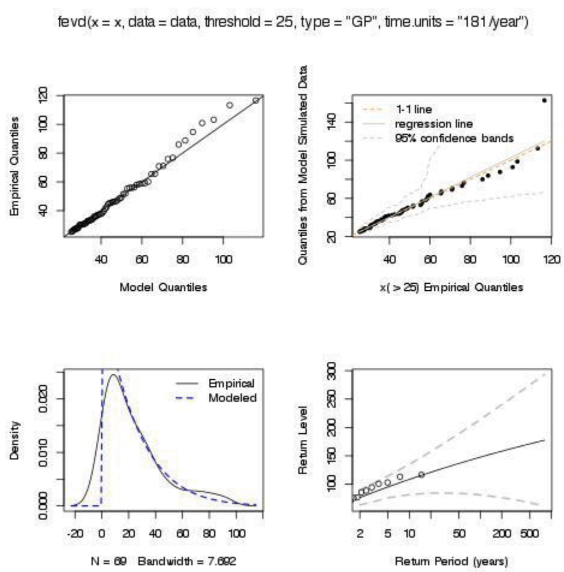

6E

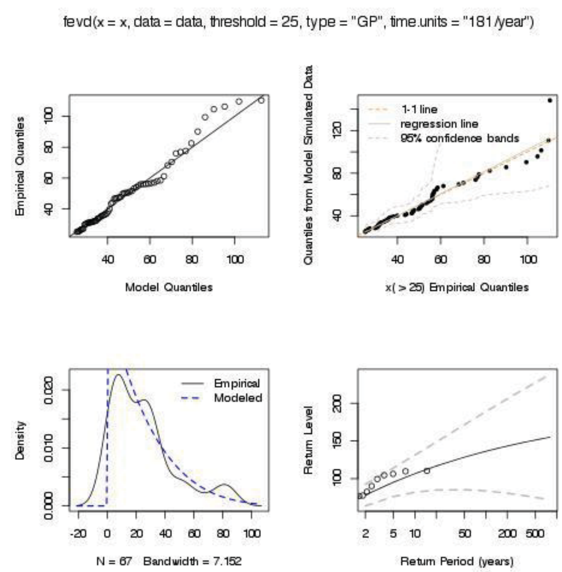

6F

72-hour Gridded Diagnostic Plots Dry Season Threshold = 25 mm

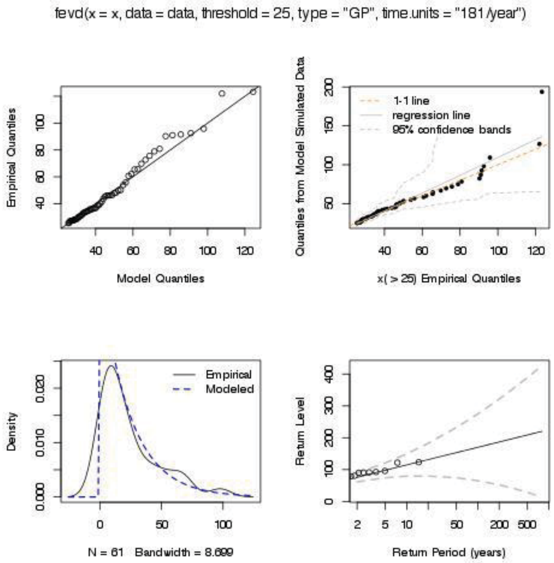

5C

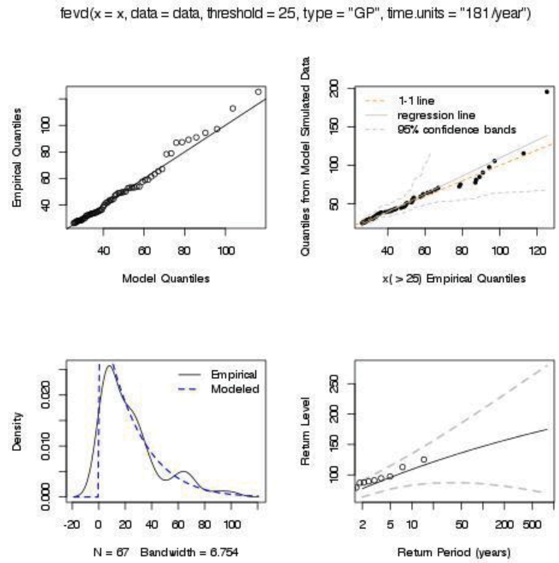

5D

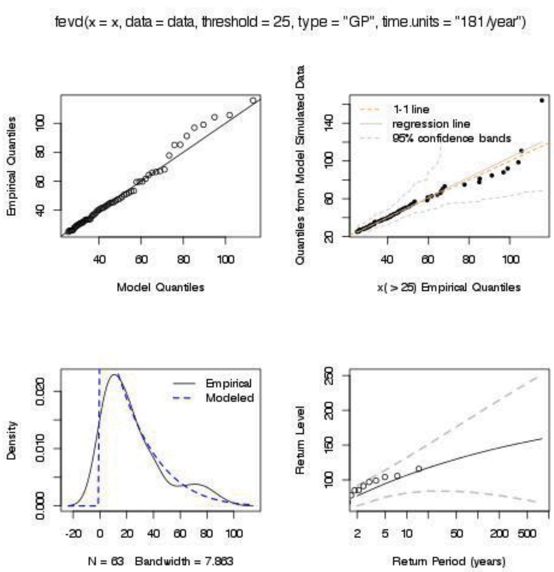

5E

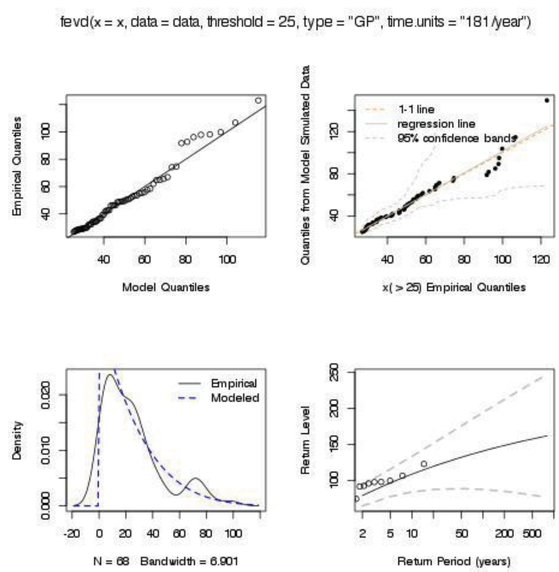

5F

72-hour Gridded Diagnostic Plots Dry Season Threshold = 25 mm

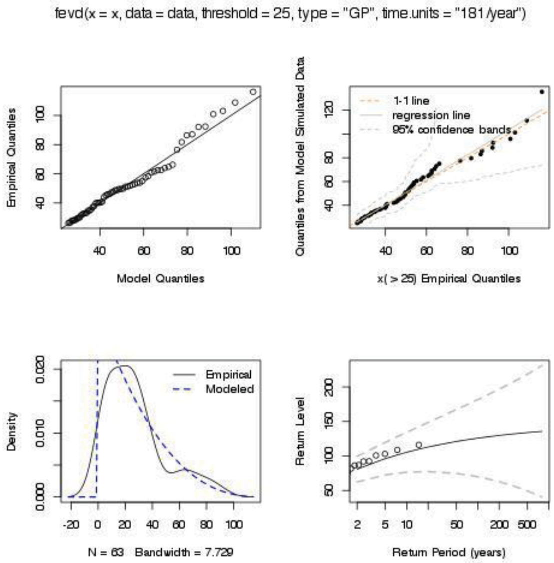

5G

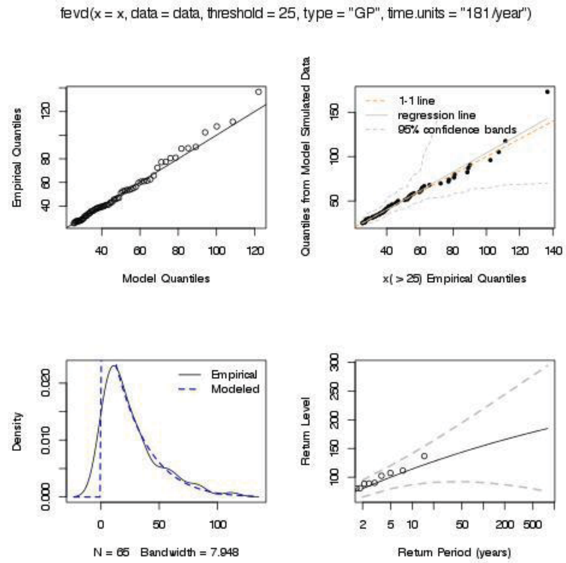

5H

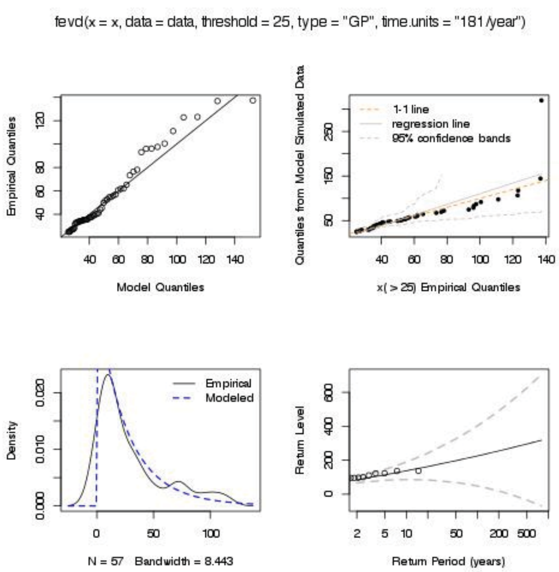

4C

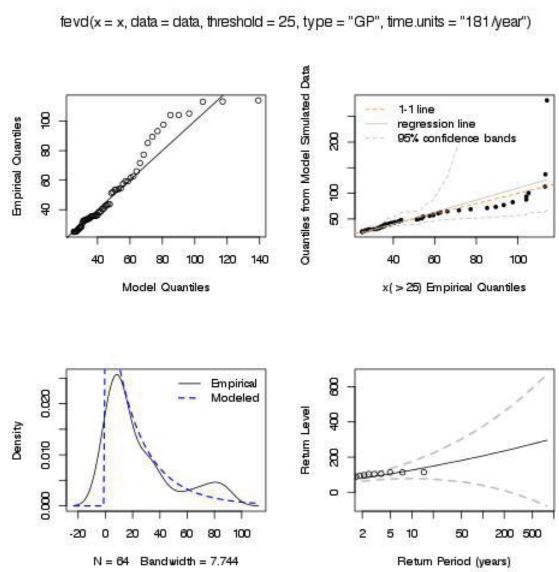

4D

72-hour Gridded Diagnostic Plots Dry Season Threshold = 25 mm

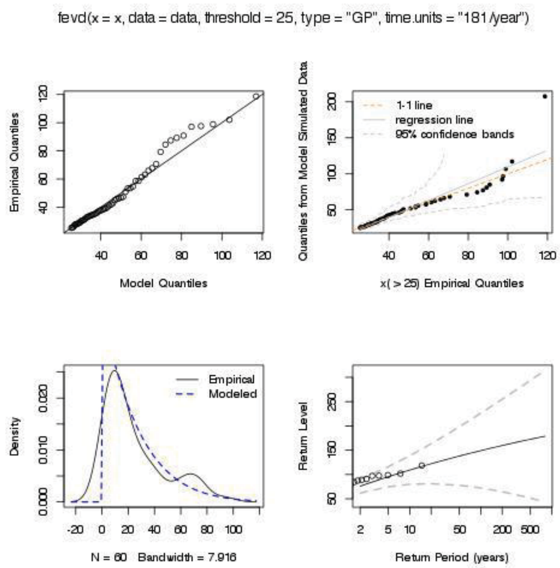

4E

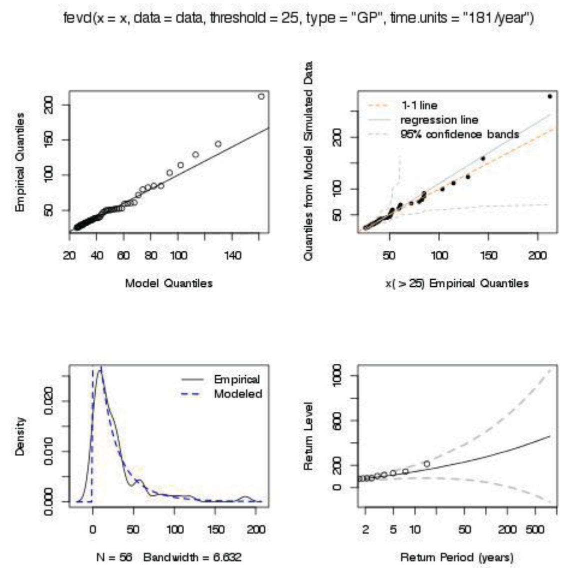

4F

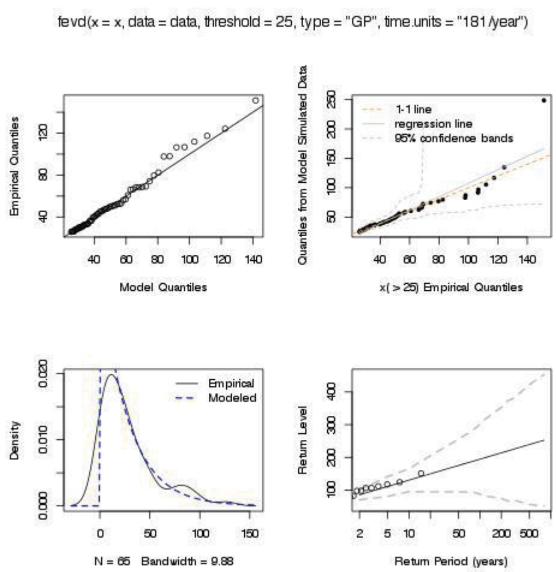

4G

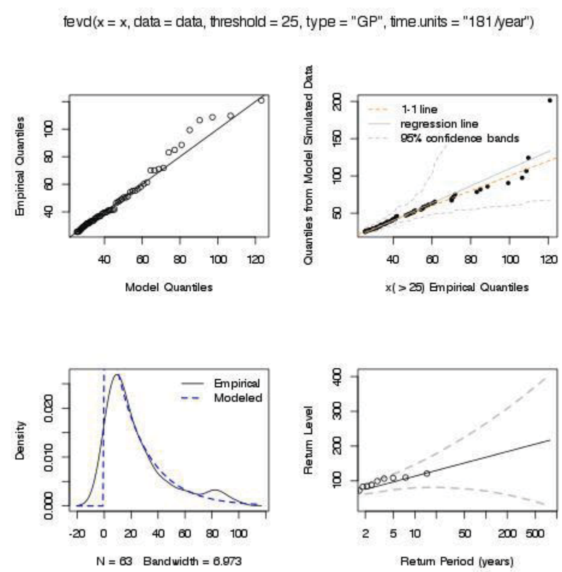

3B

72-hour Gridded Diagnostic Plots Dry Season Threshold = 25 mm

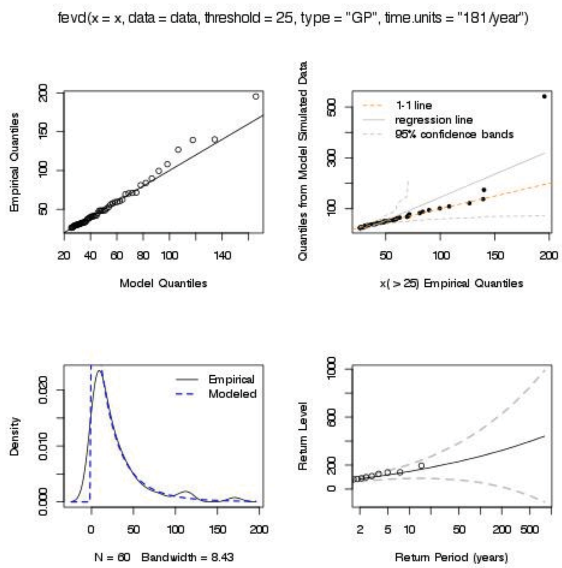

3C

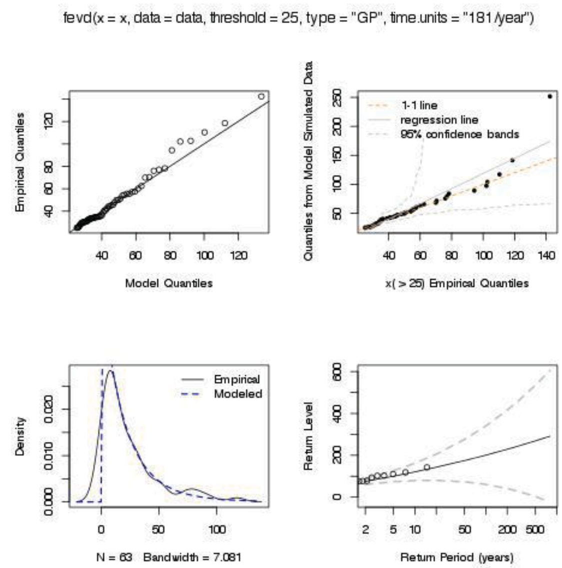

3D

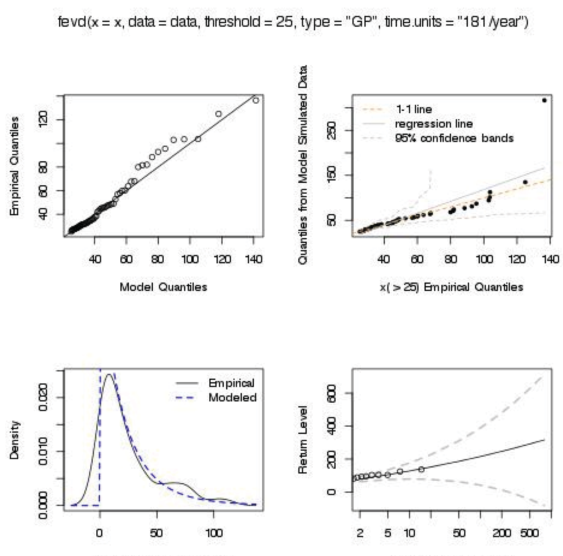

3E

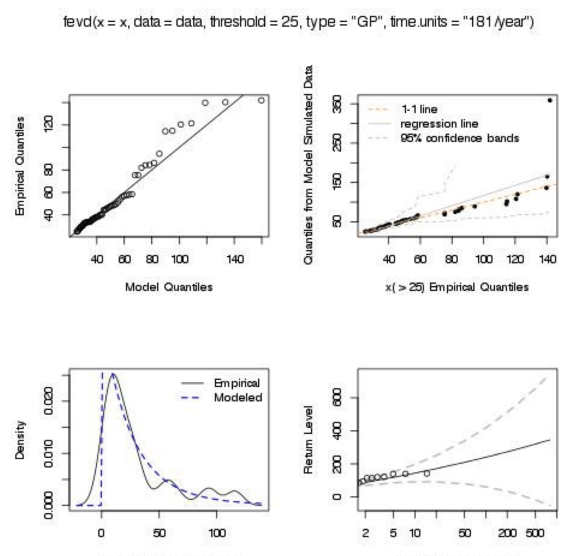

3F

72-hour Gridded Diagnostic Plots Dry Season Threshold = 25 mm

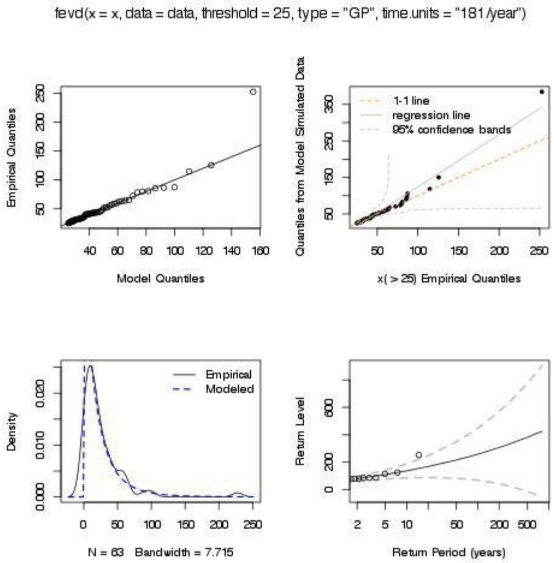

2C

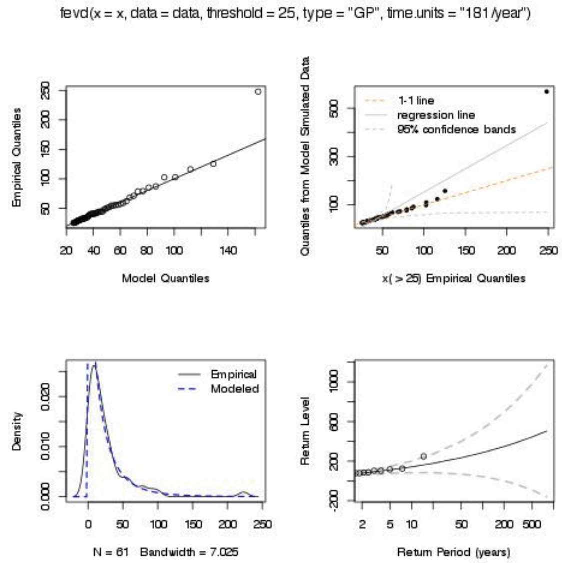

2D

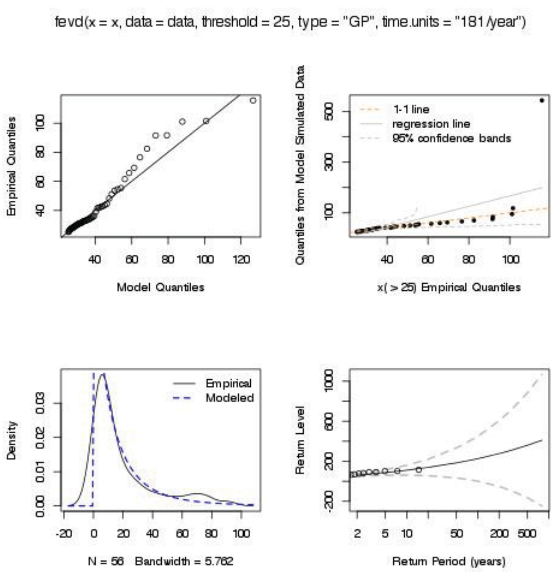

2E

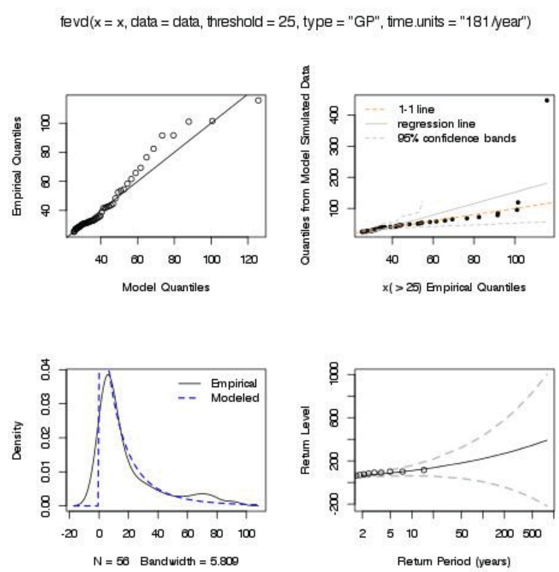

1D

72-hour Gridded Diagnostic Plots Dry Season Threshold = 30 mm

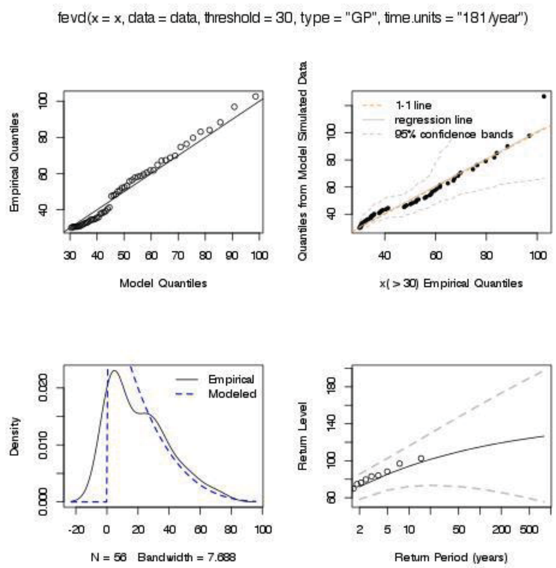

10E

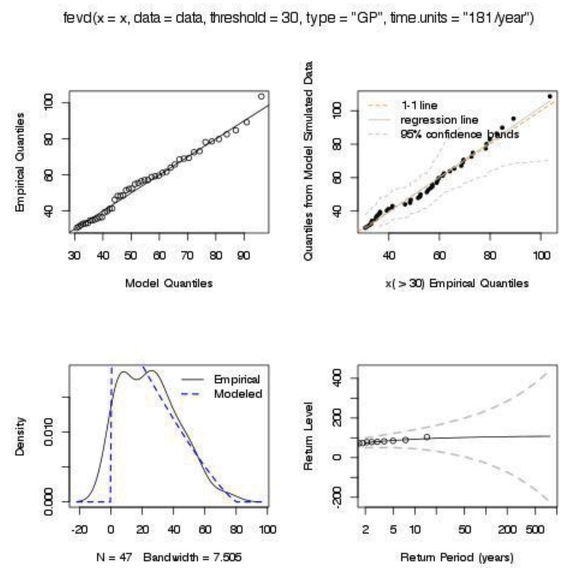

10F

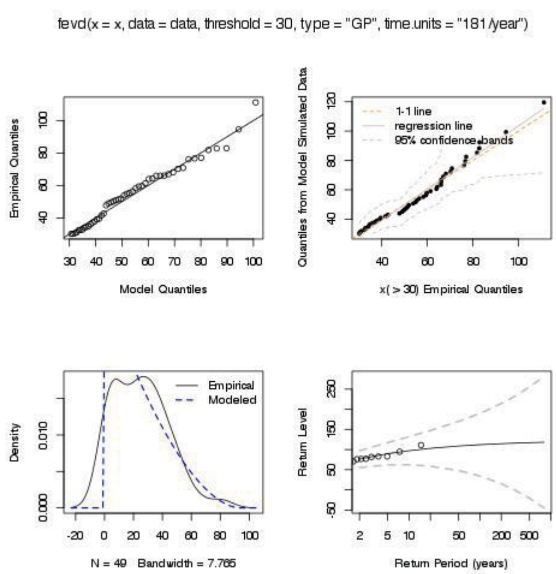

10G

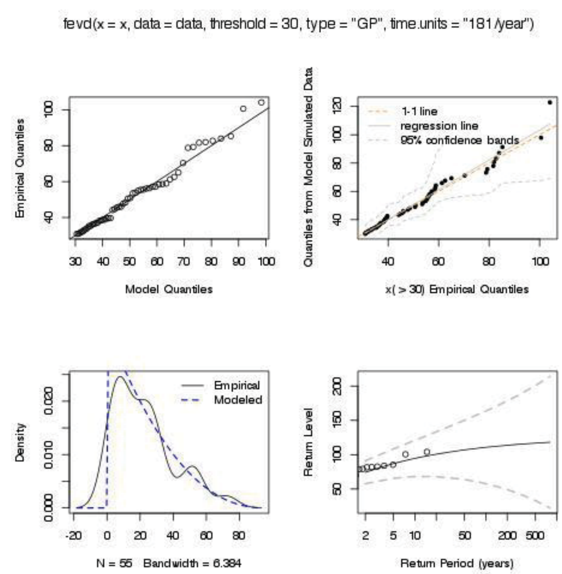

9E

72-hour Gridded Diagnostic Plots Dry Season Threshold = 30 mm

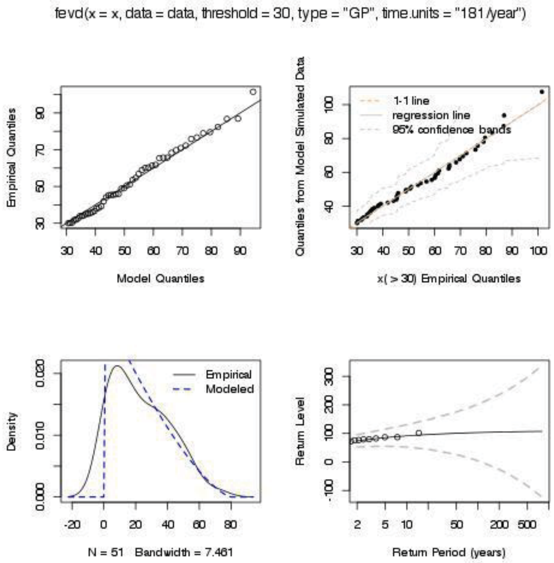

9G

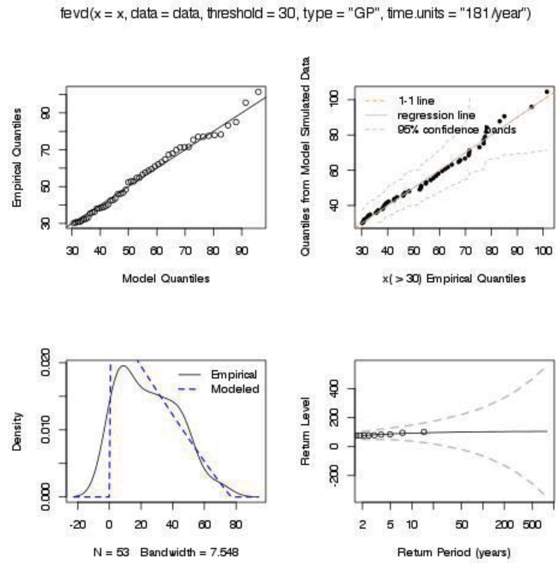

9H

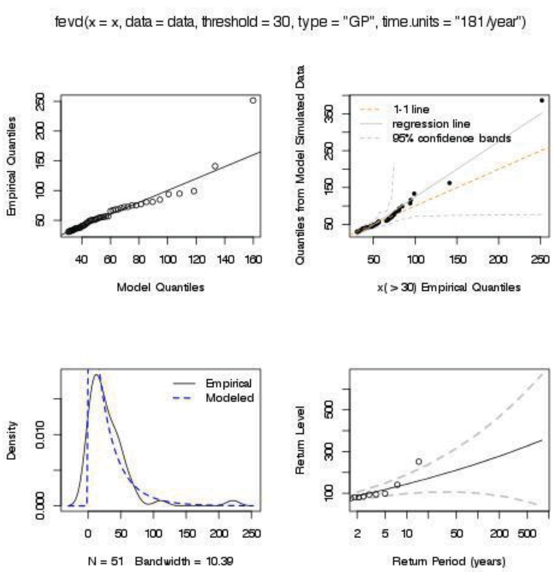

9I

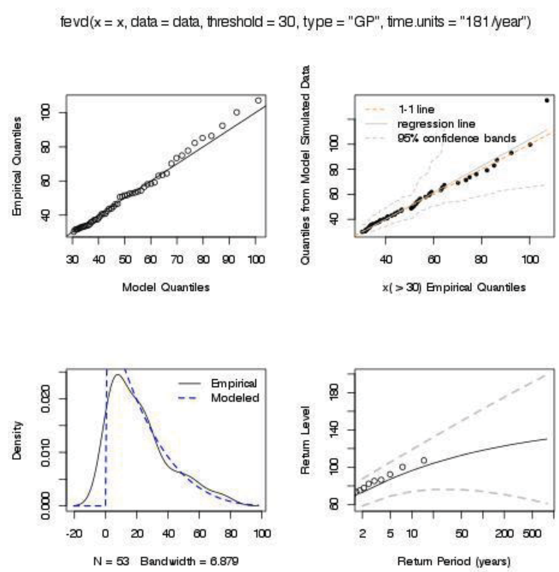

8D

72-hour Gridded Diagnostic Plots Dry Season Threshold = 30 mm

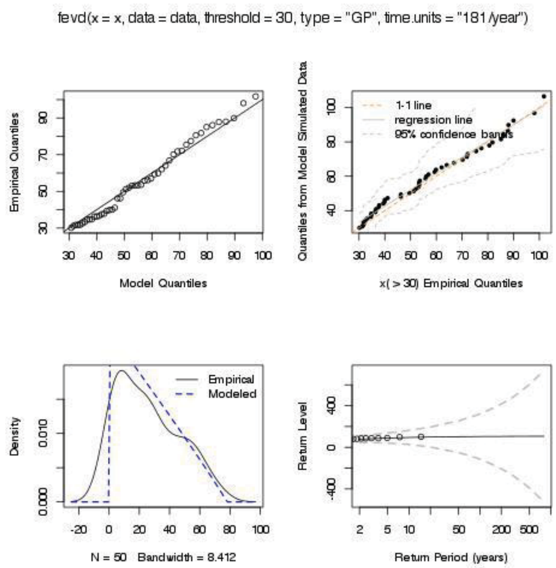

8H

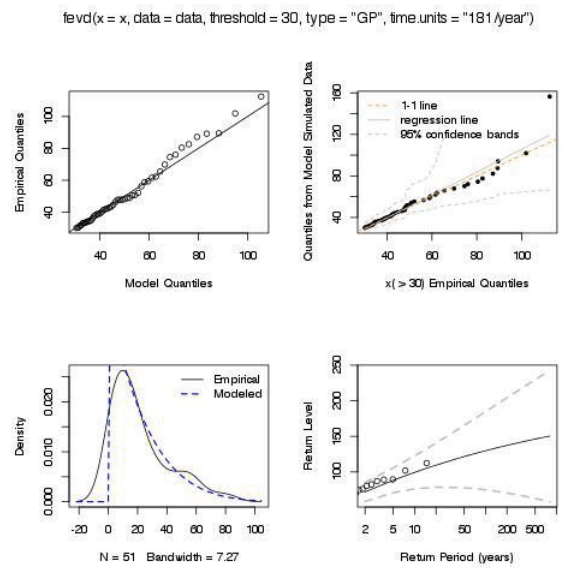

7D

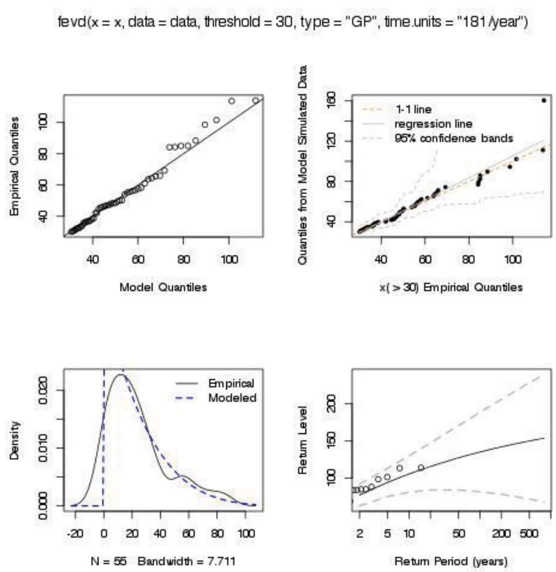

7E

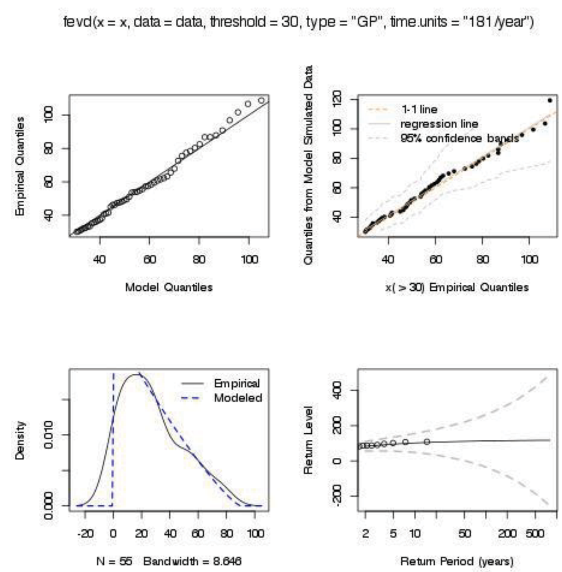

7F

72-hour Gridded Diagnostic Plots Dry Season Threshold = 30 mm

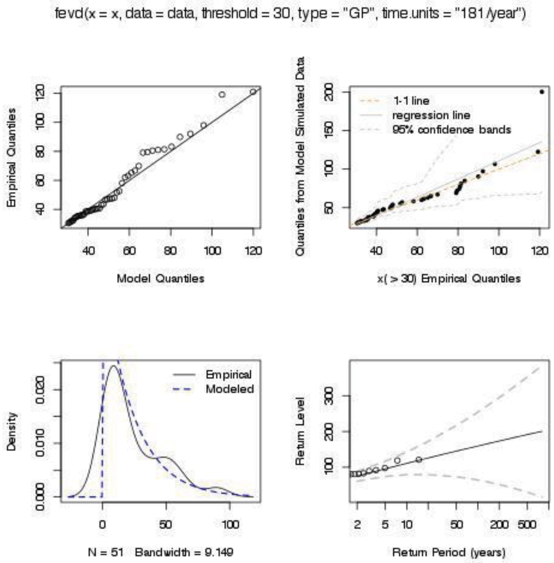

6C

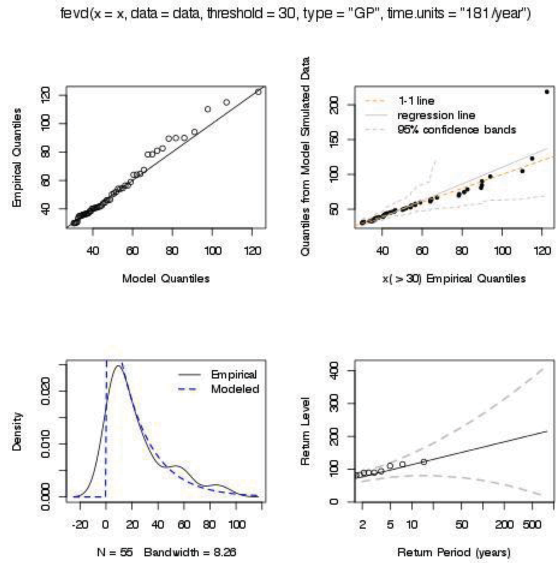

6D

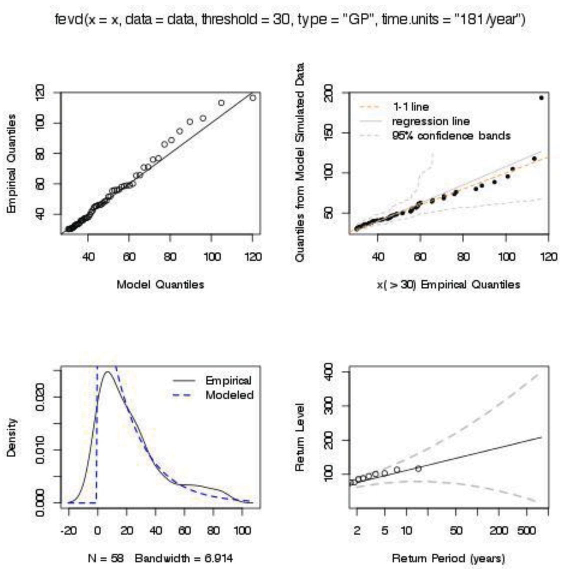

6E

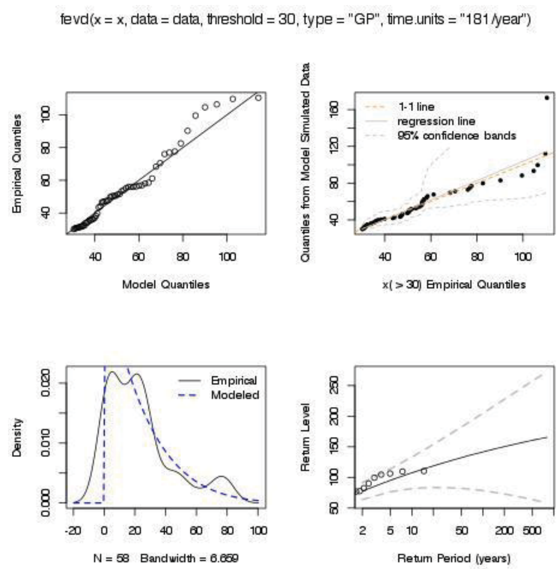

6F

72-hour Gridded Diagnostic Plots Dry Season Threshold = 30 mm

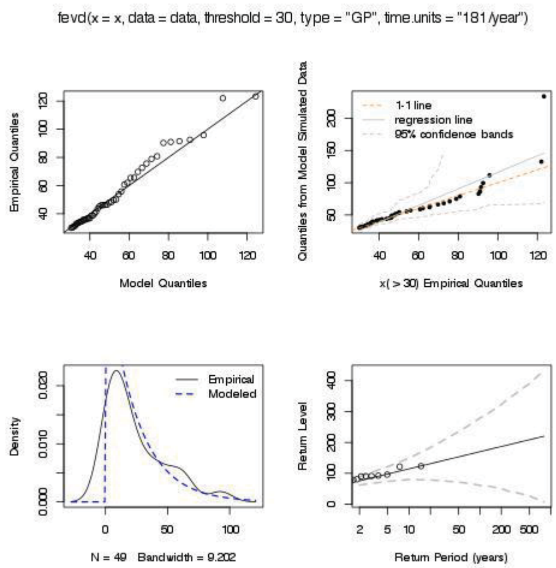

5C

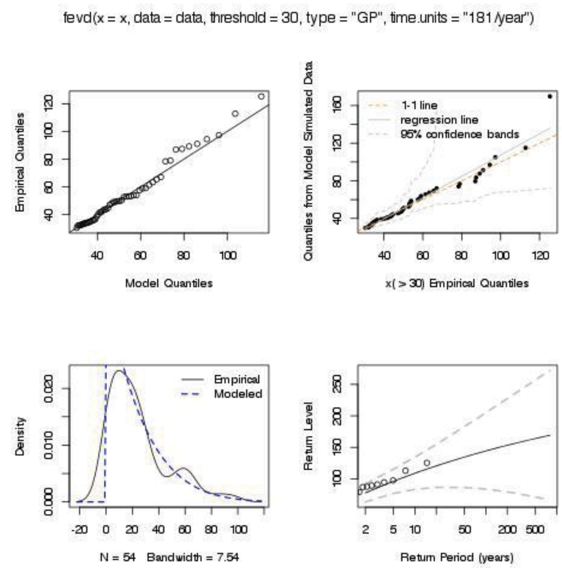

5D

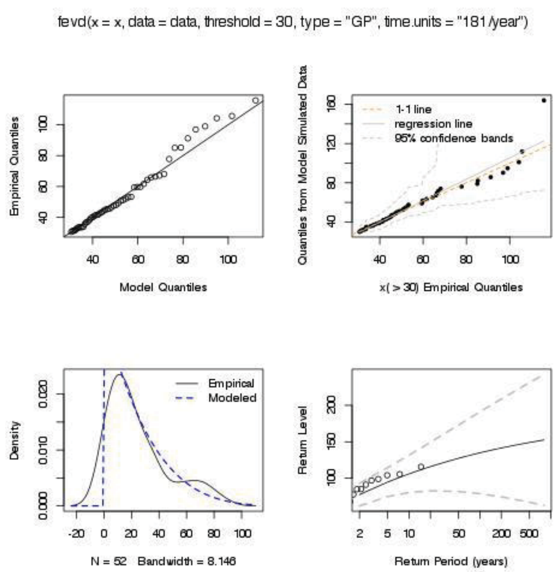

5E

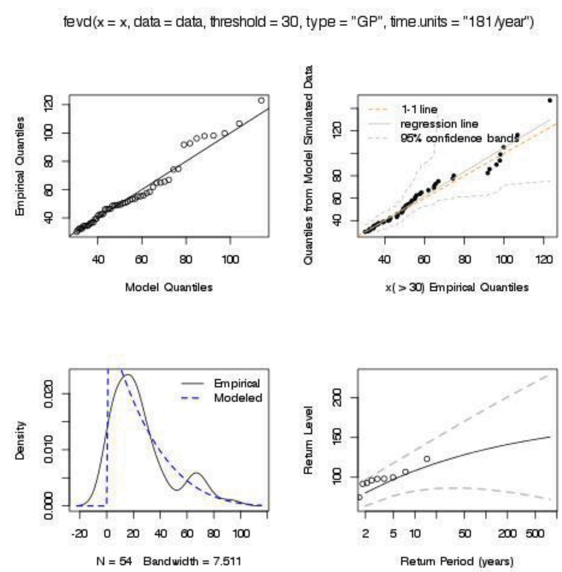

5F

72-hour Gridded Diagnostic Plots Dry Season Threshold = 30 mm

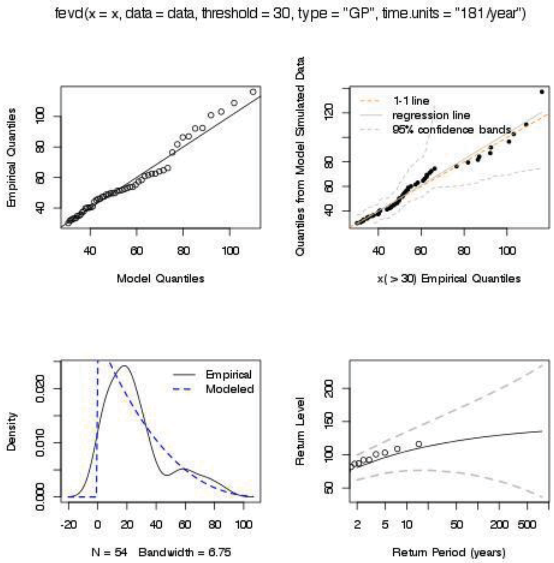

5G

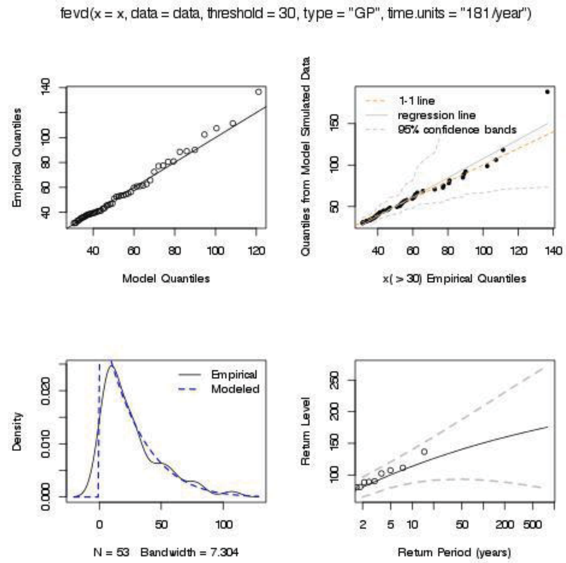

5H

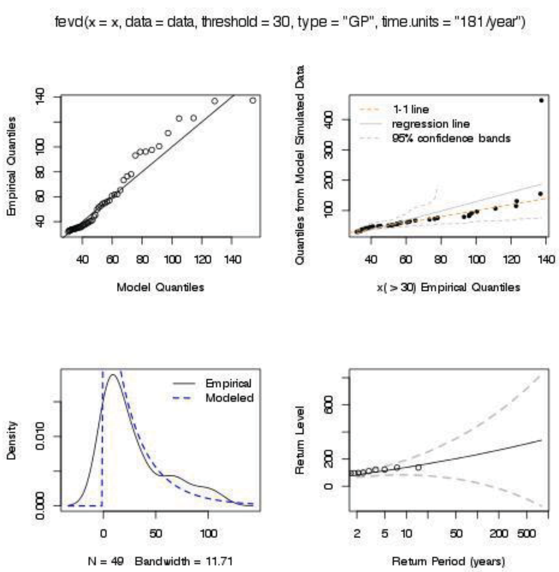

4C

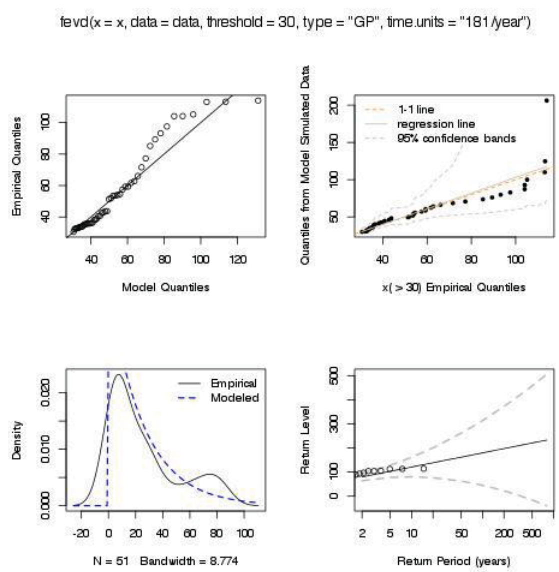

4D

72-hour Gridded Diagnostic Plots Dry Season Threshold = 30 mm

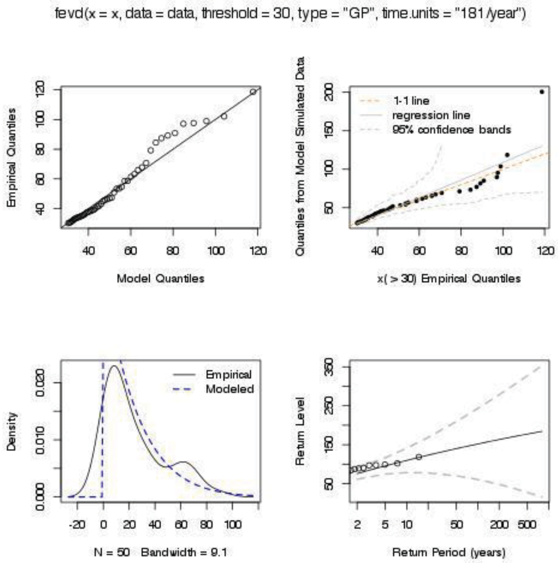

4E

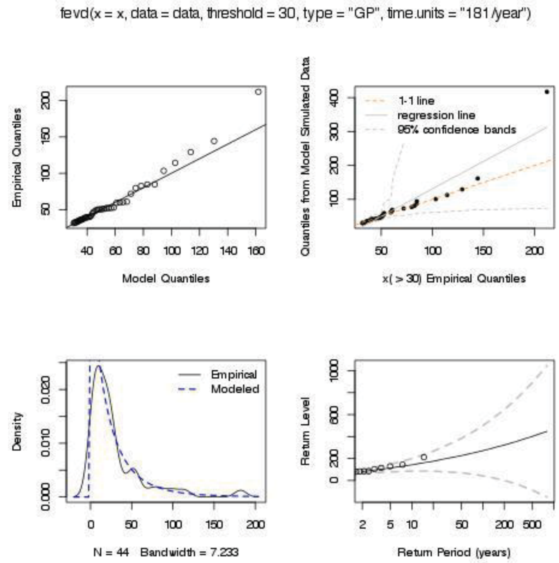

4F

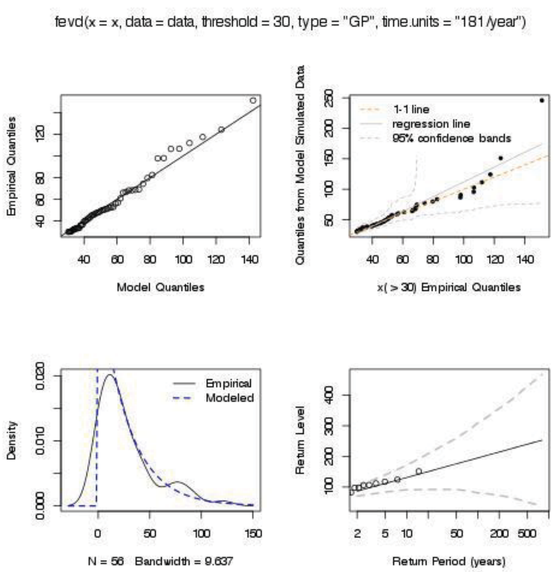

4G

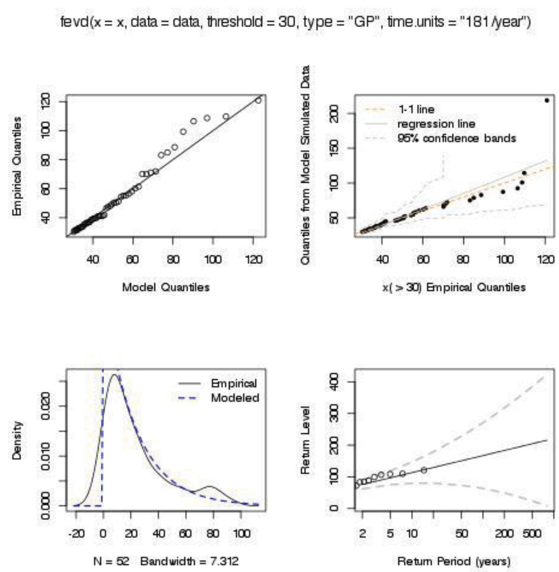

3B

72-hour Gridded Diagnostic Plots Dry Season Threshold = 30 mm

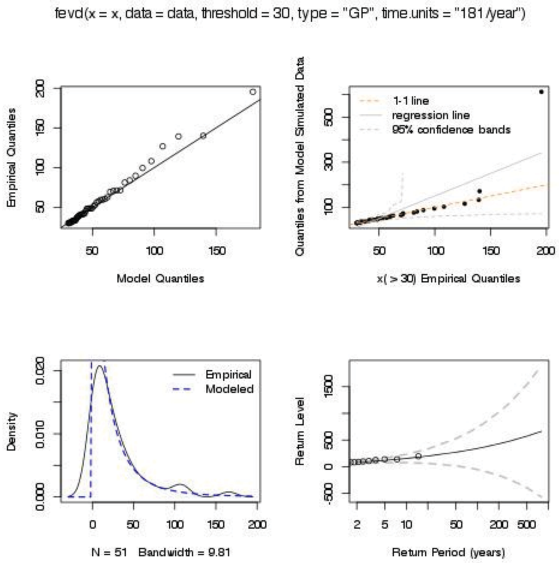

3C

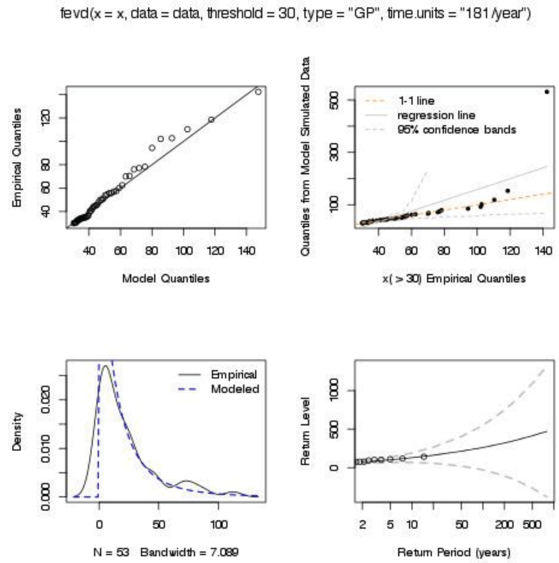

3D

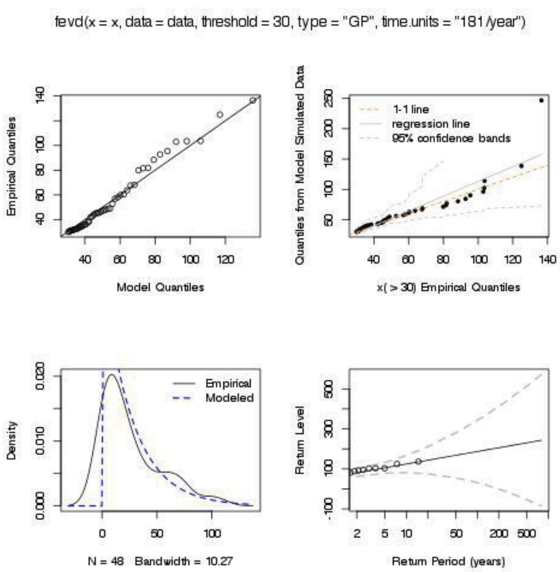

3E

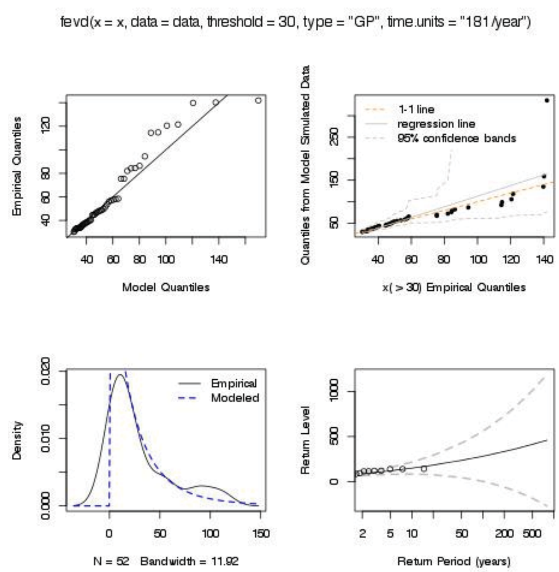

3F

72-hour Gridded Diagnostic Plots Dry Season Threshold = 30 mm

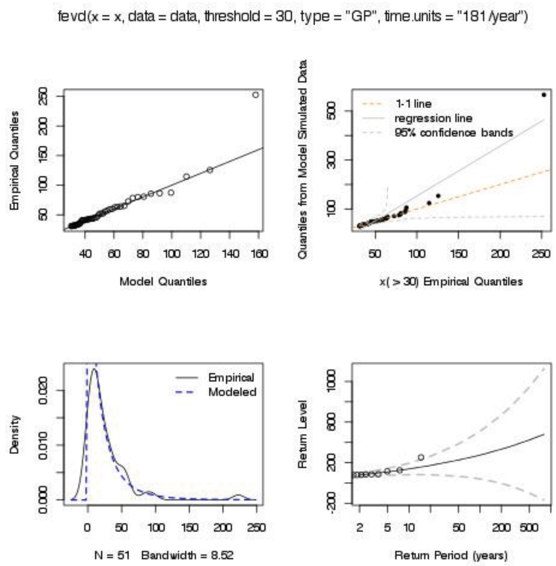

2C

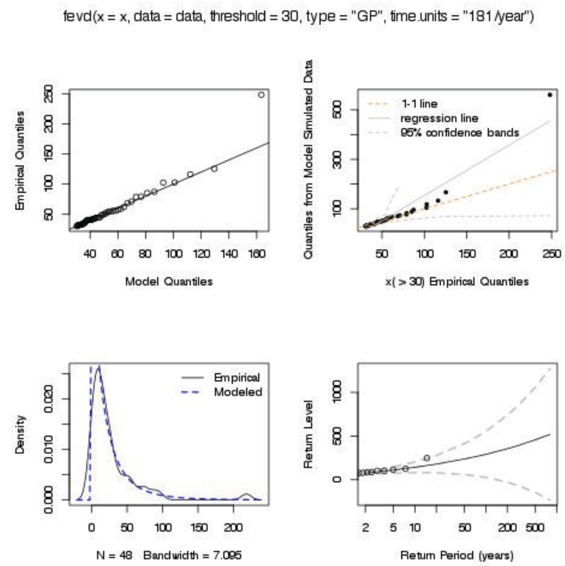

2D

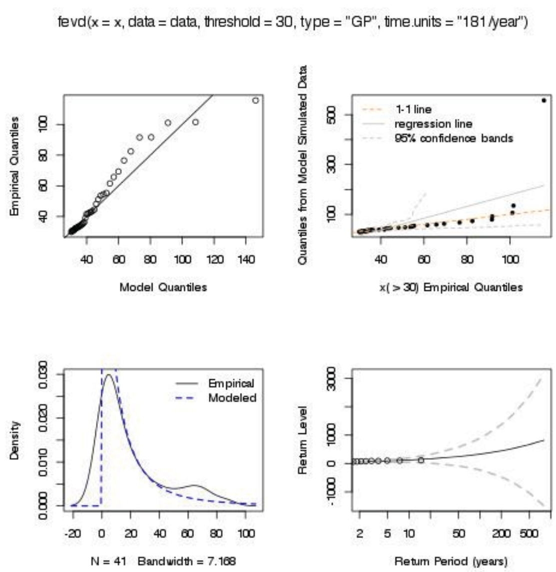

2E

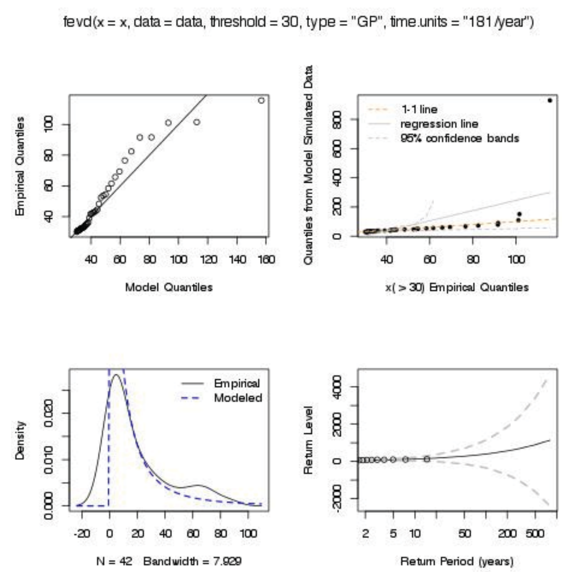

1D

72-hour Gridded Diagnostic Plots Wet Season Threshold = 40 mm

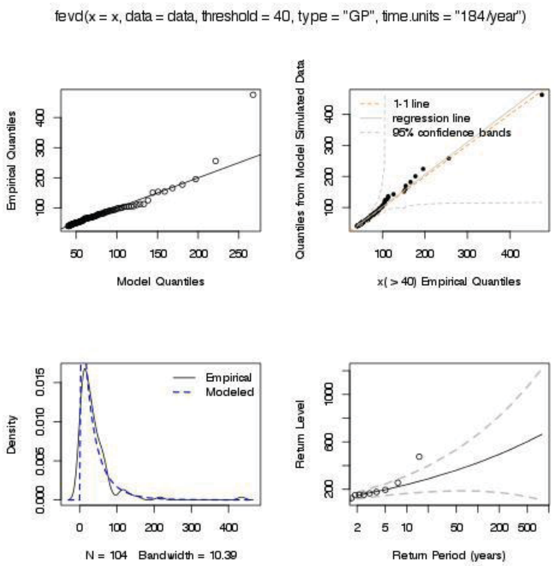

10E

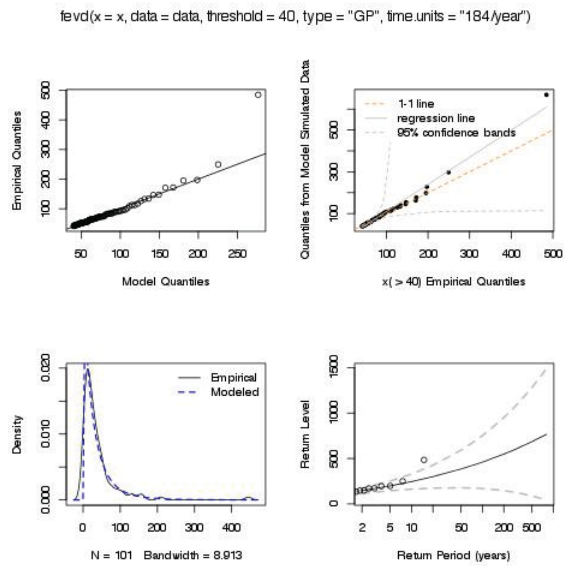

10F

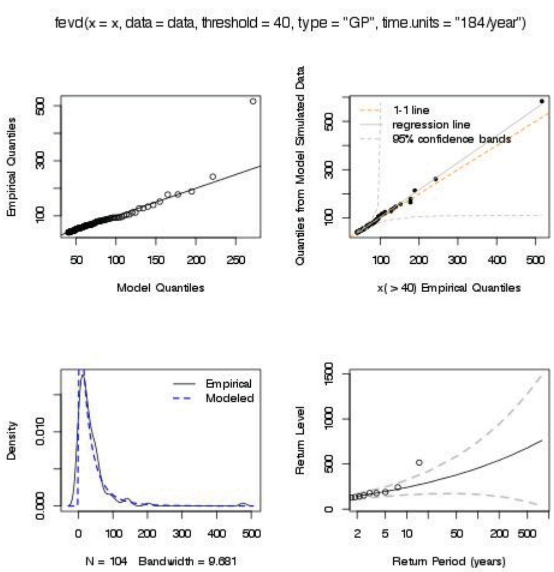

10G

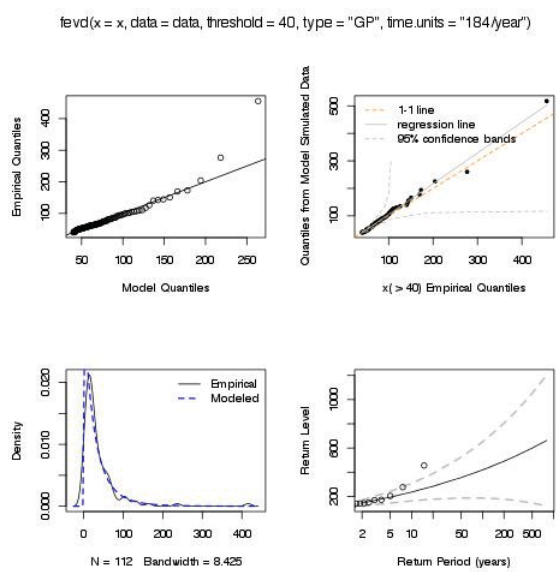

9E

72-hour Gridded Diagnostic Plots Wet Season Threshold = 40 mm

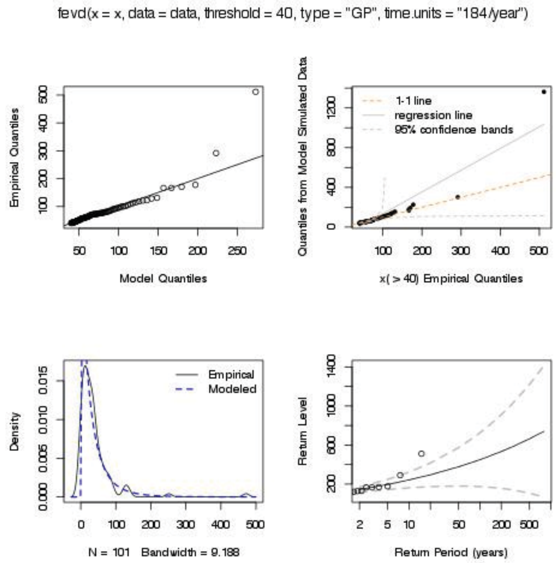

9G

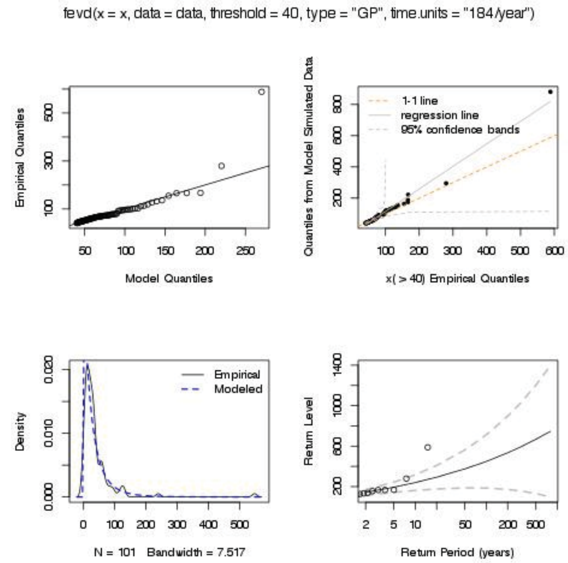

9H

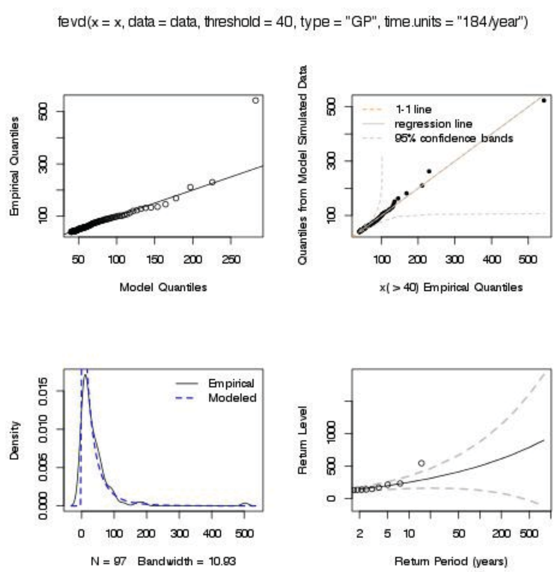

9I

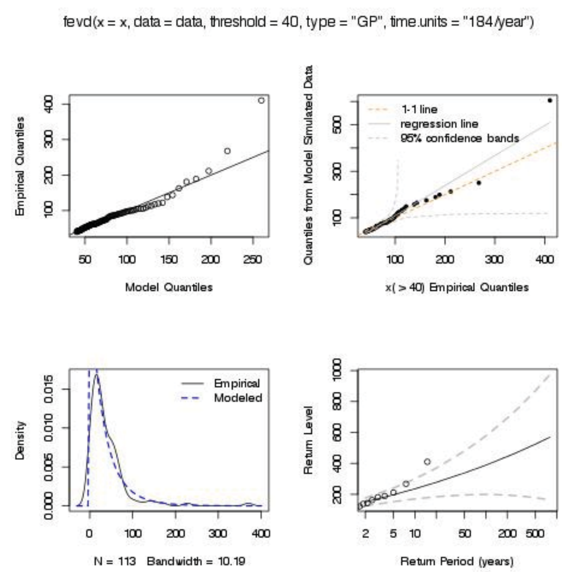

8D

72-hour Gridded Diagnostic Plots Wet Season Threshold = 40 mm

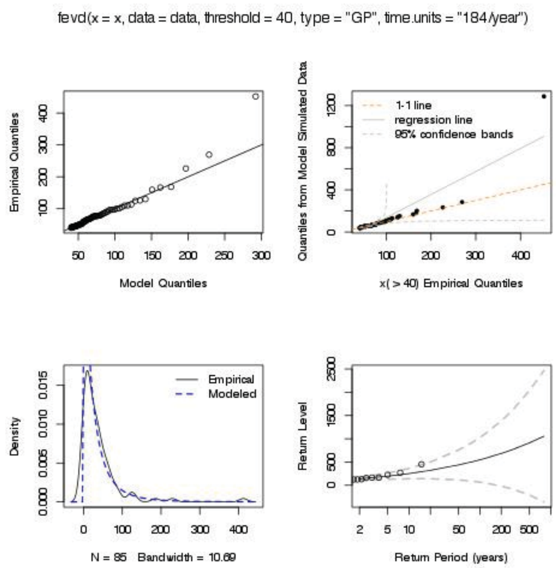

8H

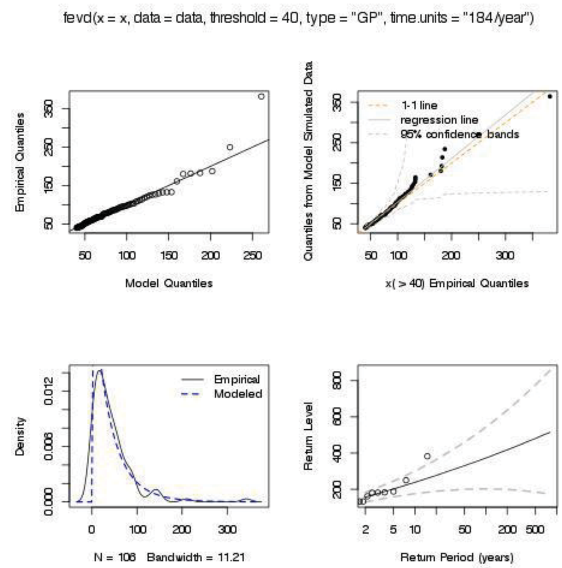

7D

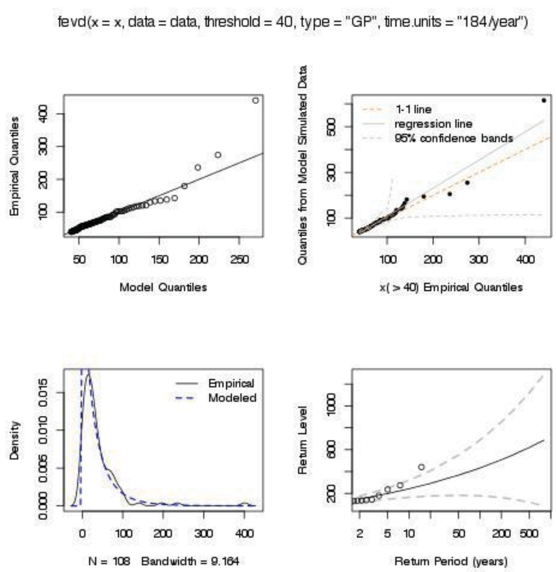

7E

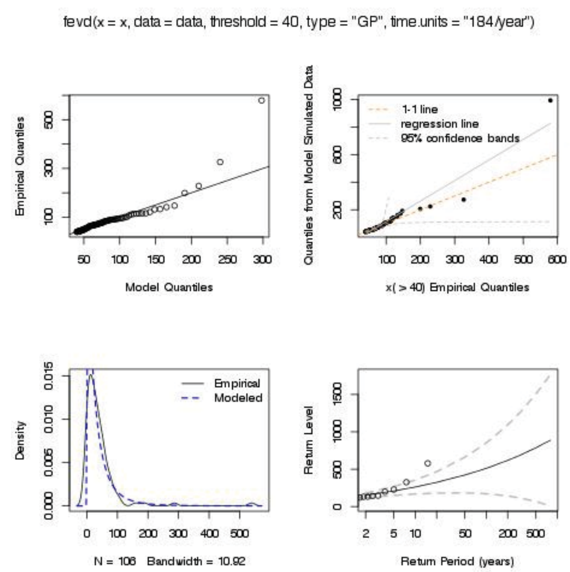

7F

72-hour Gridded Diagnostic Plots Wet Season Threshold = 40 mm

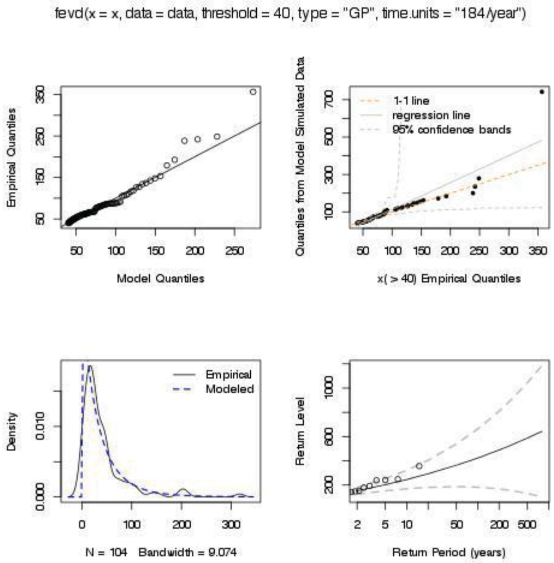

6C

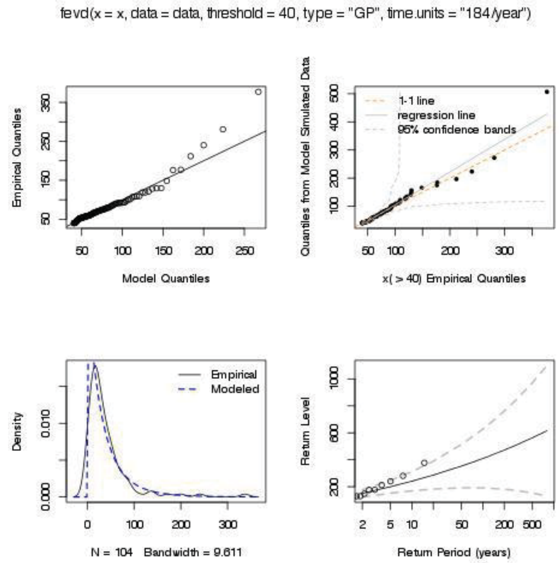

6D

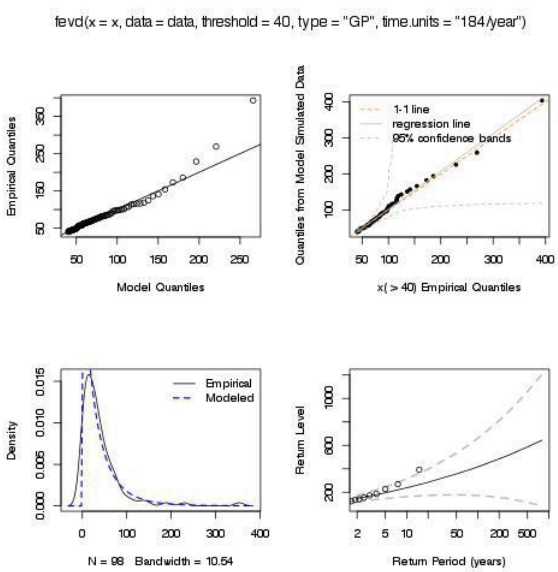

6E

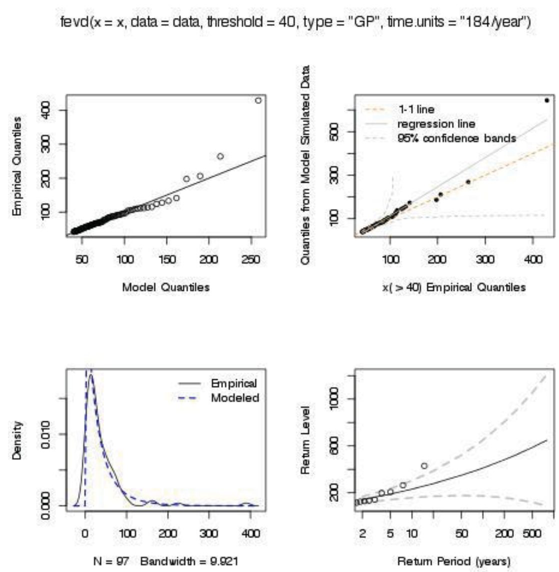

6F

72-hour Gridded Diagnostic Plots Wet Season Threshold = 40 mm

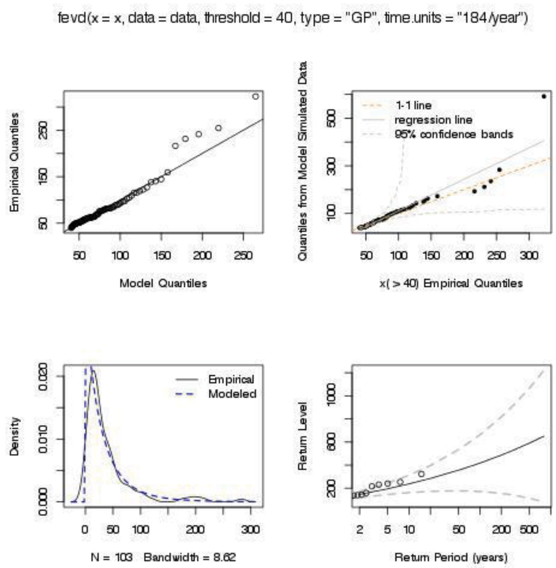

5C

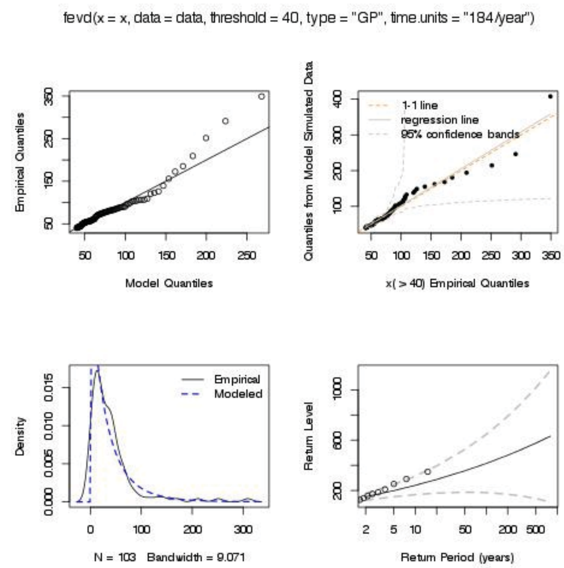

5D

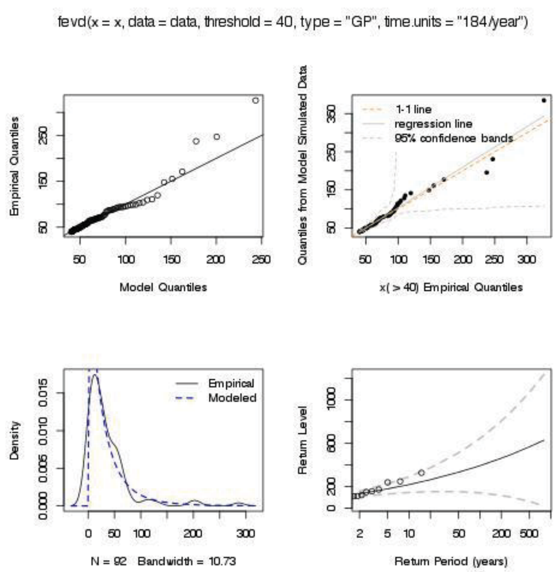

5E

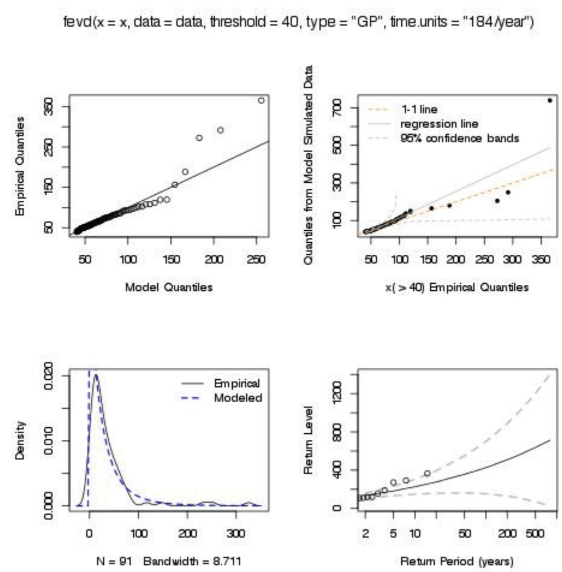

5F

72-hour Gridded Diagnostic Plots Wet Season Threshold = 40 mm

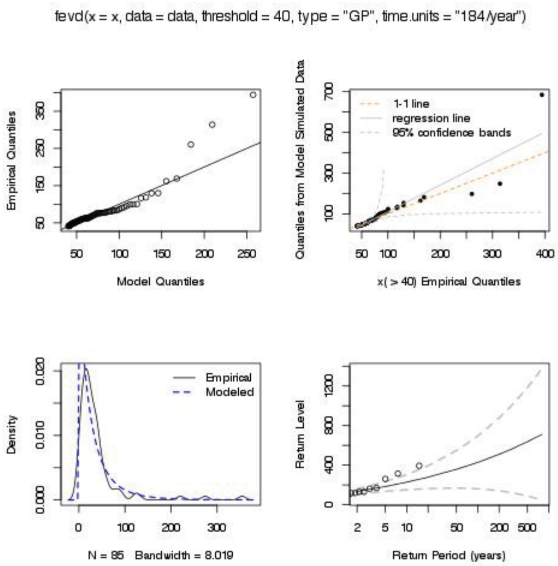

5G

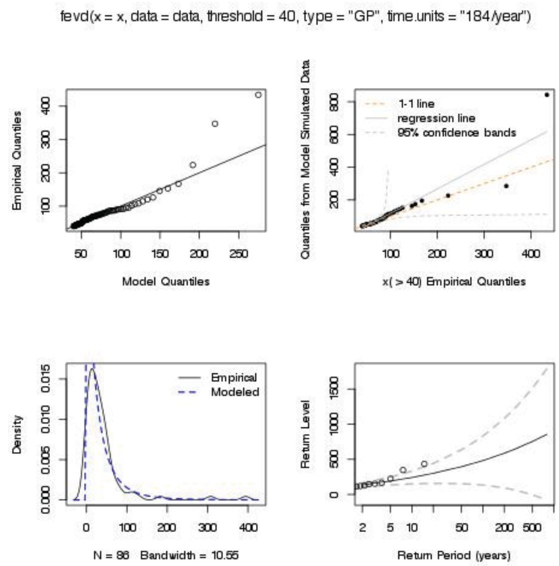

5H

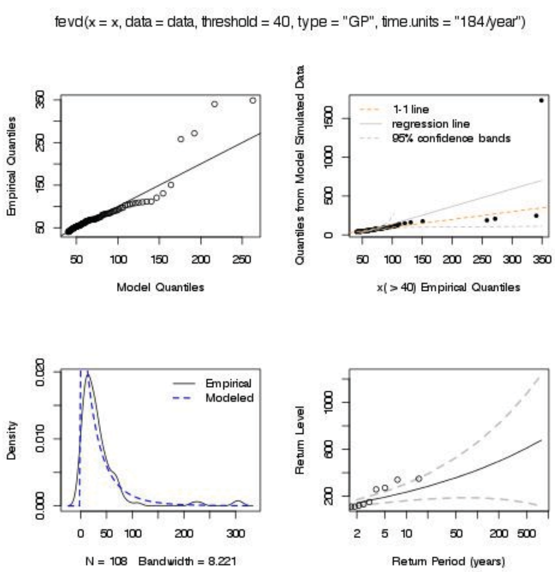

4C

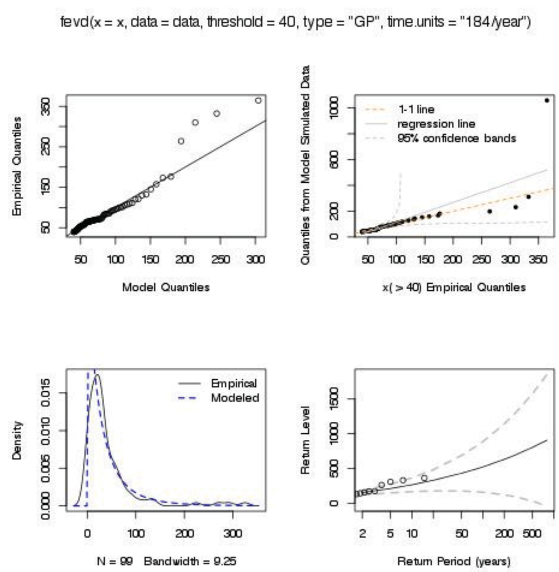

4D

72-hour Gridded Diagnostic Plots Wet Season Threshold = 40 mm

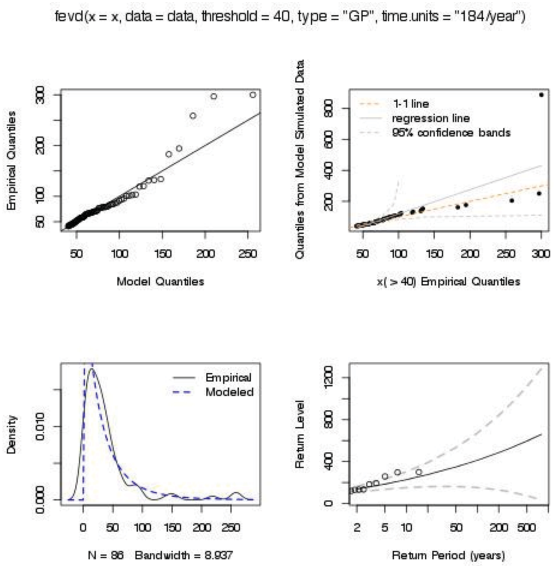

4E

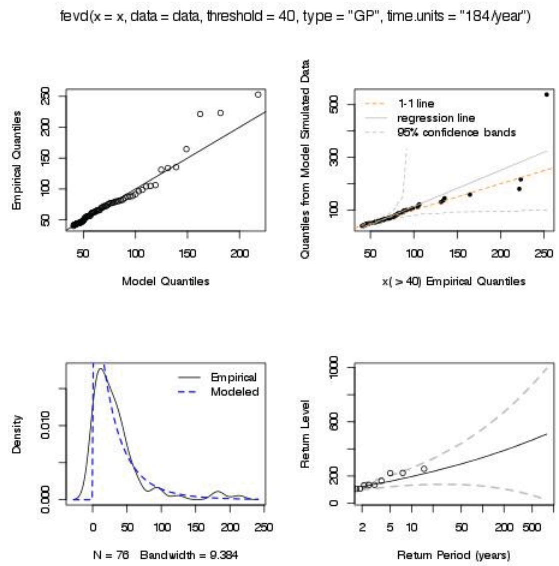

4F

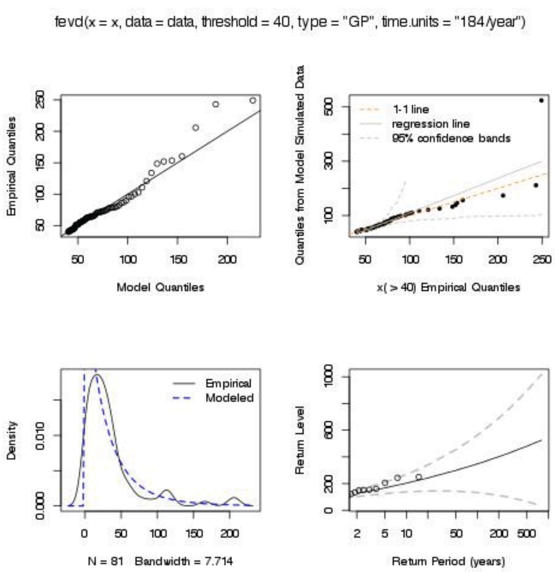

4G

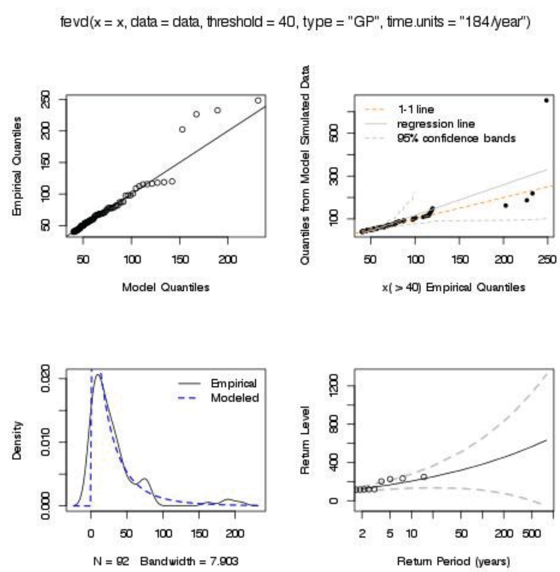

3B

72-hour Gridded Diagnostic Plots Wet Season Threshold = 40 mm

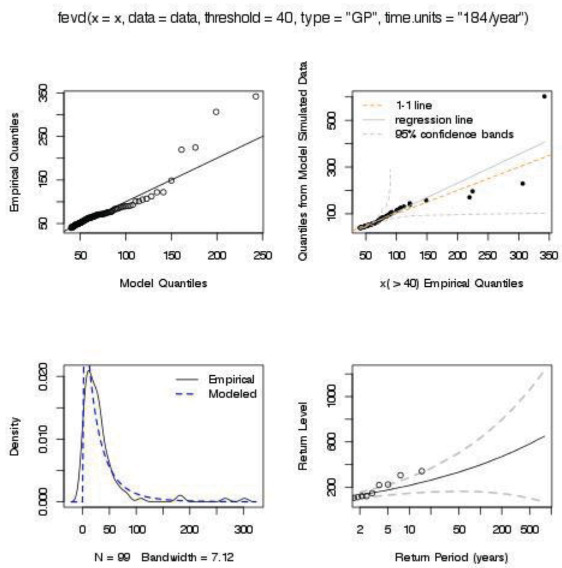

3C

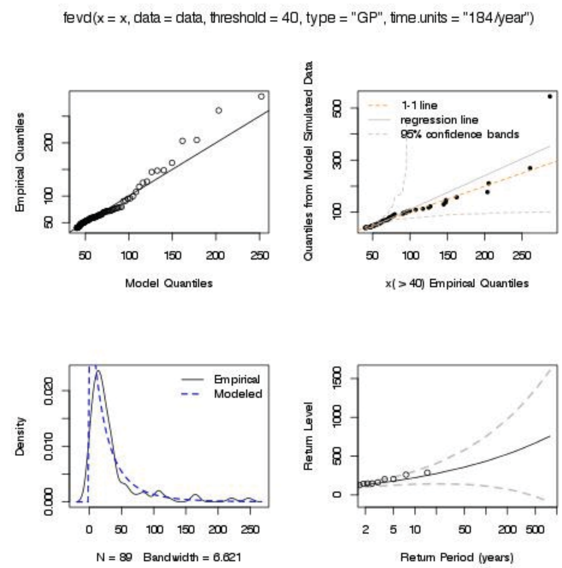

3D

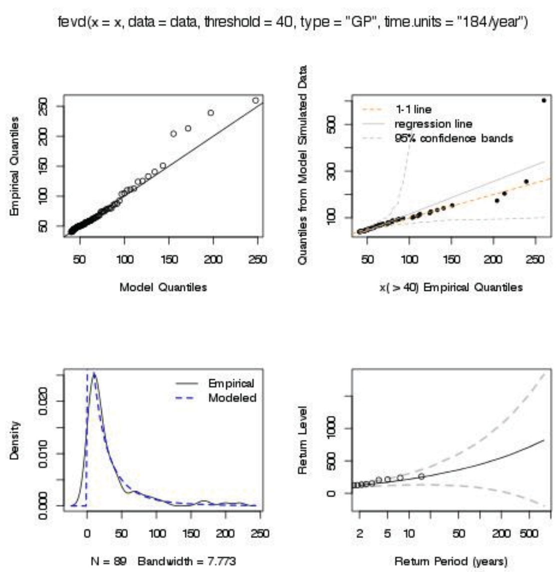

3E

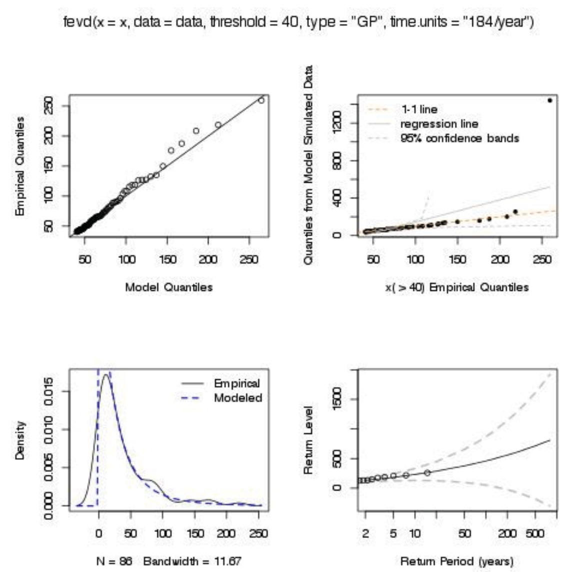

3F

72-hour Gridded Diagnostic Plots Wet Season Threshold = 40 mm

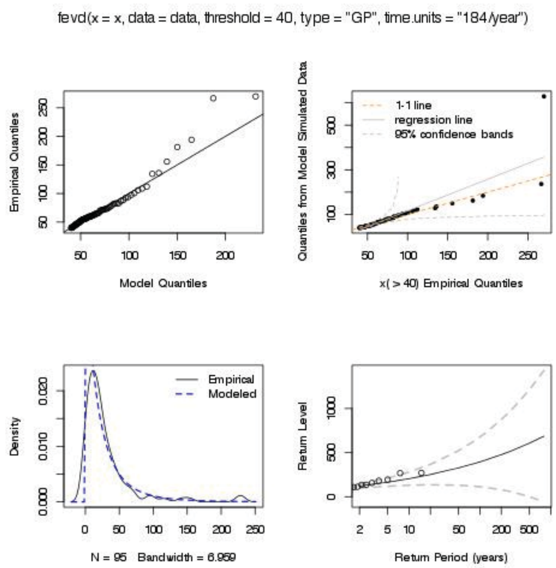

2C

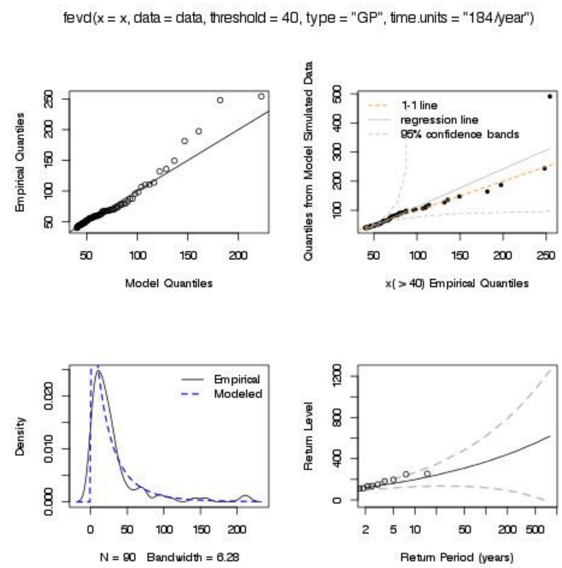

2D

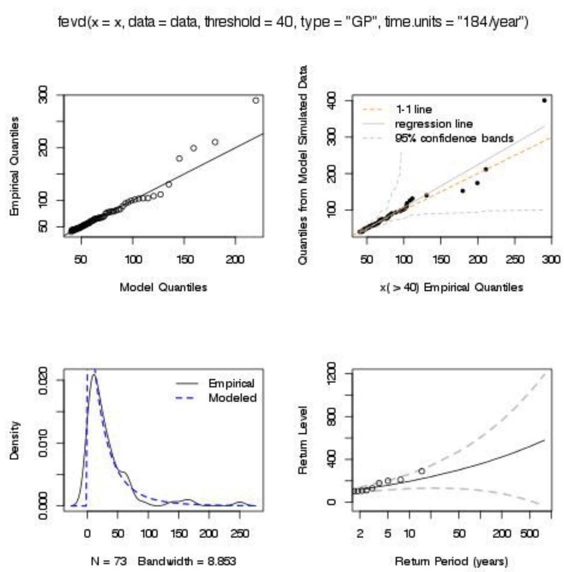

2E

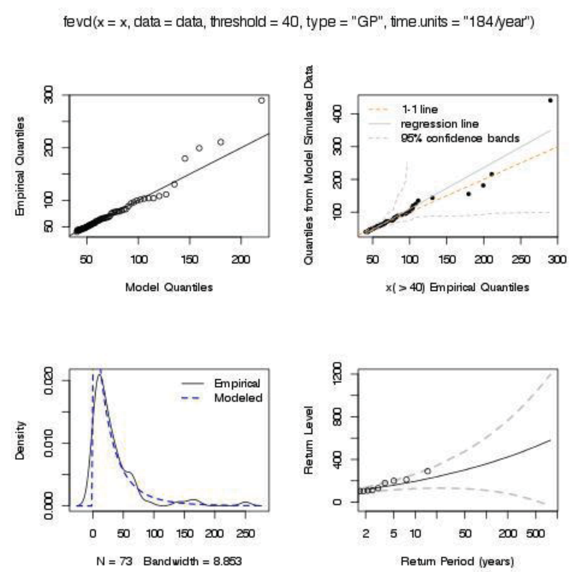

1D

72-hour Gridded Diagnostic Plots Wet Season Threshold = 45 mm

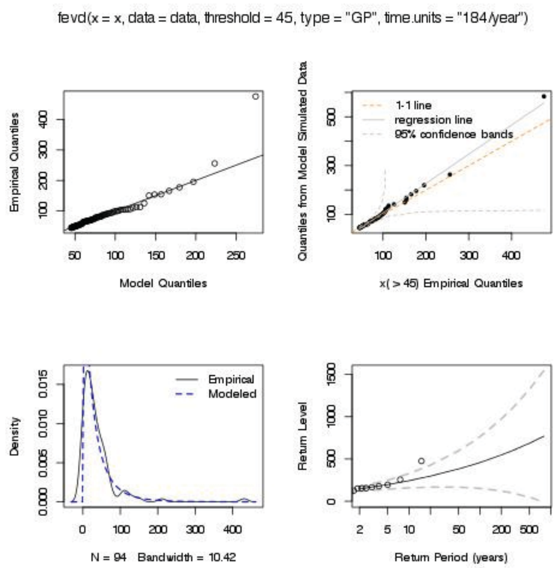

10E

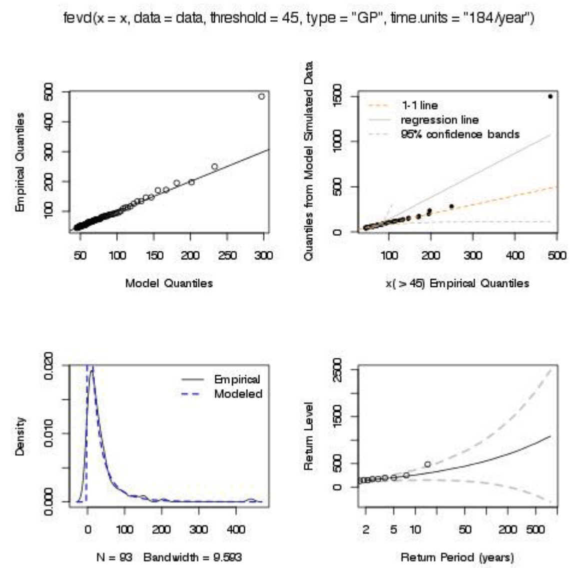

10F

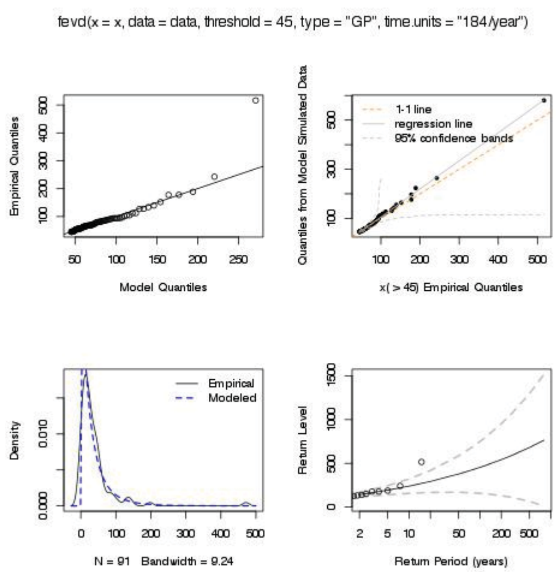

10G

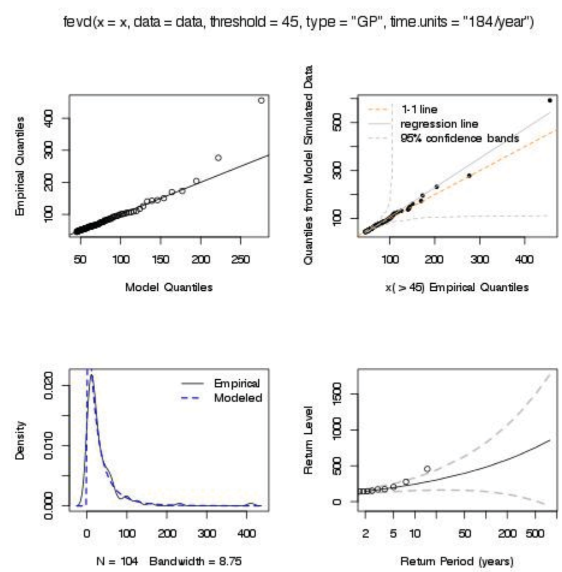

9E

72-hour Gridded Diagnostic Plots Wet Season Threshold = 45 mm

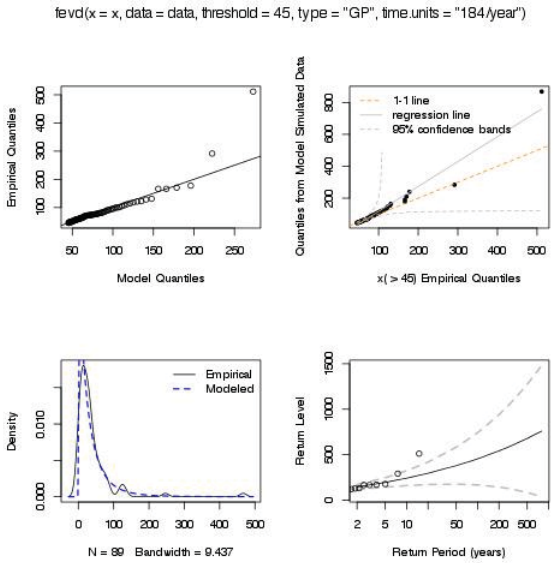

9G

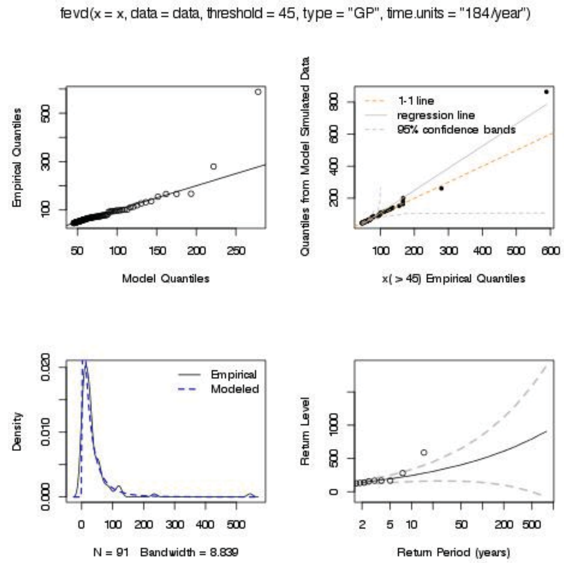

9H

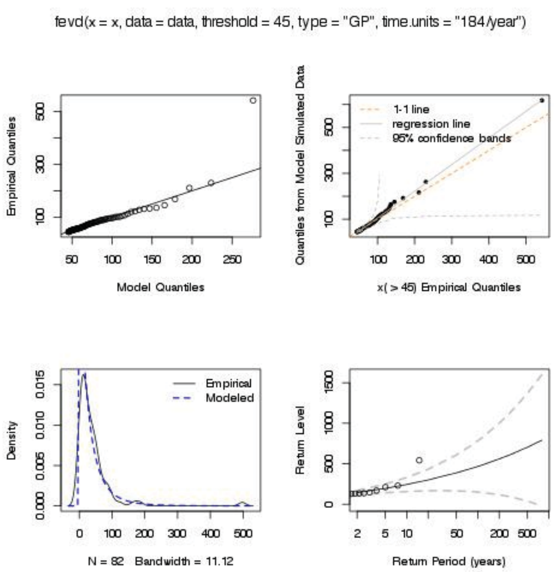

9I

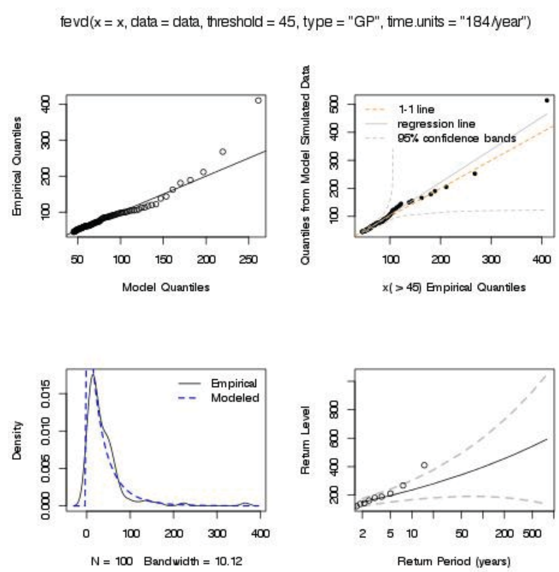

8D

72-hour Gridded Diagnostic Plots Wet Season Threshold = 45 mm

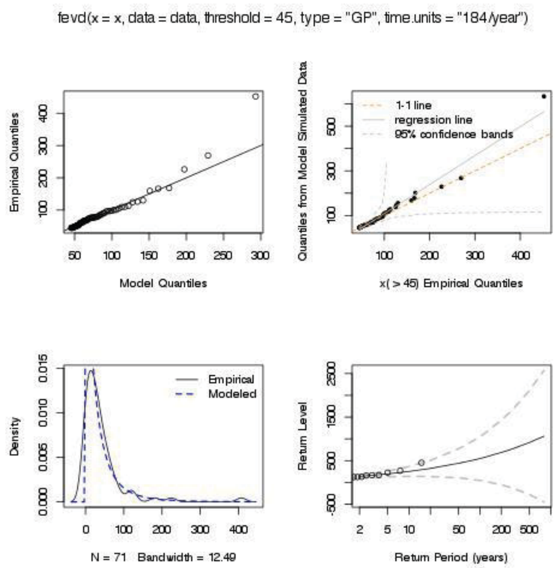

8H

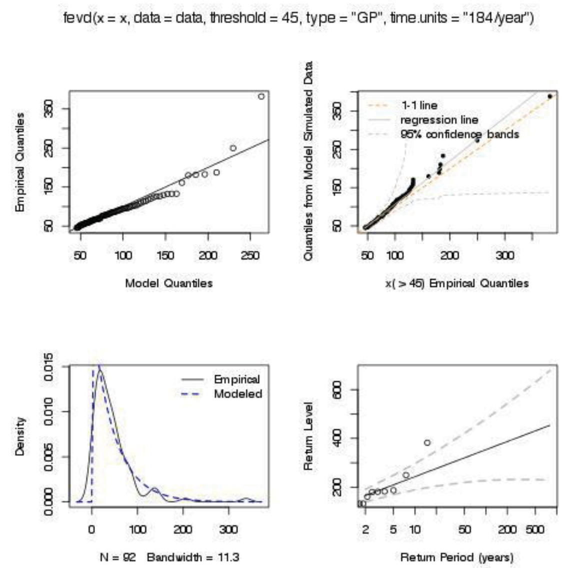

7D

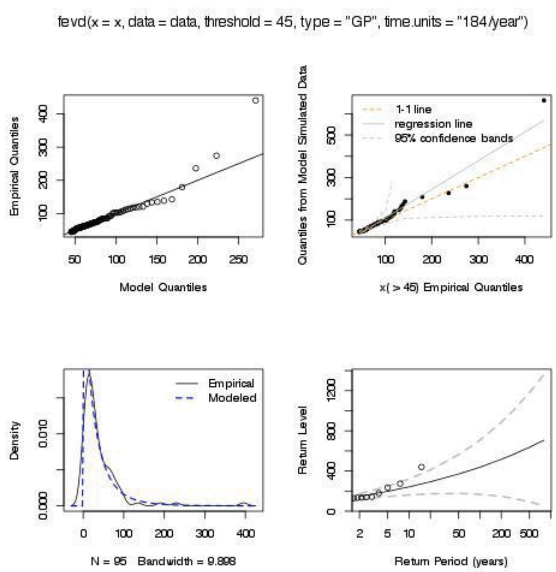

7E

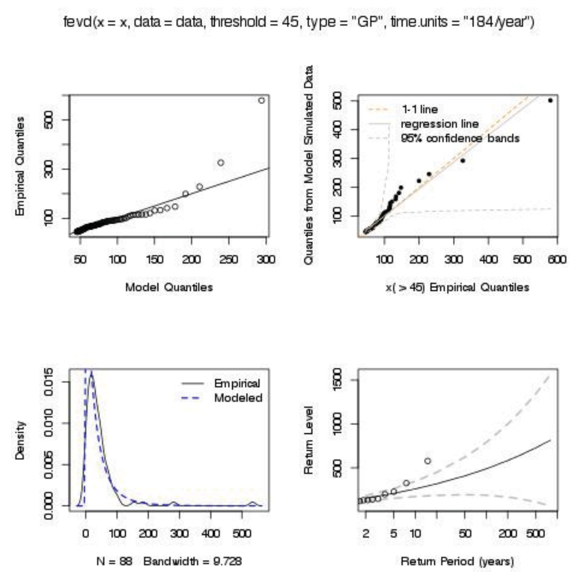

7F

72-hour Gridded Diagnostic Plots Wet Season Threshold = 45 mm

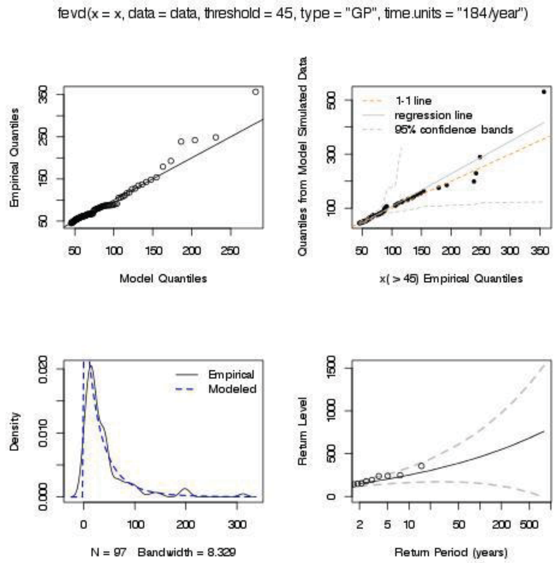

6C

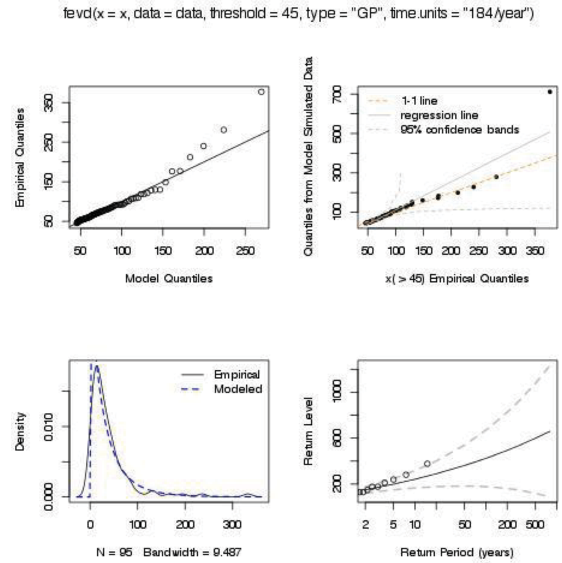

6D

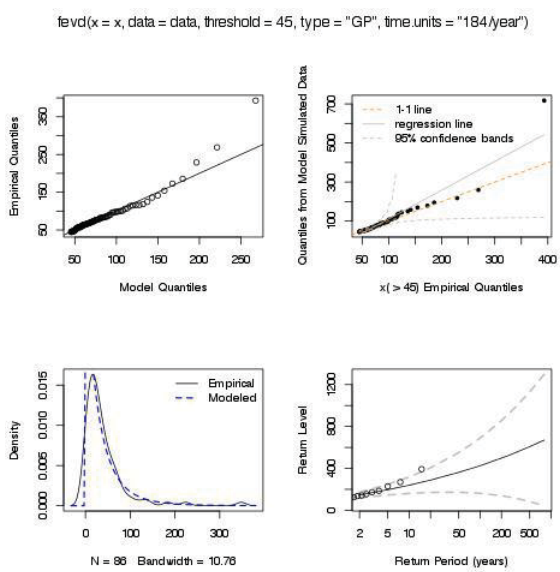

6E

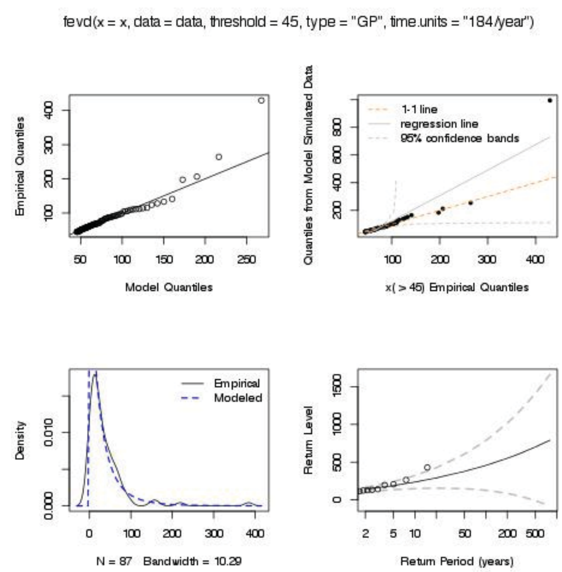

6F

72-hour Gridded Diagnostic Plots Wet Season Threshold = 45 mm

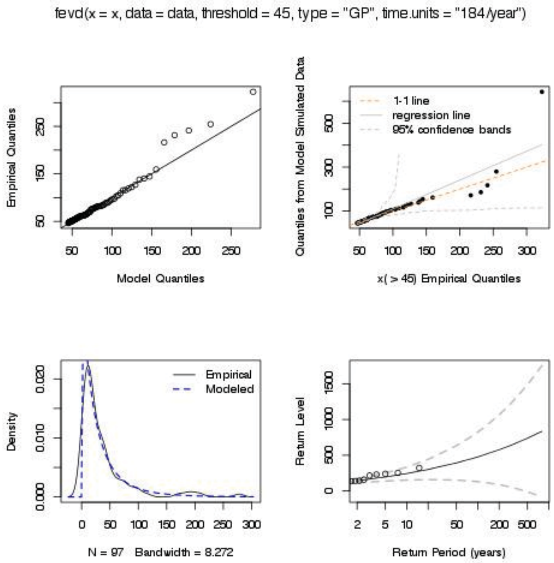

5C

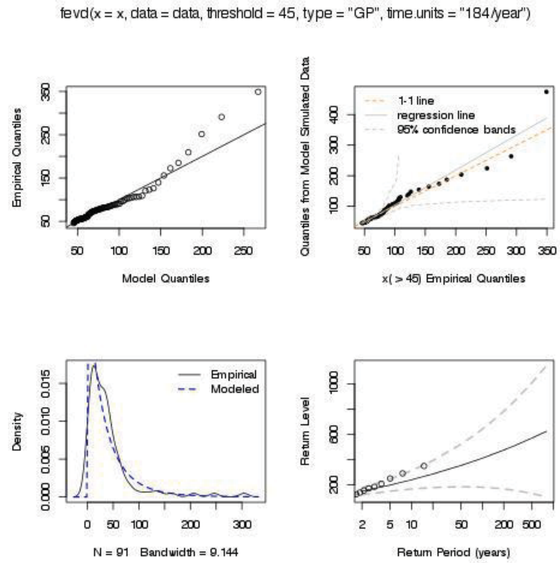

5D

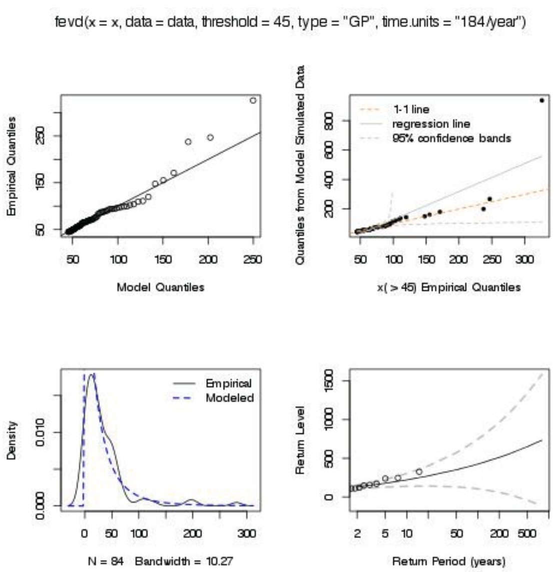

5E

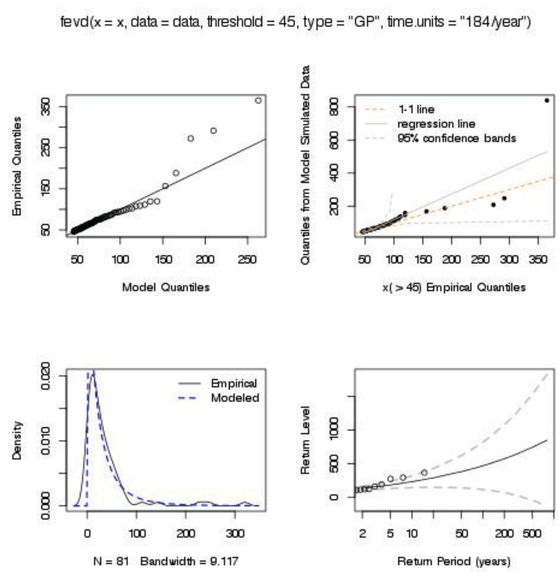

5F

72-hour Gridded Diagnostic Plots Wet Season Threshold = 45 mm

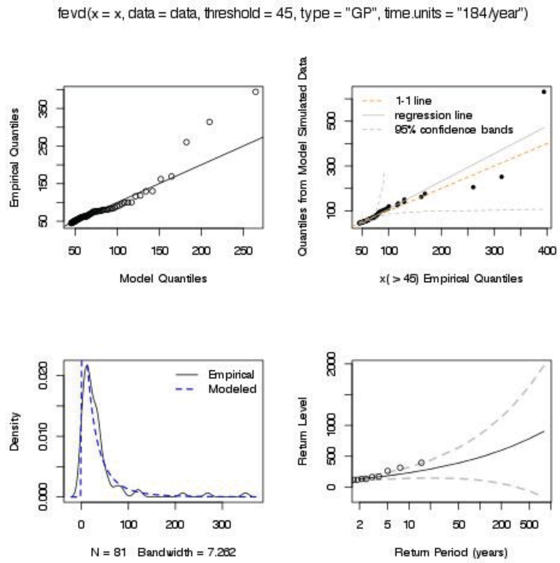

5G

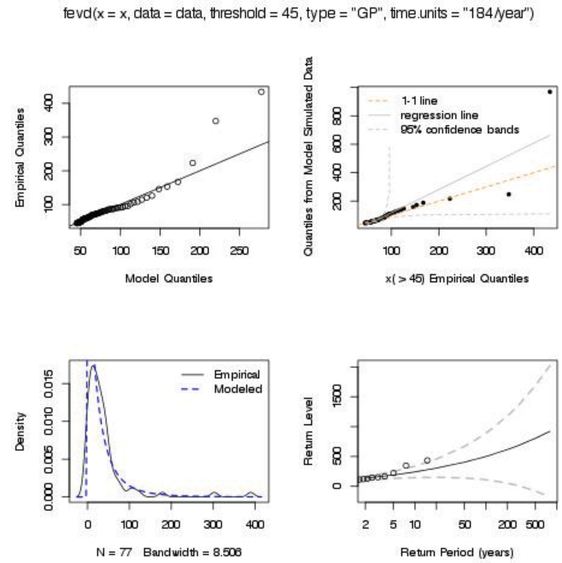

5H

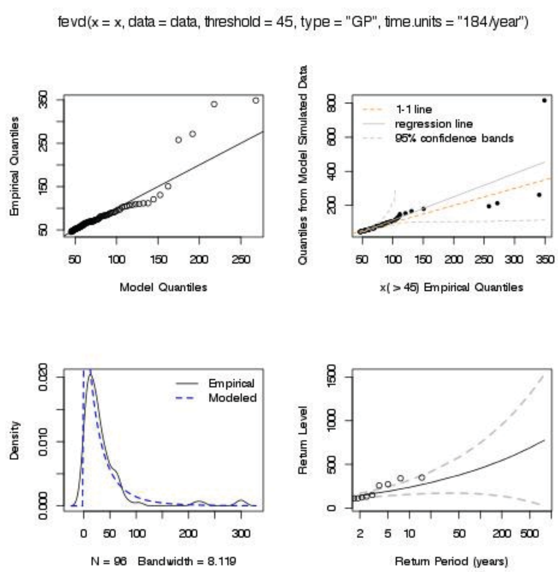

4C

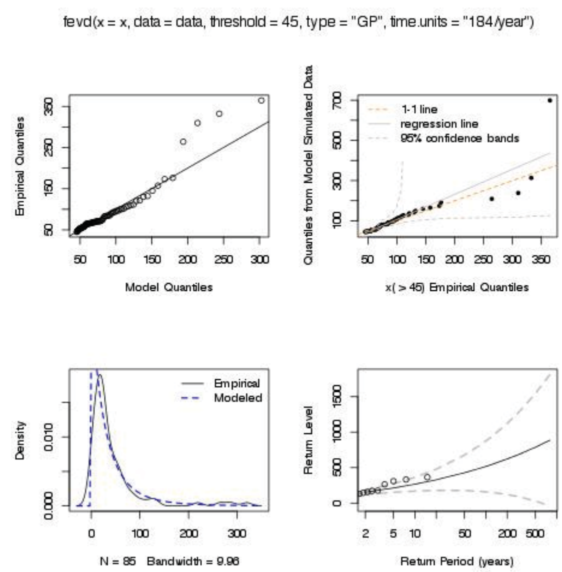

4D

72-hour Gridded Diagnostic Plots Wet Season Threshold = 45 mm

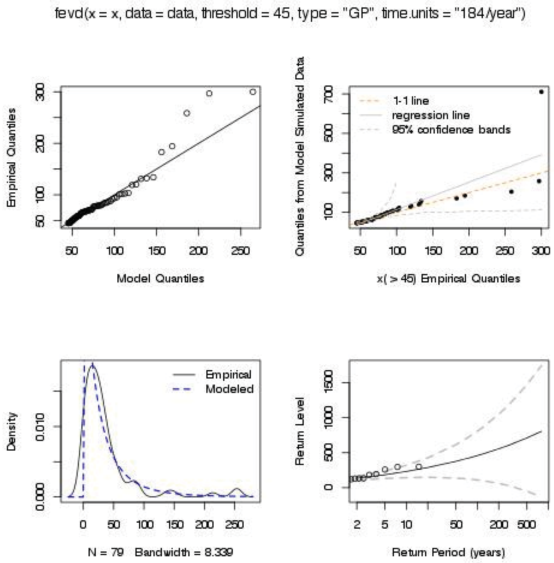

4E

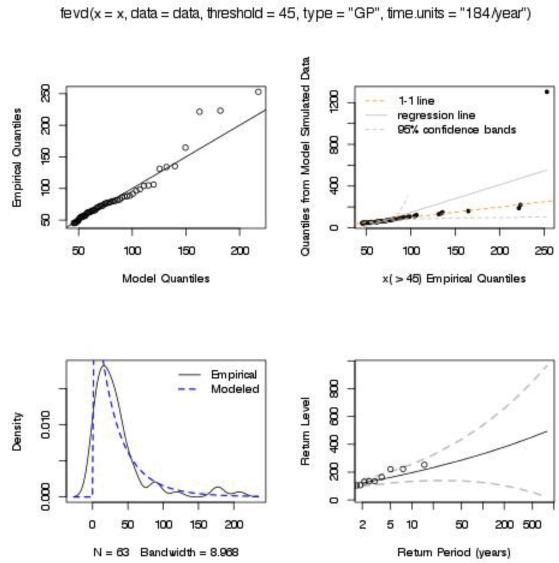

4F

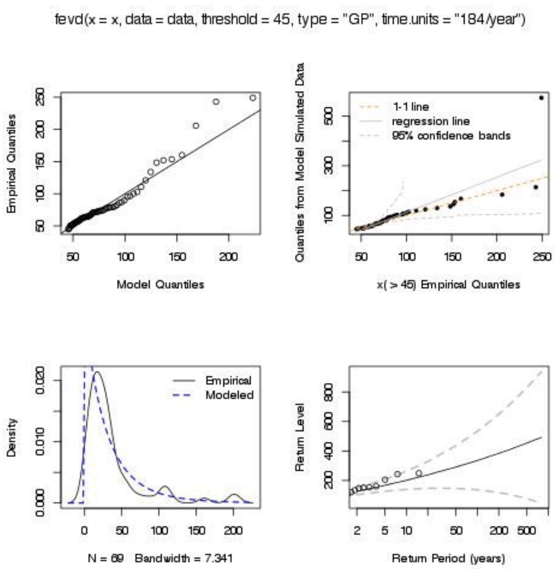

4G

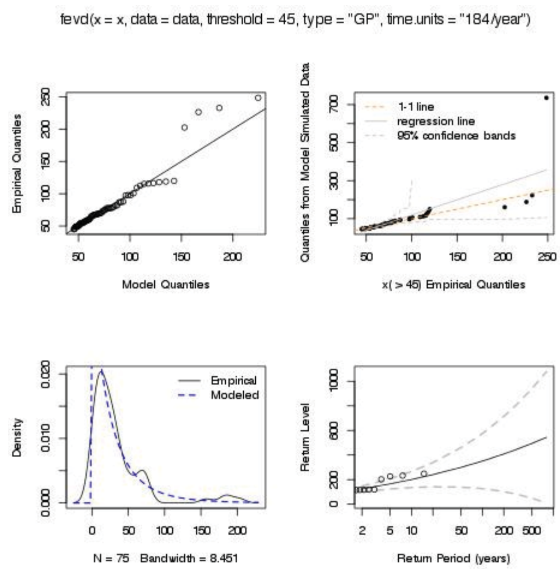

3B

72-hour Gridded Diagnostic Plots Wet Season Threshold = 45 mm

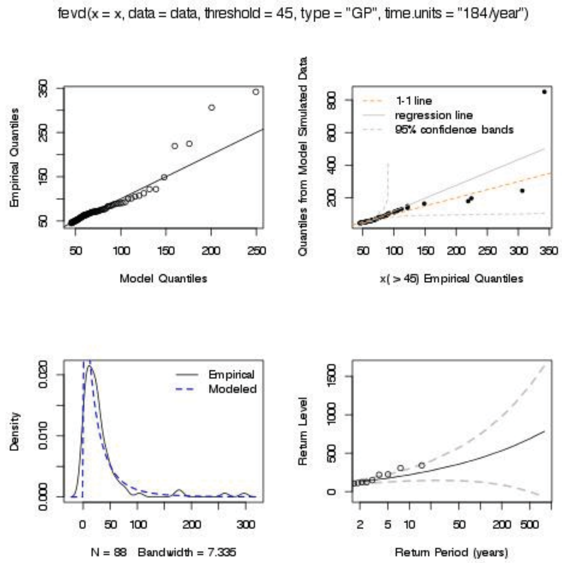

3C

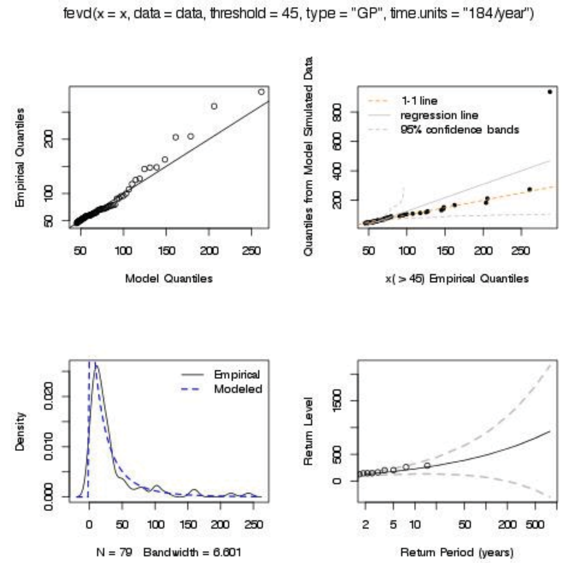

3D

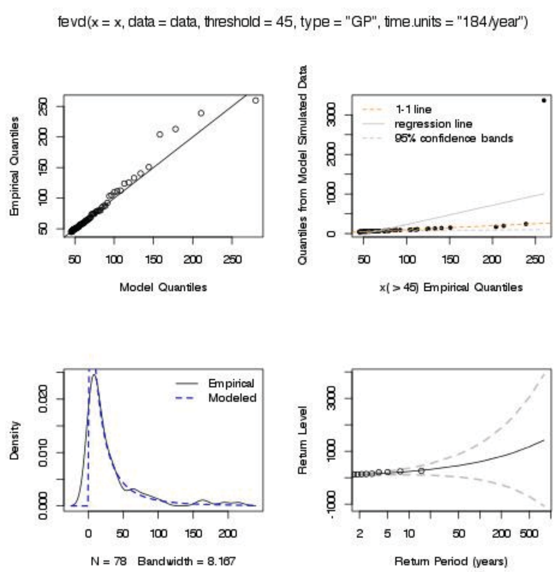

3E

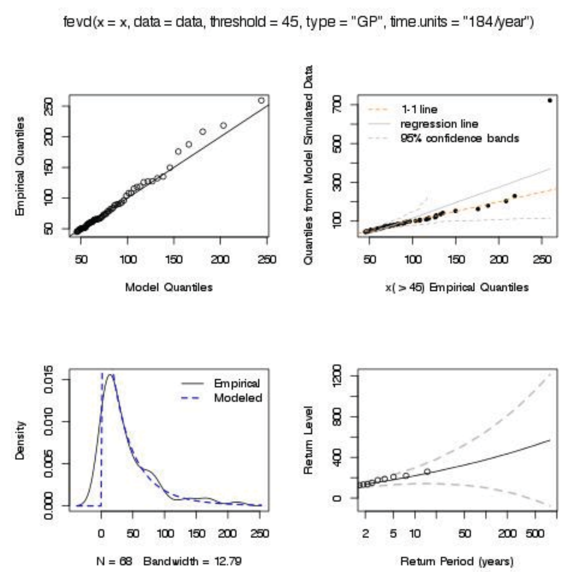

3F

72-hour Gridded Diagnostic Plots Wet Season Threshold = 45 mm

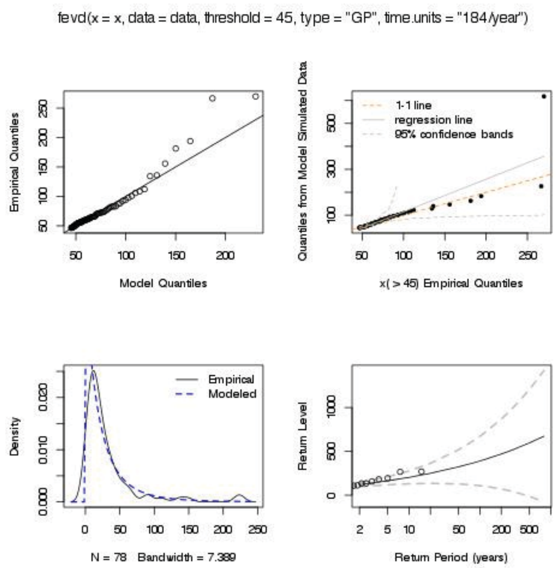

2C

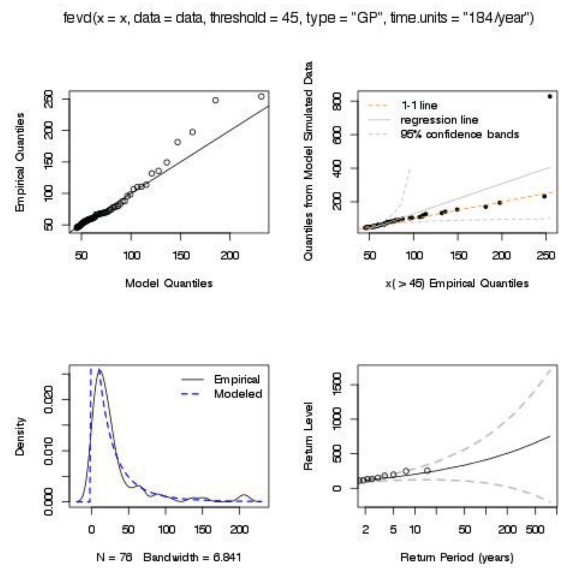

2D

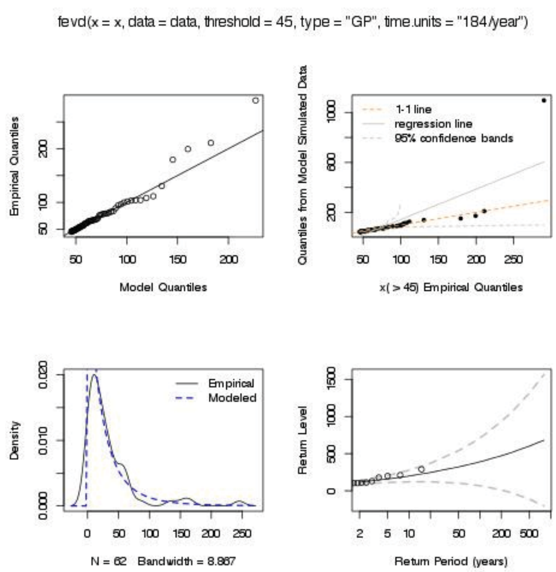

2E

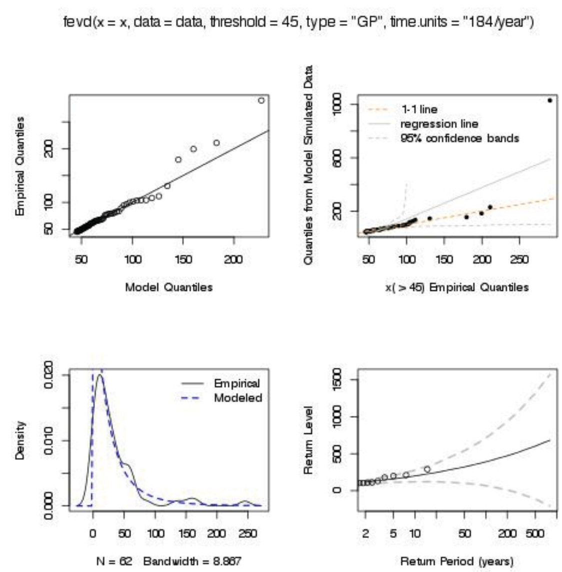

1D

72-hour Gridded Diagnostic Plots Wet Season Threshold = 50 mm

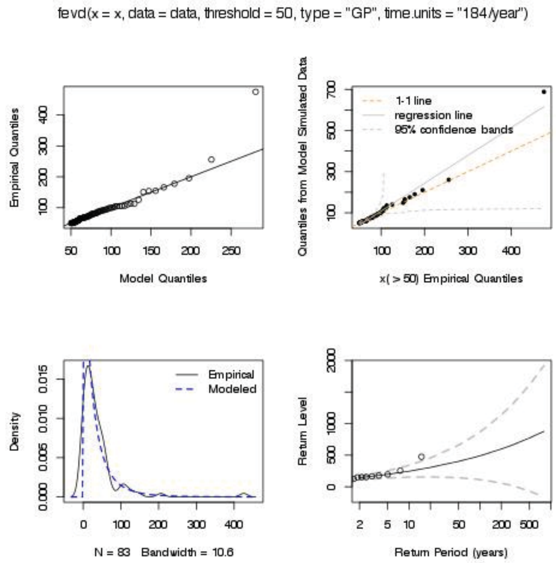

10E

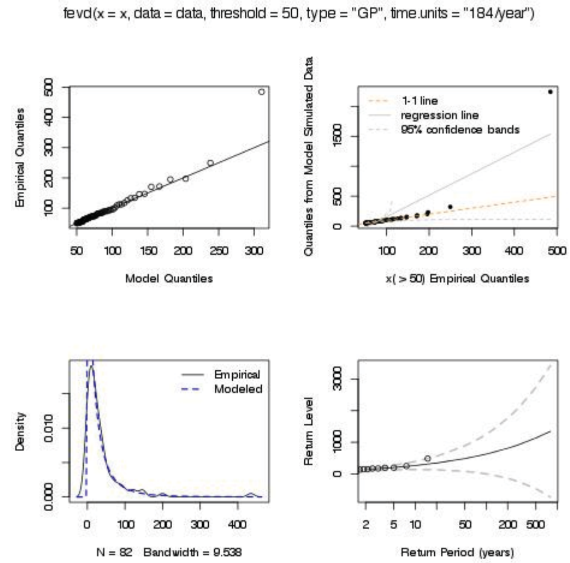

10F

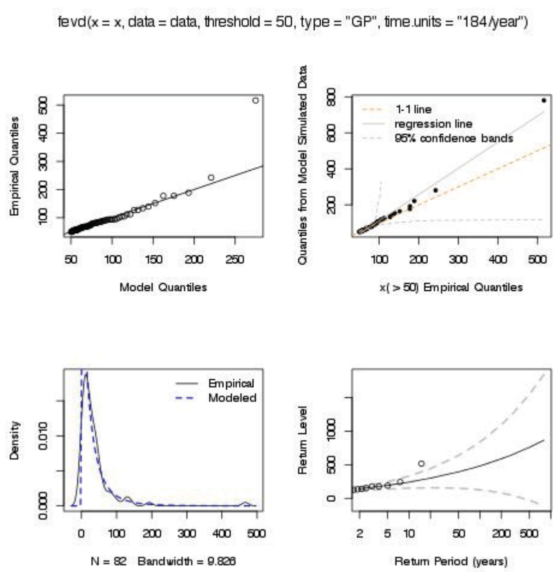

10G

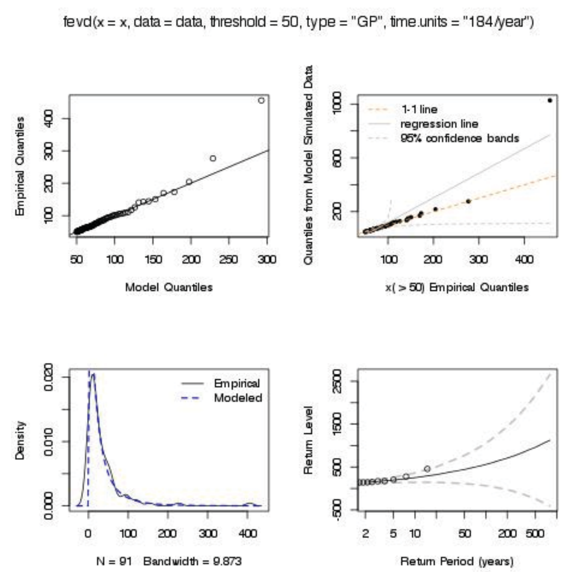

9E

72-hour Gridded Diagnostic Plots Wet Season Threshold = 50 mm

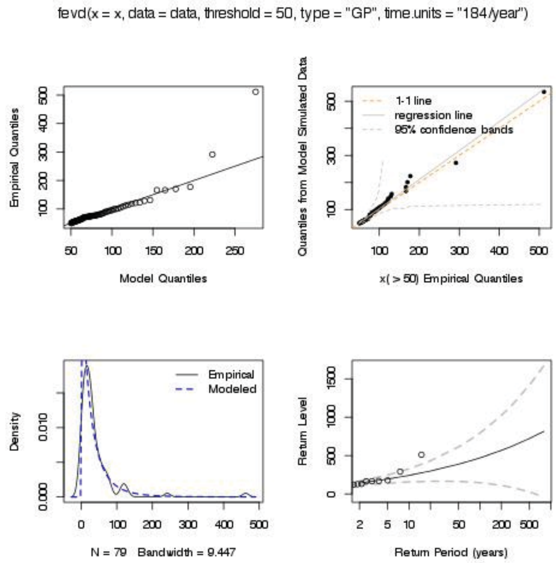

9G

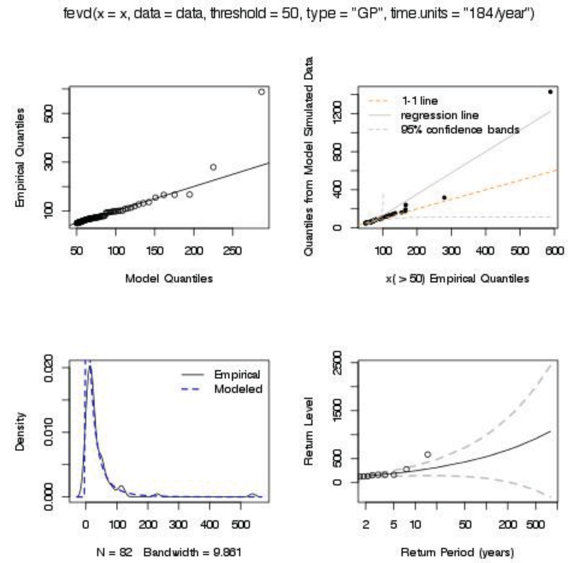

9H

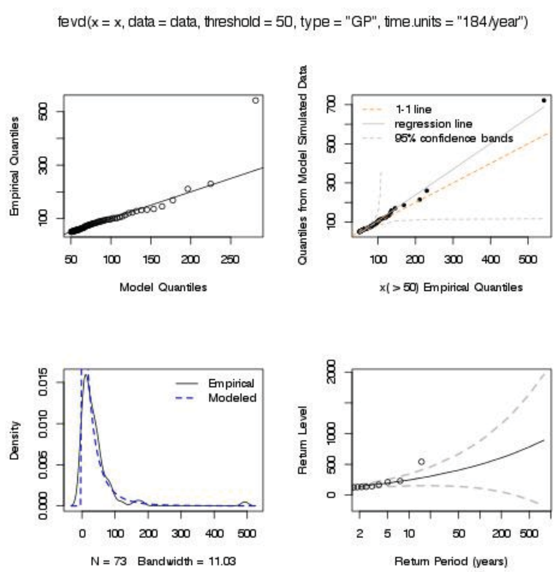

9I

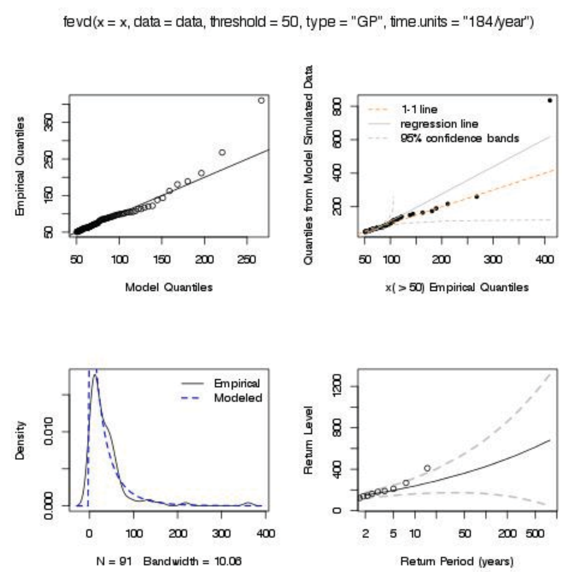

8D

72-hour Gridded Diagnostic Plots Wet Season Threshold = 50 mm

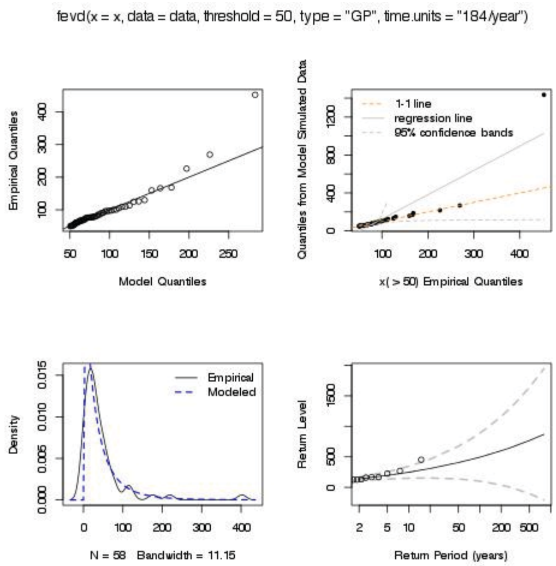

8H

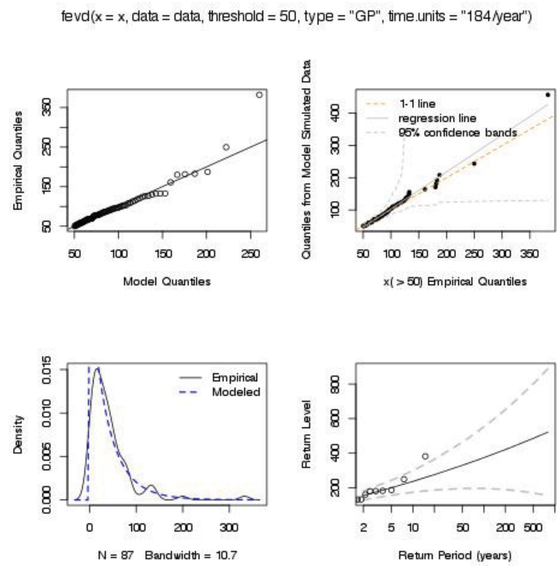

7D

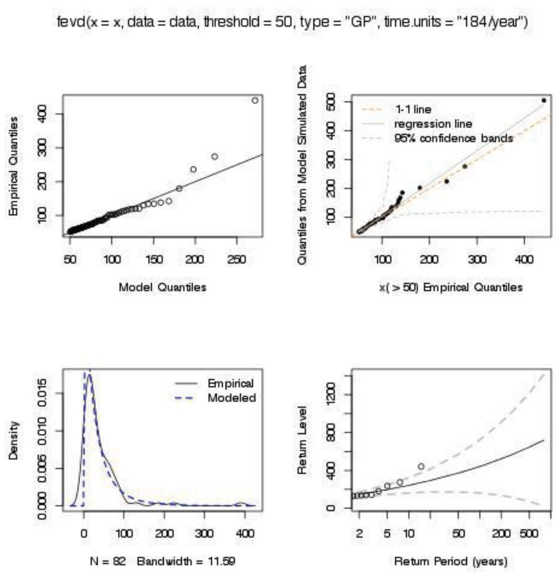

7E

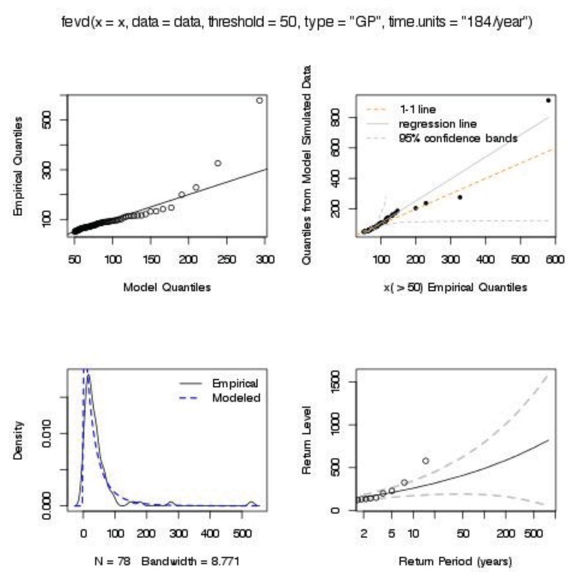

7F

72-hour Gridded Diagnostic Plots Wet Season Threshold = 50 mm

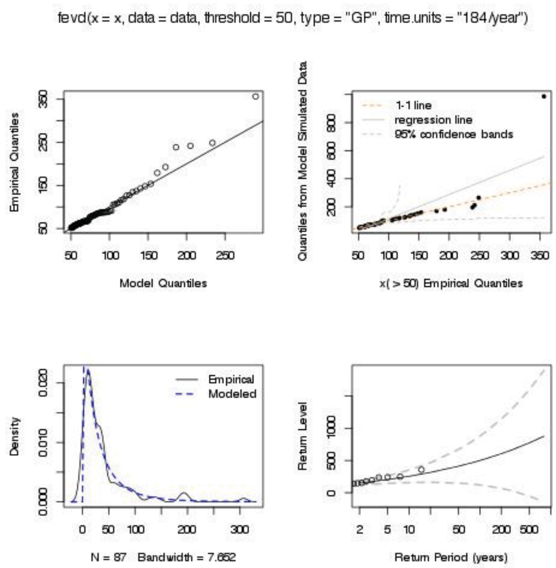

6C

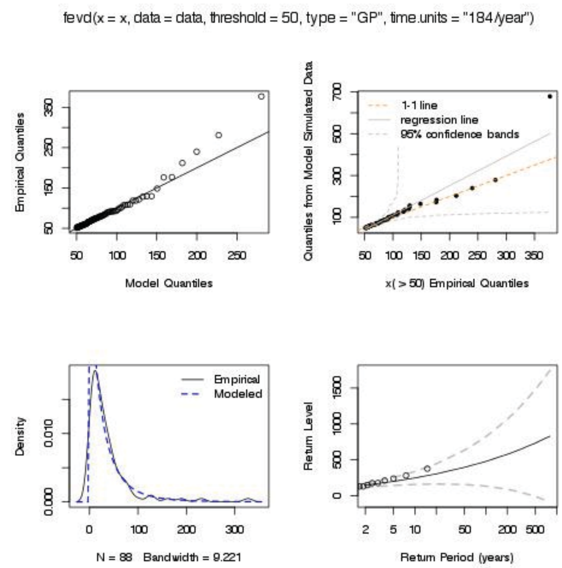

6D

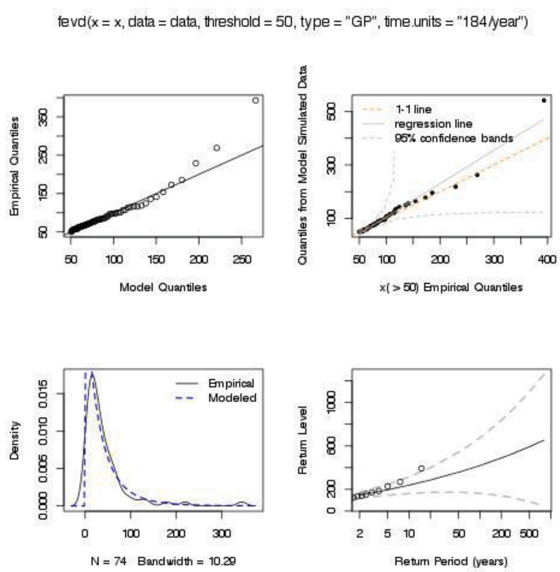

6E

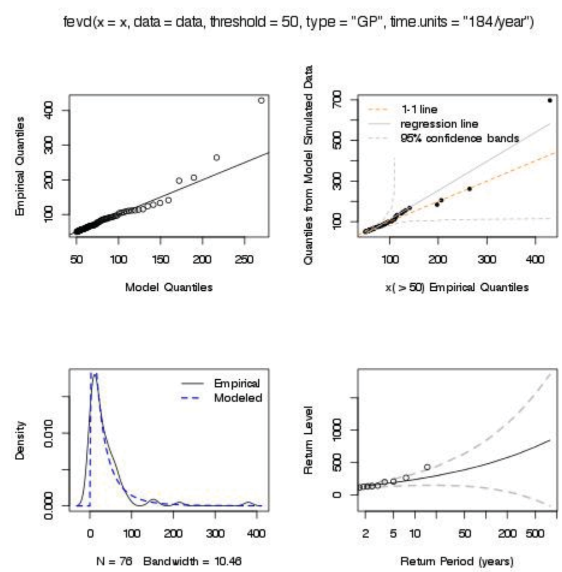

6F

72-hour Gridded Diagnostic Plots Wet Season Threshold = 50 mm

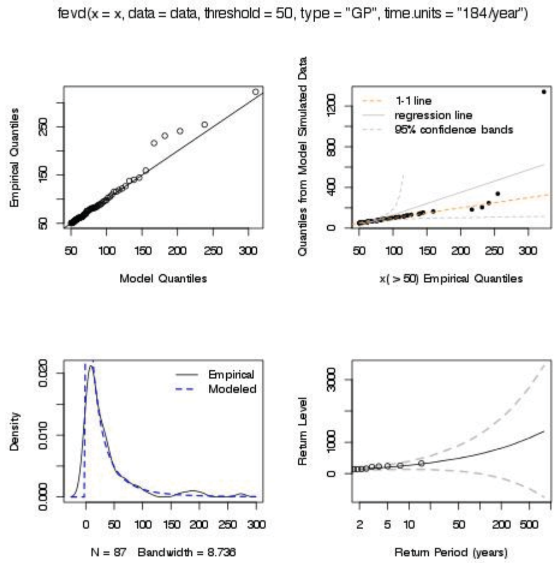

5C

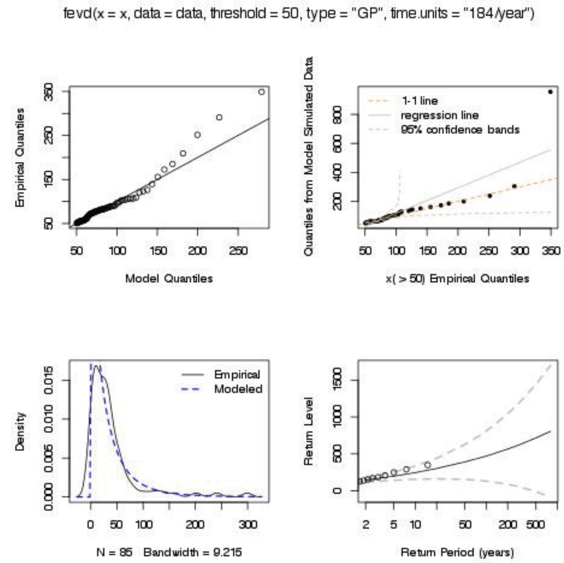

5D

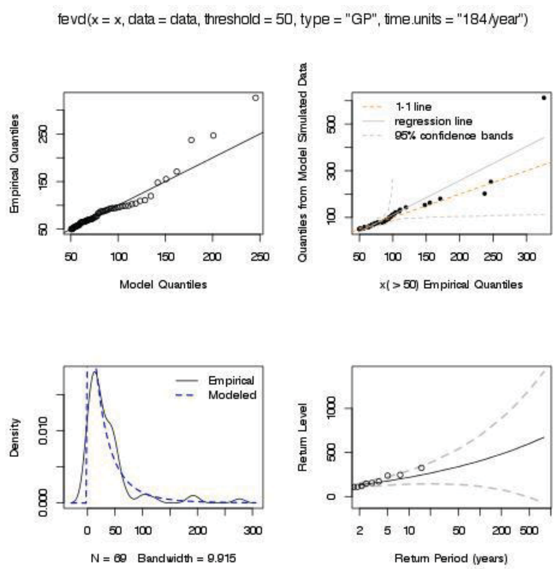

5E

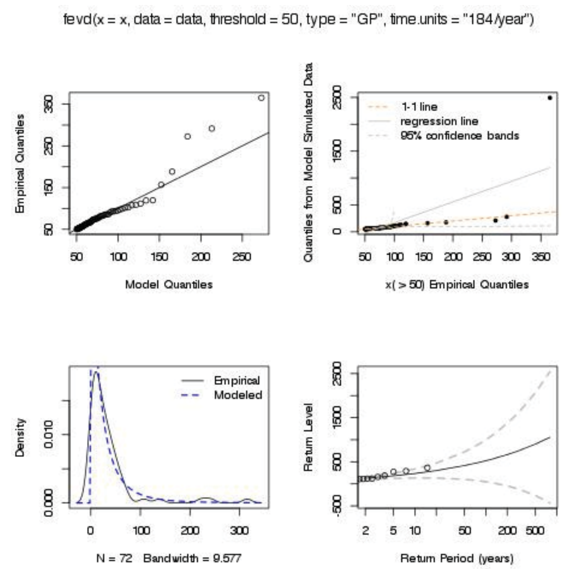

5F

72-hour Gridded Diagnostic Plots Wet Season Threshold = 50 mm

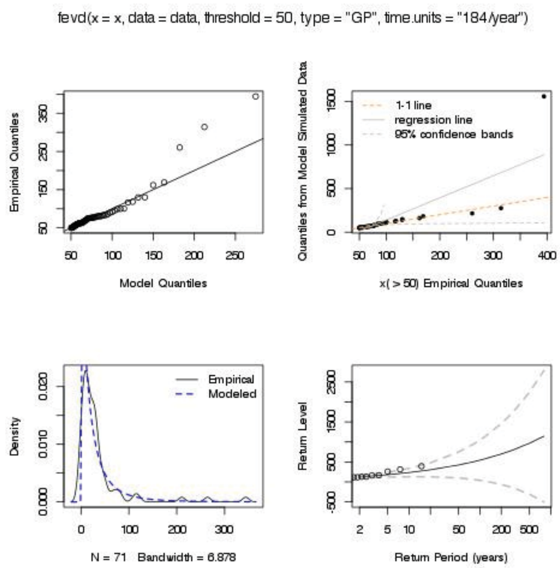

5G

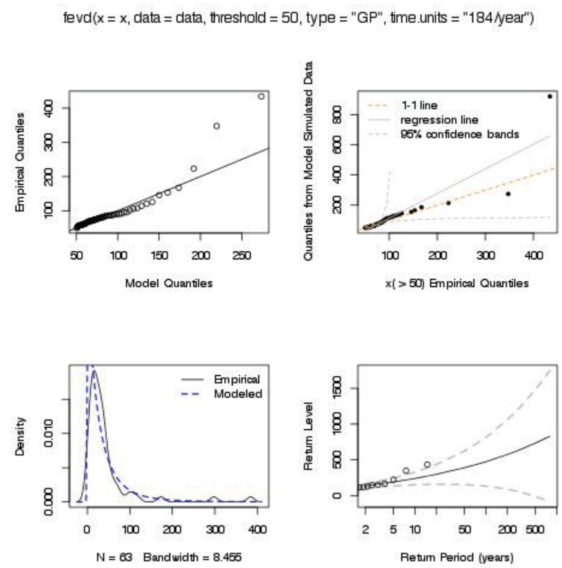

5H

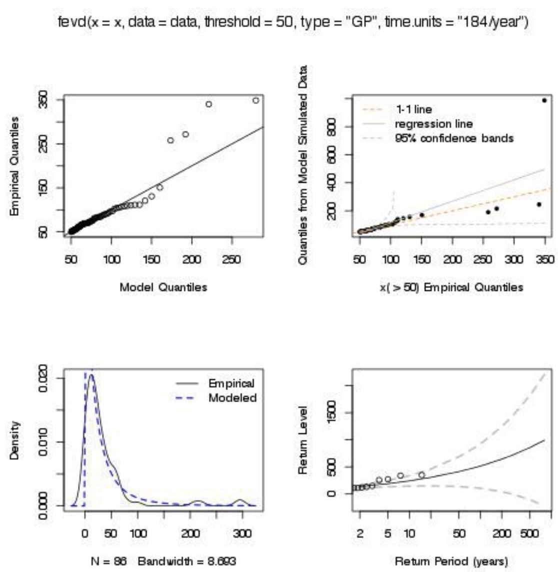

4C

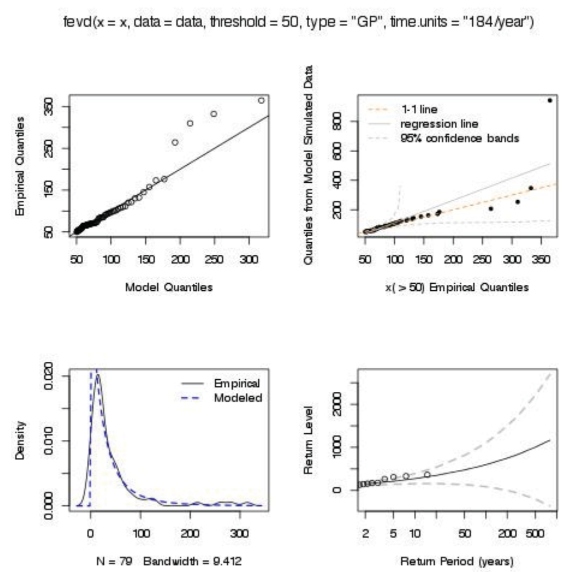

4D

72-hour Gridded Diagnostic Plots Wet Season Threshold = 50 mm

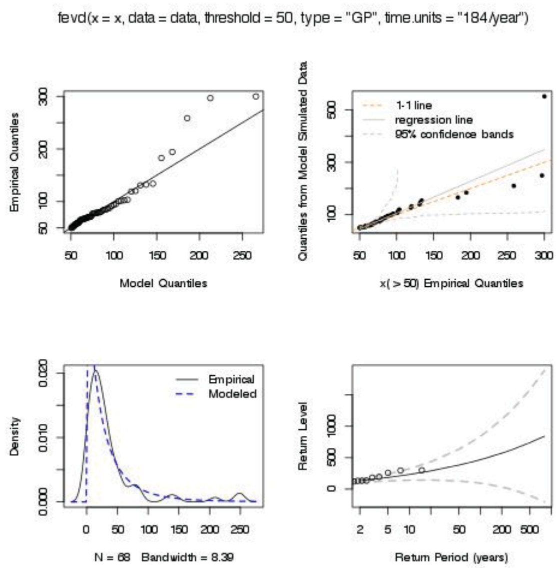

4E

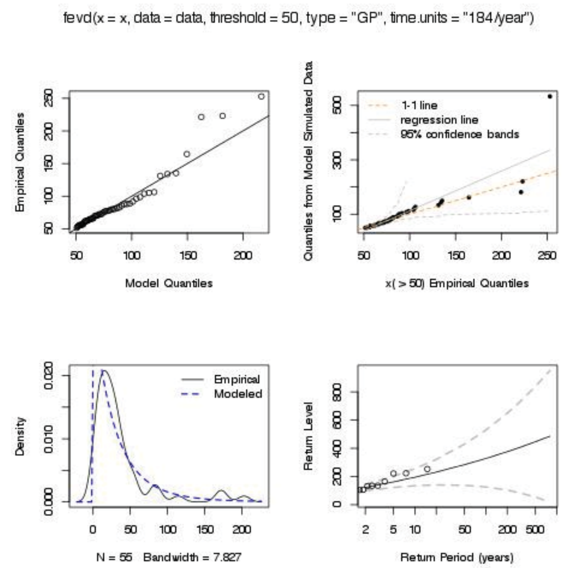

4F

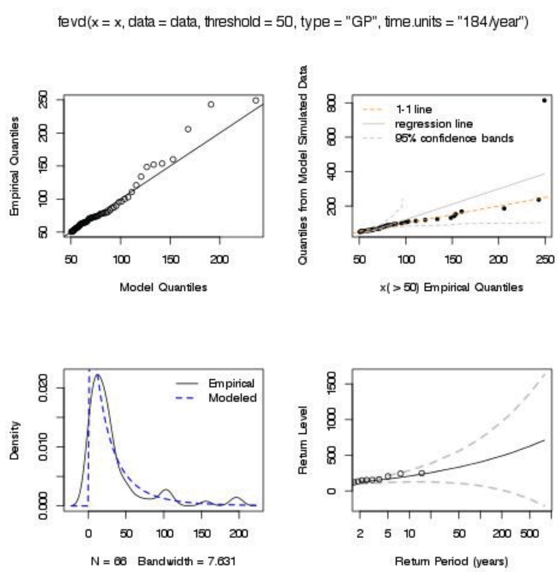

4G

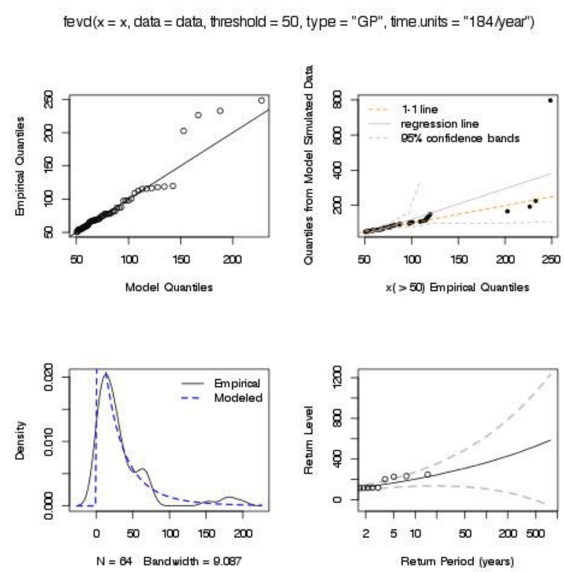

3B

72-hour Gridded Diagnostic Plots Wet Season Threshold = 50 mm

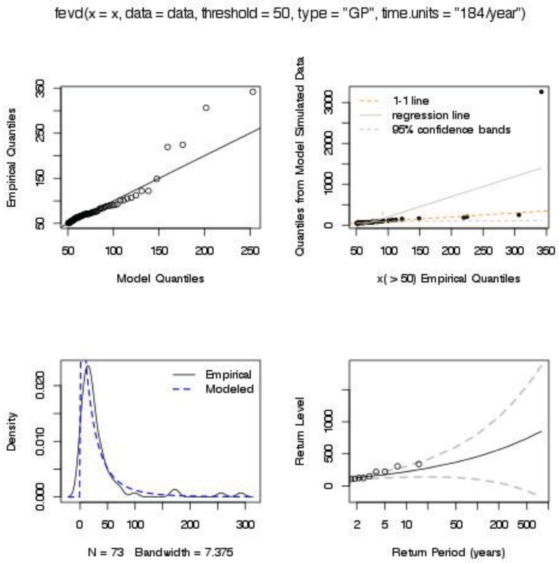

3C

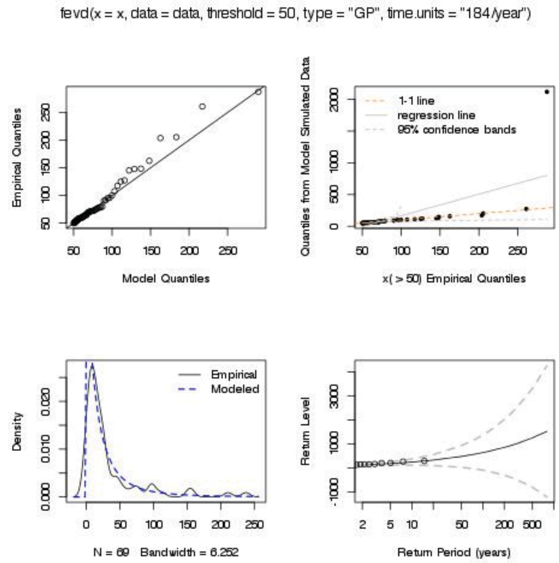

3D

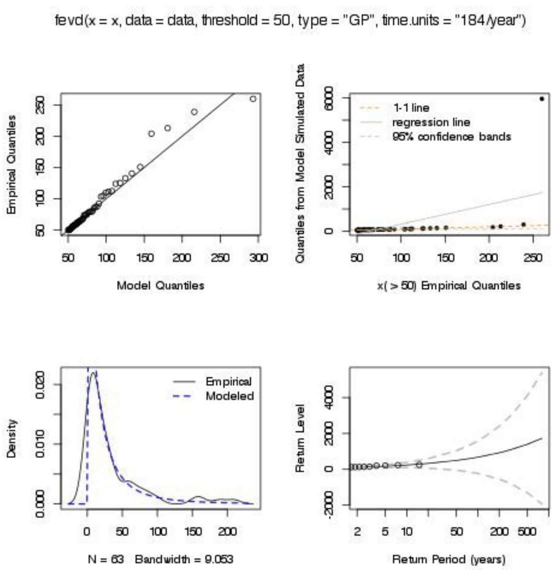

3E

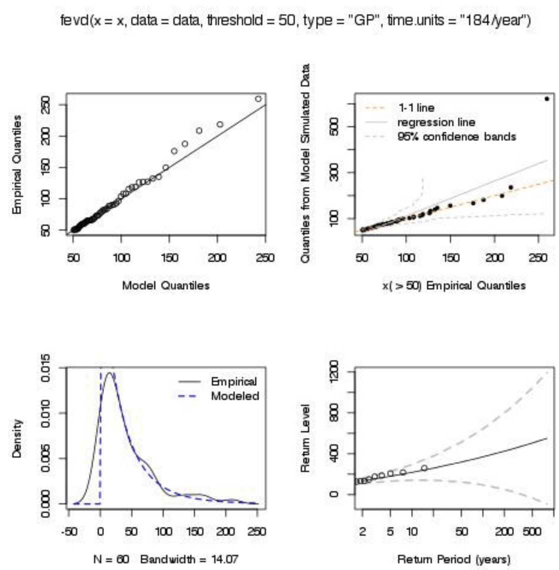

3F

72-hour Gridded Diagnostic Plots Wet Season Threshold = 50 mm

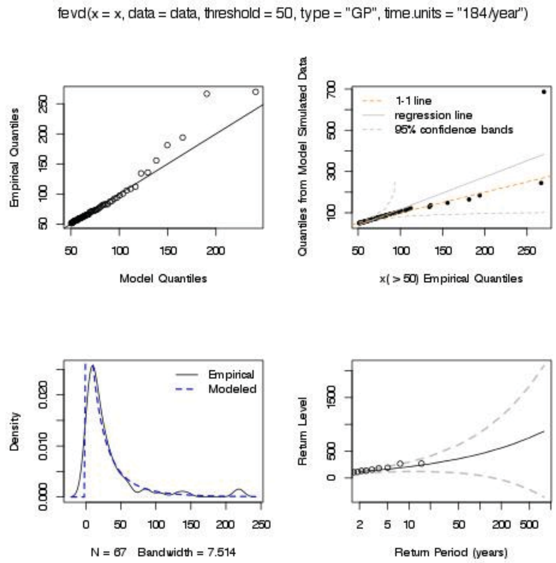

2C

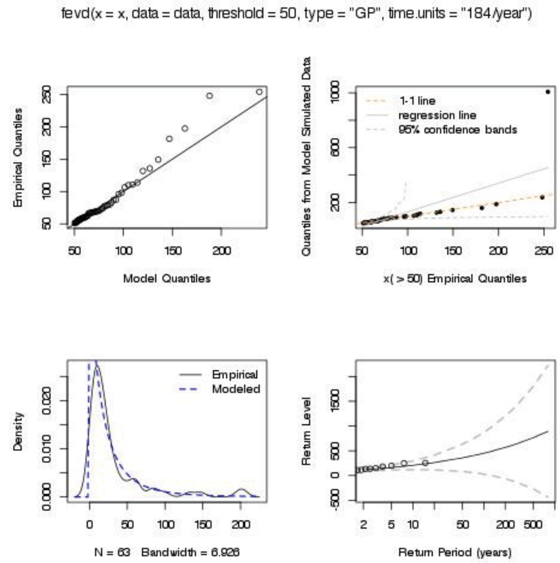

2D

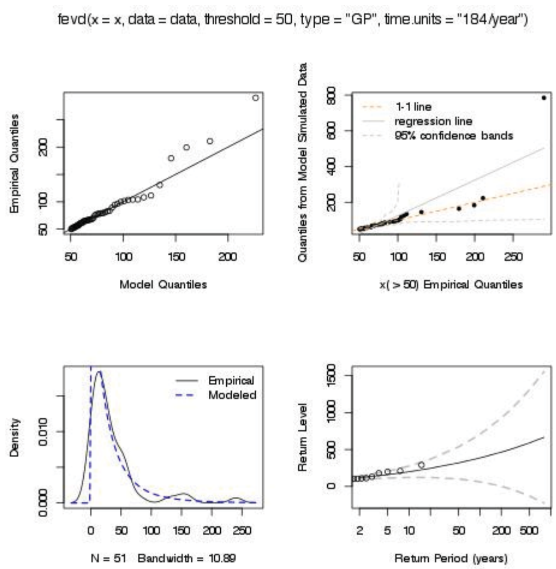

2E

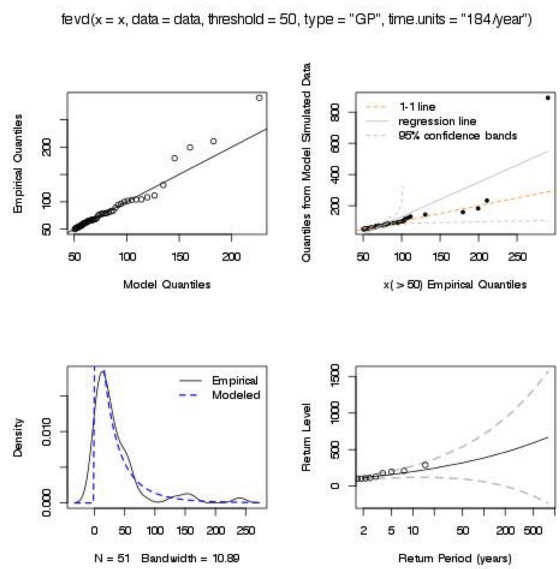

1D